



# RIOAO OPTILAS 2025

## Program and Abstracts

Santa Cruz de la Sierra, Bolivia

---



November 17 to 21, 2025  
UPB, Santa Cruz de la Sierra, Bolivia

---

Omar Ormachea, Ph.D.  
Eric Rosas, Ph.D.



# RIOA OPTILAS 2025 Meeting

## XII Meeting Optics Meeting / XV Latin American Meeting on Optics, Lasers and Applications

### Table of Contents

<b>RIOA OPTILAS 2025 Meeting</b>	<b>1</b>
Introduction	6
Presentation	6
Organization	7
Scientific Committee	8
RIOA-OPTILAS 2025 meeting venue	8
RIOA-OPTILAS 2025 inaugural speeches	9
Conference Program	11
<b>Plenary Talks</b>	<b>12</b>
Structuring ultrafast laser pulses for their application in attosecond science	12
Light Manipulation in Multilayered Photonic Structures	12
Future Perspectives of Optical Fiber Sensors	13
Applications of Gallium Oxide-Based Photomemristors in Neuromorphic Engineering	13
Ultrafast structural dynamics in solids driven by femtosecond laser pulses: from nonthermal bond breaking to surface nanostructuring	14
Physical principles of optical interferometry for surface topography measurement	15
Some contributions to improving atmospheric observations through solar spectral analysis	16
Uncovering Science: Communicating Research to Everyone	16
Triangulation at the Standard Quantum Limit	17
<b>Posters</b>	<b>18</b>
Deformation of metallic parts measurement applied shearing interferometry and mechanical sensors	19
U-Bent MMM Optical Fiber Sensor for the Detection of Mercury and Cadmium Ions in Aqueous Solutions	20
Cost-effective 3D printed bright-field microscope	21

Latent Fingerprint Imaging via Modulated-Intensity Maps from Fringe-Pattern Deflectometry	22
Solar Concentrator	23
Thin-Film Deposition and Optical Testing of a First-Surface Mirror for Astronomical Applications	24
Differentiation of air pollution sources in Montevideo using NO <sub>2</sub> , CO trace gas columns, and atmospheric aerosol properties	25
Application of photonic principles for medical samples transportation: Radiative cooling fabrics in warm tropical weather	26
Manufacture of aspherical mirrors for the implementation of a classic Cassegrain astronomical telescope	27
Spatial polarization modulation using two LCDs in tandem	28
Evaluating gait recognition performance on privacy preserving images	29
An Infrared-based Aedes-aegypti Identification Trap	30
A Data-based Protocol for a Low-cost Mobile Spectrometer Calibration	31
Analysis of Atmospheric Factors in Free-Space Optical (FSO) Communications for High-Altitude Urban Environments in La Paz, Bolivia	32
Effects of Atmospheric Conditions on Infrared Data Transmission: Experimental Analysis in La Paz, Bolivia	33
Detection of microstructural patterns in optical coherence tomography images using artificial intelligence tools to differentiate melanoma from melanocytic nevus	34
Optical sensors based on optical fibers in Mach-Zehnder type interferometry configuration for measuring ethanol concentration	35
Optical sensors based on balloon-shaped optical fibers with tip-induced deformation in a Mach-Zehnder interferometer configuration for measuring ethanol concentration	36
Enhancement of atomic emission intensity of heavy metals in LIBS using silver nanoparticles to increase the detection sensitivity of Cu and Pb	37
Optical design of double lens for the refractor telescope CST-80 KU by G-sum Method	38
Three-dimensional measurement of human face topography using fringe projection profilometry	39
Contouring of residual limb by white light profile for medical prosthetics	40
Thickness analysis of South American Camelid Wool Fiber by Fraunhofer Diffraction	41
Bridging Theory and Practice: A Remote Solar Laboratory for Energy Transition Education	42
Bio-inspired retinal analysis theoretical model based on mantis shrimp vision for monitoring the progression of Sanfilippo syndrome	43
Optimization of projection selection and measurement time in compressive single-pixel imaging	44
Temperature fiber sensor with variable sensitivity based on the Vernier effect and the bend-induced linear birefringence with tension	45
Stepping stones to engineer pulse propagation through multifrequency nonlinearities	46
Stochastic Modeling of the Polarization Effect on Light-Induced Mass Transport in Azopolymers	47
Photoinduced Optical Properties in Layer-by-Layer Azopolymer Films and Polyamines	48
Laser tuning of IR radiative properties of metals	49
Optical sensor based on a Mach-Zehnder interferometric curved optical fiber for measuring refractive index	50
Second-order electrogyration in Bi <sub>12</sub> SiO <sub>20</sub> crystals analyzed by a dualrotation Mueller–Stokes polarimeter	51
Axial Thermal Gradient Localization and Its Role in LHPG Fiber Integrity	52

Design of Aplanatic Imaging Systems printed using Stereolithography	53
<b>Oral Presentations</b>	<b>54</b>
Photonic Crystal Mode Control in Semiconductor Lasers	55
Thickness analysis of South American Camelid Wool Fiber by Fraunhofer Diffraction	56
Upgraded emissometer at the University of the Basque Country based on a new control-design paradigm	57
Spatial polarization modulation using two LCDs in tandem	58
Gravity-compensated focus-tunable lenses. Aberration analysis	59
An Infrared-based Aedes-aegypti Identification Trap	60
Coexistence of Aplanatism and Achromatism in Optical System Design	61
Optimization of projection selection and measurement time in compressive single-pixel imaging	62
Advanced characterization of oxide nanomaterials using infrared spectroscopy	63
Precision Tissue Classification via LIBS and ML: Toward Intraoperative Pathology Screening	64
Optical Multispectral Characterization of Photonic and Plasmonic Properties of Living Biostructures and Optical Ranging Biodiversity Assessment	65
Spatio-chromatic vision changes following cataract surgery with multifocal diffractive intraocular lens implantation	66
Ablation volume analysis in laser induced breakdown spectroscopy diagnosis on colon tissues	67
Application of photonic principles for medical samples transportation: Radiative cooling fabrics in warm tropical weather	68
Bio-inspired retinal analysis theoretical model based on mantis shrimp vision for monitoring the progression of Sanfilippo síndrome	69
Contouring of residual limb by white light profile for medical prosthetics	70
Fiber-based acoustic and optic fused couplers	71
Point sensors and fiber characterization techniques based on forward stimulated Brillouin scattering	72
Optical Fiber Sensor Based on CS-TA Functionalized E-SMS Structure for the Selective Detection of Microplastics in Water	73
Sensing Fiber Twist through State of Polarization-Induced Phase Shifts	74
Low-Coherence Interferometry for Analog Optical Communication	75
Figure-8 fiber laser with dynamically controlled switching characteristic	76
U-Bent MMM Optical Fiber Sensor for the Detection of Mercury and Cadmium Ions in Aqueous Solutions	77
Analysis of Atmospheric Factors in Free-Space Optical (FSO) Communications for High-Altitude Urban Environments in La Paz, Bolivia	78
Optical sensors based on optical fibers in Mach-Zehnder type interferometry configuration for measuring ethanol concentration	79
Optical sensors based on balloon-shaped optical fibers with tip-induced deformation in a Mach-Zehnder interferometer configuration for measuring ethanol concentration	80
Emissions into the atmosphere from the Ing. Héctor R. Lara Sosarefinery, Cadereyta de Jiménez, Nuevo León, México	81
The GEMM initiative by OPTICA & AGU and the BEACO2N sensors	82

Analysis of spectral structures influencing the detection of atmospheric trace gases	83
Differentiation of air pollution sources in Montevideo using NO <sub>2</sub> , CO trace gas columns, and atmospheric aerosol properties	84
A Data-based Protocol for a Low-cost Mobile Spectrometer Calibration	85
Enhancement of atomic emission intensity of heavy metals in LIBS using silver nanoparticles to increase the detection sensitivity of Cu and Pb	86
Effects of Atmospheric Conditions on Infrared Data Transmission: Experimental Analysis in La Paz, Bolivia	87
Experimental study of polarization in the Normal Zeeman effect	88
A Comparison of Metallic Nanoantenna Configurations for Single-Photon Emitters	89
Optical Bullets with Angular Momentum in Nonlinear Waveguides	90
Design and Simulation of GeSbS-Based Microcavities for Advanced Nonlinear Photonics	91
Optical Characterization of Infrared Key Fiber Materials: Transmission and Kerr Coefficient Measurements	92
From Lab to Factory: Applied Photonics Solutions for Industry	93
Plasmonic–Magnetic Hybrid Nanostructures for Efficient Photocatalytic Arsenic Remediation in Water	94
Thin-Film Deposition and Optical Testing of a First-Surface Mirror for Astronomical Applications	95
Modeling of ultrashort laser pulse nanostructuring of materials	96
Aniseikonia with Sphero-Cylindrical Lenses	97
First Peruvian binoculars: Improvements	98
Manufacture of aspherical mirrors for the implementation of a classic Cassegrain astronomical telescope	99
Optical design of double lens for the refractor telescope CST-80 KU by G-sum Method	100
Solar Concentrator	101
Multiple Interferometry Applied to Radio Telescope Techniques	102
Remote Automated Laboratory for Real-Time Optimization of Coagulation-Flocculation mediated UV Processes in Arsenic- Contaminated Water Treatment	103
A Hybrid Solar Street Lights Remote Laboratory	104
Bridging Theory and Practice: A Remote Solar Laboratory for Energy Transition Education	105
Remote Multisensor System for Indirect Measurement of Nanoparticle Surface Charge under UV Illumination	106
A Remote Photovoltaic Laboratory at Latitude 0o for Supporting 24/7 Online Self-learning and Inverted-classroom Teaching	107
Fringe projection system calibration based on Radon transform	108
Fast phase unwrapping by polynomial fitting	109
Surface Profilometry with a Smartphone-Based Fringe Projection System	110
Simplified Chromatic Aberration Compensation in Digital Camera Lenses for Fringe Projection Profilometry	111
Automatic orthogonal recording polarimeter applied to bio-samples	112
Evaluating gait recognition performance on privacy preserving images	114
Cost-effective 3D printed bright-field microscope	115

---

Detection of microstructural patterns in optical coherence tomography images using artificial intelligence tools to differentiate melanoma from melanocytic nevus	116
Three-dimensional measurement of human face topography using fringe projection profilometry	117
Measurement and characterization of reflective convex surfaces using Ronchi deflectometry	118
Deformation of metallic parts measurement applied shearing interferometry and mechanical sensors	119
Latent Fingerprint Imaging via Modulated-Intensity Maps from Fringe-Pattern Deflectometry	120
Optical Design and prototyping of terrestrial telescope	121
A Remote Solar Photovoltaic Laboratory for Energy Dispatch Analysis	123
Nailfold capillaroscopy	124
3D scanning of objects by color multi-line structured light projection	125
Second Harmonic Generation from LIPSS on GaAs	126
<b>Photographs of RIOA-OPTILAS 2025</b>	<b>127</b>
<b>Detailed Conference Program</b>	<b>141</b>
<b>Final Comments</b>	<b>152</b>

## Introduction

The RIAO OPTILAS Meeting is the premier triennial academic gathering dedicated to bringing together Ibero-American researchers, professors, and students working in the vast field of Optics, Photonics, and their applications. Its fundamental goal is to facilitate the dissemination of project results and to strengthen scientific and academic collaboration across Latin America, Europe, and North America.

This event proudly hosts two major activities: the XII Iberoamerican Optics Meeting (RIAO) and the XV Latin-American Meeting on Optics, Lasers and Applications (OPTILAS).

### **The Historic 2025 Edition in Santa Cruz**

We are honored to welcome the scientific community to the RIAO/OPTILAS 2025 Meeting in Santa Cruz, Bolivia. This edition marks a historical milestone, as it is the first time this prestigious event is held in Bolivia.

The Local Organizing Committee is pleased to announce that the meeting will take place from November 17 to 21, 2025, at the UPB Campus (Universidad Privada Boliviana) in Santa Cruz, Bolivia. We thank all researchers and students for their contributions and look forward to a successful and productive week of scientific exchange.

## Presentation

The 2025 edition of the RIAO-OPTILAS Congress represents a milestone for the Ibero-American scientific community. This international meeting, which has brought together RIAO and OPTILAS since 1998 in Cartagena de Indias, Colombia, reaffirms the commitment of the Ibero-American Optics Network (RIAO) to strengthening optics and photonics in Ibero-America, promoting collaboration, academic exchange and the training of new generations of researchers.

Academic participation in this 2025 event is characterised by the diversity, quality and dynamism of the Bolivian optical community, which did not hesitate for a moment to offer its academic spaces for this celebration at the event in Bolivia. This edition is summarised as follows:

- Nine keynote speakers from leading global optical research institutions.
- 64 oral presentations initially confirmed, covering topics such as quantum optics, biophotonics, metrology, nonlinear optics, instrumentation, among others.
- 10 poster presentations, selected for their quality and scientific relevance.
- 25 additional posters presented by students who are also participating in oral presentations, as part of the Student Poster Competition, an initiative that seeks to stimulate scientific communication among young researchers.
- Total number of confirmed oral presentations: 73, including last-minute additions and active student participation.

This volume of contributions reflects the dynamism and interest in strengthening scientific collaboration networks. RIOA-OPTILAS 2025 stands out for its strong youth component. The active participation of students in the poster competition and oral sessions demonstrates:

- RIOA's commitment to training new generations of scientists.
- The promotion of scientific communication and critical thinking skills.
- The creation of collaborative networks between young and established researchers.

This approach guarantees the renewal and sustainability of the scientific ecosystem in optics and photonics. The choice of Bolivia as the venue for the RIOA-OPTILAS 2025 Congress is the result of a strong local initiative led by Prof. Omar Ormachea, director of the Optical and Energy Research Center, together with his scientific, academic and administrative team. Their efforts have been key to positioning the Bolivian Private University as an international scientific meeting place.

This event also marks the beginning of a new institutional cycle, with Dr María Sagrario Millán taking over as chair of the RIOA Council for the period 2025–2028. A renowned European scientist in the field of optics, her leadership heralds a period of consolidation, expansion and strengthening of RIOA in its academic, institutional and geographical dimensions.

RIOA-OPTILAS 2025 is not only a high-level academic event, but also a historic opportunity to strengthen science in Bolivia and the Ibero-American region. The event's attendance figures, the prominence of young people, the institutional support and the international reach are testament to RIOA's commitment to scientific development, equality and cooperation.

Dr. José Luis Paz  
Chair of the Council 2022–2025  
Red Iberoamericana de Óptica  
November 2025

## Organization

The RIOA-OPTILAS 2025 Local Organizing Committee was integrated by the following members of the faculty of the UPB: Omar Alberto Ormachea Muñoz (Chair), Edgar Eduardo Salazar Florez, Juan Pablo Gonzales Arce, César Alejandro Pérez Fernández and Alex Stephan Villazón Torrico.

The RIOA-OPTILAS 2025 Technical Program Committee was integrated with the following distinguished colleagues of the Iberian-American optics and photonics community: Íñigo González de Arrieta Martínez of the Universidad del País Vasco in Spain; Telmo Echániz of the Universidad del País Vasco in Spain; Silvia Ledesma of the Universidad de Buenos Aires in Argentina; Inocencio R. Martín of the Universidad de La Laguna in Spain, and Aura Higuera Rodríguez of Signify in The Netherlands.

The RIOA-OPTILAS 2025 Steering Committee was integrated by representatives of the optics and photonics societies of the member countries, Spain, Portugal, Mexico, Cuba, Colombia, Venezuela, Ecuador and Argentina.

The steering committee included: José Luis Paz Rojas (President, Peru), Eric Rosas (Secretary), Myrian Tebaldi (Counselor, Argentina), Freddy Rafael Pérez (Counselor, Colombia), Juan Gualberto Darías González (Counselor, Cuba), César Costa Vera (Counselor, Ecuador), Aníbal de la Piedad Beneítez (Counselor, Mexico), Manuel Filipe Costa (Counselor, Portugal), Augusto Beléndez Vázquez (Counselor, Spain) and Vincent Piscitelli (Counselor, Venezuela).

## Scientific Committee

The members of the RIAO-OPTILAS 2025 International Scientific Committee were:

- Ramón Carriles Jaimes, Centro de Investigaciones en Óptica, México
- Manuel Filipe Costa, University of Minho, Portugal
- Luis David Badilla, Universidad Nacional, Costa Rica
- Christian Cuadrado-Laborde, IFIR Conicet, Argentina
- Jesús Garduño-Mejía, Instituto de Ciencias Aplicadas y Tecnología UNAM, México
- Julio Gutiérrez, Tecnológico de Monterrey, México
- Gerardo Gutiérrez-Juárez, Universidad de Guanajuato, México
- María Sagrario Millán García-Varela, Universitat Politècnica de Catalunya, España
- Rubén Ramos-García, Instituto Nacional de Astrofísica, Óptica y Electrónica, México
- Pedro Torres, Universidad Nacional de Colombia, Colombia
- Marcelo Trivi, Centro de Investigaciones Ópticas, Argentina
- J. Benito Vázquez-Dorrío, University of Vigo, España
- Miguel V. Andrés, University of Valencia, España
- John Fredy Barrera Ramírez, Universidad de Antioquia, Colombia
- Victor H. Granados, Universidad Nacional, Costa Rica
- Jorge Enrique Mejía Sánchez, Universidad de Guadalajara, México

## RIAO-OPTILAS 2025 meeting venue

The main venue for the conference is the UPB Campus in Santa Cruz, Bolivia. The academic activities will be hosted in two dedicated, independent areas:

Main Auditorium (Room 1): This space has a capacity for 150 participants and will be used for plenary sessions, opening ceremony, plenary talks, oral presentations, and the closing ceremony.

Meeting room (Room 2): This area has capacity for 100 participants and will be used for the various workshops in simultaneous sessions. It will be designated as the official poster exhibition, including the awards for the best student posters.

The UPB facilities will ensure that both rooms function independently to guarantee the smooth execution of the academic program.

---

## RIAO-OPTILAS 2025 inaugural speeches

**Carlos Foronda, Ph.D.**  
**Vice-President, UPB**

Dear colleagues, researchers, professors, students, and distinguished guests:

It is a great pleasure and an honor for UPB to welcome you to RIAO/OPTILAS 2025, here in the vibrant city of Santa Cruz de la Sierra, Bolivia.

This event brings together the 12th Ibero-American Optics Meeting and the 15th Latin American Meeting on Optics, Lasers, and Applications. It also marks a historic moment: this is the first time that a scientific conference of this size is held in our country. For UPB, and for Bolivia, this is more than an academic event. It shows the growth and strength of our scientific community. At UPB we believe that prestige is not declared — it is demonstrated. And this week is clear proof of that.

Since its foundation, UPB has grown together with Bolivia. Its prestige comes from generations of professors, researchers, and students who have pursued academic excellence with ethical commitment. It comes from a nation that keeps moving forward and a university that chooses to support that progress through knowledge.

To all our guests from Latin America, Europe, and North America: welcome to UPB and welcome to Bolivia.

RIAO/OPTILAS is held every three years in a different Ibero-American country and brings together some of the brightest minds in optics and photonics. This 2025 edition, the first in Bolivia, is truly special. We are honored to host keynote speakers and researchers from many nations, and we are proud that UPB professors and students will also present their work.

Researchers from twelve countries join us this week, all united by a shared passion for knowledge. For UPB, recognized as the most prestigious private non-profit university in Bolivia, this event reflects our mission: to educate talented professionals under international standards of excellence, and to serve our country through science.

Hosting this event confirms that UPB's reputation is built every day — in the classroom, in the laboratory, and through applied research and global cooperation.

The true value of this week is not only in the presentations. It is in the conversations, the new partnerships, and the ideas that will travel across borders and create real solutions. Progress grows through cooperation, rigor, and purpose.

UPB has expanded internationally while staying rooted in Bolivia. We have shown that it is possible to prepare professionals for the world, from Bolivia, for Bolivia, with global reach.

Our partnership with the University of London, our international academic networks, and the recognition received by our faculty show our strong commitment to science and education. That is why we say with confidence: the best come to UPB, because at UPB, the best teach.

UPB is a non-profit foundation. This means that every achievement and every innovation is reinvested in what matters most: our students, our professors, and our country. We believe in an academic model that opens its doors to society and to the world. This is how we serve Bolivia: by cultivating knowledge, inspiring talent, and preparing for tomorrow while working today.

On behalf of UPB, I want to express our sincere gratitude to the International Organizing Committee, the scientific and technical teams, and every participant who made this meeting possible.

From November 17 to 21, Santa Cruz will be the heart of Ibero-American optics and photonics. May this week be full of learning, collaboration, and inspiration.

And when it ends, may we proudly say that Bolivia rose to the level of international science.

Thank you very much.

**Omar Ormachea, Ph.D.**

**Chair, Local Organizing Committee**

We have finally reached this moment, the inauguration of the RIAO OPTILAS 2025 Congress, which also hosts two meetings of the Ibero-American Optics Community and which RIAO has generously allowed us to organize. This moment represents the fruit of two years of work by a group of colleagues from the UPB.

Although organizing an international event has been a challenging experience for most of us, it will be an unforgettable experience for everyone. However, even though all the hours worked and the preparations made have already left their mark on our memories, the most important part is yet to come. During this week, we will have the opportunity to hear presentations from Ibero-American specialists in many areas of research in optics, photonics, lasers, and their many and diverse applications, but we will also be joined by distinguished international researchers who will share their knowledge and experiences.

In addition, we will have the participation of students from our university, institutes, and research centers, who will have the opportunity to attend as listeners or participate as exhibitors in the oral and poster presentation modalities of our conference. The opportunity to learn about other works, other approaches, and the researchers who carry them out is part of the outcome.

I would also like to thank all my colleagues on the Organizing Committee, Eric Rosas, Manuel Philipe Costa, and the UPB for all their support during this time. Finally, we thank you all for attending this opening ceremony and hope that this will be a very beneficial week for everyone.

Thank you very much.

## Conference Program

Hour	Monday, November 17th	Tuesday, November 18th	Wednesday, November 19th	Thursday, November 20th	Friday, November 21st
7:45 - 8:30	Registration of participants				
8:30 - 8:55		Quantum Optics School / Parallel sessions	Quantum Optics School / Parallel sessions		Oral Presentation Session
9:00 - 9:30	<b>Opening</b>				
9:30 - 10:00	First IPS-RIOA Topical Workshop on Quantum Optics - Quantum Optics School	Coffee break	Coffee break	Coffee break	Coffee break
10:00 - 10:15		Parallel sessions	Parallel sessions	Quantum Optics School / Parallel sessions	Oral Presentation Session
10:15 - 10:45					
10:50 - 11:30					
11:30 - 12:30	Plenary 1 Peter de Groot	Plenary 3 Mike McKee	Plenary 5 Emiliano Descrovi	Plenary 7 Erna Frins	Plenary 9 John Howell
12:30 - 13:45	Lunch break	Lunch break	Lunch break / Giving your first international technical presentation	Lunch break	<b>Closing Ceremony Cocktail</b>
14:00 - 14:20	Oral Presentation Session	Oral Presentation Session	Oral Presentation Session	Oral Presentation Session	
14:20 - 14:40					
14:40 - 15:00					
15:00 - 15:20					
15:20 - 15:40					
15:40 - 15:55	Coffee break	Coffee break	Coffee break	Coffee break	
16:00 - 17:00	Plenary 2 Carlos Hernández	Plenary 4 Marina Sparvol	Plenary 6 Martin E. Garcia	Plenary 8 Orlando Frazão	
17:00 - 18:30	Posters Session / <b>Welcome Cocktail</b>	Communicating Science to the public / Mike McKee	RIOA OPTILAS General Assembly	IPS-Peer review ethics / Carmiña Londoño IPS-Entrepreneurs hip / Natalia Cañas	
18:30 - 19:00					
19:00 - 23:00			<b>Official Event Dinner</b>		

## Plenary Talks

### Structuring ultrafast laser pulses for their application in attosecond science

Carlos Hernández-García

University of Salamanca, Spain

**Bio:** Carlos Hernández is an associate professor at Universidad de Salamanca (Spain). PhD in Physics (2013). After a European Marie Skłodowska Curie postdoctoral stay at JILA, University of Colorado at Boulder (USA), he returned to Universidad de Salamanca where he leads the Unit on Structured Light and Matter (LUMES) and the ERC Starting Grant project ATTOSTRUCTURA. His work focuses on the generation and applications of structured laser pulses, with durations in the attosecond timescale. Together with his colleagues and collaborators, he has designed theoretical tools to understand and combine quantum simulations with highly non-linear strong-field processes. Co-author of >80 peer-reviewed publications. Recipient of the Fresnel Prize 2019, the IUPAP Young Scientist Prize 2021, and the ICO Prize 2023.

**Abstract:** Ultrafast laser technology has transformed our understanding of science, enabling the observation and control of matter on femtosecond ( $10^{-15}$  s) and attosecond ( $10^{-18}$  s) timescales. The generation of attosecond pulses through high harmonic generation (HHG)—recognized with the 2023 Nobel Prize in Physics—has established a foundation for attosecond science as a transformative field impacting applied —photonics, nanotechnology, spectroscopy, imaging— and fundamental—physics, chemistry, biology— fields. A pivotal development in attosecond science is the capability of structuring ultrafast laser sources, particularly in their spin and orbital angular momentum properties. These advances enable time-dependent studies of chiral systems, magnetic materials, and ultrafast electronic and spin dynamics with unprecedented precision. The ability to generate structured attosecond pulses via HHG has driven several breakthroughs in nonlinear optics, allowing the creation of EUV/soft x-ray pulses with tailored angular momentum and spatiotemporal profiles. In this talk we will review several works that have boosted the field of attosecond structured pulses during the last decade. We will focus not only on the ability to tailor the angular momentum properties of attosecond pulses, but also on how through the topology of the EUV/soft x-ray pulses we can retrieve information about ultrafast electronic dynamics of matter. Since the early work on HHG driven by vortex beams, the use of driving field configurations with custom orbital angular momentum properties has opened opportunities for controlling spatiotemporal high-order harmonic properties. Notable advancements include the generation of attosecond vortices with controlled polarization, high harmonic pulses with time-dependent orbital angular momentum or self-torque, EUV vector harmonic pulses, attosecond vortex pulse trains, spatially-structured harmonic beams from graphene, or EUV spatiotemporal and spatio-spectral optical vortices.

### Light Manipulation in Multilayered Photonic Structures

Emiliano Descrovi

Politecnico di Torino and European Optical Society, Italy

**Bio:** Emiliano Descrovi is Associate Professor in Physics at the Department of Applied Science and Technology, Politecnico di Torino, Italy. He obtained his master degree in Physics from the University of Torino in 1999 and the PhD in Microtechnique from the Université de Neuchâtel, Switzerland, in 2005. His research interests fall in the domain of dielectric nanophotonics and light-responsive polymer photonics, targeting novel tunable devices controlled by light. In the past years, he focused on optical phenomena involving surface modes on planar dielectric multilayers. In 2020 he joined the European Optical Society (EOS) board and presently serves as President since September 2024.

**Abstract:** Recent results on light manipulation by means of Bloch surface waves (BSW) on multilayers are presented. Planar multilayers sustaining either TE or TM-polarized BSW offer new opportunities for light management at the micro and nanoscale. BSWs can be considered as the dielectric equivalent of Surface Plasmon for metals. Compared to SPPs, BSWs present some advantages, such as lower absorption, narrower mode resonances, stronger near-field surface enhancement effects, longer propagation length, spectral and polarization tunability. In this talk, I will show how light can be confined and propagated by means of BSW coupling, in a 2D optics fashion, wherein light is flowing on an almost flat surface with weak perturbations. In addition, I will discuss how the presence of the high photonic LDOS associated to BSW can change the emission behavior of organic dipoles located on the multilayer surface. The concept of a BSW planar cavity is introduced and the corresponding effects on the spectral and temporal signature of emitters located therein will be discussed. In addition, chiral diffractive gratings will be demonstrated to provide an outcoupling mechanism for BSW resulting in free-space propagating beams carrying specific orbital angular momenta. The presented results have potential applications in the domain of engineered sources for telecommunications and quantum technologies.

## Future Perspectives of Optical Fiber Sensors

**Orlando Frazão**

**Institute for Systems and Computer Engineering, Technology and Science, Portugal**

**Bio:** Orlando Frazão is a Senior Researcher at INESC TEC, Portugal. He obtained his PhD in Physics from the University of Porto in 1999. His research interest lies in the fields of optical fiber sensors and optical telecommunications. He has received three awards. Orlando Frazão has published more than 500 papers in peer-reviewed scientific journals and international conferences and is the author of 7 patents. He is also a Senior Member of SPIE and an EOS Fellow.

**Abstract:** Optical fiber sensors (OFS) still play a crucial role due to their unique advantages. They are immune to electromagnetic interference, making them ideal for applications in aerospace, power grids, and medical fields. Additionally, they enable long-distance remote sensing and are widely used in structural health monitoring for bridges and pipelines. Their high precision and sensitivity allow for the detection of small variations in temperature, pressure, and strain, while their resistance to extreme environments makes them essential in nuclear plants, deep-sea exploration, and space missions. They are also lightweight and miniaturized, favoring biomedical and aerospace applications. However, they face challenges such as high costs, complex integration, and competition from wireless and IoT sensors. Despite this, they continue to dominate areas like structural monitoring, oil and gas, biomedicine, defense, and aerospace. Therefore, optical fiber sensors remain relevant, especially where precision, durability, and remote sensing are indispensable, with their future depending on cost reduction and integration with smart sensor networks.

## Applications of Gallium Oxide-Based Photomemristors in Neuromorphic Engineering

**Marina Sparvoli**

**Universidade de São Paulo, Brazil**

**Bio:** Marina Sparvoli holds a Bachelor's degree in Physics Teaching (2011) and a Bachelor's degree in Physics (2005) from the University of São Paulo (USP), a Master's degree in Electrical Engineering (2007), and a Ph.D. in Electrical Engineering (2011), both from USP. She completed a postdoctoral project in Electrical Engineering at

the Polytechnic School (2012), working with infrared region sensors for aerosol detection. She was a faculty member in the Electrical Engineering, Information Systems, and Computer Science programs at UNIP (2013). She also taught in the Computer Science program at the Federal University of ABC (2015). She conducted postdoctoral research on resistive memories in the Computer Science department at the Federal University of ABC (2019). In 2021, she was a faculty member in the Instrumentation, Automation, and Robotics Engineering program at the Federal University of ABC. She completed a postdoctoral position at the Institute of Physics at USP, specializing in thin films. She is currently a professor in the Instrumentation, Automation, and Robotics Engineering program at the Federal University of ABC. Her research expertise is in Electrical Engineering, with an emphasis on Semiconductor Materials and Components, focusing primarily on the following topics: oxides and nitrides, photoelectric sensors, dip coating, memristors, and graphene.

**Abstract:** Gallium oxide ( $\text{Ga}_2\text{O}_3$ ) is an emerging wide bandgap semiconductor material that has garnered significant attention in the field of high-voltage and high-frequency power electronics. Five main crystalline phases of  $\text{Ga}_2\text{O}_3$  have been identified, including the corundum ( $\alpha$ ), monoclinic ( $\beta$ ), defect spinel ( $\gamma$ ), cubic ( $\delta$ ), and orthorhombic ( $\epsilon$ ) phases. Their thermodynamic stability follows the order of  $\gamma$ ,  $\delta$ ,  $\alpha$ ,  $\epsilon$ , and  $\beta$ . Notably, the monoclinic  $\beta$ - $\text{Ga}_2\text{O}_3$  phase is the most stable, particularly at high temperatures, while the other phases are metastable above room temperature and tend to transform into the  $\beta$  phase under specific thermal conditions. In this study, thin films were deposited using the RF sputtering technique at three different power levels: 200, 300, and 400 W. The films were deposited onto p-type silicon substrates over a process duration of 30 minutes. For analysis, Rutherford Backscattering (RBS) techniques, scanning electron microscopy (SEM), and X-ray diffraction (XRD) were employed, confirming the  $\beta$  phase. Through UV-Vis spectroscopy, the reflectance of the material was obtained, enabling the calculation of the bandgap. After depositing metallic contacts, the IxV curve was obtained to study the material non-linear behavior and light response. The three devices were subjected to electrical characterization in order to obtain key parameters such as SET and RESET voltages. It was observed that the photomemristors exhibited threshold switching behavior and photoelectric response. The devices were also evaluated in conjunction with an RC circuit, which emulates the dynamics of the neuronal membrane.

## Ultrafast structural dynamics in solids driven by femtosecond laser pulses: from nonthermal bond breaking to surface nanostructuring

Martin E. Garcia

University of Kassel, Germany

**Bio:** Martin Garcia is Professor of Theoretical Physics and Director of the Institute of Physics at the University of Kassel, Germany. He studied physics at the Instituto Balseiro in Bariloche, Argentina, and earned his PhD in Physics from the Freie Universität Berlin in 1992. Following postdoctoral appointments in the USA and Spain, he completed his Habilitation in Berlin. His research interests cover different areas of Solid-State Theory, Ultrafast Phenomena and Biophysics.

**Abstract:** When solids are exposed to ultrashort, intense laser pulses, they are driven into an extreme nonequilibrium state: the electronic system is heated within femtoseconds to temperatures of tens of thousands of Kelvin—far exceeding the surface temperature of the Sun—while the ionic lattice remains initially cold and undisturbed. In this short-lived, transient regime, the hot electrons dramatically alter the interatomic bonding landscape, exerting strong forces on the ions. These forces can trigger ultrafast structural phase transitions that are inaccessible under thermodynamic equilibrium conditions. Such «nonthermal» phenomena can be effectively described using approaches based on Density Functional Theory (DFT).

However, DFT simulations are inherently limited to small systems (typically fewer than  $\sim 1000$  atoms) and are not yet capable of fully capturing the energy exchange between electrons and ions.

Almost simultaneously with the bond modification, the sudden increase in electronic temperature enhances electron-phonon coupling, leading to stronger electron-ion collisions. These collisions initiate a flow of energy from the electronic system into the lattice, culminating in a thermalized state within a few picoseconds. At this point, both subsystems reach a common elevated temperature, giving rise to “thermal” structural responses such as melting, ablation, dislocation formation, and nanocrystallization. Both the energy exchange- and the “thermal” processes are well captured by two-temperature model molecular dynamics (TTM-MD) simulations, which, based on classical interatomic potentials, enable the study of systems containing hundreds of millions of atoms. However, such models cannot account for the initial laser-induced bond changes and associated nonthermal transformations.

In this talk, we will review the current theoretical frameworks for describing both “nonthermal” and “thermal” laser-induced phenomena and present recent efforts toward a unified description that bridges the gap between electronic excitation and large-scale material response. Particular emphasis will be placed on the role of machine learning–based interatomic potentials—especially neural network potentials—which, when properly trained on DFT data, provide a powerful route to scale quantum-accurate descriptions to previously inaccessible time and length scales.

## Physical principles of optical interferometry for surface topography measurement

**Peter de Groot**

**Zygo Corporation and SPIE, USA**

**Bio:** Peter de Groot, PhD, is fascinated by optics and its practical use for measuring things. Educated first in History then in experimental atomic Physics at the Universities of Grenoble, Maine, and Connecticut, he enjoys discovering the hidden links between academic and applied research that fuel inventions and creative solutions in science and industry. Dr. de Groot joined Zygo in 1992, and has been Executive Director of Research, Chief Scientist, and now Scientist Emeritus for the company. His work has led to 141 US patents for optical instruments and 225 technical papers and book chapters. He is a Fellow of Optica and the Institute of Physics, and is the 2025 President of SPIE, the international Society for Optics and Photonics. His research interests include optical instrument theory and design, dimensional metrology, interferometry, and quantum methods of sensing and computing. An experienced educator, Dr. de Groot has taught secondary school science in West Africa, advanced topics at universities in the USA and the UK, and professional development courses worldwide.

**Abstract:** The story of modern surface-measuring interferometry is a remarkable journey through the history of optics, beginning with the discovery of interference fringes and leading up to present-day methods. Today, laser interferometers and white-light interference microscopes are benchmark tools for high-precision measurements of form and roughness for everything from optical components with sub-nanometer tolerances to highly structured, additively manufactured parts. While basic concepts begin with a Michelson interferometer for perfectly flat and smooth mirrors, the topic becomes more complicated and interesting with real, three-dimensional (3D) surface structures. These surfaces diffract light over a range of angles, encoding topography information in a complex scattered light field. This light is then collected and imaged onto a camera, which inevitably filters the scattered light, leading to variations in response depending on spatial frequency. Furthermore, even for low spatial frequencies, data processing that converts measured light intensities to height

data can suffer from measurement nonlinearities and uncertainty, particularly with parts that have semi-transparent coatings or variations in material composition over the measured area.

In our research at Zygo, in collaboration with international partners, we are building a better understanding of the fundamental metrological characteristics of topography-measuring interferometers. A suite of modeling techniques tackles these issues, from conventional or “elementary” Fourier optics to full 3D transfer functions and methods for solving the inverse problem for complex surface structures. Key aspects of our work include the translation of complex physics concepts into new capabilities, as well as meaningful, easily understood specifications and guidance for optimizing instrument setup for specific measurement tasks. Tools include open-source software models as well as engagement with international standards organizations such as ISO, for consistency and confidence in the use of interferometers for areal surface topography measurement.

## Some contributions to improving atmospheric observations through solar spectral analysis

**Erna Frins**

**Universidad de la República de Uruguay, Uruguay**

**Bio:** Erna Frins is Professor of Physics at the Physics Institute of the Engineering School, Universidad de la República, Uruguay. Dipl.-Phys. (1992) from the TU-Berlin and a PhD in physics (1998) from the Wolfgang Goethe-University, Germany. Frins is a laureate of the National UNESCO – L’OREAL Award for Women in Science in 2012. Between 2007 and 2011, she was president of the Uruguayan Physical Society and is now chair of the National Scientific Committee for Antarctic Research in Uruguay. Since 2023, she has been a member of the physics science jury for the Falling Walls Prize. She leads a research group in pure and applied optics. Her research is focused on developing optical methods for atmospheric remote sensing. She joined the Aerosol Robotic Network – AERONET, NASA, Project in 2019.

**Abstract:** The Earth’s atmosphere is a physical system strongly affected by human activity at local, regional, and global scales. One example of this is the rise in global temperature, which, among other things, increases the incidence of wildfires. These fires burn a large volume of biomass, altering the chemical composition of the atmosphere and increasing the amount of particulate matter, specifically fine aerosols.

Solar radiation, in addition to inducing chemical reactions during the day, is an excellent tool for studying the atmosphere, quantifying gaseous emissions from industrial plants, and observing local changes due to biomass burning, even if it occurs kilometres away.

Here we present different approaches to improving the detection and quantification of trace gases resulting from the combustion of fossil fuel (e.g., Nitrogen oxides, Sulphur oxides, and Carbonyls), and the quantification of gas fluxes using differential optical absorption spectroscopy (DOAS). We also present some results on atmospheric aerosols that originated from biomass burning, resulting from ground-based aerosol monitoring in Montevideo through AERONET (Aerosol Robotic Network, NASA).

## Uncovering Science: Communicating Research to Everyone

**Mike McKee**

**University of Central Florida, USA**

**Bio:** Mike McKee is currently the associate director for the Bachelor of Science in Photonic Science (BSPSE) and Engineering at CREOL, The College of Optics and Photonics a position he has held since 2013 and is a joint program between the College of Engineering and Computer Science and the College of Optics and Photonics.

For nearly twenty years prior to this, he was a high school physics teacher, science instructional coach, and conducted workshops for teachers and students alike. He also was the co-director for the Science Olympiad National Tournament, hosted at the University of Central Florida in 2012 and in 2014. This event required massive coordination of all the activities for the science activities that included hosting about 7000 people, opening and closing ceremonies, and other program details. From 1999 to 2018, he was the state director for the Florida Science Olympiad, coordinating activities at seven regional competitions, a state competition at UCF, and the involvement of 200 schools across the state of Florida.

**Abstract:** The last time you told someone outside your field your topic of research, did you get a strange look, a nodding glance, or a pause before a new topic was discussed? Communicating difficult scientific topics in a way that a person can understand is important to engage more in the practice of science and attract more students into the field. Rather than “dumbing down” your explanation, speaking simply can help those who are not just young, but also in other fields who may be experts in their own right, but lack the deep understanding of your research.

This talk will present some fun “take-away” techniques you can use immediately, to help you explain your research or scientific concepts and avoid those awkward stares.

## Triangulation at the Standard Quantum Limit

**John Howell**

**Chapman University, USA**

**Bio:** Professor Howell started his career at the University of Rochester and eventually led the Center for Coherence and Quantum Optics as both a professor of physics and optics. He moved to Jerusalem in 2017 where he joined the Racah Institute as a professor of physics. In 2022, he joined the faculty at Chapman University in Southern California as a part of the Institute for Quantum Studies. His work embraces many fields of classical and quantum optics. He has received several awards and is a fellow at Optica. He is currently serving as the Past President of the ICO.

**Abstract:** The laws and principles of triangulation have been known for millennia with known uses by the Egyptians and Greeks. From star tracking, to surveying, to navigation, to robotics, its applications are pervasive in our modern society. However, for the most part, its limitations have been primarily technical. In this presentation, I will describe our theoretical and now experimentally the fundamental limits of triangulation with the intent of vastly enhancing its precision. We derived the Cramer Rao bound for a Poisson point source measured in the back focal plane of a lens. We then measured the depth of the source with nanometer-scale precision at 1.4 meters away using two balanced detectors. This is four to five orders of magnitude better than other passive depth estimation systems. I will discuss the methods allowing us to achieve these results and some applications.

# Posters

**Note:** All the contributions submitted by students in oral presentation format will also participate in the poster contest. A poster presentation room will be available for this purpose.

## Deformation of metallic parts measurement applied shearing interferometry and mechanical sensors

Ernesto Javier Ruiz-Ortega, Francisco Javier Casillas-Rodríguez, Francisco Gerardo Peña-Lecona, Jesús Muñoz-Maciel, Sergio Álvarez-Rodríguez, Miguel Mora-Gozalez

**Topic(s):** Instrumentation, measurement and metrology, Optics and photonics in the industry [ID 088]

**Institution(s):** Universidad de Guadalajara, México

Mechanical deformations are changing that materials experience when they receive impulses or external forces. Usually, to measure these deformations various mechanical sensor techniques are commonly used, such as strain gauges, piezoelectric sensors, load cells, and extensometers, among others, these types of sensors are used as transducers, which transform mechanical energy into an electrical signal [1]. In addition, optical methods such as interferometry can be used; these methods allow the changes measurement of the object under test between its initial state (when it is not being subjected to mechanical stresses) vs. its deformed state when an external force is applied [2].

In this work, different types of metals currently used in the automotive industry for the manufacture of gears, pistons, supports, and structure of automobiles will be evaluated. In which the metal part will be subjected to a tension or compression stress to measure the deformations suffered by the same material. The measurements will be carried out by optical interferometry in conjunction with strain gauges, in shearing and Wheatstone bridge configuration, respectively (as shown in Figure 1).

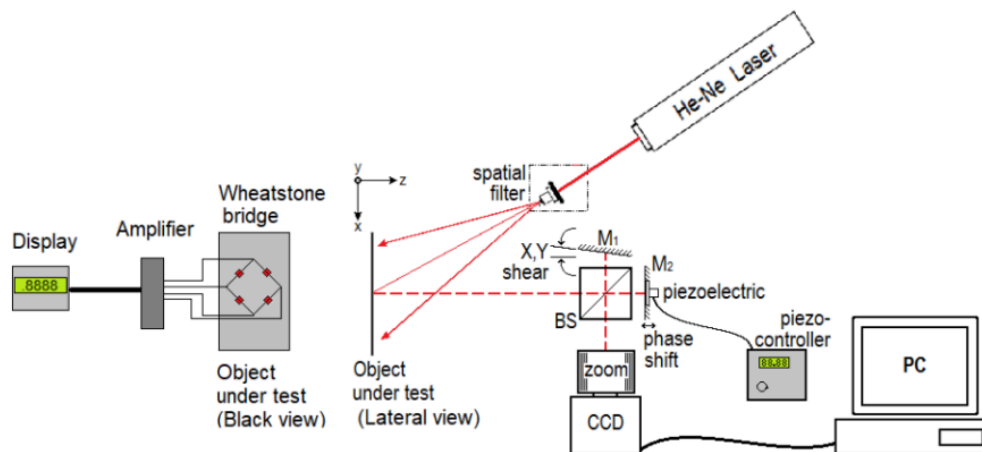


Figure 1: Electrical and optical diagrams.

A mechanical press was used to deform the object under test, a rectangular metal piece (aluminum, steel or stainless steel). The press can deliver deformations of up to 2 tons in compression or in tension configurations, respectively; the experiment has been carried out up to 0.5 tons. The gauge array can measure deformations in the piece from 1 kg up to the limit of the experiment; however, the interferometer begins to detect deformations after 10 kg, but the interferogram phase shows a 3D deformation view and it reaches up to 632nm resolution. Given these results, it can be concluded that both methods work properly for the study of our materials or our objects under test and it is possible to interpret the deformation with any of these methods.

### References

- [1] R. Pallás Areny. *Sensores y acondicionadores de señal*, 4a ed., Marcombo, 2003.
- [2] P. Hariharan. *Optical Interferometry*, 2nd ed. Elsevier Science, 2003.

**Corresponding author:** Miguel Mora. **Email:** miguel.mora@academicos.udg.mx

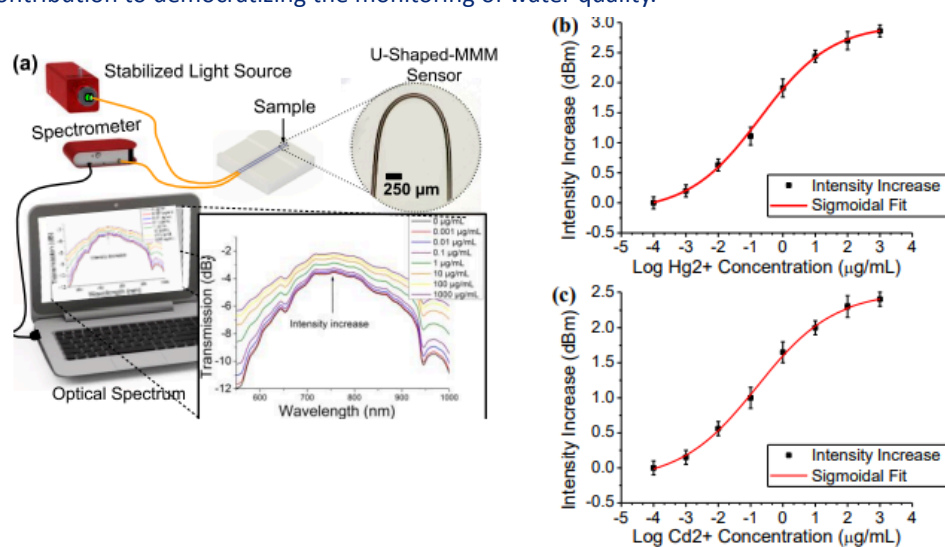
# U-Bent MMM Optical Fiber Sensor for the Detection of Mercury and Cadmium Ions in Aqueous Solutions

Arturo Gaviria-Calderón, Brayan Patiño-Jurado, and Jorge Garcia-Sucerquia

**Topic(s):** Fiber optics, sensors and optical communications [ID 042]

**Institution(s):** Universidad Nacional de Colombia, Colombia

Heavy metal contamination in water, particularly by mercury ( $\text{Hg}^{2+}$ ) and cadmium ( $\text{Cd}^{2+}$ ) ions, means significant environmental and health risks due to their toxicity and tendency to bioaccumulate [1]. Conventional detection methods are often expensive, complex, and time-consuming [2], reducing the opportunities for its democratization. In this work, the development of U-Bent multimode-multimode-multimode (U-MMM) optical fiber sensors for the sensitive and selective detection of  $\text{Hg}^{2+}$  and  $\text{Cd}^{2+}$  ions in aqueous solutions is presented. The simplicity and effectiveness of this proposal constitutes our contribution to democratizing the monitoring of water quality.



**Figure 1: (a) Experimental setup. (b) and (c) Detection results of the U-Bent MMM sensor.**

Multimode interference and enhanced light-medium interaction within a bent multimode fiber segment, are the phenomena that rule the operation of the U-MMM sensor. Figure 1 shows the sensor setup in panel (a) and its performance in panels (b) and (c). For mercury detection, the UMMM sensor surface was functionalized with a chitosan/ $\text{Fe}_2\text{O}_3$  nanocomposite film. Adsorption of  $\text{Hg}^{2+}$  ions into this coating induces changes in the local refractive index, producing measurable increase in the transmitted optical spectrum with detection capabilities down to  $0.001 \mu\text{g/mL}$  (1 ppb) with a sensitivity of  $0.053 \text{ dBm}/\mu\text{g/mL}$ , as shown in panel (b). For cadmium detection, the U-MMM fiber sensor was coated with a green-synthesized gold nanoparticle (AuNP) film stabilized by chitosan and polyvinyl alcohol (PVA). The AuNP-functionalized surface selectively binds  $\text{Cd}^{2+}$  ions, that produce measurable variations in optical transmission to  $\text{Cd}^{2+}$  concentrations up to  $0.001 \mu\text{g/mL}$  (1 ppb) with a sensitivity of  $0.041 \text{ dBm}/\mu\text{g/mL}$ , as presented in panel (c).

## References

- [1] K. G. Pavithra, P. SundarRajan, P. S. Kumar, and G. Rangasamy, "Mercury sources, contaminations, mercury cycle, detection and treatment techniques: A review," *Chemosphere*, vol. 312, p. 137314, Jan. 2023.
- [2] A. Gaviria-Calderón, J. Garcia-Sucerquia, B. Patiño-Jurado, and J. F. Botero-Cadavid, "Competitive fiber optic sensors for the highly selective detection of mercury in water," *Appl. Opt.* Vol. 62, Issue 3, pp. 592-600, vol. 62, no. 3, pp. 592–600, Jan. 2023.

**Corresponding author:** Arturo Gaviria. **Email:** argaviriaca@unal.edu.co

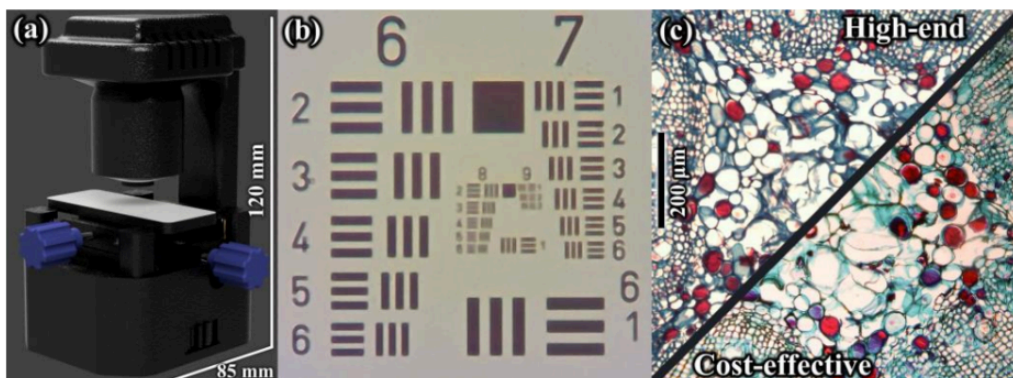
## Cost-effective 3D printed bright-field microscope

Diego A. Londono, Carlos A. Buitrago-Duque, and J. Garcia-Sucerquia

**Topic(s):** Imaging systems, Microscopy [ID 061]

**Institution(s):** Universidad Nacional de Colombia, Colombia

The development of accessible optical tools is essential to support practical science and engineering education. In recent years, various open-source and low-cost microscope initiatives have emerged to address this need [1]. This work contributes to that effort by presenting a digitally integrated, cost-effective bright-field optical microscope. The system is built with off-the-shelf materials: a SonyIMX335 CMOS sensor (available for \$30 USD), frequently used in CCTV systems, and a pair of interchangeable webcam lenses. While previous works have demonstrated the use of similar lens systems for portable microscopy [2], up to the best knowledge of the authors this is the first implementation combining such a lens set with a fully 3D-printed mechanical platform, as illustrated in panel (a) of Fig. 1. The optical setup employs an inverted short focal length (2 or 5 mm) lens operating as the objective; this lens projects the image to infinity when the sample is positioned at its working distance. A second lens with a larger focal length (25 mm), used as the tube lens, then focuses the image onto the sensor. The mechanical platform was fabricated using fused deposition modeling 3D printing and assembled with M3x0.5 screws and 3 mm steel rods, providing up to 20 mm of low-backlash, controlled motion along the X and Y axes and up to 13 mm along the Z axis. The illumination is provided by a diffuse white LED powered via a USB Type-C port, which also serves as the interface for connecting the camera to a computer or mobile device. Panel (b) shows the image of a USAF 1951 resolution target obtained with the proposed microscope prototype; the smallest resolved object is group 8, element 1, corresponding to a feature size of approximately 2 microns, allowing clear observation of typical biological specimens. In panel (c) a direct comparison of the optical performance of the cost-effective microscope and a high-end optical microscope equipped with a Nikon Plan 10x/0.25 objective is presented. While the commercial microscope provided superior image quality with minimal distortions, the cost-effective proposal delivered comparable visible detail, demonstrating its viability as an effective alternative to image complex biological samples as, for instance, a dicotyledonous plant. The total cost of the proposed bright-field microscope is around \$45, inviting its open fabrication and adaptation; its modular design allows users to customize or upgrade the components to meet specific educational or experimental needs, including easily swapping objective lenses for varying magnification.



**Figure 1: Cost-effective 3D printed bright field microscope. (a) Picture of the built microscope. (b) Image of the USAF 1951 test target. (c) Comparison of the imaging performance between a high-end commercial microscope and the cost-effective proposal.**

### References

- [1] J. S. Cybulski, J. Clements, and M. Prakash, PLOS ONE 9, e98781 (2014).
- [2] C. Yu, S. Li, C. Wei, S. Dai, X. Liang, J. Li, Micromachines 13, 869 (2022).

**Corresponding author:** Diego Londono-Zapata. **Email:** dilondonoz@unal.edu.co

# Latent Fingerprint Imaging via Modulated-Intensity Maps from Fringe-Pattern Deflectometry

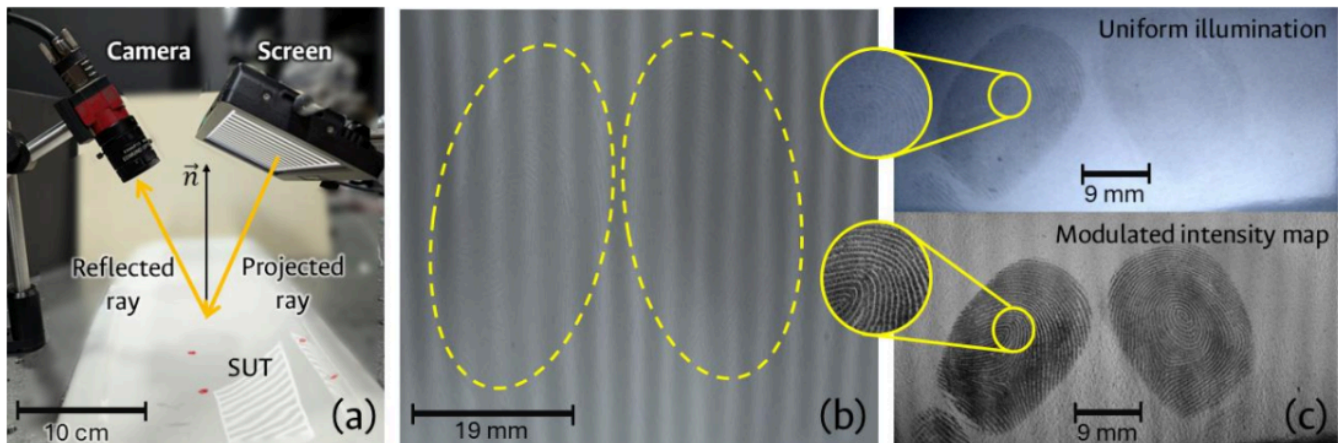
Julian Perez-Carvajal, Carlos A. Buitrago-Duque, and J. Garcia-Sucerquia

**Topic(s):** Image processing, vision and artificial intelligence, Instrumentation, measurement and metrology, Optics and photonics in the industry [ID 066]

**Institution(s):** Universidad Nacional de Colombia, Colombia

Unlike conventional methods for revealing latent fingerprints, which are based on physical or chemical labeling of the surface [1], this work presents a contactless and non-destructive approach for latent fingerprint imaging using fringe pattern deflectometry [2]. The setup of the method is shown in Fig. 1(a). It requires only a regular screen to display a sinusoidal fringe pattern, whose fully- or partially-reflection on a surface under test (SUT) is recorded by a digital camera. The recording codifies height variations of the steady SUT in the form of intensity modulations, as shown in Fig. 1(b). To retrieve the surface information, four controlled phase shifts of  $\pi/2$  steps are introduced into the sinusoidal pattern, such that the recorded intensity can be modeled as  $I_n(x, y) = I_0 + I_m(x, y) * \cos [\varphi(x, y) + n\pi/2]$ .  $n \in [0,3]$  equation (1).

$I_0$ ,  $I_m(x, y)$ , and  $\varphi(x, y)$  correspond to the background intensity, the modulated intensity, and the pattern-phase variations induced by the SUT, respectively [3]. In each recording,  $I_m(x, y)$  codifies the subtle local reflectivity variations of the SUT in the form of changes in the reflected fringe intensity; for case of study in this contribution, those changes can be caused by the presence of oily residues on the surface, such as those left by fingerprint marks [1]. Using a conventional phase-shifting formalism, the modulated intensity can be extracted from the recorded set as  $I_m(x, y) = 1/2\sqrt{(I_3 - I_1)^2 + (I_2 - I_0)^2}$  equation (2). As illustrated in Fig.1(c), the  $I_m$  map, in the lower right corner, provides a significantly enhanced contrast of the fingerprint marks when compared to a direct capture under uniform illumination, as shown in the upper right corner of Fig. 1(c). This method opens new possibilities for contactless forensic analysis and the evaluation of macroscopic alterations in surface reflectivity. Furthermore, the setup simplicity, requiring only a screen for pattern projection and a camera for recording, opens a way for accessible instrumentation innovations and field-ready systems.



**Figure 1: (a) Experimental deflectometry setup. (b) Fringe pattern recording with distorted intensity by the SUT. (c) Latent fingerprints obtained using uniform illumination (top) and the modulated intensity map (bottom).**

## References

- [1] Dhanotia, J., Chatterjee, A., Bhatia, V., & Prakash, S. (2018). A simple low cost latent fingerprint sensor based on deflectometry and WFT analysis. *Optics and Laser Technology*, 99, 214–219
- [2] Burke J, Pak A, Höfer S, Ziebarth M, Roschani M and Beyerer J (2023), Deflectometry for specular surfaces: an overview. [3] Huang, L., Idir, M., Zuo, C., & Asundi, A. (2018). Review of phase measuring deflectometry. *Optics and Lasers in Engineering*, 107, 247–257.

**Corresponding author:** Diego Londono-Zapata. **Email:** dilondonoz@unal.edu.co

## Solar Concentrator

Abraham Lopez Pacheco, María Jose Cervantes Oropeza, Bruno Méndez Sánchez, Omar Cuamani

**Topic(s):** Geometrical optics [ID 073]

**Institution(s):** Benemerita Universidad Autonoma de Puebla, México

A solar concentrator with a Fresnel lens is a system designed to maximize solar energy capture by concentrating light onto a focal point. This innovative device uses a Fresnel lens, characterized by its thin, flat shape composed of concentric rings that allow solar radiation to be focused with high efficiency. Its main goal is to make the most of solar energy, reducing the costs of electric or thermal generation.

A fundamental aspect of this type of system is the design of an automatic lighting mechanism, which adjusts the concentrator's orientation based on solar intensity. For this, light sensors and solar tracking systems are integrated to ensure precise positioning toward the sun throughout the day. This not only enhances energy performance but also optimizes the use of available resources.

In the optical design, the lens is arranged appropriately to minimize light losses and concentrate the greatest amount of energy on the receiver. Simultaneously, the mechanical design focuses on providing a solid and resistant structure capable of withstanding various environmental conditions and facilitating both maintenance and system operation.

A significant advantage of this type of solar concentrator is its ability to capture diffuse sunlight, making it viable in areas with cloudy or variable climates, where other systems are less effective. This feature broadens its applicability and makes it a versatile option for different regions.

Currently, a functional prototype of the solar concentrator with Fresnel lens has already been developed, with the optical, mechanical, and tracking components completed. The only remaining component to be integrated is the photovoltaic system, which will enable efficient conversion of the concentrated solar energy into electricity.

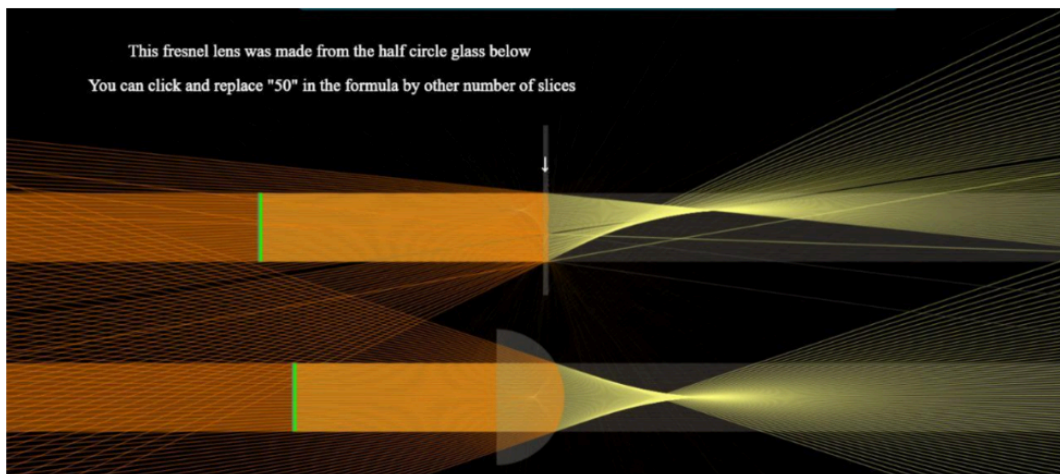


Figure 1: Solar concentrator with a Fresnel lens.

### References

- [1] (s.f.). Fresnel termosolar. <https://laenergiasolar.org/energia-termica-solar/fresnel-termosolar/>
- [2] My Magnifier. (s.f.). Lente Fresnel lineal concentradora solar. <https://www.mymagnifier.com/es/product/Linear-Fresnel-Lens-Solar-+Concentrator.html>
- [3] ScienceDirect. (s.f.). Fresnel concentrator lens. In ScienceDirect Topics. Elsevier. <https://www.sciencedirect.com/topics/engineering/fresnel-concentrator-lens>

**Corresponding author:** Maria Cervantes. **Email:** maria.cervanteso@alumno.buap.mx

# Thin-Film Deposition and Optical Testing of a First-Surface Mirror for Astronomical Applications

Ana Paula Quelopana, Gonzalo Gálvez de la Puente

**Topic(s):** Thin films [ID 091]

**Institution(s):** Pontificia Universidad Católica del Perú, Perú

The fabrication of a first-surface astronomical mirror was completed, encompassing design, manufacturing, and evaluation stages. The design phase utilized optical modeling software to determine the optimal thicknesses and refractive indices for both the aluminum and magnesium fluoride thin-film coatings. These parameters were calculated to maximize reflectivity at the desired wavelengths for astronomical observations. Prior to coating deposition, the glass substrate underwent a thorough cleaning process. This involved initial cleaning with distilled water and isopropyl alcohol, followed by an argon plasma treatment step. The plasma cleaning parameters were controlled in certain values set of voltage, current, pressure and time to eliminate any contaminants that could compromise the quality of the subsequent coatings. The aluminum layer was deposited using physical vapor deposition (PVD) under high vacuum conditions (10<sup>-6</sup> mbar), ensuring a uniform and adherent coating. This was followed by the deposition of the protective magnesium fluoride layer using similar PVD techniques [1][2]. Quality control measures were implemented throughout the manufacturing process. Specifically, the adhesion of the aluminum film to the glass substrate was assessed using the ASTM D3359 standard tape test [3], confirming a robust bond. Post-fabrication, the mirror's performance was thoroughly evaluated.

A spectrophotometer was used to measure the reflectivity across the relevant spectral range. These experimental results were then compared to simulated reflection spectra obtained using the Transfer Matrix Method, validating the accuracy of the design parameters [4][5]. Furthermore, the Ronchi test was employed to characterize the surface figure, assessing the presence and magnitude of optical aberrations [6]. The final mirror, photo 1, demonstrated excellent optical properties, meeting all specifications for its intended astronomical application.



**Figure 1: Aluminum and Magnesium fluoride coated first-surface mirror.**

## References

- [1] G. Gálvez de la Puente et al., Proceedings of SPIE, PP 740–743, 4419 (2001). “Physical effects of evaporated materials in thin films and emission patterns”.
- [2] G. Gálvez de la Puente et al., Proceedings of SPIE, pp. 560–563 107 5622 (2004) “Titanium dioxide thin films: refractive index variation as a function of the deposition rate”.
- [3] <https://store.astm.org/d3359-17.html>
- [4] H. A. Macleod, (1989) McGraw Hill, New York. “Thin Films Optical Filters”.
- [5] H. K. Pulker, (1984) Elsevier, Amsterdam. “Coatings on glass”.
- [6] DOI 10.7149/OPA.51.1.49028.

**Corresponding author:** Gonzalo Gálvez de la Puente. **Email:** ggalvez@pucp.edu.pe

# Differentiation of air pollution sources in Montevideo using NO<sub>2</sub>, CO trace gas columns, and atmospheric aerosol properties

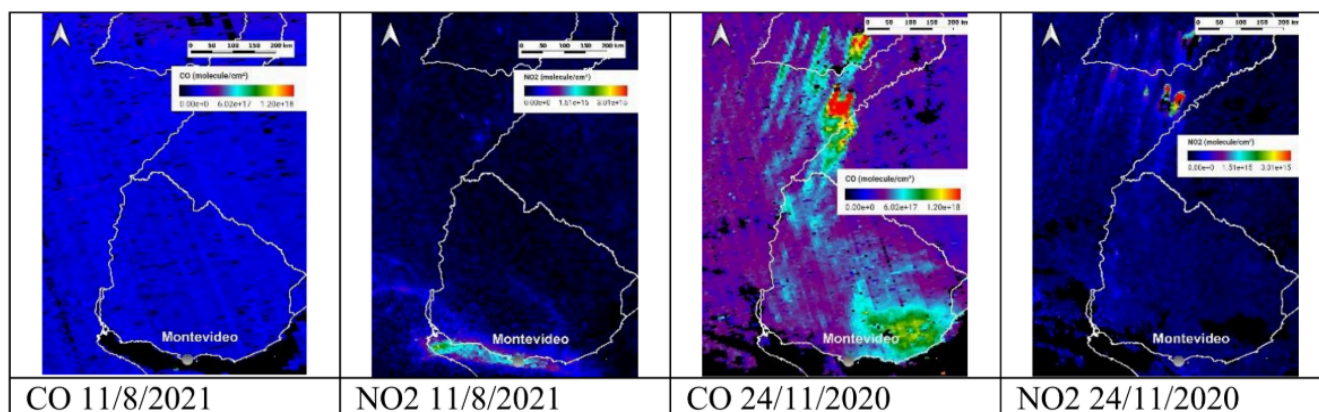
Alejandro Agesta, Erna Frins

**Topic(s):** Atmospheric and ocean optics, Remote sensing and sensors, Spectroscopy [ID 051]

**Institution(s):** Universidad de la República, Uruguay

The differentiation of atmospheric pollution sources is essential for environmental management and air quality studies. In this study we aim to differentiate urban emissions into the atmosphere from emission originating from large-scale biomass burning. This paper analyzes the results of combining satellite data of NO<sub>2</sub> and CO columns (TROPOMI) with aerosol properties from the AERONET station [2, 3] in Montevideo (Montevideo\_FING) to characterize and distinguish between these two types of sources. The analysis is based on the premise that forest fires emit large quantities of NO<sub>2</sub> and CO, with the typical atmospheric half-life of NO<sub>2</sub> being a few hours, while that of CO is several days [1].

Aerosols resulting from biomass burning possess properties that distinguish them from urban aerosols. In comparison, they are smaller in size, exhibit greater absorption of solar radiation, and have higher Angstrom exponent values [4]. On August 11, 2021, satellite images in Montevideo show an episode of high NO<sub>2</sub> column values (likely originating from Buenos Aires) as seen in Fig. 1, an aerosol fine mode fraction (FMF) of 0.79, and an Angstrom exponent of 1.55 according to the AERONET station. However, these increases are not accompanied by high CO column values. In contrast, on November 24, 2020, a CO transport event due to biomass burning (with NO<sub>2</sub> confined near the sources, an event previously studied by Osorio et al. [5]), registered an FMF of 0.94 and an Angstrom exponent of 2.1. These results show the potential of this approach, taking into account various parameters including local instruments and satellites, to identify and separate the contributions of different atmospheric pollution sources in the region.



**Figure 1:** Comparison of NO<sub>2</sub> and CO columns obtained from TROPOMI on 11/8/2021 with those from 24/11/2020. Panels a) and b) show urban pollution, and panels b) and c) show biomass burning.

## References

- [1] Wan, N. et al., (2023). ACP, 23(1), 711–724. <https://doi.org/10.5194/acp-23-711-2023>
- [2] O'Neill, et al., (2001). JGR, 106(D9), 9787–9806. <https://doi.org/10.1029/2000JD900245>
- [3] Dubovik, O. et al., JGR, 105(D16), 20673–20696. <https://doi.org/10.1029/2000JD900282>
- [4] Mattoo, S. et al., [https://doi.org/10.5067/MODIS/MOD04\\_L2.061](https://doi.org/10.5067/MODIS/MOD04_L2.061)
- [5] Osorio, M. et al., <https://doi.org/10.5194/acp-24-7447-2024>

**Corresponding author:** Alejandro Agesta. **Email:** aagesta@fing.edu.uy

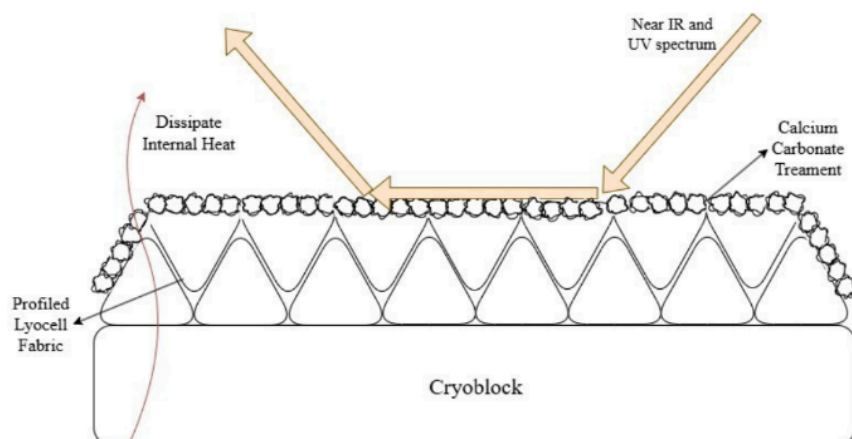
# Application of photonic principles for medical samples transportation: Radiative cooling fabrics in warm tropical weather

Alicia Zelada-Acosta, Alejandra Oviedo-Cortés, Ariana Y. Miranda-Jimenez, Erwin D. Moreno-Añez

**Topic(s):** Bio photonics and biomedical applications [ID 094]

**Institution(s):** Universidad Privada Boliviana, Bolivia

Rural areas with high temperatures and a lack of reliable electricity complicate cold-chain storage for the transportation of medical samples. To address this, we introduce a fabric bag with cooling properties to maintain samples at cold temperatures without electricity. This prototype is based on the principle of radiative cooling, which allows materials to reject solar radiation while emitting thermal energy in the mid-infrared spectrum. Our design consists of a portable cooling bag that combines cryoblock racks with an outer case fabric treated with poly(2-hydroxyethyl acrylate) and ions of calcium carbonate and barium sulfate [1]. This creates a surface that reflects sunlight and dissipates heat as shown in Figure 1, mimicking the effect of photonic films but with more accessible and affordable materials. To evaluate the efficiency of our design, we propose a series of comparative experiments consisting of temperature measurements of physiological serum exposed to sunlight while wrapped in our fabric. This work represents a first step towards the development of affordable, off-grid cooling solutions for biomedical applications in remote rural areas where conventional refrigeration is not feasible.



**Figure 1: Schematic diagram.**

## References

[1] Patamia, E. D., Yee, M. K., & Andrew, T. L. (2024). Microstructured Reflective Coatings on Commodity Textiles for Passive Personal Cooling. *ACS Applied Materials & Interfaces*, 16(43), 59424-59433. <https://doi.org/10.1021/acsami.4c15984>

**Corresponding author:** Alicia Zelada-Acosta. **Email:** antoniozelada1@upb.edu

## Manufacture of aspherical mirrors for the implementation of a classic Cassegrain astronomical telescope

P. Gallardo, A. Romero, A. Escudero, F. Gonzales

**Topic(s):** Optical design and fabrication [ID 044]

**Institution(s):** Pontificia Universidad Católica del Perú, Perú

This work presents the processes of design, manufacturing, and optical testing of aspheric mirrors (paraboloids and hyperboloids) for the implementation of a classical Cassegrain astronomical telescope [1]. The work begins with the simulation of the optical system using Ansys Zemax OpticStudio (student version), where the behavior of the system components (mirrors) is evaluated. This is followed by the manufacturing process of the mirrors according to the design specifications. Subsequently, the final shapes of the reflective optical surfaces (mirrors) are assessed, and a metallic thin film is applied.

Finally, the proposed system is assembled, and its performance is evaluated [2,3]. The material used to fabricating the mirrors is Pyrex glass.

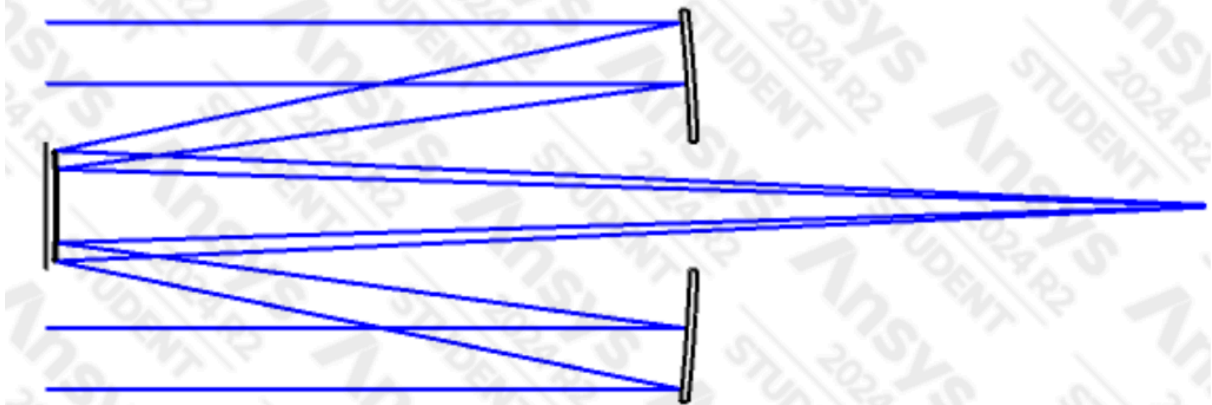


Figure 1: Simulation of the telescope Cassegrain.

### References

- [1] Rutten H., Van Venrooij M. (1988) Telescope Optics. Willmann\_Bell, Inc.
- [2] Baldwin, G., Ochoa, J., & Gonzales, F. Kinematic characterization of a polishing machine for the design of petal tools and its application in the parabolization of reflective optical surfaces. *Óptica Pura y Aplicada* (2022).
- [3] Gonzales, F., Baldwin, G. E., Romero, S., Tupia, W., & Gálvez, G. Design and manufacture of a small Newtonian telescope for lunar observation. *Óptica Pura y Aplicada*, 51. (2018).

---

**Corresponding author:** Pablo Gallardo. **Email:** a20206447@pucp.edu.pe

## Spatial polarization modulation using two LCDs in tandem

Federico Guglielmucci Nazar, Facundo Rouquaud, Sebastián Bordakevich, Silvia Ledesma

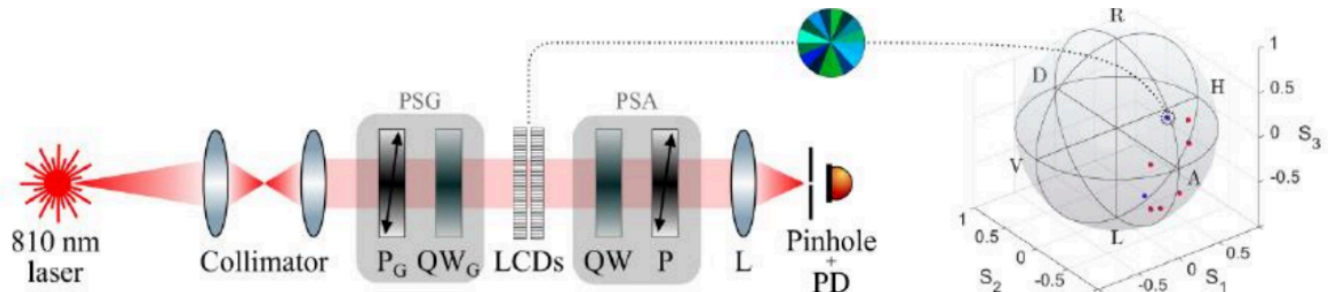
**Topic(s):** Fourier optics and signal processing, Imaging systems [ID 101]

**Institution(s):** Universidad de Buenos Aires; (CONICET), Argentina

Liquid crystal displays (LCDs), widely used in optical applications, are essential as spatial light modulators as they allow precise manipulation of beam properties, including amplitude, phase, and polarization [1]. In previous works, the advantage of using two twisted nematic LCDs in series has been demonstrated [2], optimizing the configuration to achieve complete modulation of amplitude and phase, or optimal polarization modulation covering a surface on the Poincaré sphere [3].

The experimental setup proposed for this work uses the optimized configuration from [3] to spatially modulate polarization. As shown in the Figure, it comprises a polarization state generator (PSG), two TN LCDs, and a polarization state analyzer (PSA). The LCDs, extracted from a commercial videoprojector, are controlled via its green (G) and blue (B) channels and act as a single compound modulator. The output's Stokes parameters were obtained via projective measurements, and spatial averaging was achieved by detecting the intensity at the center of the Fourier plane.

The LCDs were divided into  $N$  regions (from 4 to 256), each assigned a different polarization from one of eight zones of the surface of accessible states. Simulations using a density matrix formalism predicted the expected average state for each zone. Experiments matched simulations for low  $N$ , but fidelity dropped below 0.9999 beyond a critical threshold of  $N = 64$ , indicating practical limitations due to resolution, alignment, and inhomogeneities. These results demonstrate the effectiveness of using two TN LCDs in tandem for spatial modulation, while also revealing a practical constraint on their application. Moreover, the approach enables precise and programmable polarization control with commercially available components.



**Figure 1: Experimental setup and polarization modulation results.**

A collimated 810 nm laser illuminates a PSG (polarizer + quarter-wave plate), two TN LCDs in tandem, and a PSA (quarter-wave plate + polarizer). The beam is spatially filtered with a pinhole in the center of the Fourier plane to measure its average intensity with a photodiode (PD). Top: polarization image for  $N = 16$ , jointly modulated by channels G and B of the video projector. Right: average Stokes vectors on the Poincaré sphere (experimental: red; simulation: blue).

### References

- [1] Y. Q. Yang, A. Forbes, and L. C. Cao. *Opto-Electron Sci* 2, 230026 (2023). "A review of liquid crystal spatial light modulators: devices and applications".
- [2] A. Márquez et al, *Opt. Express* 16, 1669-1685 (2008). "Mueller-Stokes characterization and optimization of a liquid crystal on silicon display showing depolarization".
- [3] S. Bordakevich, L. Rebón, and S. Ledesma, *Appl. Opt.* 61, 969-977 (2022). "Optimization for maximum modulation of a double-pass twisted nematic liquid crystal display".

**Corresponding author:** Silvia Ledesma. **Email:** author: ledesma@df.uba.ar

## Evaluating gait recognition performance on privacy preserving images

Loana Velasquez-Omonte, Guillermo Sahonero-Alvarez, Edgar Salazar, Laura Galvis

**Topic(s):** Image processing, vision and artificial intelligence, Machine vision, Optics in computing, Other topic [ID 104]

**Institution(s):** Universidad Catolica Boliviana; Universidad Privada Boliviana, Bolivia; Pontificia Universidad Católica de Chile, Chile; Universidad Industrial de Santander, Colombia

The growing concern for privacy in computer vision systems has driven the development of privacy preserving techniques at the optical level, preventing the capture of sensitive visual information during image acquisition. Recent advances in privacy-preserving optics have demonstrated the potential of hardware-level protection by directly degrading sensitive visual information at the point of image acquisition. In this work, we explore the impact of using the privacy-preserving optical encoder proposed by [1], which was originally designed for privacy-preserving human pose estimation, as part of a conventional gait recognition framework. Inspired by the Gait Energy Image (GEI) representation, we computed an average image for the degraded images or Degraded Gait Signature (DGS). Before computing the DGS, all images were binarized by background subtraction, with respect to a reference frame available in the videos, and thresholding. Then, the DGS for each subject and sequence were classified by a deep learning model. For our experiments, we used the OAK-Gait8 dataset that contains 8 subjects, 6 sequences, and 3 variations from 5 camera angles. In total, we used 504 videos for training, 144 for validation and 72 for testing, representing 70%, 20% and 10% of the dataset respectively. The total number of videos used was 720. We only used RGB videos. Our results, based on simulations and comparative analyses show that, although the lens significantly diffuses the image and does not preserve a human-like gait shape, the system is still able to classify individuals with approximately 71% accuracy. This indicates that the optical degradation produces a representation more similar to a spectral or abstract pattern than a recognizable human form, yet it still contains sufficient information for biometric classification. These findings provide insight into the trade-off between privacy protection and biometric recognition when using PSF-based privacy-preserving optics.

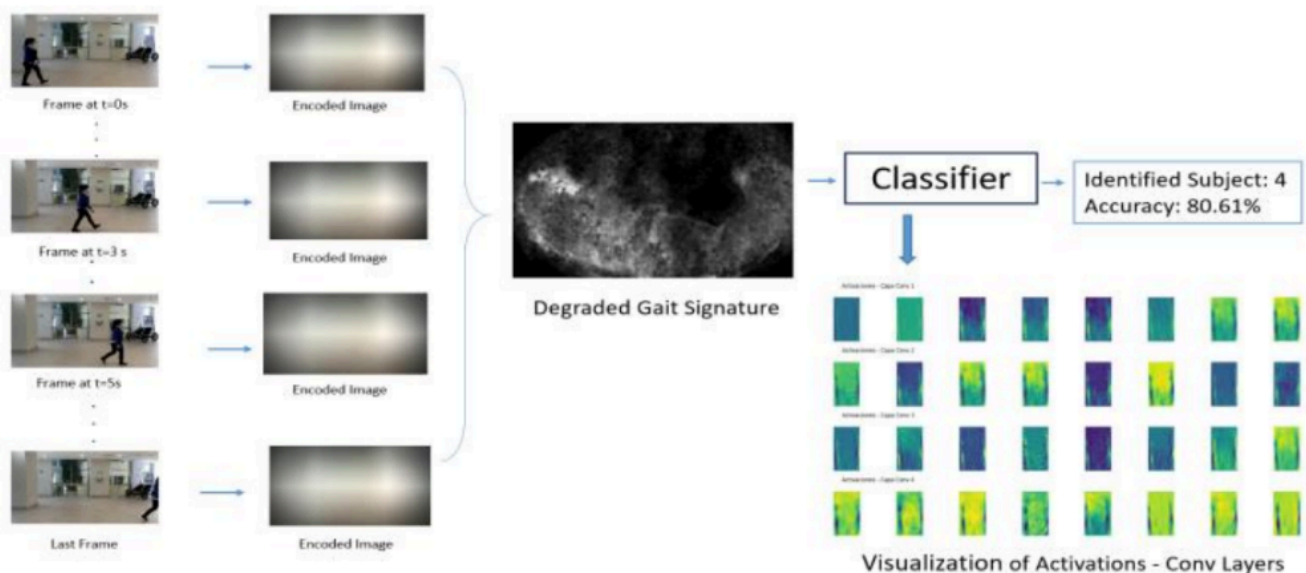


Figure 1: Degraded Gait Signature generation and classification from a video sequence.

### References

[1] C. Hinojosa, J. C. Niebles, and H. Arguello, "Learning Privacy-Preserving Optics for Human Pose Estimation," in Proceedings of the IEEE/CVF International Conference on Computer Vision (ICCV), 2021, pp. 2573–2582. [Online]. Available: <https://carloshinojosa.me/project/privacy-hpe>

**Corresponding author:** Edgar Salazar. **Email:** edgarsalazar@upb.edu

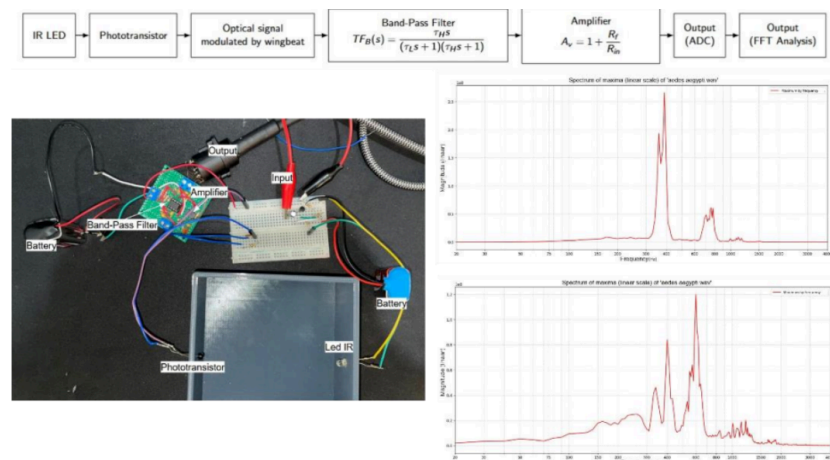
# An Infrared-based Aedes-aegypti Identification Trap

Amina Antonio, Miguel Angel Quiroz, Edgar Salazar

**Topic(s):** Optoelectronics, detectors and sources [ID 087]

**Institution(s):** Universidad Privada Boliviana, Bolivia

Dengue is one of the most common seasonal diseases in tropical areas. With more than 3 million confirmed cases world-wide, and 1400 deaths in 2025, this disease is a constant threat especially for vulnerable people (infants and elders) [1]. The transmission of Dengue is done by the aedes aegypti, thus, several efforts have been made to eradicate this insect. Such attempts include fumigation and preventive campaigns, genetic modification for female sterilization, or classical mosquito traps [2]. Some contemporary researchers, on the other hand, have worked extensively in the characterization of insects through quantifying the frequency of the wingbeat using spectral analysis and optical methods for data acquisition [3]. In this paper, we propose an Infrared-red based wingbeat acquisition method by using an IR Light Emitting Diode (LED) with its respective receptor. By interrupting the emitter-receptor light path, a pattern that is proportional to the insect movement is captured, and after proper analog filtration (band-pass filter from 150Hz to 600Hz) and amplification, its spectral content is calculated using conventional FFT methods. To test our model, we reproduced an aedes aegypti sound [4] and, through a common-emitter amplifier, modulated the IR-emitter signal. Even though some similar ideas and prototypes have been formulated, our method is the first of its kind in the context of Bolivia. This is the first step towards and comprehensive discrimination process that will eventually lead to a trap that only reacts to Aedes-aegypti with proper electromechanical actuators.



**Figure 1: Schematic and results of the experiment. Top: Block diagram of the system. Bottom-left: Implemented hardware. Bottom-right: Acquired spectral signatures of the aedes aegypti wingbeat.**

A collimated 810 nm laser illuminates a PSG (polarizer + quarter-wave plate), two TN LCDs in tandem, and a PSA (quarter-wave plate + polarizer). The beam is spatially filtered with a pinhole in the center of the Fourier plane to measure its average intensity with a photodiode (PD). Top: polarization image for  $N = 16$ , jointly modulated by channels G and B of the video projector. Right: average Stokes vectors on the Poincaré sphere (experimental: red; simulation: blue).

## References

- [1] Dengue Worldwide Overview, European Centre for Disease Prevention and Control, <https://www.ecdc.europa.eu/en/dengue-monthly>
- [2] S. T. Ogunlade, M. T. Meehan, A. I Adekunle, & E. S. McBryde. A systematic review of mathematical models of dengue transmission and vector control: 2010–2020. *Viruses*, 15(1), 254, 2023.
- [3] E. Joelianto, et. al. Convolutional neural network-based real-time mosquito genus identification using wingbeat frequency: A binary and multiclass classification approach. *Ecological Informatics*, 80, 102495, 2024.
- [4] H. Mukundarajan, F. J. H Hol, E. A. Castillo, C. Newby, & Prakash, M. (2017). Using mobile phones as acoustic sensors for high-throughput mosquito surveillance. *elife*, 6, e27854, 2017.

**Corresponding author:** Miguel Quiroz. **Email:** mickyquiroz9@gmail.com

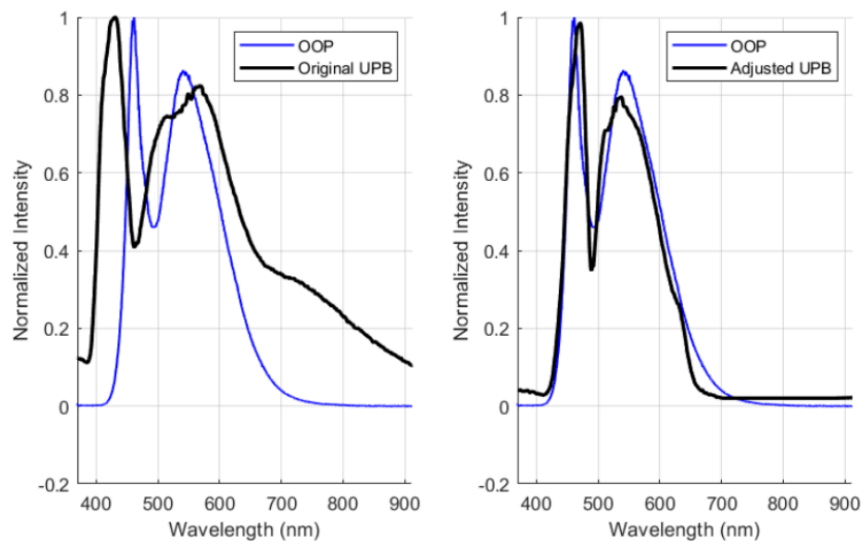
## A Data-based Protocol for a Low-cost Mobile Spectrometer Calibration

Marco De la Fuente Villarroel, Facundo Aliaga, Edgar Salazar

**Topic(s):** Spectroscopy [ID 086]

**Institution(s):** Universidad Privada Boliviana, Bolivia

Spectrometry is a well-established technique that has been extensively used for different purposes, including for example, biomedical, life-sciences and water testing [1]. Nevertheless, dedicated hardware for conducting spectral analysis is expensive, and its price increases with the spectral resolution. Recently, several attempts have been made to design spectrometers with off-the-self components, with similar performance as the one shown by commercial solution, being the one proposed by Ormachea et al. [2] (UPB) highlighted over the others due to its reduced cost and adaptability to mobile phone cameras, as well as its reproducibility. In this study, we propose and develop a comprehensive protocol that allows for the calibration of the UPB spectrometer taking as reference the OCEAN OPTICS USB 4000 (OOP). For that, we simultaneously took spectral signatures with UPB and OOP from a conventional White Light Emitting Diode (LED) under low-light conditions, with previous calibration. Afterwards, we pre-processed the data by point-wise matching the wavelengths with posterior interpolation and intensity normalization. We then implemented a Dynamic Warping (DW) algorithm that finds the minimum distant of the two signatures and, through indexation and interpolation using 14 control points, the UPB curve is adjusted to the OOP. Results of the calibration protocol can be seen in Fig. 1.



**Figure 1: Left: OOP and original UPB White LED spectrum. OOP and adjusted UPB White LED spectrum.**

### References

- [1] A. Das. Portable UV–Visible Spectroscopy–Instrumentation, Technology, and Applications. Portable Spectroscopy and Spectrometry, 179-207, (2021).  
 [2] A. Villazon, O. Ormachea, A. Zenteno, & A. Orellan. A low-cost spectrometry remote laboratory. In International Conference on Remote Engineering and Virtual Instrumentation (pp. 198-209). Cham: Springer International Publishing (2022).

**Corresponding author:** Edgar Salazar. **Email:** edgarsalazar@upb.edu

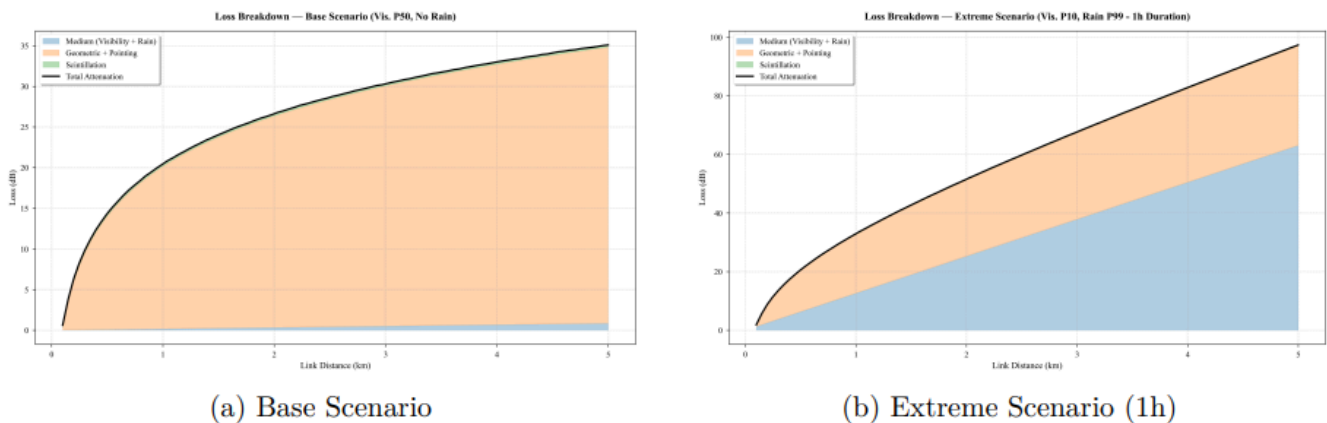
# Analysis of Atmospheric Factors in Free-Space Optical (FSO) Communications for High-Altitude Urban Environments in La Paz, Bolivia

Carlos Gironda, Rene Sosa

**Topic(s):** Fiber optics, sensors and optical communications, Laser and laser optics [ID 072]

**Institution(s):** Universidad Privada Boliviana, Bolivia

Free Space Optical (FSO) communications are a promising technology, whose performance is severely affected by atmospheric conditions. This study provides a comprehensive analysis of FSO link performance in the Bolivian Altiplano, a high-altitude region with distinctive climatic features. Unlike sea-level links where atmospheric turbulence is a critical limiting factor, the conducted analysis reveals that at elevations of approximately 3700 m a.s.l., such as in the municipality of Achocalla (Bolivia), turbulence becomes negligible, contributing only 0.3 dB of attenuation. Through Monte Carlo simulations that incorporate local meteorological data and models for rain and fog attenuation, the dominant factors are identified as geometric and pointing losses (a fixed component of 34 dB at 5 km) and, crucially, attenuation due to precipitation during the wet season. A key finding is the high sensitivity of the link to the duration of rain events, with attenuations ranging between 20.1 dB and 63.1 dB for the same daily rainfall percentile (P99), depending on whether a duration of 6 or 1 hour is assumed, respectively. These results provide essential design criteria for FSO systems in high-mountain regions, indicating that efforts should focus on optimizing the optical design and allocating adequate power margins for rain, while complex turbulence mitigation schemes can be disregarded.



**Figure 1: Breakdown of attenuation components for representative operating conditions.**

## References

- [1] S. A. Al-Gailani, M. F. M. Salleh, A. A. Salem, R. Q. Shaddad, U. U. Sheikh, N. A. Alcelan, and T. A. Almohamad, "A Survey of Free Space Optics (FSO) Communication Systems, Links, and Networks," *IEEE Access*, vol. 9, pp. 7353–7373, 2021.
- [2] S. M. Yasir, N. Abas, S. Raut, N. R. Chaudhry, and M. S. Saleem, "Investigation of optimum FSO communication link using different modulation techniques under fog conditions," *Heliyon*, vol. 8, no. 12, p. e12516, 2022.
- [3] M. A. Khalighi and M. Uysal, "Survey on free space optical communication: A communication theory perspective," *IEEE Communications Surveys & Tutorials*, vol. 16, no. 4, pp. 2231–2258, 2014.

**Corresponding author:** Esteban Gironda. **Email:** estebangironda1@upb.edu

---

## Effects of Atmospheric Conditions on Infrared Data Transmission: Experimental Analysis in La Paz, Bolivia

Mariana Vasquez, Rene Sosa

**Topic(s):** Atmospheric and ocean optics, Instrumentation, measurement and metrology, Optics and photonics in the industry [ID 076]

**Institution(s):** Universidad Privada Boliviana, Bolivia

This article aims to verify whether atmospheric conditions in La Paz, such as solar radiation and low atmospheric density significantly degrade the efficiency of voice transmission via infrared (IR) in low-cost systems, in order to evaluate the feasibility of implementing this technology in high-altitude urban environments. Some atmospheric factors at high altitude can increase optical noise in basic receivers, reducing the signal-to-noise ratio (SNR) in unshielded systems. Furthermore, the presence of aerosols and high climatic variability in the Andean region could exacerbate the attenuation of IR signals, particularly in devices with economical components and limited filtering capacity. However, some argue that IR transmitters are less practical than other technologies such as RF or Li-Fi, due to their susceptibility to physical obstacles and limited range in uncontrolled conditions. Nevertheless, IR technology remains relevant in emerging applications, such as IoT security systems and data transmission in electromagnetically restricted environments, where privacy and immunity to interference are critical. In conclusion, this research will not only provide key data to optimize IR systems in Bolivia, considering local atmospheric conditions, but will also assess their competitiveness against other technologies, highlighting scenarios where their implementation would be technically and economically viable.

### References

- [1] Amaya Araujo, C. A., & Celeita Martinez, J. A. (2023). Caracterizacion de un sistema radio sobre comunicaci3n 3ptica inal3mbrica para entornos interiores.
- [2] de Electricidad, V., & Alternativas, E. (2021). Estudio complementario de impacto de la radiaci3n UV en paneles solares (datos UV de un a3o) y otros componentes expuestos en condiciones del altiplano boliviano Gestion 2021.
- [3] Gim3nez de Castro, C. G. (2023). Observando la cromosfera solar en el infrarrojo. Bolet3n de la Asociaci3n Argentina de Astronom3a, 64.

---

**Corresponding author:** Mariana Vasquez. **Email:** [marianamontserrathvasquez@gmail.com](mailto:marianamontserrathvasquez@gmail.com)

# Detection of microstructural patterns in optical coherence tomography images using artificial intelligence tools to differentiate melanoma from melanocytic nevus

Florencia Pinto, Rene Sosa

**Topic(s):** Image processing, vision and artificial intelligence [ID 070]

**Institution(s):** Universidad Privada Boliviana, Bolivia

Optical coherence tomography (OCT) has been established as a non-invasive imaging technique with high spatial resolution, which permits a detailed visualization of tissue microstructure. In melanoma diagnosis, the accurate differentiation between malignant and healthy tissue is crucial for early detection and improved clinical results.

This project proposes the development of a detection model based on convolutional neural networks (CNN's) to identify microstructural patterns in OCT images. To achieve this, publicly available databases will be used, with a focus on cross-validation and robustness against interpatient variability. Additionally, complementary techniques such as transfer learning and data augmentation will be explored to enhance system performance, especially in the context of limited datasets.

The main objective is to achieve high sensitivity and specificity in classification, minimizing false positives and negatives, and ultimately providing a reliable clinical decision-support tool for the early diagnosis of melanoma.

## References

- [1] Ayadh, M., et al. (2025). AI-assisted identification of non-melanoma skin cancer structures based on combined high-resolution morphological imaging and chemical characterisation of skin tissues. *Journal of Biomedical Optics*, 30(7), 076008. <https://doi.org/10.1117/1.JBO.30.7.076008>
- [2] Kulyabin, M., et al. (2024). OCTDL: Optical coherence tomography dataset for image-based deep learning methods. *Scientific Data*, 11, Article 3182. <https://doi.org/10.1038/s41597-024-03182-7>
- [3] Lai, P.-Y., Shih, T.-Y., Chang, Y.-H., Chang, C.-H., & Kuo, W.-C. (2025). Deep learning with optical coherence tomography for melanoma identification and risk prediction. *Journal of Biophotonics*, 18(1), e202400277. <https://doi.org/10.1002/jbio.202400277>
- [4] Naranjo, F. P., et al. (2025). A clinical study of two optical coherence tomography scanners: How resolution and depth affect skin cancer diagnostic accuracy classified by deep neural networks and foundation models. *Optica Open Preprints*. <https://preprints.opticaopen.org/articles/preprint/29492909>
- [5] Rotunno, G., Salvi, M., Deinsberger, J., Krainz, L., Weber, B., Sinz, C., & Liu, M. (2025). DERMA-OCTA: A comprehensive dataset and preprocessing pipeline for dermatological OCTA vessel segmentation. *Scientific Data*, 12, 1473. <https://doi.org/10.1038/s41597-025-05763-6>

---

**Corresponding author:** Florencia Pinto. **Email:** [tabatapinto1@upb.edu](mailto:tabatapinto1@upb.edu)

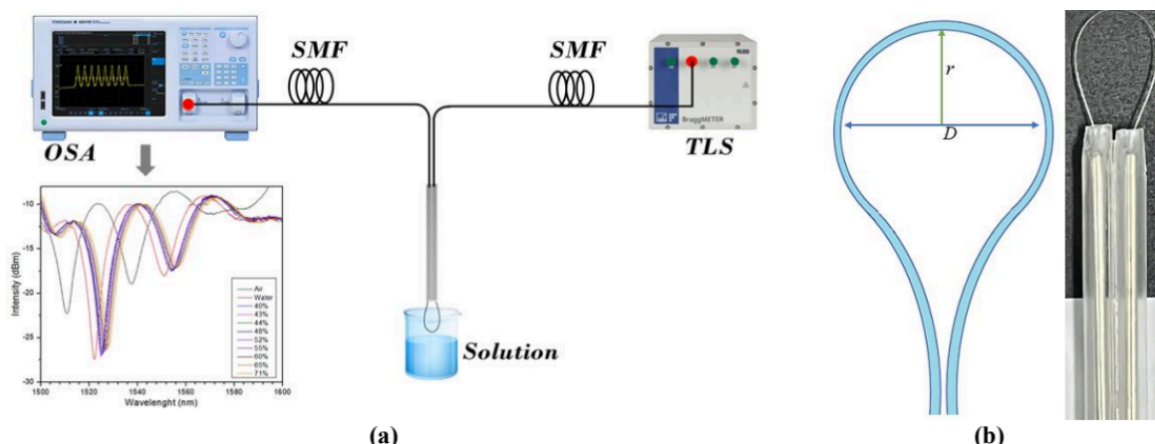
## Optical sensors based on optical fibers in Mach-Zehnder type interferometry configuration for measuring ethanol concentration

L. Espejo-Bayona, Sindi Horta, Duber Avila

**Topic(s):** Fiber optics, sensors and optical communications, Remote sensing and sensors [ID 020]

**Institution(s):** Universidad Popular del Cesar, Colombia

This study presents the development and characterization of an optical device based on a single-mode optical fiber for measuring the concentration of ethanol in an analyte. The proposed configuration consists of a curved, balloon-shaped uncoated optical fiber, whose operating principle is based on Mach-Zehnder type interferometry. This geometric arrangement takes advantage of the high sensitivity of fiber optic interferometers, allowing changes in ethanol concentration to be detected by shifting the peaks of minimum intensity in the interference patterns of the optical signal. The device fabrication involved bending a section of bare single-mode optical fiber into a balloon shape, the ends of which were secured using a standard protective sleeve to ensure mechanical stability. Figure 1a illustrates both the conceptual design and the implemented physical configuration. For the experimental characterization, a setup was used that included a tunable laser source (TLS) in the 1500–1600 nm range and an optical spectrum analyzer (OSA, Yokogawa model AQ6370E), allowing the measurement of the signal transmitted through the device. The results demonstrate that the balloon-shaped configuration improves the interaction between the guided mode and the analyte, thus increasing the sensitivity compared to conventional geometries [1]. This approach offers advantages such as manufacturing simplicity, low cost, and high sensitivity, making it promising for applications in fluid monitoring and quality control in the food and pharmaceutical industries.



**Figure 1: (a) Experimental setup developed in the experiment, (b) Schematic diagram and final device developed.**

In this study, the device's parameters were evaluated, demonstrating its ability to measure ethanol concentrations ranging from 40% to 71%. Analysis of the interference patterns revealed peaks of minimum intensity, associated with destructive interference characteristic of asymmetric Mach-Zehnder interferometers. These peaks exhibited a shift toward longer wavelengths with increasing ethanol concentration, confirming their dependence. The sensor's sensitivity was quantified at 0.109%/nm, highlighting its high reproducibility and repeatability in measurements. Although its sensitivity is comparable to that of traditional devices [1], this configuration offers significant advantages in terms of manufacturing simplicity, low cost, and ease of implementation. These results suggest that the sensor has high potential for applications in the food and pharmaceutical industries.

### References

[1] V. Cardoso, P. Caldas, M. Giraldo, O. Frazão, J. Costa, J.L. Santos, *Sensors* 22, 7652 (2022). "Optical Strain Gauge Prototype Based on a High Sensitivity Balloon-like Interferometer and Additive Manufacturing".

**Corresponding author:** Luis Espejo. **Email:** lespejo@unicesar.edu.co

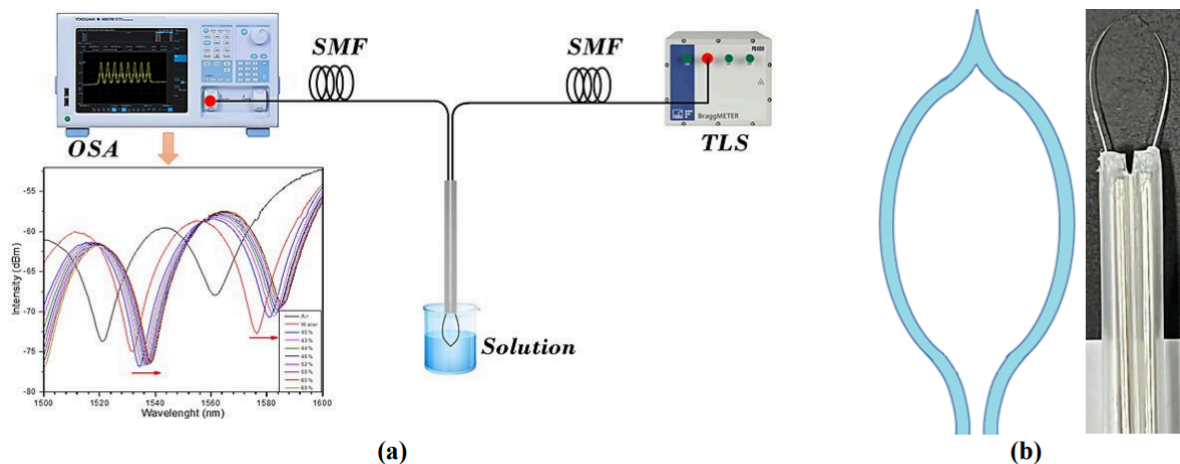
# Optical sensors based on balloon-shaped optical fibers with tip-induced deformation in a Mach-Zehnder interferometer configuration for measuring ethanol concentration

L. Espejo-Bayona, Sindi Horta, Duber Avila

**Topic(s):** Fiber optics, sensors and optical communications, Remote sensing and sensors [ID 045]

**Institution(s):** Universidad Popular del Cesar, Colombia

This study presents the development and characterization of an optical device based on a single-mode optical fiber for measuring ethanol concentration in an analyte. The proposed configuration consists of an uncoated optical fiber curved in the shape of a balloon with a deformation in the sensing zone with a controlled electric arc. This geometric arrangement takes advantage of the high sensitivity of fiber optic interferometers, allowing changes in ethanol concentration to be detected by shifting the minimum intensity peaks in the interference patterns of the optical signal. The device manufacturing involved bending a section of bare single-mode optical fiber into a balloon shape, to which an electric arc was applied over the sensing area of the fiber, to ensure mechanical stability the ends of the fiber were fixed using a standard protective sleeve. Figure 1 illustrates both the experimental design and the physical configuration implemented. For the experimental characterization, a setup was used that included a tunable laser source in the range of 1500–1600 nm and an optical spectrum analyzer, allowing the measurement of the signal transmitted through the device. The results demonstrate that the balloon-shaped configuration with an electric arc improves the interaction between the guided mode and the analyte, thus increasing the sensitivity compared to conventional geometries [1].



**Figure 1: (a) Experimental setup developed in the experiment, (b) Schematic diagram and final device developed..**

In this study, the parameters of the proposed device were evaluated, demonstrating its ability to measure ethanol concentrations ranging from 40% to 65%. Analysis of the interference patterns revealed peaks of minimum intensity, associated with destructive interference characteristic of asymmetric Mach-Zehnder interferometers. These peaks exhibited a shift toward longer wavelengths with increasing alcohol concentration, confirming their dependence. The sensor's sensitivity was measured at 0.183%/nm, highlighting its high reproducibility and repeatability in measurements. Although its sensitivity is comparable to that of traditional devices, this configuration offers significant advantages in terms of manufacturing simplicity, low cost, and ease of implementation.

## References

[1] L. Jing, H. Yu, Z. Tong, W. Zhang, Y. Tao and J. Mu, Applied Physics B 130, 151 (2024). "Temperature-insensitive optical fiber sensor based on SMF-NCF-FMF-NCF-SMF spindle shaped structure for refractive index measurement".

**Corresponding author:** Luis Espejo. **Email:** lespejo@unicesar.edu.co

## Enhancement of atomic emission intensity of heavy metals in LIBS using silver nanoparticles to increase the detection sensitivity of Cu and Pb

Elder Espinoza-Sanchez, Jhenry F. Agreda-Delgado, M. A. Valverde-Alva, W. Aldama-Reyna

**Topic(s):** Spectroscopy [ID 078]

**Institution(s):** Universidad Nacional de Trujillo, Perú

The application of the NELIBS technique (nanoparticles-enhanced LIBS) was studied to improve the atomic emission intensity of heavy metals (Cu and Pb) [1]. The samples used were copper (99.9% purity) and lead (99% purity) cubes, both with dimensions of 1 cm × 1 cm × 1 cm. On each sample, 10 μL of a silver nanoparticles (AgNPs) colloid in deionized water, previously synthesized by laser ablation in liquids [2], was deposited using a micropipette. The solvent was evaporated, and to increase the nanoparticles concentration, the process was repeated by adding an additional 10 μL onto the same pretreated surface. The LIBS spectra were obtained by irradiating the samples with a pulsed Nd:YAG laser (1064 nm), operating at  $(10.94 \pm 0.38)$  mJ/pulse for Cu + AgNPs and  $(7.16 \pm 0.42)$  mJ/pulse for Pb + AgNPs. The laser radiation was directed using a high-reflectance mirror and focused onto the sample with a 10 cm focal length lens; the sample was positioned at 7 cm, achieving an irradiation spot size of 1.5 mm. The complete experimental setup is shown in Fig. 1. The analysis of the atomic emission spectra revealed that, in the presence of AgNPs, the intensity of the characteristic Cu emission lines increased threefold compared to the samples without nanoparticles, while the Pb lines showed an approximate 70% enhancement. This signal amplification can be attributed to the coupling of surface plasmon generated by the nanoparticles [3]. These results highlight the potential of the NELIBS technique to improve sensitivity and detection limits in the spectroscopic analysis of heavy metals using LIBS.

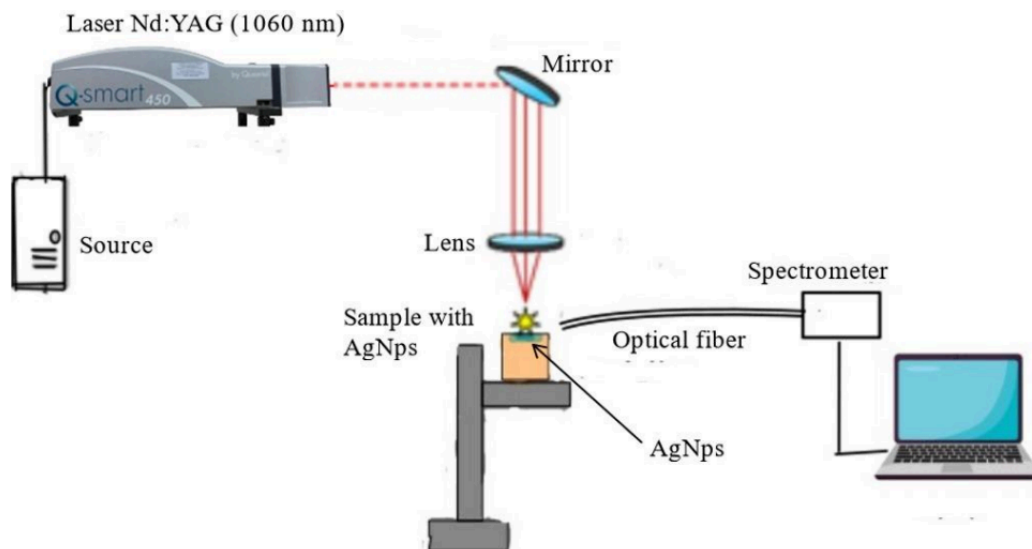


Figure 1: Schematic diagram..

### References

- [1] D. A. Cremers and L. J. Radziemski, Handbook of Laser-Induced Breakdown Spectroscopy, 2nd ed., Wiley, 2013. volume number to make it bold".
- [2] Aldama-Reyna, W., et al. "Photoacoustic study of changes in optical properties of colloids with silver nanoparticles produced by laser ablation." Int. J. Appl. Eng. Res 13 2018: 1408-1414.
- [3] J. Liu et al., "Enhancement mechanisms in nanoparticle-enhanced laser-induced breakdown spectroscopy," Spectrochimica Acta Part B, vol. 87, pp. 43–53, 2013.

**Corresponding author:** Elder Espinoza. **Email:** t1521200121@unitru.edu.pe

## Optical design of double lens for the refractor telescope CST-80 KU by G-sum Method

Jenifer Garcia, Franco Gonzales and Ivan Choque

**Topic(s):** Geometrical optics, Optics in computing, Optical design and fabrication [ID 034]

**Institution(s):** Universidad Nacional Jorge Basadre Grohmann; Pontificia Universidad Católica del Perú, Perú

Students of our university are interested in Astronomical Observation, but our telescope, CST-80 KU, was discontinued over 30 years ago, consequently it is impossible to buy a replacement lens, for that reason it is important for us to design an appropriate lens for improving the observation. The present work shows a design of an achromatic doublet lens by the G-sum method. This technique allows us to find parameters for proper correction for spherical, coma and chromatic aberration [1-2]. The design process was first carried out by computer simulation using Ansys Zemax OpticStudio Student. Lens parameters such as: radii curvatures, diameters, thickness, sagittas and refraction indexes are included in the simulation. Glasses N-BK7 and N-SF5 are used in this study, they were chosen by their suitable combination of optical properties, such as dispersion and transmission, which make them compatible and efficient for optical system design [3]. Simulation results allow us to visualize the proposed three-dimensional design, to analyze the mentioned aberrations by spot diagrams, and to optimize the optical system [4]. In the future, the proposed design will facilitate the lens manufacture with a high degree of precision.

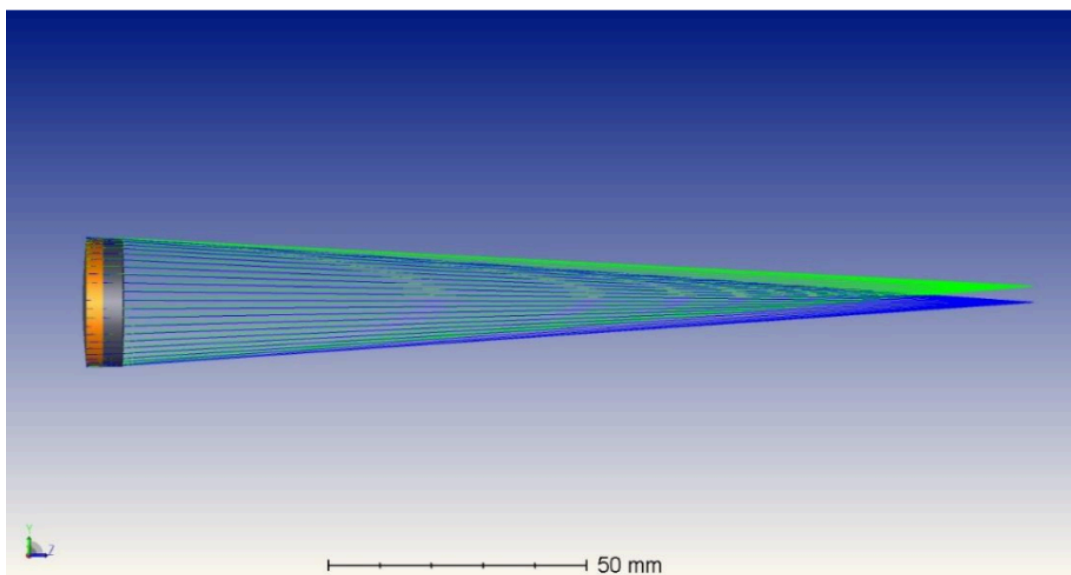


Figure 1: TComputer simulation of a doublet lens by using Zemax OpticStudio.

### References

- [1] Gee AE. The design of telescope objectives by the G-sum method. *Amateur Telescope Making*.1953;III:208.
- [2] Smith JA. Third-order aberration theory and calculation. In: *Modern Optical Engineering*. 4th ed. New York: McGraw-Hill; 2010. p. 105–122.
- [3] Yu SM, Jung MS. Selection of optical glasses using a chromatic-aberration correction method for the whole visible range plus a telecentric lens design applying the method. *Korean J Opt Photonics*. 2015;26(4):217–25.
- [4] Zemax R. Manual del usuario del programa de diseño óptico. Zemax LLC; 2012.

**Corresponding author:** Jenifer Garcia. **Email:** jegarcia@unjbg.edu.pe

## Three-dimensional measurement of human face topography using fringe projection profilometry

Riquelme P-Cruz, Ivan Choque, Edith Paredes

**Topic(s):** Instrumentation, measurement and metrology, Optics in computing, Optics at surfaces [ID 032]

**Institution(s):** Universidad Nacional Jorge Basadre Grohmann, Perú

Every year, thousands of people experience deformities in their facial structure as a result of surgical interventions or pathological processes, since the purpose of these procedures is to treat the disease [1]. In this work, the three-dimensional topography of the human face is measured using fringe projection profilometry (FPP). The profilometer comprises a multimedia projector and a monochrome CMOS camera. Human face samples were taken from five volunteers aged between 20 and 40 years. Fringe patterns with sinusoidal profiles were projected onto samples under study, and the phase shift between two consecutive fringe patterns was  $\pi/3$  [2]. Images were recorded and processed in Matlab software. Images were demodulated using a six-step phase-shift algorithm (PSA). Preliminary results display three-dimensional human face topographies with high resolution; this confirms the feasibility of the employed technique. Finally, our results can be useful as recorded morphology for future developments in the design and manufacture of facial prostheses [3].

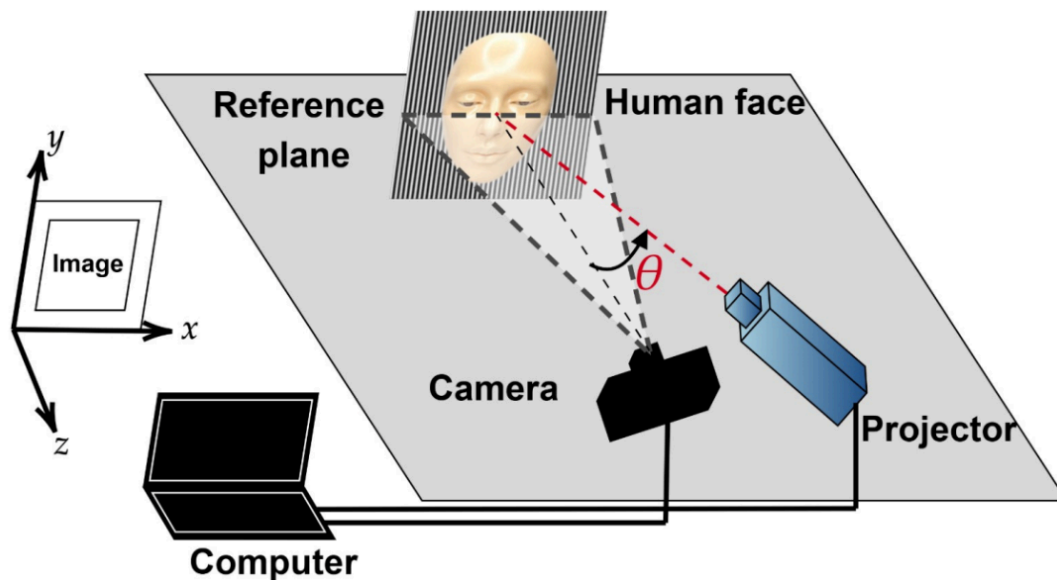


Figure 1: Experimental setup of a Fringe Projection Profilometer (FPP).

### References

- [1] Xue J, Zhang Q, Li C, Lang W, Wang M, Hu Y. 3D face profilometry based on a galvanometer scanner with infrared fringe projection at high speed. *Appl Sci.* 2019;9(7):1458.
- [2] M. Servin, J. A. Quiroga, J. M. Padilla, et al., *Fringe pattern analysis for optical metrology*, Wiley Online Library (2023).
- [3] Bockey S, Berssenbrügge P, Dirksen D, Wermker K, Klein M, Runte C. Computer-aided design of facial prostheses by means of 3D-data acquisition

**Corresponding author:** Riquelme P-Cruz. **Email:** riquelmepc@unjbg.edu.pe

## Contouring of residual limb by white light profile for medical prosthetics

Joaquin S. Rivera, Daniel Aquino S., Rodrigo C. Salcedo, Ivan Choque Aquino

**Topic(s):** Bio photonics and biomedical applications, Instrumentation, measurement and metrology, Optics in computing [ID 048]

**Institution(s):** Universidad Nacional Jorge Basadre Grohmann, Perú

Surface topology is essential in the fabrication of medical prosthetics [1], a properly designed surface can minimize friction and enhance compatibility with the patient's tissue, preventing irritation or discomfort. To address this, we present an experimental method for digitizing a 3D residual limb as a sample using white line projection [2,3]. A profilometer utilizing white line profiles was employed to scan the sample. The sample examined belongs to a volunteer. Initial findings reveal a 3D model of the sample, which was subsequently used for 3D printing the measured structure. Carefully controlled surface characteristics will contribute to improving material strength, reducing early wear, and extending the prosthesis's durability.

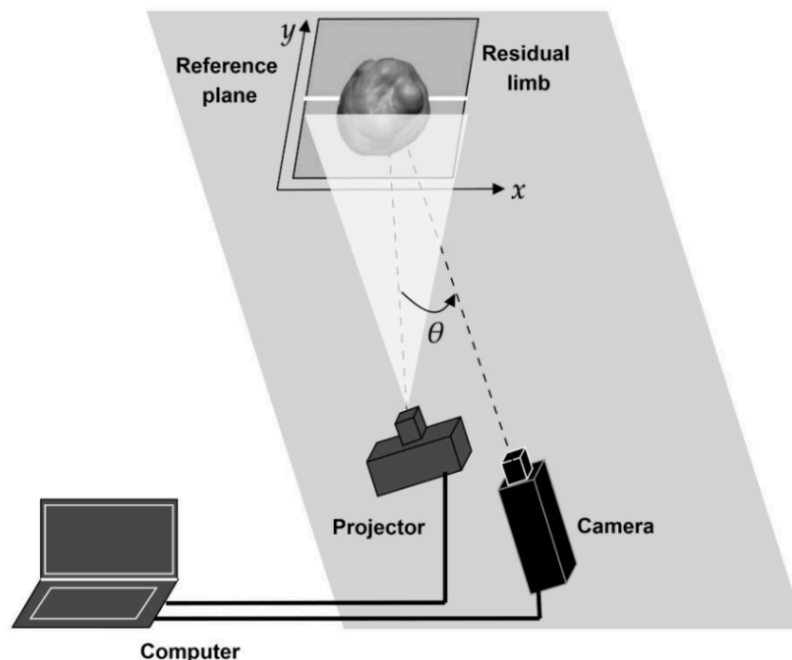


Figure 1: Experimental setup of a white line projection technique.

### References

- [1] Xue, J., Zhang, Q., Li, C., Lang, W., Wang, M., & Hu, Y., *Applied Sciences*, 9(7), 1458 (2019). "3D face profilometry based on a galvanometer scanner with infrared fringe projection at high speed".
- [2] Vilchez-Rojas, H. L., Rayas, J. A., & Martínez-García, A., *Optics and Lasers in Engineering*, 134, 106295 (2020). "Use of white light profiles for the contouring of objects".
- [3] Cutti, A. G., Santi, M. G., Hansen, A. H., & Fatone, S., *Sensors*, 24(7), 2350 (2024). "Accuracy, repeatability, and reproducibility of a hand-held structured-light 3D scanner across multi-site settings in lower limb prosthetics".

**Corresponding author:** Joaquin Sifuentes. **Email:** jsifuentesri@unjbg.edu.pe

## Thickness analysis of South American Camelid Wool Fiber by Fraunhofer Diffraction

Jade Aguayo, Ivan Choque and Riquelme P-Cruz

**Topic(s):** Diffraction and gratings, Laser and laser optics, Optics in computing [ID 031]

**Institution(s):** Universidad Nacional Jorge Basadre Grohmann, Perú

In Tacna, Peru, the thickness of the South American Camelid (SAC) fiber wool is related with their price, for that reason it is important to measure it with high accuracy, and to quantize the appropriate cost. This work describes a detailed procedure to analyze the wool fiber thickness of the SAC by Fraunhofer diffraction. Twenty samples of fibers wools are obtained from each kind of SAC. A single fiber sample per species was mounted on a sample holder. Diffraction patterns are obtained from an experimental setup, as shown in Figure 1. A green laser beam ( $\lambda = 532 \text{ nm}$ ) goes to the sample and the fiber runs as a diffracting device, generating a Fraunhofer diffraction pattern onto a screen. Each fiber was stretched as straight as possible in order to avoid deformation or rupture. Recorded diffraction patterns are processed using a MATLAB routine, this is useful to analyze the intensity distribution and to estimate the fiber thickness [1-2]. Preliminary results show similar values for those obtained by  $20.21 \pm 0.49 \mu\text{m}$ ,  $19.21 \pm 0.88 \mu\text{m}$ ,  $22.28 \pm 1.11 \mu\text{m}$  and  $14.1 \mu\text{m}$  for alpaca, llama, vicuña and guanaco; respectively [3]. This technique is a non-destructive and a low-cost alternative for quantitative assessment of SAC wool, it can be used in fair trade and product certification.

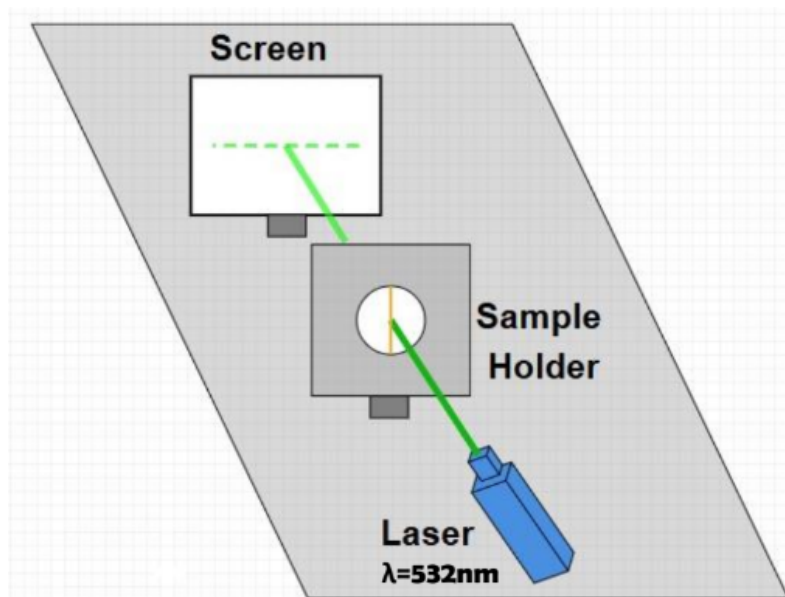


Figure 1: Experimental setup for Fraunhofer diffraction.

### References

- [1] Z. Zhang, H. Bai, G. Yang, F. Jiang, Y. Ren, J. Li, K. Yang, and H. Yang, Comp. Simul. Fraunhofer Diffract. Based on MATLAB, J. Phys. Educ. 45, 123 (2020).
- [2] J. A. Cortes Osorio, J. A. Chaves Osorio, and J. A. Mendoza, Estudio de la difracción de Fraunhofer de una ranura simple mediante tratamiento digital de imágenes, Univ. Tecnol. De Pereira, Dep. de Física (2013).
- [3] A. Flores Gutiérrez, Caracterización etnozootécnica de las poblaciones de Camélidos Sudamericanos domésticos en comunidades de la Provincia de Tacna, Perú, Tesis de Maestría, Univ. de Buenos Aires, Área Producción Animal, 2009.

**Corresponding author:** Jade Aguayo. **Email:** jaguayoj@unjbg.edu.pe

# Bridging Theory and Practice: A Remote Solar Laboratory for Energy Transition Education

Juan Peralta-Jaramilo, Emerita Delgado-Plaza, Doménica León-Moreira, Henry Fuentes

**Topic(s):** Solar energy [ID 111]

**Institution(s):** Escuela Superior Politécnica del Litoral, Ecuador

Within the framework of the Erasmus+ project EU-BEGP (Modernising Digital Education in Energy Transition for Circular Economy in Latin America), a remote photovoltaic laboratory has been developed at CDTs–ESPOL to bridge the gap between theoretical learning and real-world practice in renewable energy education. This innovative platform enables undergraduate and postgraduate students to remotely interact with a 1.65 kWp solar PV system (three 550 W panels, 3.3 kW on-grid inverter), instrumented with ESP32 sensors and connected to a SCADA system for real-time acquisition of electrical and environmental variables.

Students can perform hands-on activities such as I–V and P–V curve analysis, evaluation of energy efficiency under different tilt angles, thermographic inspection to detect hotspots, and preventive maintenance procedures. These experiences strengthen analytical, diagnostic, and decision-making skills, allowing learners to understand how environmental conditions and system configurations influence photovoltaic performance and grid integration.

This remote laboratory represents an innovative educational strategy that modernises energy training, expands access to high-quality practical experiences, and enhances the development of professional competences in renewable energy, supporting the goals of energy transition and circular economy promoted by the EU-BEGP project.



Panel de Supervisión y control Solar, Hídrico y Aerotermia



**Figure 1: (a) Panel de supervisión y control del sistema solar, hídrico y aerotérmico conectado al laboratorio remoto del CDTs–ESPOL, (b) Instalación y calibración de los módulos fotovoltaicos de 1.65 kWp desarrollado en el marco del proyecto Erasmus+ EU-BEGP.**

**Acknowledgments:** This work was partially funded by the Erasmus+ project “EU-BEGP” (Project No. 101081473).

## References

- [1] E. Delgado, P. Plaza, D. León-Moreira, J. D. Cabrera Abad, B. M. Briones Morante et al., “Energy efficiency training: Evaluation and optimization of its implementation in secondary education,” Proc. 23rd LACCEI International Multi-Conference for Engineering, Education and Technology (LACCEI): “Engineering, Artificial Intelligence, and Sustainable Technologies in service of society”, January 2025. DOI: 10.18687/LACCEI2025.1.1.2079
- [2] R. S. Herrera, M. A. Márquez, A. Mejías, R. Tirado, and J. M. Andújar, “Exploring the usability of a remote laboratory for photovoltaic systems,” IFAC-PapersOnLine, vol. 48, no. 29, pp. 190–195, Dec. 2015. doi: 10.1016/j.ifacol.2015.11.205

**Corresponding author:** Juan Peralta. **Email:** jperal@espol.edu.ec

# Bio-inspired retinal analysis theoretical model based on mantis shrimp vision for monitoring the progression of Sanfilippo síndrome

Adriana M. Suárez Oña, Mayra F. Ocampo Valdivia

**Topic(s):** Bio photonics and biomedical applications, Image processing, vision and artificial intelligence, Medical optics and biotechnology, Vision, color, and visual optics [ID 113]

**Institution(s):** Universidad Privada Boliviana, Bolivia

Mucopolysaccharidosis type III (MPS III), commonly known as Sanfilippo syndrome, is a lysosomal storage disease characterized by the accumulation of heparan sulfate, which causes neuronal degeneration [1]. A bioindicator associated with this pathology is the structural and functional changes in the retina, the monitoring of which is essential for evaluating disease progression [2]. This paper proposes a bio-inspired theoretical model based on the vision of the mantis shrimp (*Odontodactylus scyllarus*), a marine crustacean whose optical specializations include high sensitivity to polarized light, spectral resolution, and highly accurate spatial filtering [3]. This model is based on the computational simulation of these capabilities applied to fundus autofluorescence (FAF) images previously acquired using standard clinical equipment. The analysis flow consists of four stages (Fig. 1): FAF image preprocessing, multispectral analysis, computational polarimetry using Gabor filters and receptive field spatial filtering, combining wavelets and Gabor filters [4]. Although the model's accuracy does not replace that of a clinical examination or a real polarimetric sensor, it allows for a non-invasive, sensitive, reproducible, and cost-effective analysis of retinal micro-alterations associated with MPS III.

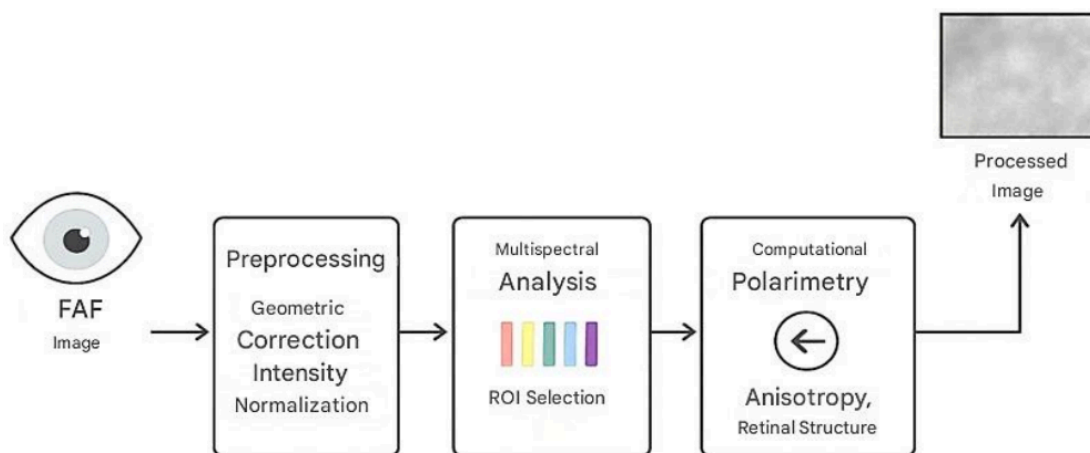


Figura 1: Analysis flow of the bioinspired model for the detection of retinal alterations in MPS III.

## References

- [1] N. Benetó, L. Vilageliu, D. Grinberg y I. Canals, "Sanfilippo syndrome: molecular basis, disease models and therapeutic approaches," *International Journal of Molecular Sciences*, vol. 21, no. 21, art. 7819, Oct. 2020.
- [2] M. S. García y J. A. Pérez, "Retinal autofluorescence analysis in lysosomal diseases," *Public Library of Science (PMC)*, 2014.
- [3] A. Altaqui, P. Sen, H. Schrickx, J. Rech, J.-W. Lee, M. Escuti, W. You, B. J. Kim, R. Kolbas, B. T. O'Connor y M. Kudenov, "Mantis shrimp-inspired organic photodetector for simultaneous hyperspectral and polarimetric imaging," *Science Advances*, vol. 7, n.º 10, art. eabe3196, mar. 2021. 2014.
- [4] Autonomous University of Madrid, "Image processing for the detection of [4] retinal biomarkers," *UAM Institutional Repository*, 2018.

**Corresponding author:** Adriana Suárez. **Email:** adrianasuarez1@upb.edu

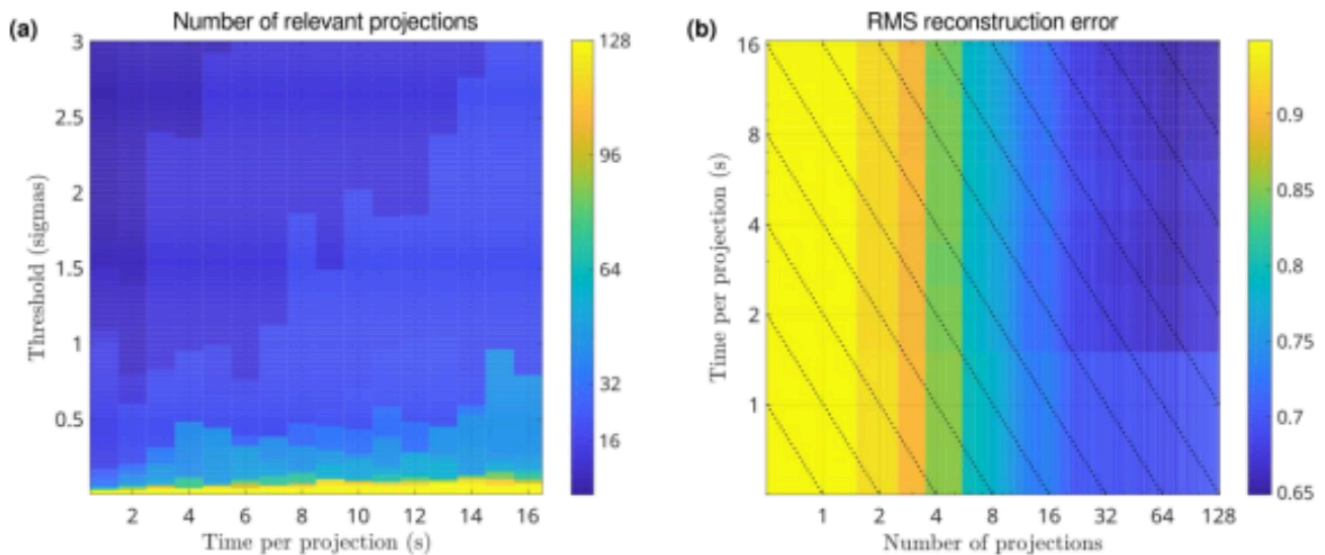
# Optimization of projection selection and measurement time in compressive single-pixel imaging

Sebastián Bordakevich, Lorena Rebón, Silvia Ledesma

**Topic(s):** Fourier optics and signal processing, Imaging systems, Other topic [ID 106]

**Institution(s):** Universidad de Buenos Aires; Universidad Nacional de La Plata, Argentina

Single-pixel cameras [1] use a single fixed detector to capture scenes by sequentially projecting onto basis elements via an SLM. Compressive sensing reduces measurement time by sampling only relevant projections. The presented approach extends [2], optimizing element selection given available measurement time. We use a nonlinear crystal photon source, a reflective twisted nematic LCD (projecting a binary triangle onto Hadamard basis), and single photon counting detectors. Typically, compressive imaging uses a short preliminary scan, ranking projections by photon count to measure the most relevant. However, too short scans reduce confidence in discriminating consecutively ranked projections, risking exclusion of relevant ones and inclusion of less relevant ones. Thus, we applied thresholds to the count differences between consecutively ranked projections: if not exceeded, projections cannot be discriminated and require uniform treatment to avoid misselection. Since differences typically decrease, there is a last projection beyond which all lower-ranked projections are significantly less relevant, defining a set of relevant projections. As seen in Figure (a), this set's size increases with looser thresholds (admitting smaller differences) or longer scans (better statistics). Given this set, we analyzed what minimizes RMS reconstruction error: measuring all those projections for a certain time, or a subset with longer times per projection. Figure (b) shows that reconstruction quality improves when increasing measured projections and their measurement time. However, under constrained total measurement time (dotted lines), results show that beyond a certain total time, adding further projections increase RMS error, thus favoring extending measurement time per projection. This avoids measuring irrelevant projections and validates the previous analysis: total measurement time can be allocated exclusively among the most relevant projections.



**Figure:** (a) Number of relevant projections according to the preliminary scan, as a function of the difference threshold and the time per projection. (b) RMS error of the reconstruction as a function of the number of measured projections and their measurement time; dotted lines mark constant total measurement time.

## References

- [1] G. Gibson, S. Johnson, and M. Padgett. Optics Express 28 (19) 28190 (2020)  
 [2] S. Bordakevich, L. Rebón, and S. Ledesma. FiO+LS Conference 2024, paper JW4A.29 (2024).

**Corresponding author:** Sebastián Bordakevich. **Email:** sbordakevich@df.uba.ar

## Temperature fiber sensor with variable sensitivity based on the Vernier effect and the bend-induced linear birefringence with tension

I. Armas-Rivera, M. Durán-Sánchez, B. Ibarra-Escamilla, M. Delgado-Pinar, A. Díez, J. L. Cruz, and M. V. Andrés

**Topic(s):** Fiber optics, sensors and optical communications [ID 019]

**Institution(s):** Instituto Nacional de Astrofísica, Óptica y Electrónica (INAOE), México; Universidad de Valencia, España

Fiber optic temperature sensors based on the Vernier effect have recently received great interest due to their benefits such as corrosion resistance, small size, immunity to electromagnetic interference, among others [1]. Due to this, we proposed and demonstrated a temperature fiber sensor with variable sensitivity based on the Vernier effect [2] and the bend-induced linear birefringence with tension [3].

The experimental setup shown in Fig. 1, includes two Lyot filters (LF) in cascaded configuration, the reference and the sensing LF. Each LF consists of a birefringent element placed between two linear polarizers (PBS, Polarizing Beam Splitter) at 45 degrees respect to the birefringent element axes.

The reference LF includes a 1.885 m highly birefringent fiber (Hi-Bi) with linear birefringence  $= 1.979 \times 10^3 \text{ m}^{-1}$  at 1550 nm and 30-m long SMF-28 fiber coiled onto a 2 cm radius cylinder as a tunable birefringent element. The bend-induced linear birefringence can be increased by increasing the fiber strain. By aligning the birefringent elements axes, e.g. fast-axes, both birefringences add constructively. The sensing LF includes a 2.02 m Hi-Bi fiber. As a light source, we used a supercontinuum (SC) laser providing a wide spectrum. In the initial configuration (0 strain), the produced Vernier envelope was 91.68 nm. The sensing Hi-Bi fiber was heated from 20 to 21 °C by a thermal bath with 0.2 °C steps. In this configuration, the temperature sensitivity of the fiber sensor was  $-43.87 \text{ nm}/^\circ\text{C}$  corresponding to a magnification factor  $M = 22.07$ . The  $M$  factor compares the temperature sensitivity enhancement with respect to single LF, in this case  $-1.987 \text{ nm}/^\circ\text{C}$ . By increasing the fiber strain, the Vernier envelope was increased to 106.31 nm and to 208.15 nm, increasing the sensor sensitivity to  $-70.16 \text{ nm}/^\circ\text{C}$  ( $M = 35.3$ ) and  $-132.46 \text{ nm}/^\circ\text{C}$  ( $M = 66.66$ ), respectively.

Numerically, it was found that the sensor sensitivity tends to infinity when the fiber strain is near 4 mε. Experimentally, the sensor sensitivity reaches a limit when the spectral period of the Vernier envelope exceeds the measurement bandwidth, preventing to track the shift of the envelope minimum or maximum.

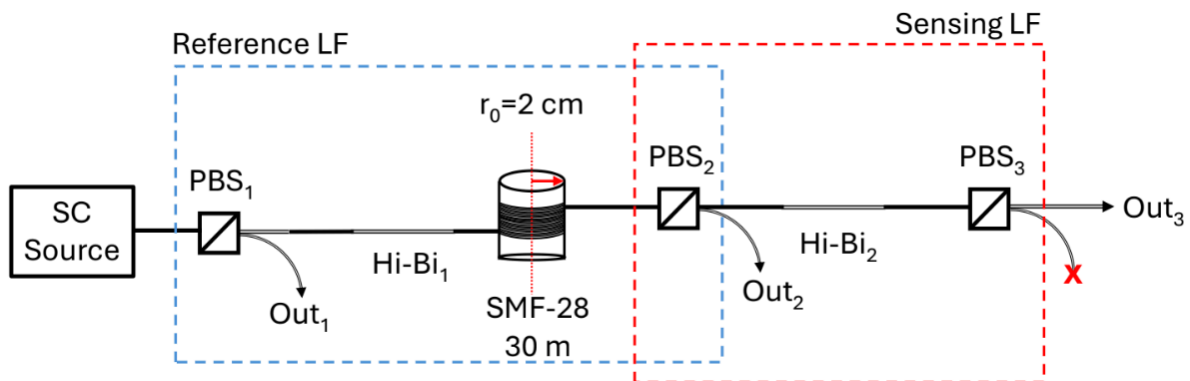


Figure 1: Temperature fiber sensor experimental setup.

### References

- [1] H. Huang, C. Jiang, S. Sun, H. Li, T. Cao, L. Zhang, Y. Shu, and G. Jiang, *Appl. Phys. B* 131,35 (2025).
- [2] R. Xu, S. Liu, Q. Sun, P. Lu, and D. Liu, *IEEE Photonics Technol. Lett.* 24, 23 (2012).
- [3] I. Armas-Rivera, L. A. Rodríguez-Morales, S. Cortés-López, M. Durán-Sánchez, M. V. Andrés, and B. Ibarra-Escamilla, *Opt. and Laser Technol.* 175, 110816 (2024).

**Corresponding author:** Iván Armas. **Email:** ivan\_rr1@hotmail.com

## Stepping stones to engineer pulse propagation through multifrequency nonlinearities

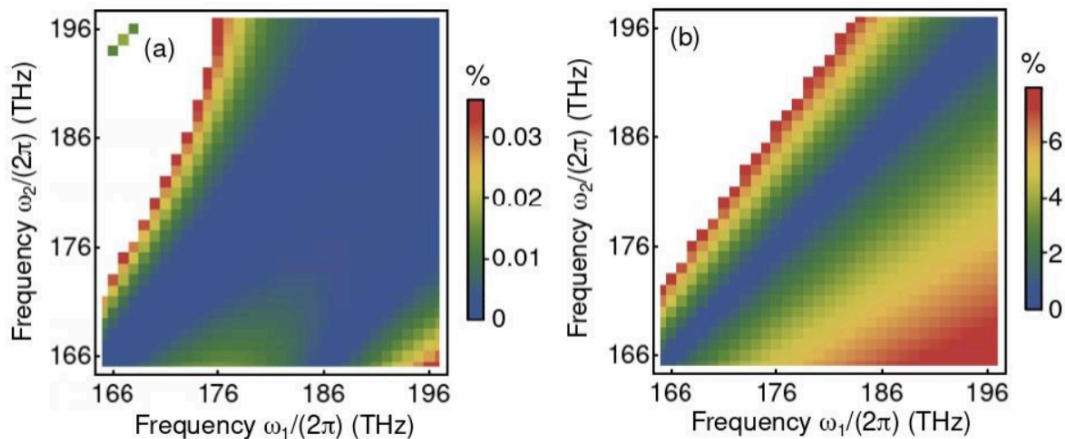
M. A. Bosch & M. P. Safont, D. Castelló-Lurbe, E. Silvestre, M. Delgado-Pinar, A. Díez, and M. V. Andrés

**Topic(s):** Fiber optics, sensors and optical communications, Nonlinear optics [ID 028]

**Institution(s):** Universidad de Valencia, España

Group-velocity-dispersion (GVD) engineering plays a crucial role to control nonlinear pulse propagation in fibers, e.g., for supercontinuum (SC) generation. However, the interplay between nonlinearities and the dispersion resulting from the frequency dependence of the effective index leads to some limitations to pulse propagation. In this regard, the need of short femtosecond pulses to produce coherent SC is a paradigmatic case [1]. If the only dispersive parameter is the effective index, then the anomalous GVD easing pulse spectral broadening also promotes instabilities and hence, a coherence loss during SC generation. As a result, demanding initial conditions, namely, relatively wideband pumping pulses, are required to mitigate the impact of instabilities [1]. If the nonlinearity also depends on frequency significantly, then instabilities can be cancelled even under anomalous GVD, offering renewed opportunities for coherent SC even in the picosecond pulse regime [1]. Being largely unexplored, this investigation entails major challenges that our group are steadily tackling.

On the theoretical side, the generalized nonlinear Schrödinger equation (GNLSE) fails to capture the dependence on multiple frequencies of the nonlinearity and, as such, it does not suit this research track. Consequently, we had first to derive the multifrequency nonlinear Schrödinger equation (MFnLSE) to account for this feature rigorously while keeping the numerical advantages of the GNLSE [2]. Second, using our MFnLSE, we have also analytically obtained the nonlinearity dispersion enabling coherent spectral broadening of picosecond pulses under anomalous GVD, showcasing the impact of its multifrequency nature. On the experimental side, we have collected solid evidence supporting the feasibility of a method to determine higher-order dispersion accurately, extending the approach that we had demonstrated experimentally measuring nonlinearities precisely in fibers [3,4].



**Figure 1:** For nonlinear processes  $2\omega_1 \rightarrow \omega_2 + \omega_3$ , with  $\omega_3 = 2\omega_1 - \omega_2$ , relative error between the multifrequency nonlinearity and its approximated values employed in (a) the MFnLSE, and (b) the GNLSE.

### References

- [1] D. Castelló-Lurbe, *Opt. Lett.* 47, 1299 (2022).
- [2] D. Castelló-Lurbe, E. Silvestre, and M. V. Andrés, *Opt. Lett.* 49, 4713 (2024).
- [3] D. Castelló-Lurbe et al., *Opt. Lett.* 45, 4432 (2020).
- [4] D. Castelló-Lurbe & C. Cuadrado-Laborde et al., *Opt. Lett.* 48, 493 (2023).

**Corresponding author:** David Castelló. **Email:** david.castello-lurbe@uv.es

# Stochastic Modeling of the Polarization Effect on Light-Induced Mass Transport in Azopolymers

Franco Lucio Tambosco, Silvia Adriana Ledesma, María Gabriela Capeluto

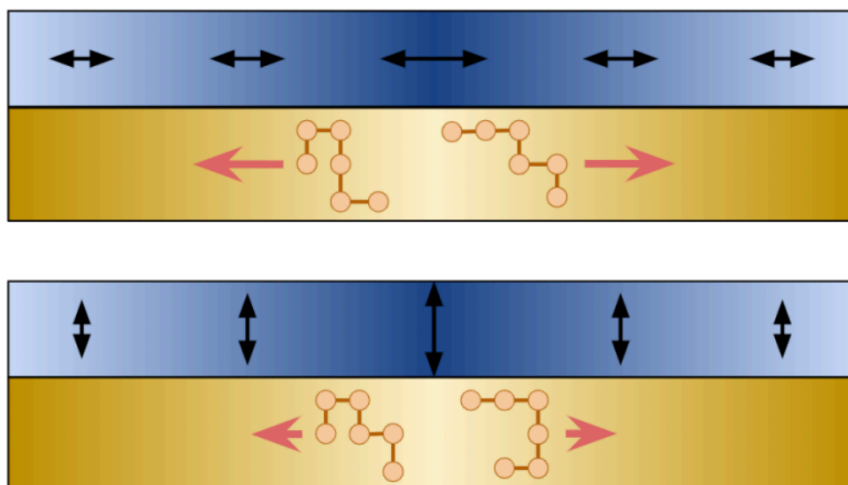
**Topic(s):** Nano photonics and metamaterials [ID 057]

**Institution(s):** Universidad de Buenos Aires, Argentina

Azobenzene-functionalized polymers (azopolymers) have attracted significant attention in recent years due to their photoinduced response, which arises from the photoisomerization of these functional groups. In particular, certain azopolymers exhibit mass migration when exposed to spatial variations in light intensity, phase, or polarization. The illumination with interference pattern leads to the formation of surface relief gratings (SRGs) [1]. Typically, mass migrates from high- to low-intensity regions, with enhanced efficiency when the intensity gradient is aligned with the light polarization. This optomechanical response has enabled a wide range of applications, including polarization holography [2], lithography [3], and actuation of nanoscale objects [4]. Despite numerous experimental and theoretical studies, the microscopic mechanism responsible for this transport remains under debate.

In the present work, we employ a stochastic model to simulate photoinduced mass transport in azopolymers. Polymer chains are generated using the self-avoiding walk (SAW) method on a two-dimensional square lattice, and the monomer motion is driven by photoisomerization probabilities and diffusion coefficients. An efficiency factor is introduced to account for the effects of light polarization variation across the SRG. We applied the model to a variety of structured illumination conditions, exploring different spatial distributions of light intensity and polarization.

The simulations successfully reproduce key features of experimentally observed surface relief formation [5], supporting the idea that mass transport can be effectively explained by a stochastic mechanism primarily driven by photoisomerization. This concept is schematically illustrated in Fig. 1, which shows examples of material displacement under different illumination patterns, emphasizing the role of both intensity and polarization distributions in guiding mass movement.



**Figure 1: Schematic illustration of light-induced mass transport, highlighting the influence of intensity and polarization patterns. The blue gradient shows light intensity, the yellow gradient mass distribution, the arrows indicate polarization (black), and chain displacement (red).**

## References

- [1] A. Natansohn and P. Rochon, *Chem. Rev.* 102, 4139 (2002).
- [2] G. Ateev, L. Nedelchev et al., *Photonics* 10, 728 (2023).
- [3] B. Yang, M. Yu et al., *ChemPlusChem* 85, 2166 (2020).
- [4] M. Capeluto, R. Salvador et al., *Optical Materials* 66, 247 (2017).
- [5] N. S. Yadavalli and S. Santer, *J. Appl. Phys.* 113, 224304 (2013).

**Corresponding author:** Franco Tambosco. **Email:** ftambosco@df.uba.ar

## Photoinduced Optical Properties in Layer-by-Layer Azopolymer Films and Polyamines

Franco Lucio Tambosco, Candelaria Rico, Gaspar Ariel Casaburi, Florencia Di Salvo, María Gabriela Capeluto

Topic(s): Photonics [ID 059]

Institution(s): Universidad de Buenos Aires, Argentina

Azobenzene-based materials are of great interest due to their photoinduced properties, which stem from the trans–cis photoisomerization of the azobenzene units. Repeated isomerization cycles induce a preferential molecular reorientation that minimizes light absorption, resulting in macroscopic birefringence. In some functionalized azopolymers, photoisomerization also produces mass transport under illumination gradients, leading to material migration from more to less illuminated regions [1].

This work investigates the photoinduced optical response of layer-by-layer (LbL) films composed by the azopolymer PAZO (Figure 1a) combined with protonated polyamines in their chloride salt form. The well-known PAH/PAZO system [2] (Figure 1b, c) is used as a reference, alongside two alternative systems employing PDADMAC (poly(diallyldimethylammonium chloride)) and PEI (poly(ethylenimine hydrochloride)).

Films with varying numbers of bilayers and immersion times were fabricated and characterized to determine the influence of these parameters and the identity of the polyamine on the photoinduced effects. Figure 1c illustrates photoinduced birefringence, in which azobenzene molecules orient perpendicular to the electric field (indicated by the blue arrow). Figure 1d shows the typical recording cycle, including the writing, relaxation, and erasure processes. The results provide insights into optimizing the optical performance of azopolymer-based multilayers through tailored film assembly.

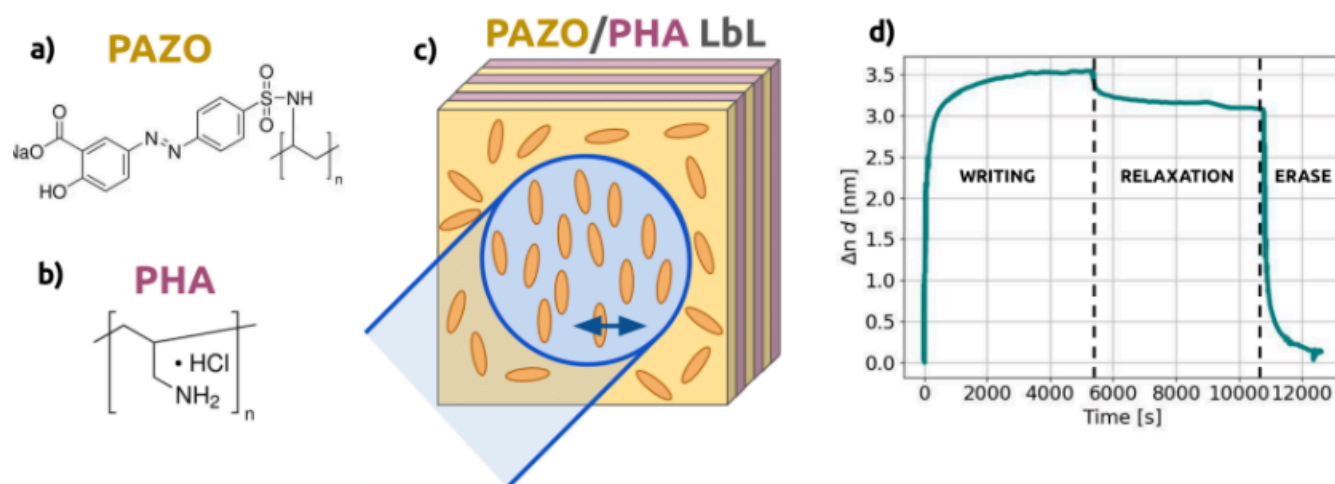


Figure 1: Structure of PAZO (a) and PHA (b). (c) Schematic of a PAZO/PHA LbL film, showing the orientation of azobenzenes on the illuminated area and (d) example of a birefringence curve, showing the writing, relaxation and erase steps.

### References

- [1] M. G. Capeluto, R. Falcione et al., *Opt. Mater.* 90, 281 (2019).  
 [2] M. Raposo, Q. Ferreira et al., *J. Appl. Phys.* 118, 114504 (2015).

Corresponding author: Maria Capeluto. Email: maga@df.uba.ar

## Laser tuning of IR radiative properties of metals

J. Gabirondo López, M. Soldera, J.M. Igartua, A.F. Lasagni, G.A. López

**Topic(s):** Diffraction and gratings, Instrumentation, measurement and metrology, Laser and laser optics, Materials processing with lasers [ID 016]

**Institution(s):** University of the Basque Country, España; Institut für Fertigungstechnik, Technische Universität Dresden, Germany

In this contribution, the feasibility of tailoring the radiative properties of stainless steel via Direct Laser Interference Patterning (DLIP) is introduced. By fabricating periodic micro- and nanostructures, emissivity is enhanced and made directionally dependent, as evidenced by direct spectral measurements and supported by Rigorous Coupled-Wave Analysis (RCWA) simulations. The experimental findings reveal that the modified surface acts as a spectrally selective emitter with a strong dependence on the emission direction, which is in good overall agreement with the predictions made by Maxwell's equations. These results show DLIP's potential for high-throughput, mask-free surface modification, with significant implications for fine-tuning of thermal management, radiative cooling, and related photonic applications.

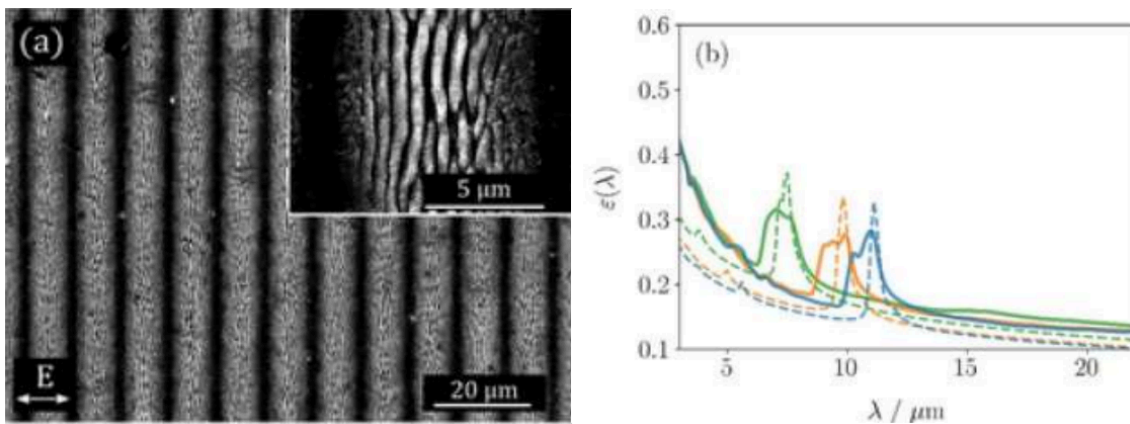


Figure 1: a) SEM image of the DLIP-structured stainless steel sample. b) Measured and simulated IR emissivity of the patterned samples.

**Corresponding author:** Gabriel López. **Email:** gabrielalejandro.lopez@ehu.eus

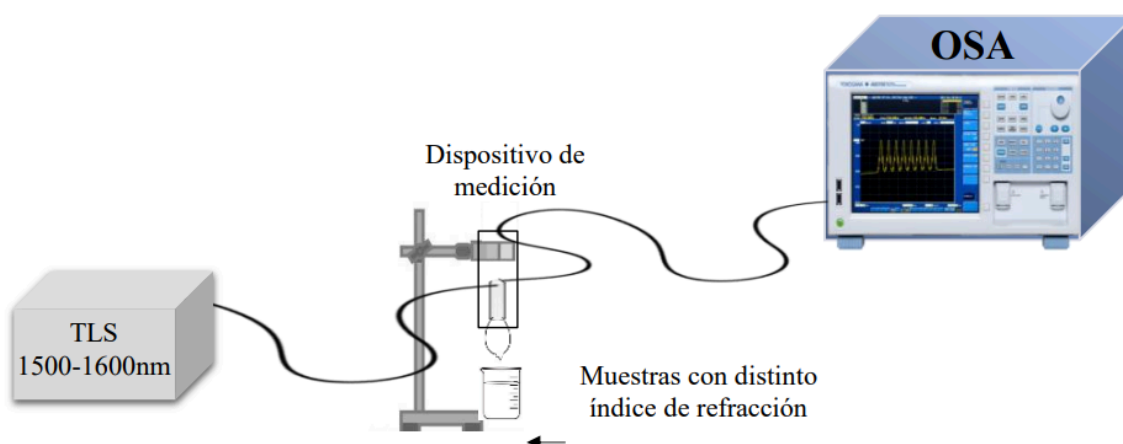
## Optical sensor based on a Mach-Zehnder interferometric curved optical fiber for measuring refractive index

Camila Noreña, Sindi Horta, Duber Ávila

**Topic(s):** Fiber optics, sensors and optical communications, Optics and photonics in the industry [ID 075]

**Institution(s):** Universidad Popular del Cesar, Colombia

This research proposes the development and analysis of an optical sensing system for the measurement of refractive indices of analytes, using a configuration based on a Mach-Zehnder interferometric curved optical fiber. The interferometric bent configuration was designed using a standard single-mode optical fiber of reference SMF-28, which was manually bent and supported on a piece manufactured from a 3D printer. The transmission spectral response was evaluated using a light source in the 1500 nm to 1600 nm range and an OSA optical spectrum analyzer (see figure 1); sucrose water samples in the 1.33 - 1.42 RIU range were used for the measurements, finding a sensitivity of 287.60 nm/RIU, evidenced by spectral modulations as the refractive index of the analyte was varied. The results obtained reveal the versatility and efficiency of these optical fiber-based configurations for optical sensing, being these sensing and detection tools with promising applications that can allow the detection of different variables [1-3], which evidences their potential in environmental monitoring, biomarkers and variations in physical parameters of interest that can be analyzed from changes in their refractive indices.



**Figure 1: a) Experimental setup implemented for the measurement of the transmission spectrum.**

### References

- [1] Zhang, J., Li, Y., & Yao, G. (2022). High Sensitivity Balloon-Like Sensor Based on Twin-Core and Twin-Hole Fiber. *IEEE Photonics Journal*, 14(4), 1-7.
- [2] Cardoso, V. H., Caldas, P., Giraldo, M. T. R., Frazão, O., Costa, J. C. A., & Santos, J. L. (2022). Optical strain gauge prototype based on a high sensitivity balloon-like interferometer and additive manufacturing. *Sensors*, 22(19), 7652.
- [3] Zhang, Y., Liu, Y., Huang, Z., Huang, P., Tang, X., Liu, Z., ... & Yuan, L. (2023). Simultaneous Measurement of Microdisplacement and Temperature Based on Balloon-Shaped Structure. *Sensors*, 23(20), 8521.

**Corresponding author:** Carmiña Noreña. **Email:** candreanorena@unicesar.edu.co

# Second-order electrogyration in $\text{Bi}_{12}\text{SiO}_{20}$ crystals analyzed by a dualrotation Mueller–Stokes polarimeter

María Alejandra Guerrero-V, Luis-A Guerra, Jorge Enrique Rueda-P

**Topic(s):** Instrumentation, measurement and metrology, Optoelectronics, detectors and sources [ID 082]

**Institution(s):** Universidad de Pamplona, Colombia; CONICET, Argentina

We report the experimental discovery and quantitative analysis of a second-order electrogyration (EG) effect in (110)-cut  $\text{Bi}_{12}\text{SiO}_{20}$  (BSO) crystals[1], investigated using a dualrotation Mueller–Stokes polarimeter [2]. By applying electric fields both parallel and perpendicular to the [001] crystallographic direction, we confirmed a nonlinear optical activity proportional to the square of the applied field—a behavior previously unreported in BSO. Through analytical modeling of the polarimetric response, we successfully isolated the electro-optic (EO) and EG contributions from intensity-based measurements. The extracted second-order EG coefficients were  $-4.86 \times 10^7$  and  $-1.87 \times 10^7 \text{ pm}^2/\text{V}^2$  for longitudinal and transverse geometries, respectively—exceeding by more than three orders of magnitude the values reported for materials like quartz or  $\text{TeO}_2$ . Additionally, the EO coefficient  $r_{41}$  was measured to be  $1.17 \pm 0.03 \text{ pm}/\text{V}$  at 660.5 nm. Our results support the hypothesis that the quadratic EG response may stem from defect-induced mechanisms, such as interstitials or substitutional impurities, which alter the intrinsic optical activity. This study not only provides new insights into the nonlinear optical behavior of BSO, but also demonstrates the capability of Mueller–Stokes polarimetry for accurate electro-optic characterization in complex photonic materials.

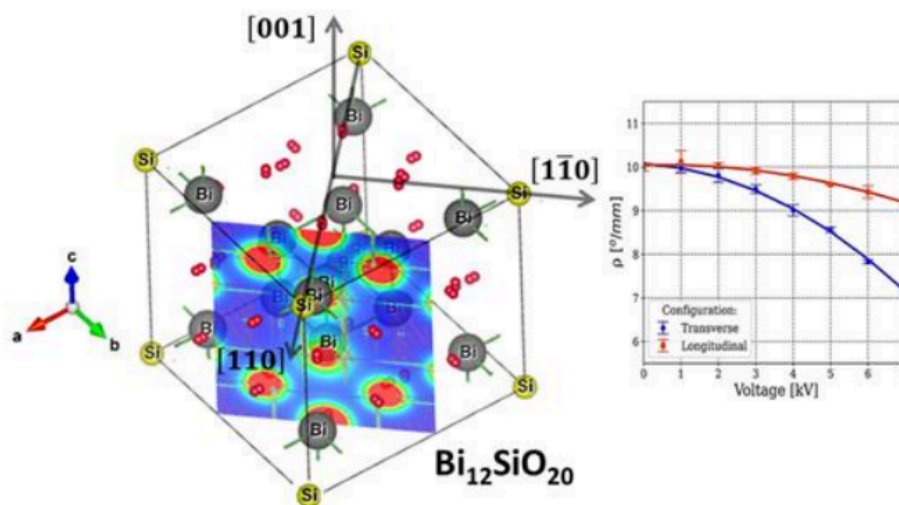


Figure 1: Electric field configurations applied to the BSO crystal under study: Transverse ( $E_{app} \parallel [110]$ ) and Longitudinal ( $E_{app} \parallel [001]$ ). Light incides on the (110) face.

## References

- [1] M.A. Guerrero-V, J.E. Rueda-P, “Second-order electrogyration effect in BSO crystal”, *Appl. Phys. B*, 130, 197 (2024). <https://doi.org/10.1007/s00340-024-08327-5>
- [2] D.H. Goldstein, “Mueller matrix dual-rotating retarder polarimeter”, *Appl. Opt.*, 31(31), 6676 (1992). <https://doi.org/10.1364/ao.31.006676>

**Corresponding author:** Jorge Rueda. **Email:** jruedap2003@unipamplona.edu.co

## Axial Thermal Gradient Localization and Its Role in LHPG Fiber Integrity

Jorge Enrique Rueda-P, João Rodrigues, Antonio Carlos Hernandes

**Topic(s):** Diffraction and gratings, Instrumentation, measurement and metrology, Laser and laser optics, Materials processing with lasers [ID 083]

**Institution(s):** Universidad de Pamplona, Colombia; Universidade de São Paulo, Brazil

The laser-heated pedestal growth (LHPG) technique enables the production of monocrystalline fibers with high pulling rates due to steep axial thermal gradients[1]. However, such high gradients can induce thermal stresses that lead to internal cracks when the fiber radius exceeds a critical threshold.

In this work, we present a new perspective on axial thermal gradient localization during LHPG growth, based on the finding that the maximum gradient occurs not at the traditional liquid/fiber interface, but within the fiber itself, at a certain distance  $\Delta$  from the interface[2]. An analytical model based on a Gaussian temperature profile was developed, allowing the calculation of axial and radial thermal gradients and the position of maximum thermal stress. Using this approach, we derived an expression for the critical radius ensuring crack-free fiber growth. The model was validated through the experimental growth of  $\text{SrTiO}_3$  and  $\text{Al}_2\text{O}_3$  fibers—both high-melting-point materials ( $>2300$  K)— and the corresponding optimal cooling rates were identified:  $210$  °C/min for  $\text{SrTiO}_3$  and  $296$  °C/min for  $\text{Al}_2\text{O}_3$ . These results reinforce the importance of accurately locating the point of maximum axial gradient to ensure structural integrity in LHPG-grown fibers, and provide a practical guideline for defect-free growth of oxide crystals with high thermal demands.

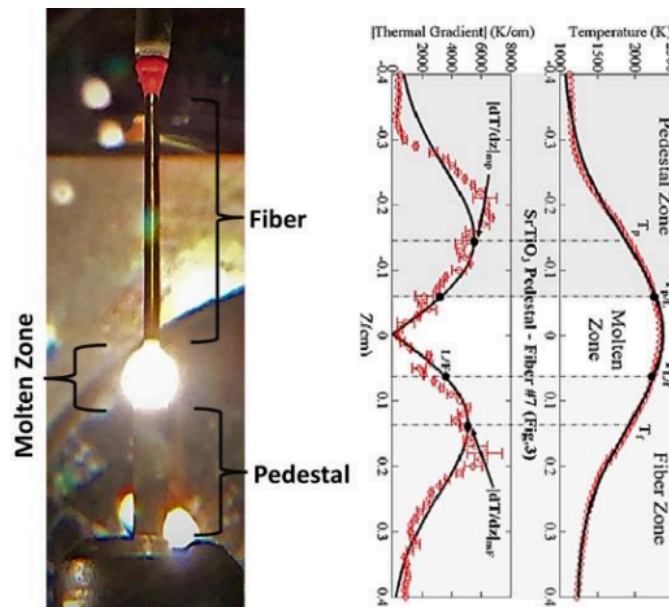


Figure 1: Localization of the Maximum Axial Thermal Gradient and Critical Radius in LHPG.

### References

- [1] Andreeta, M.R.B., & Hernandes, A.C. (2002). Thermal gradient control at the solid-liquid interface in the laser-heated pedestal growth technique. *Journal of Crystal Growth*, 234, 754–761. [https://doi.org/10.1016/S0022-0248\(01\)01736-5](https://doi.org/10.1016/S0022-0248(01)01736-5)
- [2] Rueda-P, J.-E., Rodrigues, J.E.F.S., & Hernandes, A.C. (2021). Monocrystalline fiber growth technique: New critical radius considerations. *Journal of Crystal Growth*, 574, 126199. <https://doi.org/10.1016/j.jcrysgro.2021.126199>

**Corresponding author:** Gabriel López. **Email:** gabrielalejandro.lopez@ehu.es

## Design of Aplanatic Imaging Systems printed using Stereolithography

Angie Sandoval, Alberto Silva, Rafael Torres

**Topic(s):** Imaging systems, Optical design and fabrication, Optics at surfaces[ID 067]

**Institution(s):** Universidad industrial de Santander, Colombia

Current optical design is typically performed using specialized software such as Zemax or OSLO. Although powerful, these tools require high computational resources and rely on complex optimization algorithms. These methods can correct high-order optical aberrations [1, 2], but at a high computational cost, especially in complex designs where optimization processes may take weeks or even months.

The Optics and Signal Processing Research Group (GOTS) at the Industrial University of Santander has developed a generalized theory of Descartes' ovoid's [3], based on physical principles of optics rather than computational optimization. This theory describes optical surfaces using so-called GOTS parameters, adaptable to different configurations. As a result, aplanatic optical systems with a single lens (singlets) have been designed [4], representing a conceptual breakthrough compared to the state of the art in optics, where multiple elements are typically required to achieve this property.

Since conventional manufacturing of high-quality optical lenses requires specialized machinery—often inaccessible in regions like Latin America— an alternative approach based on stereolithography 3D printing is proposed [6]. This approach is complemented by post-curing, sanding, and polishing processes to enhance the final optical quality, facilitating experimental implementation. A Shack-Hartmann sensor is used to characterize the fabricated lenses, measuring optical aberrations via Zernike polynomials [7].

In this framework, the designed surfaces correspond to intersections of Descartes' ovoids, which are quartic surfaces. Such systems allow control and minimization of optical aberrations without conventional optimization methods. This capability represents a significant contribution to modern optical design, demonstrating that high optical performance can be achieved with substantially reduced computational and technological costs.

### References

- [1] Zemax. (n.d.). Aspheric surfaces part 1: Introduction to aspherical surfaces in optical design. Zemax Support. Retrieved April 27, 2025, from <https://support.zemax.com/hc/en-us/articles/31584981420691-Aspheric-Surfaces-Part-1-Introduction-to-Aspherical-Surfaces-in-Optical-Design>
- [2] Lambda Research Corporation. (n.d.). OSLO Optics Reference Manual. Retrieved April 27, 2025, from [https://lambdaresearch.com/hubfs/Support/support/OSLOOpticsReference\\_Sep21.pdf](https://lambdaresearch.com/hubfs/Support/support/OSLOOpticsReference_Sep21.pdf).
- [3] Alberto Silva-Lora and Rafael Torres, "Superconical aplanatic ovoid singlet lenses," *J. Opt. Soc. Am. A* 37, 1155-1165 (2020)
- [5] Alberto Silva-Lora and Rafael Torres, "Aplanatism in stigmatic optical systems," *Opt. Lett.* 45, 6390-6393 (2020)
- [7] Formlabs. (2023). Creating camera lenses with stereolithography. Formlabs Blog. Retrieved April 28, 2025, from <https://formlabs.com/blog/creating-camera-lenses-with-stereolithography/>.
- [6] R. Paschotta, article on "Shack-Hartmann Wavefront Sensors" in the RP Photonics Encyclopedia, retrieved 2025-04-28, (<https://doi.org/10.61835/jcv>).

---

**Corresponding author:** Rafael Torres. **Email:** [rafael.torres@saber.uis.edu.co](mailto:rafael.torres@saber.uis.edu.co)

---

# Oral Presentations

# Photonic Crystal Mode Control in Semiconductor Lasers

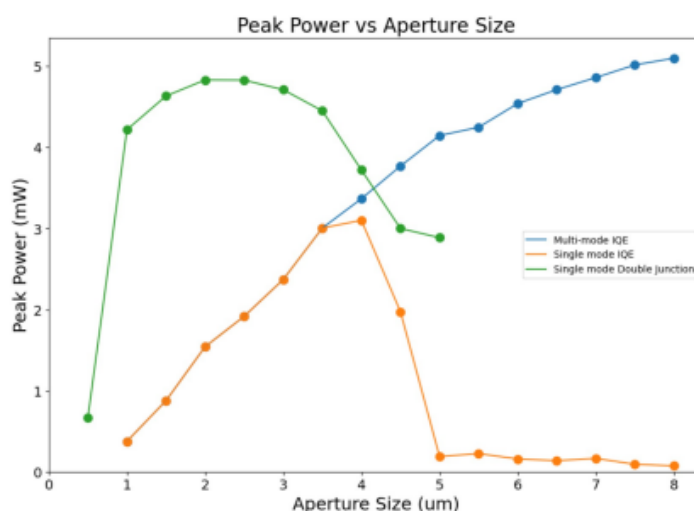
E. Raftery, C. Armstrong, D. Pflug, and K. D. Choquette

**Topic(s):** Laser and laser optics [ID 029]

**Institution(s):** University of Illinois at Urbana-Champaign, USA

High brightness semiconductor lasers are a critical technology for many applications. Semiconductor laser diodes exhibit the highest efficiencies of any type of laser, although the output power is often distributed over many optical modes supported by the laser cavity. The most efficient semiconductor laser diodes are thus multi-mode and have inferior brightness. Photonic crystals, either a 1- or 2-dimensional periodic pattern of refractive indices introduced into the laser cavity, can be used to control the optical modes [1, 2]. We report our recent progress of 850 nm single mode photonic crystal vertical cavity surface emitting lasers (VCSELs) using a single and double-junction optical cavity.

As apparent in Figure 1 for oxide apertures [3] less than  $4 \times 4 \mu\text{m}^2$  in size, the VCSEL output is single mode (defined as greater than 10dB side mode suppression ratio). Thus, for output powers  $> 3\text{mW}$ , the multi-mode VCSEL has reduced brightness. Note using a double-junction active region (with intra-cavity tunnel junction [3]), the single mode output can easily exceed 5 mW. Further details regarding photonic crystal VCSELs will be discussed.



**Figure 1: Maximum output power versus aperture size for single and double-junction VCSELs. Due to photodetector limitations, the output power is saturated for  $\geq 5\text{mW}$ .**

## References

- [1] K. D. Choquette, D. S. Siriani, A. M. Kasten, M. P. Tan, J. D. Sulkin, P. O. Leisher, J. J. Raftery, Jr., A. J. Danner, "Single Mode Photonic Crystal Vertical Cavity Surface Emitting Lasers," *Advances in Optical Technologies*, D280920 (2012).
- [2] K. Hirose, Y. Liang, Y. Kurosaka, A. Watanabe, T. Sugiyama, and S. Noda, "Watt-class highpower, high-beam-quality photonic-crystal lasers," *Nat. Photonics*, vol. 8, pp. 406–411 (2014).
- [3] Y. Xiao, J. Wang, H. Liu, P. Miao, Y. Gou, Z. Zhang, G. Deng, and S. Zhou, "Multi-junction cascaded vertical cavity surface emitting laser with a high power conversion efficiency of 74%," *Light*, vol. 13 (2024).

**Corresponding author:** Kent Choquette. **Email:** choquett@illinois.edu

## Thickness analysis of South American Camelid Wool Fiber by Fraunhofer Diffraction

Jade Aguayo, Ivan Choque and Riquelme P-Cruz

**Topic(s):** Diffraction and gratings, Laser and laser optics, Optics in computing [ID 031]

**Institution(s):** Universidad Nacional Jorge Basadre Grohmann, Perú

In Tacna, Peru, the thickness of the South American Camelid (SAC) fiber wool is related with their price, for that reason it is important to measure it with high accuracy, and to quantize the appropriate cost. This work describes a detailed procedure to analyze the wool fiber thickness of the SAC by Fraunhofer diffraction. Twenty samples of fibers wools are obtained from each kind of SAC. A single fiber sample per species was mounted on a sample holder. Diffraction patterns are obtained from an experimental setup, as shown in Figure 1. A green laser beam ( $\lambda = 532 \text{ nm}$ ) goes to the sample and the fiber runs as a diffracting device, generating a Fraunhofer diffraction pattern onto a screen. Each fiber was stretched as straight as possible in order to avoid deformation or rupture. Recorded diffraction patterns are processed using a MATLAB routine, this is useful to analyze the intensity distribution and to estimate the fiber thickness [1-2]. Preliminary results show similar values for those obtained by  $20.21 \pm 0.49 \mu\text{m}$ ,  $19.21 \pm 0.88 \mu\text{m}$ ,  $22.28 \pm 1.11 \mu\text{m}$  and  $14.1 \mu\text{m}$  for alpaca, llama, vicuña and guanaco; respectively [3]. This technique is a non-destructive and a low-cost alternative for quantitative assessment of SAC wool, it can be used in fair trade and product certification.

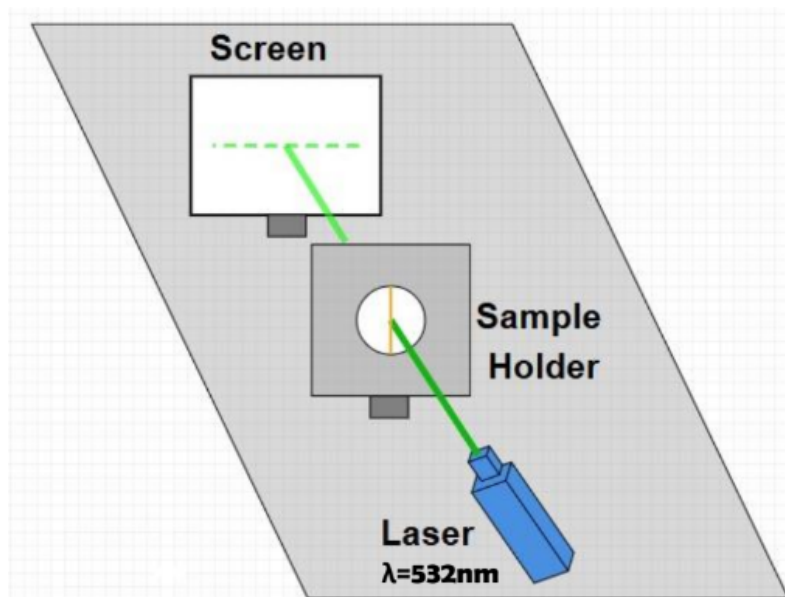


Figure 1: Experimental setup for Fraunhofer diffraction.

### References

- [1] Z. Zhang, H. Bai, G. Yang, F. Jiang, Y. Ren, J. Li, K. Yang, and H. Yang, Comp. Simul. Fraunhofer Diffract. Based on MATLAB, J. Phys. Educ. 45, 123 (2020).
- [2] J. A. Cortes Osorio, J. A. Chaves Osorio, and J. A. Mendoza, Estudio de la difracción de Fraunhofer de una ranura simple mediante tratamiento digital de imágenes, Univ. Tecnol. De Pereira, Dep. de Física (2013).
- [3] A. Flores Gutiérrez, Caracterización etnozootécnica de las poblaciones de Camélidos Sudamericanos domésticos en comunidades de la Provincia de Tacna, Perú, Tesis de Maestría, Univ. de Buenos Aires, Área Producción Animal, 2009.

**Corresponding author:** Jade Aguayo. **Email:** jaguayoj@unjbg.edu.pe

## Upgraded emissometer at the University of the Basque Country based on a new control-design paradigm

T. Echániz, J. Gabirondo-López, M. Sainz-Menchón, I. González de Arrieta, I. López-Ferreño, I. Arredondo, J. M. Igartua, and G. A. López

**Topic(s):** Fourier optics and signal processing, Optics at surfaces, Spectroscopy [ID 022]

**Institution(s):** University of the Basque Country (UPV/EHU), España

The HAIRL emissometer (High Accuracy Infrared Radiometer, Leioa) is a mid-infrared emissometer that was designed and built at the University of the Basque Country (UPV/EHU) [1]. The instrument can measure spectral directional emissivity in the range between 0.83 and 25  $\mu\text{m}$ , and it is equipped with an electric heater that can increase the surface temperature of the samples up to 1273 K. During 20 years of service, the instrument has undergone instrumental and methodological updates, such as the development of specific uncertainty budgets and the implementation of a Monte Carlo method to propagate uncertainties when integrating spectral and directional data [2].

However, the emissometer required an update to replace some of its core components, such as the FTIR spectrophotometer, which led to an integral upgrade that went beyond the mere substitution of the instruments. We present the total renovation performed to the HAIRL, which consists of three blocks: hardware, software and methodology. The hardware renewal is based on the use of control-design paradigms that allow the construction of scalable and maintainable instruments. Based on this philosophy, we have upgraded or replaced most of the devices that constitute the instrument. Among other modifications, we replaced the previous FTIR by a Bruker Vertex 80v, improved the sample heating system, redesigned the temperature measurement system and installed three new blackbodies.

Regarding the software, we have not only rebuilt all the communication protocols between the different devices and the control-computer using an expandable software-design, but we have also implemented a monitoring system based on new technologies such as InfluxDB and Grafana. The system can be completely controlled and monitored remotely, and it will be able to measure autonomously. All these technical improvements permitted us to adopt a new uncertainty budget, which treats statistically magnitudes such as the spectra measured by the FTIR or surface temperatures, and allows discarding anomalous data. Finally, a thermal radiative properties database named EKHI that follows the FAIR guidelines is being constructed. This database facilitates intercomparisons between research teams, measuring methods and uncertainty budgets, and provides the industry with high-accuracy digital data.

**Acknowledgments:** This work was funded by the University of the Basque Country, Spain (GIU19/019) and the Basque Government, Spain (IT-1714-22 and PIBA-2021-1-0022). J. Gabirondo-López, M. Sainz-Manchón and I. González de Arrieta also acknowledged financial support from pre-and post-doctoral fellowships by these institutions (University of the Basque Country, Spain: PIF 21/06; Basque Government, Spain: PRE-2022-1-0086, POS-2021-2-0022).

### References

- [1] L. Del Campo, R. B. Pérez-Sáez, X. Esquisabel, I. Fernández and M. J. Tello, New experimental device for infrared spectral directional emissivity measurements in a controlled environment, *Review of scientific instruments*, vol. 77 (2006), 113111.
- [2] I. González de Arrieta, T. Echániz, R. Fuente, J. M. Campillo-Robles, J. M. Igartua and G. A. López, Updated measurement method and uncertainty budget for direct emissivity measurements at the University of the Basque Country, *Metrología*, vol. 57 (2020) 045002.

---

**Corresponding author:** Telmo Echániz. **Email:** telmo.echaniz@ehu.es

## Spatial polarization modulation using two LCDs in tandem

Federico Guglielmucci Nazar, Facundo Rouquaud, Sebastián Bordakevich, Silvia Ledesma

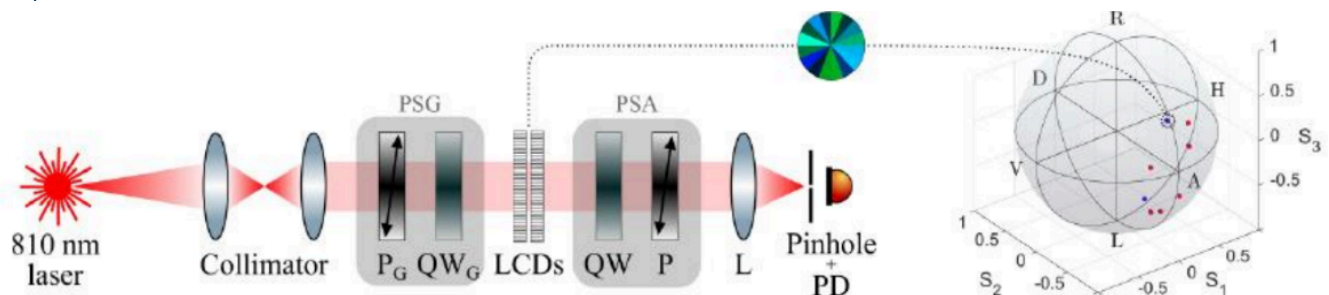
**Topic(s):** Fourier optics and signal processing, Imaging systems [ID 101]

**Institution(s):** Universidad de Buenos Aires; (CONICET), Argentina

Liquid crystal displays (LCDs), widely used in optical applications, are essential as spatial light modulators as they allow precise manipulation of beam properties, including amplitude, phase, and polarization [1]. In previous works, the advantage of using two twisted nematic LCDs in series has been demonstrated [2], optimizing the configuration to achieve complete modulation of amplitude and phase, or optimal polarization modulation covering a surface on the Poincaré sphere [3].

The experimental setup proposed for this work uses the optimized configuration from [3] to spatially modulate polarization. As shown in the Figure, it comprises a polarization state generator (PSG), two TN LCDs, and a polarization state analyzer (PSA). The LCDs, extracted from a commercial videoprojector, are controlled via its green (G) and blue (B) channels and act as a single compound modulator. The output's Stokes parameters were obtained via projective measurements, and spatial averaging was achieved by detecting the intensity at the center of the Fourier plane.

The LCDs were divided into  $N$  regions (from 4 to 256), each assigned a different polarization from one of eight zones of the surface of accessible states. Simulations using a density matrix formalism predicted the expected average state for each zone. Experiments matched simulations for low  $N$ , but fidelity dropped below 0.9999 beyond a critical threshold of  $N = 64$ , indicating practical limitations due to resolution, alignment, and inhomogeneities. These results demonstrate the effectiveness of using two TN LCDs in tandem for spatial modulation, while also revealing a practical constraint on their application. Moreover, the approach enables precise and programmable polarization control with commercially available components.



**Figure 1: Experimental setup and polarization modulation results.**

A collimated 810 nm laser illuminates a PSG (polarizer + quarter-wave plate), two TN LCDs in tandem, and a PSA (quarter-wave plate + polarizer). The beam is spatially filtered with a pinhole in the center of the Fourier plane to measure its average intensity with a photodiode (PD). Top: polarization image for  $N = 16$ , jointly modulated by channels G and B of the video projector. Right: average Stokes vectors on the Poincaré sphere (experimental: red; simulation: blue).

### References

- [1] Y. Q. Yang, A. Forbes, and L. C. Cao. *Opto-Electron Sci* 2, 230026 (2023). "A review of liquid crystal spatial light modulators: devices and applications".
- [2] A. Márquez et al, *Opt. Express* 16, 1669-1685 (2008). "Mueller-Stokes characterization and optimization of a liquid crystal on silicon display showing depolarization".
- [3] S. Bordakevich, L. Rebón, and S. Ledesma, *Appl. Opt.* 61, 969-977 (2022). "Optimization for maximum modulation of a double-pass twisted nematic liquid crystal display".

**Corresponding author:** Silvia Ledesma. **Email:** author: ledesma@df.uba.ar

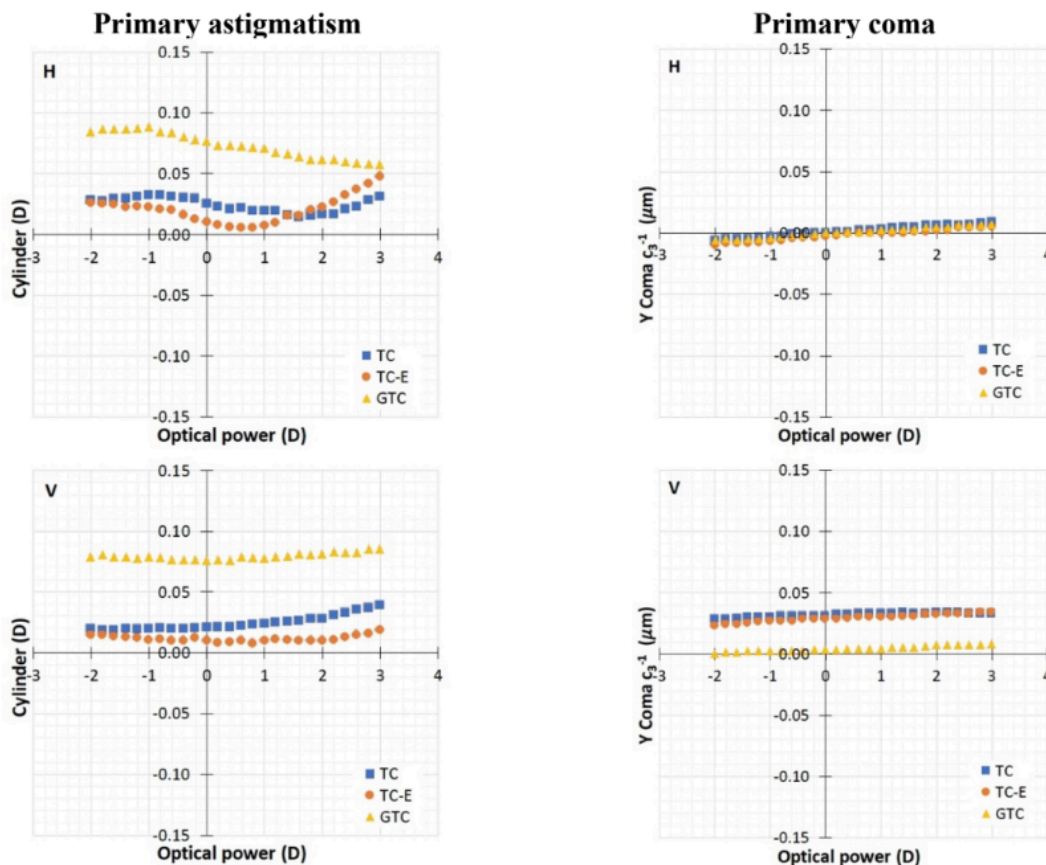
# Gravity-compensated focus-tunable lenses. Aberration analysis

Elisabet Pérez-Cabré, Fátima Cuéllar, Laura Clavé, María S. Millán

**Topic(s):** Imaging systems, Optoelectronics, detectors and sources [ID 027]

**Institution(s):** Universitat Politècnica de Catalunya, España

An electrically-addressed focus-tunable lens (FTL) enables fine, continuous, and dynamic power adjustment across a range of diopters. In many applications, the FTL is oriented horizontally with a vertical optical axis. However, applications requiring alternative orientations may suffer from aberrations due to gravitational effects on the optical fluid and elastic membrane of this device. This experimental study investigates the optical performance of a new gravity-compensated FTL, Optotune EL-16-40-GTC-VIS-5D (GTC), [1] in terms of the addressed optical power and measured wavefront error, in both horizontal and vertical lens orientation [2]. The results were compared with two standard, uncompensated models from the same manufacturer, EL-16-40-TC-VIS-5D (TC) and EL-16-40-TC-VIS-5D-E (TC-E). All the analyzed FTLs demonstrated excellent optical power performance regardless of orientation [2]. The gravity-compensated FTL effectively corrected vertical coma in the upright orientation, but induced greater astigmatism compared to the standard models. These findings provide valuable insights for vision testing and adaptive optics applications.



**Figure 1:** Wavefront analysis of GTC, TC, and TC-E FTLs in horizontal (H) and vertical (V) orientations versus addressed optical power (D). Left column: Measured cylinder magnitude (D). Right column: Vertical coma (Zernike coef.  $c_{3,-1}$ ) in microns.

**Funding:** Spanish Government (Grant ref. PID2020-114582RB-I00/AEI/10.13039/501100011033).

## References

- [1] Optotune (2024). Electrically tunable lens EL-16-40 (5D version). <https://www.optotune.com/>  
 [2] E. Pérez-Cabré et al.; J.Phys.Photonics (under review, 2025).

**Corresponding author:** Maria Millán. **Email:** m.millan@upc.edu

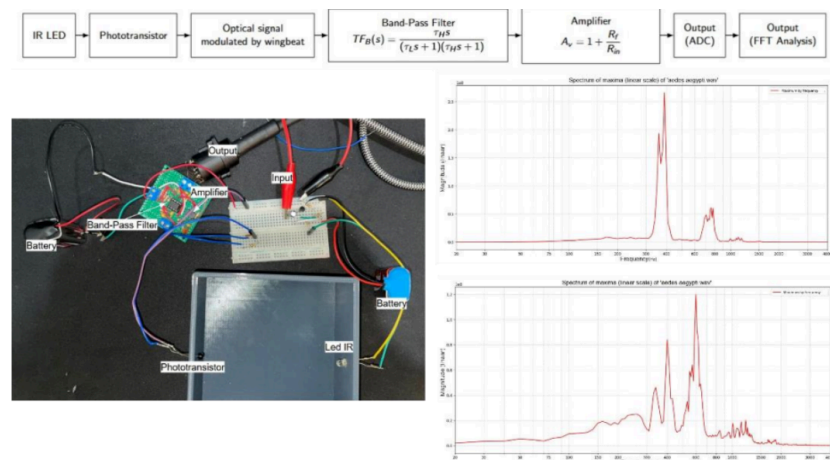
# An Infrared-based Aedes-aegypti Identification Trap

Amina Antonio, Miguel Angel Quiroz, Edgar Salazar

**Topic(s):** Optoelectronics, detectors and sources [ID 087]

**Institution(s):** Universidad Privada Boliviana, Bolivia

Dengue is one of the most common seasonal diseases in tropical areas. With more than 3 million confirmed cases world-wide, and 1400 deaths in 2025, this disease is a constant threat especially for vulnerable people (infants and elders) [1]. The transmission of Dengue is done by the aedes aegypti, thus, several efforts have been made to eradicate this insect. Such attempts include fumigation and preventive campaigns, genetic modification for female sterilization, or classical mosquito traps [2]. Some contemporary researchers, on the other hand, have worked extensively in the characterization of insects through quantifying the frequency of the wingbeat using spectral analysis and optical methods for data acquisition [3]. In this paper, we propose an Infrared-red based wingbeat acquisition method by using an IR Light Emitting Diode (LED) with its respective receptor. By interrupting the emitter-receptor light path, a pattern that is proportional to the insect movement is captured, and after proper analog filtration (band-pass filter from 150Hz to 600Hz) and amplification, its spectral content is calculated using conventional FFT methods. To test our model, we reproduced an aedes aegypti sound [4] and, through a common-emitter amplifier, modulated the IR-emitter signal. Even though some similar ideas and prototypes have been formulated, our method is the first of its kind in the context of Bolivia. This is the first step towards and comprehensive discrimination process that will eventually lead to a trap that only reacts to Aedes-aegypti with proper electromechanical actuators.



**Figure 1: Schematic and results of the experiment. Top: Block diagram of the system. Bottom-left: Implemented hardware. Bottom-right: Acquired spectral signatures of the aedes aegypti wingbeat.**

A collimated 810 nm laser illuminates a PSG (polarizer + quarter-wave plate), two TN LCDs in tandem, and a PSA (quarter-wave plate + polarizer). The beam is spatially filtered with a pinhole in the center of the Fourier plane to measure its average intensity with a photodiode (PD). Top: polarization image for  $N = 16$ , jointly modulated by channels G and B of the video projector. Right: average Stokes vectors on the Poincaré sphere (experimental: red; simulation: blue).

## References

- [1] Dengue Worldwide Overview, European Centre for Disease Prevention and Control, <https://www.ecdc.europa.eu/en/dengue-monthly>
- [2] S. T. Ogunlade, M. T. Meehan, A. I Adekunle, & E. S. McBryde. A systematic review of mathematical models of dengue transmission and vector control: 2010–2020. *Viruses*, 15(1), 254, 2023.
- [3] E. Joelianto, et. al. Convolutional neural network-based real-time mosquito genus identification using wingbeat frequency: A binary and multiclass classification approach. *Ecological Informatics*, 80, 102495, 2024.
- [4] H. Mukundarajan, F. J. H Hol, E. A. Castillo, C. Newby, & Prakash, M. (2017). Using mobile phones as acoustic sensors for high-throughput mosquito surveillance. *elife*, 6, e27854, 2017.

**Corresponding author:** Miguel Quiroz. **Email:** mickyquiroz9@gmail.com

---

# Coexistence of Aplanatism and Achromatism in Optical System Design

Alberto Silva, Rafael Torres

**Topic(s):** Geometrical optics, Imaging systems, Optical design and fabrication [ID 068]

**Institution(s):** Universidad Industrial de Santander, Colombia

This work introduces a novel optical design methodology that utilizes Descartes' ovoid refractive surfaces to achieve high-performance optical systems, which we term ultra-achromatic systems.

The use of Descartes' ovoids in optical designs has demonstrated rigorous correction of geometric aberrations [1], specifically achieving zero spherical aberration and zero coma [2]. While recent research has extended these capabilities to address achromatism [3], enabling designs with properties like achromatic astigmatism and achromatic aplanatism, their practical realization is limited by the availability of materials with ideal dispersion characteristics. The reliance on industry-standard materials introduces both chromatic and residual geometric aberrations, presenting a fundamental challenge: optimizing one type of aberration often worsens the other. To overcome this, our methodology focuses on designing isoplanatic systems, which are crucial for practical applications requiring superior performance. We present a detailed approach for creating stigmatic optical systems that exhibit minimal coma and chromatic aberrations simultaneously. This advancement represents a significant step forward in the development of high-performance optical instruments.

## References

[1] Alberto Silva-Lora and Rafael Torres, "Superconical aplanatic ovoid singlet lenses," *J. Opt. Soc. Am. A* 37, 1155-1165 (2020)

[2] Silva-Lora, A., & Torres, R. Aplanatism in stigmatic optical systems. *Optics Letters*, 45(23), 6390-6393 (2020).

[3] Silva-Lora, A., & Torres, R. Achromatic stigmatism: achromatic Cartesian ovoid. *Journal of the Optical Society of America A*, 39(9), 1524-1532 (2022).

---

**Corresponding author:** Rafael Torres. **Email:** rafael.torres@saber.uis.edu.co

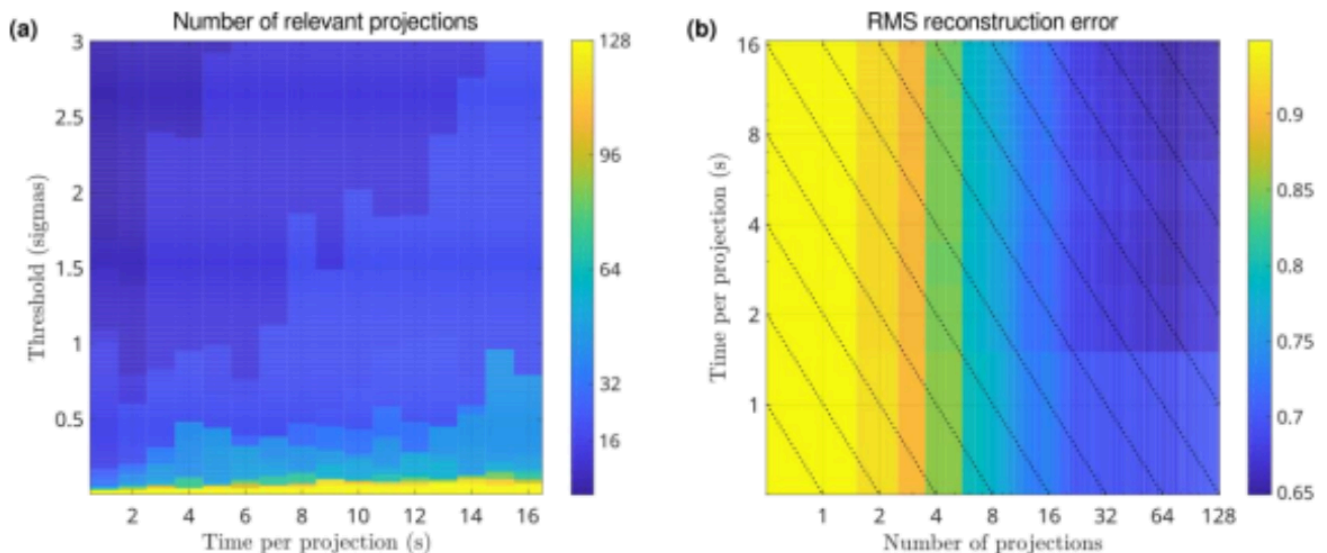
# Optimization of projection selection and measurement time in compressive single-pixel imaging

Sebastián Bordakevich, Lorena Rebón, Silvia Ledesma

**Topic(s):** Fourier optics and signal processing, Imaging systems, Other topic [ID 106]

**Institution(s):** Universidad de Buenos Aires; Universidad Nacional de La Plata, Argentina

Single-pixel cameras [1] use a single fixed detector to capture scenes by sequentially projecting onto basis elements via an SLM. Compressive sensing reduces measurement time by sampling only relevant projections. The presented approach extends [2], optimizing element selection given available measurement time. We use a nonlinear crystal photon source, a reflective twisted nematic LCD (projecting a binary triangle onto Hadamard basis), and single photon counting detectors. Typically, compressive imaging uses a short preliminary scan, ranking projections by photon count to measure the most relevant. However, too short scans reduce confidence in discriminating consecutively ranked projections, risking exclusion of relevant ones and inclusion of less relevant ones. Thus, we applied thresholds to the count differences between consecutively ranked projections: if not exceeded, projections cannot be discriminated and require uniform treatment to avoid misselection. Since differences typically decrease, there is a last projection beyond which all lower-ranked projections are significantly less relevant, defining a set of relevant projections. As seen in Figure (a), this set's size increases with looser thresholds (admitting smaller differences) or longer scans (better statistics). Given this set, we analyzed what minimizes RMS reconstruction error: measuring all those projections for a certain time, or a subset with longer times per projection. Figure (b) shows that reconstruction quality improves when increasing measured projections and their measurement time. However, under constrained total measurement time (dotted lines), results show that beyond a certain total time, adding further projections increase RMS error, thus favoring extending measurement time per projection. This avoids measuring irrelevant projections and validates the previous analysis: total measurement time can be allocated exclusively among the most relevant projections.



**Figure: (a) Number of relevant projections according to the preliminary scan, as a function of the difference threshold and the time per projection. (b) RMS error of the reconstruction as a function of the number of measured projections and their measurement time; dotted lines mark constant total measurement time.**

## References

- [1] G. Gibson, S. Johnson, and M. Padgett. Optics Express 28 (19) 28190 (2020)  
 [2] S. Bordakevich, L. Rebón, and S. Ledesma. FiO+LS Conference 2024, paper JW4A.29 (2024).

**Corresponding author:** Sebastián Bordakevich. **Email:** sbordakevich@df.uba.ar

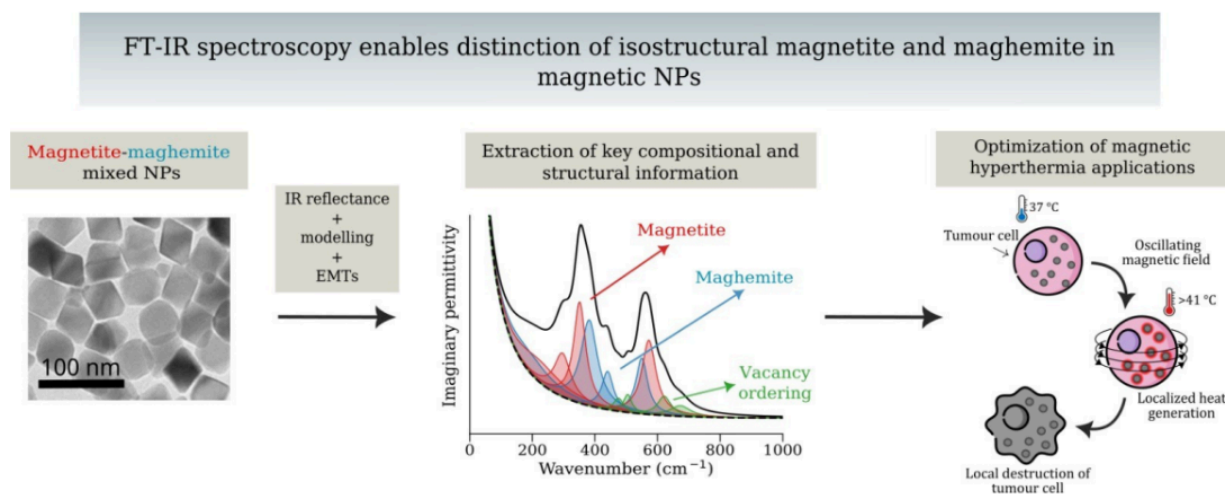
# Advanced characterization of oxide nanomaterials using infrared spectroscopy

M. Sainz-Menchón, I. González de Arrieta, T. Echániz, G. A. López

**Topic(s):** Bio photonics and biomedical applications, Instrumentation, measurement and metrology, Spectroscopy [ID 017]

**Institution(s):** University of the Basque Country (UPV/EHU), España

Spectroscopic techniques are essential tools for the characterization of novel nanomaterials and nanocomposites. For example, Raman spectroscopy is widely used to study vibrational modes and how they change with decreasing particle size. In the case of infrared spectroscopy, however, its application to nanomaterials has been traditionally more qualitative, mainly concerned with the rough identification of phases and adsorbed molecules. This is because quantitative studies require extracting the dielectric function, for which it is necessary to consider the influences of porosity, network connectivity, and particle shape and arrangement on the electromagnetic response of the matrix + nanomaterial composite. To this end, we show that a method based on reflectance spectroscopy and effective medium theories can provide quantitative results regarding the structural properties of dielectric nanomaterials. In particular, extending the measurements to the far infrared allows quantifying low-frequency modes, which are absent in most reported spectra but rich in features that can be used to identify phases with similar crystal structures. The fundamentals of the technique are demonstrated in a reference material, CeO<sub>2</sub> [1], and its generality is proven through several case studies: phase discrimination in (γ,δ)-Al<sub>2</sub>O<sub>3</sub> [2] and mixed Fe<sub>3</sub>O<sub>4</sub>/γ-Fe<sub>2</sub>O<sub>3</sub> nanoparticles [3], as well as quantification of short-range order in the case of vitreous SiO<sub>2</sub> [4].



**Figure 1: Schematic representation of the proposed characterization, with potential applications [3].**

## References

- [1] I. González de Arrieta, L. del Campo and D. De Sousa Meneses, *Phys. Chem. Chem. Phys.* 23, 13095 (2021).
- [2] I. González de Arrieta et al., *Spectrochim. Acta Part A* 298, 122795 (2023).
- [3] M. Sainz-Menchón et al., *Phys. Chem. Chem. Phys.* 27, 8498 (2025).
- [4] M. Sainz-Menchón et al., *Appl. Spectrosc.* 78, 209 (2024).

**Corresponding author:** Iñigo Gonzáles. **Email:** igonzalesdea@gmail.com

# Precision Tissue Classification via LIBS and ML: Toward Intraoperative Pathology Screening

R. Sosa - Santos, J.L. Arce-Diego, F. Fanjul-Vélez

**Topic(s):** Bio photonics and biomedical applications, Medical optics and biotechnology, Optics and photonics in the industry, Spectroscopy [ID 099]

**Institution(s):** Universidad de Cantabria, España; Universidad Privada Boliviana, Bolivia

Laser-Induced Breakdown Spectroscopy (LIBS) enables rapid, multielemental analysis of ex vivo biological tissues without complex preparation, capturing unique spectral signatures determined by elemental composition (e.g., C, O, Na, Ca, K) [1,2]. This work addresses the critical challenge of transforming raw spectral data into robust tissue discrimination through an optimized computational pipeline. Following ablation, spectra undergo rigorous preprocessing: spectral consolidation, noise reduction (Savitzky-Golay filtering), baseline correction, and intensity normalization [1,2]. Feature extraction then identifies discriminative variables—including peak intensities, elemental ratios (e.g., Ca/K), and full-width-at-half-maximum (FWHM) metrics—with dimensionality reduction techniques (e.g., PCA) selecting optimal feature subsets [3]. Supervised machine learning classifiers are trained on this refined dataset to achieve precise tissue differentiation. Support Vector Machine (SVM), Random Forest (RF), and K-Nearest Neighbors (KNN) models, among others, are benchmarked for discriminating five tissue types: connective tissue, small intestine, large intestine, aorta, and nervous tissue [4]. Model performance is validated via stratified 10-fold cross-validation, with class imbalance mitigated by synthetic oversampling (SMOTE, ADASYN). This integration establishes a versatile framework for biomedical diagnostics and forensic applications, supporting real-time tissue identification in surgical margins, biopsy validation, and pathological screening, with potential for intraoperative deployment.

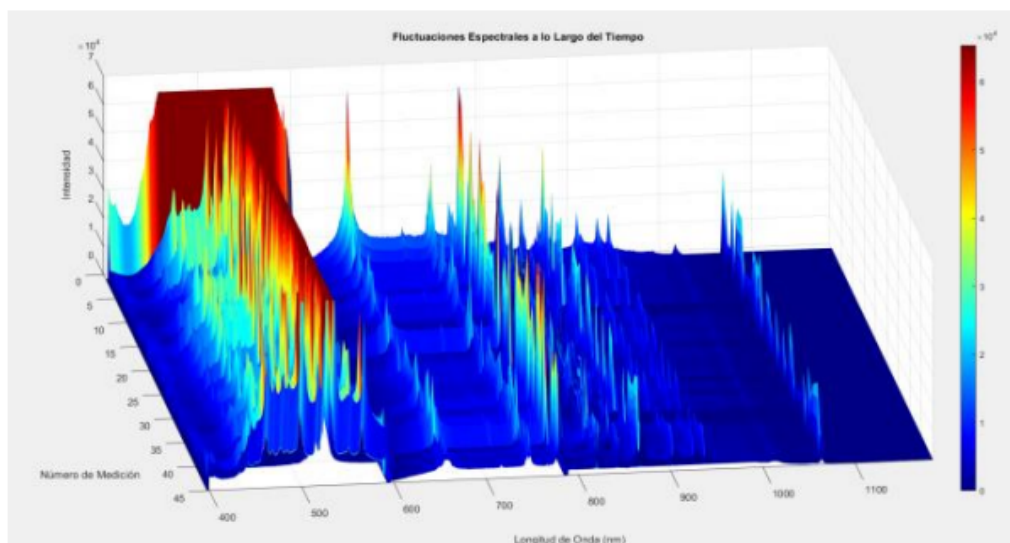


Figure 1: LIBS spectrum of muscle tissue.

## References

- [1] S. J. Rehse, "A review of the use of laser-induced breakdown spectroscopy for bacterial classification, quantification, and identification", *Spectrochim. Acta Part B At. Spectrosc.*, vol. 154, pp. 50-69, abr. 2019, doi: 10.1016/j.sab.2019.02.005.
- [2] M. A. Kasem, J. J. Gonzalez, R. E. Russo, y M. A. Harith, "LIBS analysis of artificial calcified tissue matrices", *Talanta*, vol. 108, pp. 53-58, abr. 2013, doi: 10.1016/j.talanta.2013.02.062.
- [3] Félix Fanjul-Vélez; Sandra Pampín-Suárez; José Luis Arce-Diego. "Application of classification algorithms to diffuse reflectance spectroscopy measurements for ex vivo characterization of biological tissues". *Entropy*. 22, pp. 736-1 - 736-16. 07/2020.
- [4] R. F. Sosa-Santos, J. L. Arce-Diego, F. Fanjul-Vélez, "Análisis predictivo del volumen de ablación en el diagnóstico mediante LIBS en tejidos de colon", *Actas del Congreso Anual de la Sociedad Española de Ingeniería Biomédica*, 2024.

**Corresponding author:** Rene Sosa. **Email:** rene-fernando.sosa@alumnos.unican.es

# Optical Multispectral Characterization of Photonic and Plasmonic Properties of Living Biostructures and Optical Ranging Biodiversity Assessment

Queenny K. Lopez, Jose Gonzalez, Angel Mendez, Juan Javier Naranjo, Juan Molina, Victor Santos, Mikkel Brydegaard, Cesar Costa Vera

**Topic(s):** Bio photonics and biomedical applications [ID 095]

**Institution(s):** Escuela Politécnica Nacional, Ecuador; CONICET, Argentina; Lund University, Sweden

We have developed cost-competitive dedicated methods and instruments to evaluate 1) the multispectral photonic and plasmonic responses of biological insect wings, resolved in angle and polarization under laboratory conditions, and 2) the far field responses in natural locations of large populations of flying insects (birds and bats, incidentally also). Three devices were designed, built, and tested to accomplish the former, [1-3] and for the latter, a portable self-sustaining Scheimpflug entomological Lidar was constructed and demonstrated in field campaigns in natural, highly biodiverse rainforests. [4] The methodological and instrumental details of these developments will be presented. Suitable application examples will be used to validate their corresponding performance and utility. These will include 1) the correlation between the multispectral diffuse reflectance of butterfly wings with the ecological and developmental biological niches inhabited by the corresponding insects. 2) We compare the performance of two different interrogation techniques, PiMICS and BioSpace, designed to obtain the multispectral angle and polarization photonic responses of insect wings. In both the 1) and 2) cases, the nano and microstructures of the wings underlying the optical responses and structure stability are also determined by SEM and thermogravimetric analysis. Finally, 3) measurements of the aerofauna biodiversity in a rainy forest were made under clear and foggy conditions. The advantages of the optical interrogation, both at the near and the far field, in very diverse settings, will be demonstrated.



**Figure 1: Optical methods for biostructure characterization and ranging.**

## References

- [1] Q. Lopez et al., *Materials* 17 (20), 5084 (2024)
- [2] H. Månefjord, *Rev. Sci. Instrum.* 93 113709 (2022).
- [3] J. C Howell et al., arXiv:2412.04679
- [4] V. Santos et al., *Applied Spectroscopy* 77(6).593 (2023)

**Corresponding author:** Cesar Costa. **Email:** cesar.costa@epn.edu.ec

# Spatio-chromatic vision changes following cataract surgery with multifocal diffractive intraocular lens implantation

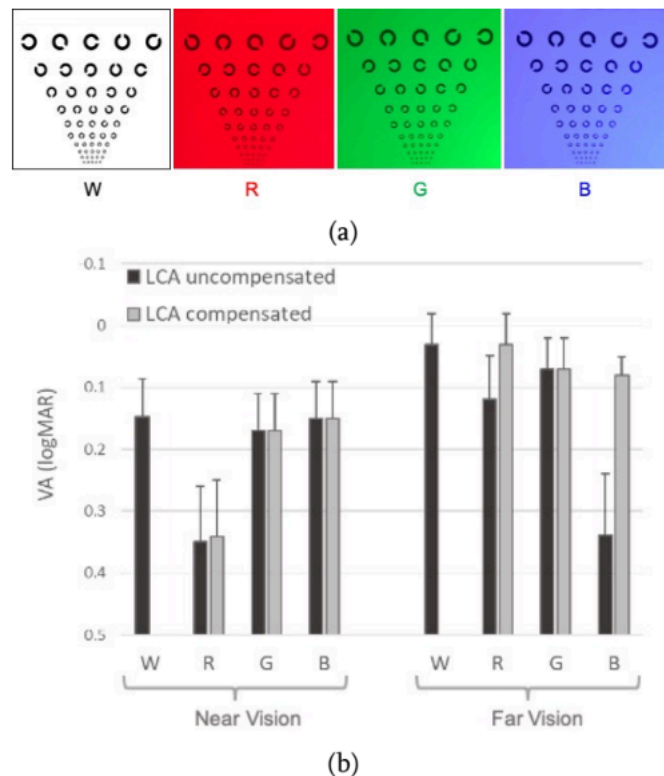
M. S. Millán, L. Clavé, A. Torrents, J. Armengol, F. Vega

**Topic(s):** Bio photonics and biomedical applications, Diffraction and gratings, Vision, color, and visual optics [ID 025]

**Institution(s):** Universitat Politècnica de Catalunya, España

Cataract surgery with intraocular lens (IOL) implantation can restore human vision far beyond the degradation produced by the loss of transparency of the natural lens. Current IOL designs are intended to compensate for common refractive errors (myopia, hyperopia, astigmatism) and age-related insufficiencies such as loss of accommodation or presbyopia. Presbyopia-correcting IOLs based on coaxial multifocality provide at least a lower power focus for distance vision and a higher power focus for near vision. We investigated multifocal diffractive IOLs and their effects on vision. Our study consisted of an in-vitro optical characterization using an on-bench eye model and an in-vivo IOL evaluation through clinical visual acuity (VA) assessment (logMAR units) of implanted patients.

We found asymmetric alterations in the spatio-chromatic vision of subjects implanted with trifocal diffractive intraocular lenses, with significant changes in resolution depending on the object distance and the spectral band of the illumination. These alterations can be detected with methods and materials of ordinary clinical examination. The alterations depend strongly on the characteristics of the diffractive design, in particular the diffraction orders used for far vision and presbyopia correction and the spectral band of the illumination [1].



**Figure 1: (a) Chart under white (W), red (R), green (G), and blue (B) light; (b) Clinical results: VA outcomes (mean  $\pm$  std dev) for far and near vision under W, R, G, B lights. LCA (longitudinal chromatic aberration).**

**Funding:** Spanish Government (Grant ref. PID2020-114582RB-I00/AEI/10.13039/501100011033).

## References

[1] Millan et al. Eye and Vision 10, 32 (15 pp) (2023).

**Corresponding author:** Maria Millán. **Email:** m.millan@upc.edu

# Ablation volume analysis in laser induced breakdown spectroscopy diagnosis on colon tissues

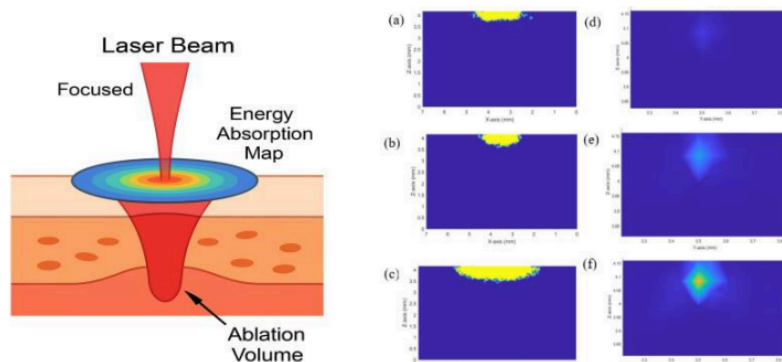
R. Sosa - Santos, J.L. Arce-Diego, F. Fanjul-Velez

**Topic(s):** Bio photonics and biomedical applications, Medical optics and biotechnology, Spectroscopy [ID 098]

**Institution(s):** Universidad de Cantabria, España; Universidad Privada Boliviana, Bolivia

Among surgical techniques, laser surgery enables precise and controlled ablation of biological tissue. The light-matter interaction underlying this process, based on photoablation or plasma-induced ablation [1], also forms the foundation of spectroscopic diagnostic techniques. Laser-Induced Breakdown Spectroscopy (LIBS) utilizes high-energy laser pulses to generate localized ablation and transient microplasmas on samples. As the plasma expands and cools, excited atoms/ions emit characteristic light captured by spectrometers, enabling elemental identification via spectral lines.

LIBS is a powerful tool for ex vivo biological tissue analysis due to its real-time multi-element detection and minimal sample preparation [2]. Precise control of the ablation volume is critical for LIBS reliability. An undersized ablation volume produces weak, noisy spectral signals, compromising elemental detection accuracy. Conversely, an oversized volume increases collateral thermal damage and dilutes tissue-specific spectral signatures by integrating elements from underlying layers or non-target cell types. This impedes accurate tissue discrimination [3], a cornerstone objective in applications like tumor margin identification. Each tissue exhibits a distinct chemical composition and spectral fingerprint [4]. Optimizing ablation depth and minimizing residual thermal energy are essential for robust LIBS signals and tissue safety. Monte Carlo simulations [5] model laser-tissue interactions to predict: (Figure 1, right, a,b,c) ablation depth profiles based on laser parameters and tissue optics, and (d,e,f) spatial distribution of stored energy deposited but not consumed by ablation. As conceptually illustrated in Figure 1 (left, tissue cross-section), these simulations map the ablation crater geometry and quantify adjacent energy accumulation using contour lines or heatmaps. Minimizing stored energy reduces thermal damage risk, while achieving optimal ablation depth ensures strong, tissue-specific LIBS signals.



**Figure 1: Ablation context and results of the simulation.**

## References

- [1] F. Fanjul-Vélez, I. Salas-García, J. L. Arce-Diego, "Analysis of laser surgery in non-melanoma skin cancer for optimal tissue removal", *Laser Physics* 25, 025606, 2015.
- [2] S. J. Rehse, "A review of the use of laser-induced breakdown spectroscopy for bacterial classification, quantification, and identification", *Spectrochim. Acta Part B At. Spectrosc.*, vol. 154, pp. 50-69, abr. 2019, doi: 10.1016/j.sab.2019.02.005.
- [3] M. A. Kasem, J. J. Gonzalez, R. E. Russo, y M. A. Harith, "LIBS analysis of artificial calcified tissue matrices", *Talanta*, vol. 108, pp. 53-58, abr. 2013.
- [4] Q. Wang, W. Xiangli, G. Teng, X. Cui, y K. Wei, "A brief review of laser-induced breakdown spectroscopy for human and animal soft tissues: pathological diagnosis and physiological detection", *Appl. Spectrosc. Rev.*, vol. 56, n.o 3, pp. 221-241, mar. 2021.
- [5] R. F. Sosa-Santos, J. L. Arce- Diego, F. Fanjul-Vélez, "Análisis predictivo del volumen de ablación en el diagnóstico mediante LIBS en tejidos de colon", *Actas del Congreso Anual de la Sociedad Española de Ingeniería Biomédica*, 2024.

**Corresponding author:** Rene Sosa. **Email:** rene-fernando.sosa@alumnos.unican.es

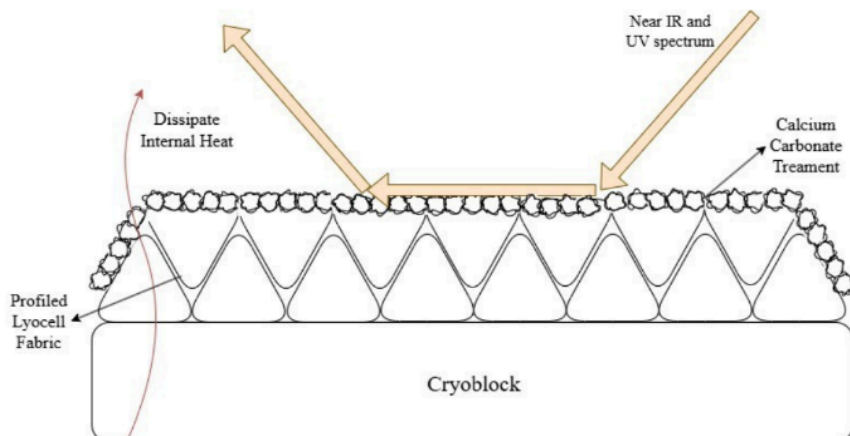
# Application of photonic principles for medical samples transportation: Radiative cooling fabrics in warm tropical weather

Alicia Zelada-Acosta, Alejandra Oviedo-Cortés, Ariana Y. Miranda-Jimenez, Erwin D. Moreno-Añez

**Topic(s):** Bio photonics and biomedical applications [ID 094]

**Institution(s):** Universidad Privada Boliviana, Bolivia

Rural areas with high temperatures and a lack of reliable electricity complicate cold-chain storage for the transportation of medical samples. To address this, we introduce a fabric bag with cooling properties to maintain samples at cold temperatures without electricity. This prototype is based on the principle of radiative cooling, which allows materials to reject solar radiation while emitting thermal energy in the mid-infrared spectrum. Our design consists of a portable cooling bag that combines cryoblock racks with an outer case fabric treated with poly(2-hydroxyethyl acrylate) and ions of calcium carbonate and barium sulfate [1]. This creates a surface that reflects sunlight and dissipates heat as shown in Figure 1, mimicking the effect of photonic films but with more accessible and affordable materials. To evaluate the efficiency of our design, we propose a series of comparative experiments consisting of temperature measurements of physiological serum exposed to sunlight while wrapped in our fabric. This work represents a first step towards the development of affordable, off-grid cooling solutions for biomedical applications in remote rural areas where conventional refrigeration is not feasible.



**Figure 1: Schematic diagram.**

## References

[1] Patamia, E. D., Yee, M. K., & Andrew, T. L. (2024). Microstructured Reflective Coatings on Commodity Textiles for Passive Personal Cooling. *ACS Applied Materials & Interfaces*, 16(43), 59424-59433. <https://doi.org/10.1021/acsami.4c15984>

**Corresponding author:** Alicia Zelada-Acosta. **Email:** antoniozelada1@upb.edu

# Bio-inspired retinal analysis theoretical model based on mantis shrimp vision for monitoring the progression of Sanfilippo síndrome

Adriana M. Suárez Oña, Mayra F. Ocampo Valdivia

**Topic(s):** Bio photonics and biomedical applications, Image processing, vision and artificial intelligence, Medical optics and biotechnology, Vision, color, and visual optics [ID 113]

**Institution(s):** Universidad Privada Boliviana, Bolivia

Mucopolysaccharidosis type III (MPS III), commonly known as Sanfilippo syndrome, is a lysosomal storage disease characterized by the accumulation of heparan sulfate, which causes neuronal degeneration [1]. A bioindicator associated with this pathology is the structural and functional changes in the retina, the monitoring of which is essential for evaluating disease progression [2]. This paper proposes a bio-inspired theoretical model based on the vision of the mantis shrimp (*Odontodactylus scyllarus*), a marine crustacean whose optical specializations include high sensitivity to polarized light, spectral resolution, and highly accurate spatial filtering [3]. This model is based on the computational simulation of these capabilities applied to fundus autofluorescence (FAF) images previously acquired using standard clinical equipment. The analysis flow consists of four stages (Fig. 1): FAF image preprocessing, multispectral analysis, computational polarimetry using Gabor filters and receptive field spatial filtering, combining wavelets and Gabor filters [4]. Although the model's accuracy does not replace that of a clinical examination or a real polarimetric sensor, it allows for a non-invasive, sensitive, reproducible, and cost-effective analysis of retinal micro-alterations associated with MPS III.

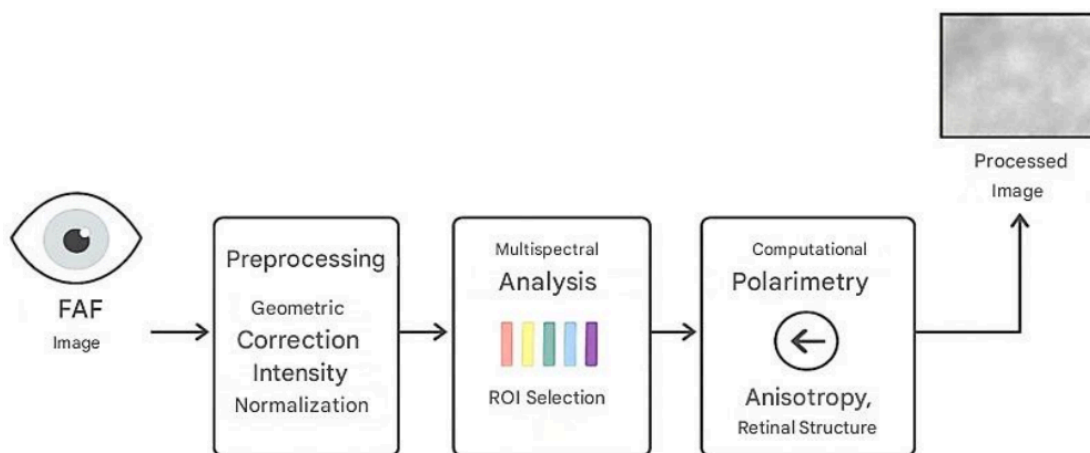


Figura 1: Analysis flow of the bioinspired model for the detection of retinal alterations in MPS III.

## References

- [1] N. Benetó, L. Vilageliu, D. Grinberg y I. Canals, "Sanfilippo syndrome: molecular basis, disease models and therapeutic approaches," *International Journal of Molecular Sciences*, vol. 21, no. 21, art. 7819, Oct. 2020.
- [2] M. S. García y J. A. Pérez, "Retinal autofluorescence analysis in lysosomal diseases," *Public Library of Science (PMC)*, 2014.
- [3] A. Altaqui, P. Sen, H. Schrickx, J. Rech, J.-W. Lee, M. Escuti, W. You, B. J. Kim, R. Kolbas, B. T. O'Connor y M. Kudenov, "Mantis shrimp-inspired organic photodetector for simultaneous hyperspectral and polarimetric imaging," *Science Advances*, vol. 7, n.º 10, art. eabe3196, mar. 2021. 2014.
- [4] Autonomous University of Madrid, "Image processing for the detection of [4] retinal biomarkers," *UAM Institutional Repository*, 2018.

**Corresponding author:** Adriana Suárez. **Email:** adrianasuarez1@upb.edu

## Contouring of residual limb by white light profile for medical prosthetics

Joaquin S. Rivera, Daniel Aquino S., Rodrigo C. Salcedo, Ivan Choque Aquino

**Topic(s):** Bio photonics and biomedical applications, Instrumentation, measurement and metrology, Optics in computing [ID 048]

**Institution(s):** Universidad Nacional Jorge Basadre Grohmann, Perú

Surface topology is essential in the fabrication of medical prosthetics [1], a properly designed surface can minimize friction and enhance compatibility with the patient's tissue, preventing irritation or discomfort. To address this, we present an experimental method for digitizing a 3D residual limb as a sample using white line projection [2,3]. A profilometer utilizing white line profiles was employed to scan the sample. The sample examined belongs to a volunteer. Initial findings reveal a 3D model of the sample, which was subsequently used for 3D printing the measured structure. Carefully controlled surface characteristics will contribute to improving material strength, reducing early wear, and extending the prosthesis's durability.

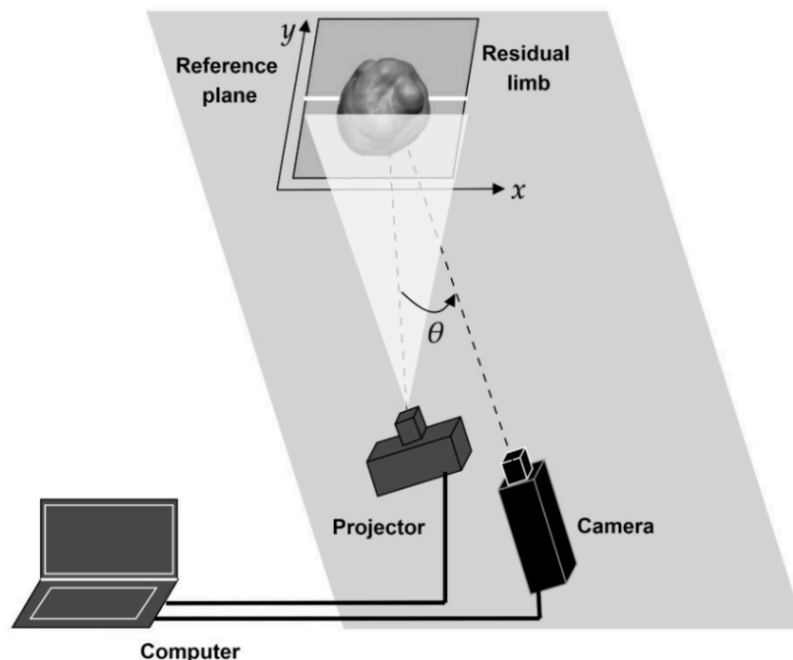


Figure 1: Experimental setup of a white line projection technique.

### References

- [1] Xue, J., Zhang, Q., Li, C., Lang, W., Wang, M., & Hu, Y., *Applied Sciences*, 9(7), 1458 (2019). "3D face profilometry based on a galvanometer scanner with infrared fringe projection at high speed".
- [2] Vilchez-Rojas, H. L., Rayas, J. A., & Martínez-García, A., *Optics and Lasers in Engineering*, 134, 106295 (2020). "Use of white light profiles for the contouring of objects".
- [3] Cutti, A. G., Santi, M. G., Hansen, A. H., & Fatone, S., *Sensors*, 24(7), 2350 (2024). "Accuracy, repeatability, and reproducibility of a hand-held structured-light 3D scanner across multi-site settings in lower limb prosthetics".

**Corresponding author:** Joaquin Sifuentes. **Email:** jsifuentesri@unjbg.edu.pe

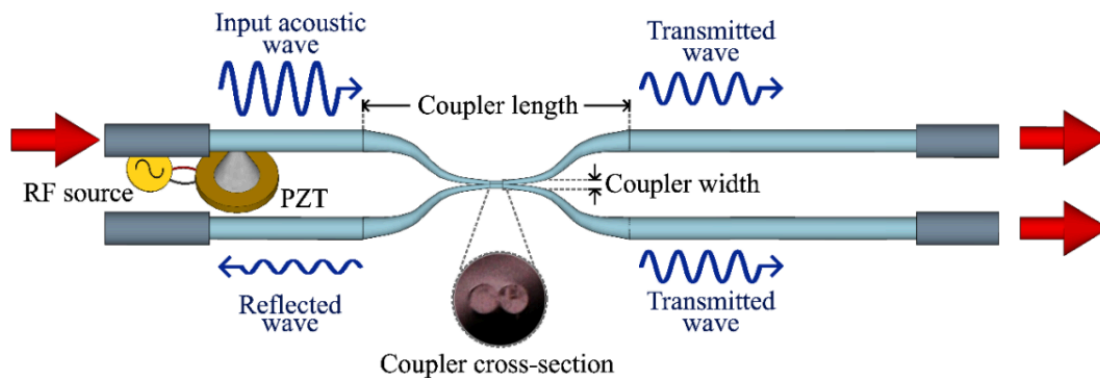
## Fiber-based acoustic and optic fused couplers

M. Bello-Jiménez, Y. Navarro-Martínez, E. Hernández-Escobar, R. López-Estopier, M. V. Hernández-Arriaga, J. Flores-González, and M. V. Andrés

**Topic(s):** Fiber optics, sensors and optical communications [ID 009]

**Institution(s):** Universidad Autónoma de San Luis Potosí, México; Universidad de Valencia, España

The experimental development of a 2×2 fiber-based acoustic and optical coupler is presented. The device consists of a fused biconical tapered structure, designed to enable dual-field operation -both acoustic and optical- through controlled tapering parameters using a standard fusing and pulling technique [1]. To investigate the acoustic field propagation, two experimental scenarios were analyzed. In the first configuration, a purely acoustic coupler with no optical coupling was fabricated, allowing a preliminary demonstration of the structure's capacity to act as a fiber-based acoustic coupler for propagating flexural acoustic waves. These waves were induced into the fiber using an aluminum horn attached to a piezoelectric disk (PZT) driven by a radio frequency (RF) source (see Figure 1) and were analyzed by measuring their amplitude at each coupler port using an extrinsic fiber-tip interferometer [2]. By varying the tapering parameters of the coupler width, different acoustic coupling ratios were achieved, ranging from 73:27 to 36:64, with excess losses between 3 and 6 dB and negligible return loss. Subsequently, by adjusting the coupler length and width, simultaneous optical and acoustic coupler was obtained. Since the acoustic frequency of the travelling flexural waves were in the 2-MHz region, the optical behavior was monitored around the 1550-nm region, where attenuation resonances can be observed. Coupling ratios of 44:56 and 47:53 were achieved for the optical and acoustic coupling, respectively. This dual-field operation highlights the potential of fused biconical fiber couplers as multifunctional platforms to allow the integration of in-fiber acousto-optic devices.



**Figure 1: Acousto-optic fiber-based coupler experimental scheme. An optical microscope image of the coupler cross section is shown at the inset.**

### References

- [1] B. S. Kawasaki, K. O. Hill, and R. G. Lamont, *Opt. Lett.* 6, 327 (1981).  
 [2] M. Bello-Jiménez, E. Hernández-Escobar, Y. Navarro-Martínez, and M. V. Andrés, *Meas. Sci. Technol.* 35, (2024).

**Corresponding author:** Yareli Navarro. **Email:** a268990@alumnos.uaslp.mx

# Point sensors and fiber characterization techniques based on forward stimulated Brillouin scattering

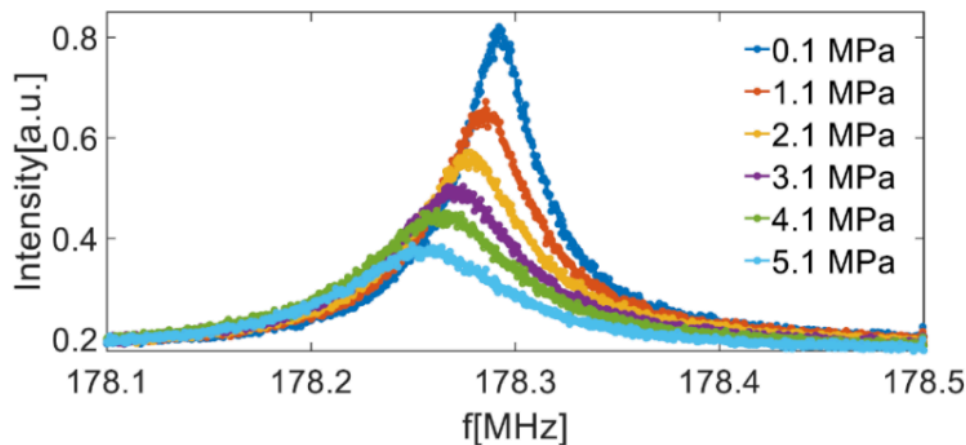
C. Álvarez-Ocampo, J. Julián-Barriel, A. I. Garrigues-Navarro, A. S. Paterno, M. Delgado-Pinar, J. L. Cruz, A. Díez, M. V. Andrés

**Topic(s):** Fiber optics, sensors and optical communications [ID 014]

**Institution(s):** Universidad de Valencia, España; Santa Catarina State University, Brazil

Forward stimulated Brillouin scattering (FSBS) in optical fibers can be exploited to develop point sensors and fiber characterization techniques. Regarding point sensor applications, we have demonstrated discriminative and simultaneous measurement of temperature and strain. We have also been able to demonstrate an all-optical mass-microbalance with a detection limit in the picogram range, showing its potential for biosensing applications. Regarding the fiber characterization techniques, FSBS has shown to be a unique tool for the measurement of Poisson's ratio of an optical fiber with record accuracy, its temperature coefficient, and its nonlinearity with strain. Similarly, optical fiber diameter variations can be measured with a resolution of a few nanometers.

The above point sensor applications and fiber characterization techniques have been developed using optical pump and probe techniques. Our work has been focused on investigating different FSBS probing methods based on optical resonances, in order to achieve higher sensitivity than using more conventional probe techniques (for example, a Sagnac interferometer). First, we investigated the use of narrow long-period fiber gratings and Bragg gratings [1]. Second, we developed a probing technique based on high Q factor whispering-gallery mode resonances of the optical fiber [2]. Third, we have investigated the use of high Q fiber ring resonators [3]. As a result, few millimeters long point sensors have been demonstrated. Recently, we have investigated a pressure sensor based on FSBS, and FSBS in silica microspheres.



**Figure 1:** Spectrum of radial acoustic resonance  $R_{0,4}$  for different pressures, in a standard optical fiber.

**Acknowledgments:** Ministerio de Ciencia, Innovación y Universidades and the European Regional Development Fund (PID2023-146725OB-I00, CNS2023-145717); Generalitat Valenciana (CIPROM/2022/30).

## References

- [1] L. A. Sánchez, A. Díez, J. L. Cruz, M. V. Andrés, *Opt. Lett.* 45, 5331 (2020).
- [2] L. A. Sánchez, M. Delgado-Pinar, A. Díez, M. V. Andrés, *Adv. Opt. Mater.* 12, 2301629, (2024).
- [3] A. I. Garrigues-Navarro, M. Delgado-Pinar, A. Díez, M. V. Andrés, *J. Lightwave Technol.*, in press (2025).

**Corresponding author:** Miguel Andrés. **Email:** miguel.andres@uv.es

# Optical Fiber Sensor Based on CS–TA Functionalized E-SMS Structure for the Selective Detection of Microplastics in Water

Brayan Patiño-Jurado, Arturo Gaviria-Calderón, Rodrigo Acuna Herrera, Pedro Torres, and Jorge Garcia-Sucerquia

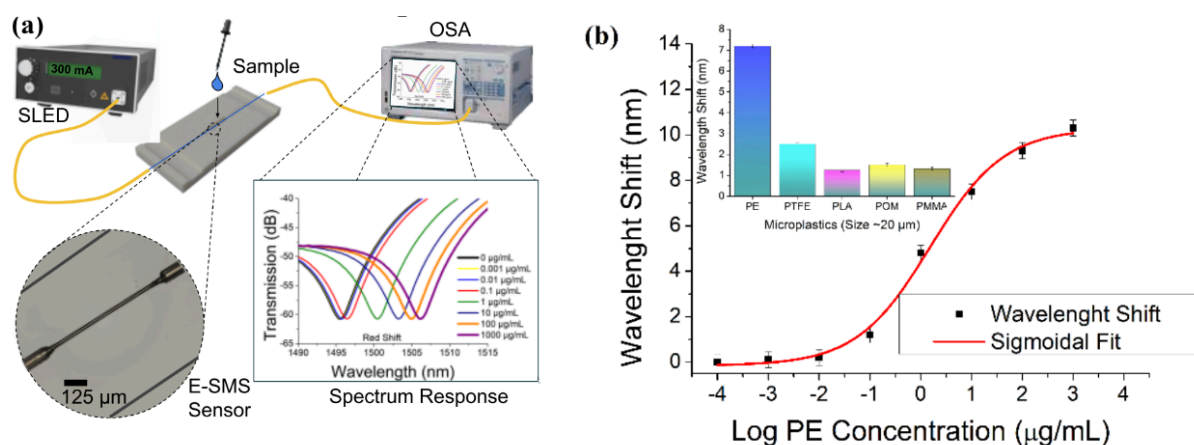
**Topic(s):** Fiber optics, sensors and optical communications [ID 041]

**Institution(s):** Universidad Nacional de Colombia, Colombia

Microplastics have emerged as a ubiquitous environmental pollutant, infiltrating marine and freshwater ecosystems and posing risks to both wildlife and human health [1]. Their small size makes their quantitative detection very challenging, demanding sensitive and selective technologies [2], that if they are cost-effective are even better. In this work, the fabrication and evaluation of a cost-effective optical fiber-based sensor for the selective detection of polyethylene (PE) microplastics in aqueous solutions is presented. The sensor consists of an E-SMS (Etched-Singlemode-Multimode-Singlemode) fiber structure, which was surface functionalized with a chitosan–tannic acid (CS–TA) conjugate. This functionalization is aimed to increase both the sensitivity and selectivity to PE microplastics, via the enhancing of the chemical affinity between the conjugate and the plastic surface.

The sensor was fabricated by splicing two single-mode fibers to a 15 mm large multimode fiber and then etched into 40% hydrofluoric acid; the resulting sensor is seen in the zoomed-in circle of panel (a) in Fig. 1 that illustrates the full setup. The functional coating was prepared by synthesizing a CS–TA conjugate through a mild aqueous reaction involving EDTA, hydrogen peroxide and ascorbic acid, to immobilize on the etched fiber surface by immersion in CS–TA conjugate and controlled heating. Microplastic samples such as PE, PMMA, PTFE, acetal and PLA, were prepared as fine powders, dispersed in water with surfactants and ultrasonication, and diluted in a concentration range from 1000 to 0.001 ppm.

From the results in Fig 1 panel (b), a concentration-dependent response to PE is evident, with a sensitivity of 3.92 nm/μg/mL and a detection limit of 0.1 μg/mL (100 ppb). Furthermore, selectivity tests demonstrated a significantly greater response to PE than to other microplastics, indicating effective molecular recognition by the CS–TA film. These results support the feasibility of using CS–TA functionalized E-SMS fiber sensors as a cost-effective, selective, and sensitive platform for microplastic detection in water samples.



**Figure 1: (a) Experimental setup with spectra obtained. (b) Detection results with selectivity test in the inset.**

## References

- [1] M. Sajjad et al., "Microplastics in the soil environment: A critical review," *Environ. Technol. Innov.*, vol. 27, p. 102408, Aug. 2022, doi: 10.1016/J.ETI.2022.102408.
- [2] Z. Huang, B. Hu, and H. Wang, "Analytical methods for microplastics in the environment: a review," *Environ. Chem. Lett.* 2022 211, vol. 21, no. 1, pp. 383–401, Sep. 2022, doi: 10.1007/S10311-022- 01525-7.

**Corresponding author:** Brayan Patiño-Jurado. **Email:** bjpatinoj@unal.edu.co

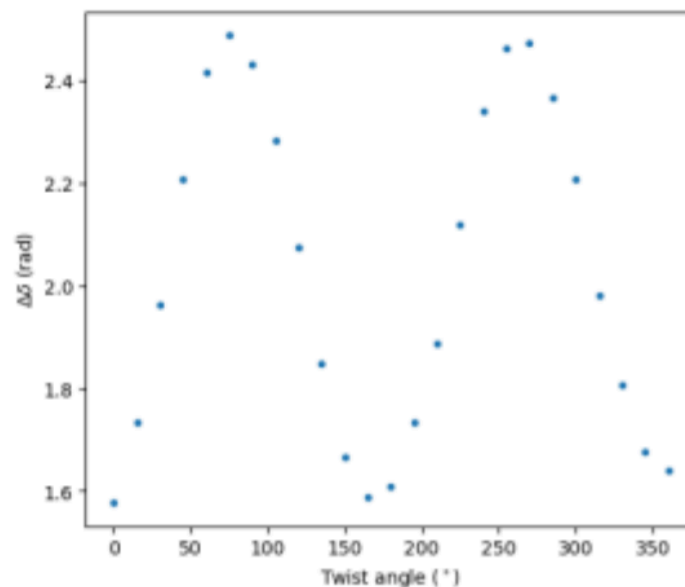
# Sensing Fiber Twist through State of Polarization-Induced Phase Shifts

Ana Teixeira, Susana Silva, Orlando Frazão

**Topic(s):** Fiber optics, sensors and optical communications, Physical optics, Remote sensing and sensors [ID 007]

**Institution(s):** INESC TEC, Portugal

In recent years, there has been growing interest in the use of optical fibers as sensors, particularly by exploiting the state of polarization (SOP) of light [1]. Polarization is a highly sensitive parameter that responds to external perturbations in the fiber, making it a powerful tool for sensing applications. In this work, we focus on understanding the twist of a fiber influences the phase of light propagating through it. To investigate this, we recorded the SOP of light at various twist angles and analyzed the corresponding phase variations. The phase variation ( $\Delta\delta$ ) was determined using the average values of the Stokes parameters,  $S_2$  and  $S_3$ , by means of  $\Delta\delta = \tan^{-1}(S_3/S_2)$  [2]. We found that the phase changes with the variation of the twist angle, with sinusoidal behavior. These findings demonstrate that the experimental setup possesses strong potential for accurately sensing twist of optical fibers.



**Figure 1:** Phase variation with applied fiber twist.

**Acknowledgements:** This work is partially supported by: "SUBMarine cableS for ReSearch and Exploration | SUBMERSE" - EU funded project (HORIZON-INFRA-2022-TECH-01 Grant agreement 101095055), and "GEOSENSE – Polarization Harnessing in Submarine Optical Cables for Global Geophysical Sensing", funded by Fundação para a Ciência e a Tecnologia (FCT), reference: 2023.15220.PEX, DOI: <https://doi.org/10.54499/2023.15220.PEX>.

## References

- [1] S. Pellegrini, G. Rizzelli, L. Andrenacci, L. Minelli, D. Pileri, G. Bosco, 2024 Italian Conference on Optics and Photonics (ICOP), 17-19 June, Italy (2024). "Polarization-based Optical Fiber Sensing: A State-of-the-Art Review". 10.1109/ICOP62013.2024.10803652
- [2] R. Talebi, F.T. Ghahfarokhi, D. Vashaei, J. Opt. Soc. Am. B 37, 2848 (2020). "Photoinduced tunable birefringence and dichroism in silver nanogratings". 10.1364/JOSAB.399604

**Corresponding author:** Ana Teixeira. **Email:** [ana.i.teixeira@inesctec.pt](mailto:ana.i.teixeira@inesctec.pt)

# Low-Coherence Interferometry for Analog Optical Communication

Eneas N. Morel, Santiago Cerrotta, Jorge R. Torga

**Topic(s):** Fiber optics, sensors and optical communications [ID 010]

**Institution(s):** Universidad Tecnológica Nacional, Argentina

We report a novel application of low-coherence interferometry (LCI) [1-2] in the field of optical communications [3-6]. This work investigates the use of LCI from a first-principles perspective, aiming to extend its applicability beyond traditional domains such as metrology and tomography [7-10]. We introduce an analog signal transmission and reception system based on LCI, including specifically designed interferometric modulation and demodulation schemes. The theoretical foundation of the proposed communication architecture is developed in detail, supported by numerical simulations that validate the concept. Finally, we present experimental results that demonstrate the feasibility and effectiveness of the system in the intended application context.

## References

- [1] B. L. Danielson and C. Y. Boisrobert, "Absolute optical ranging using low coherence interferometry," *Appl. Opt.* 30, 2975–2979 (1991)
- [2] R. Leitgeb, C. Hitzenberger, and A. Fercher, "Performance of fourier domain vs. time domain optical coherence tomography," *Opt. Express* 11, 889–894 (2003).
- [3] E. Agrell, M. Karlsson, A. R. Chraplyvy, et al., "Roadmap of optical communications," *J. Opt.* 18, 063002 (2016).
- [4] V. V. Shcherbakov, A. F. Solodkov, and A. A. Zadernovsky, "Analysis of intensity modulation response of analog fiber-optic links," in *IEEE 13th International Conference on Laser and Fiber-Optical Networks Modeling (LFNM)*, Odessa, 2016, pp. 24–26.
- [5] P. J. Winzer and R.-J. Essiambre, "Advanced optical modulation for-mats," *Proc. IEEE* 94, 952–985 (2006).
- [6] T. Hovell, R. S. Matharu, J. Petzing, et al., "Lens less fiber-deployed low-coherence interferometer for in-situ measurements in nonideal environments," *Opt. Eng.* 59, 1 (2020).
- [7] E. N. Morel, N. A. Russo, J. R. Torga, et al., "Application of a long-range swept source optical coherence tomography-based scheme for dimensional characterization of multilayer transparent objects," *Opt. Eng.* 56, 1 (2017).
- [8] I. Grulkowski, J. J. Liu, B. Potsaid, et al., "High-precision, high-accuracy ultra long range swept-source optical coherence tomography using vertical cavity surface emitting laser light source," *Opt. Lett.* 38, 673–675 (2013).
- [9] S. Cerrotta, J. R. Torga, and E. N. Morel, *Time Fourier Domain Low Coherence Interferometry* (Optica Publishing Group in Biophotonics. Congress: Biomedical Optics, 2022), pp. 3–4.
- [10] S. Cerrotta, J. R. Torga, and E. N. Morel, "Long-range frequency domain low-coherence interferometry detector for industrial applications," *J. Opt. Soc. Am. A* 40, C1–C21 (2023).

---

**Corresponding author:** Eneas Nicolas Morel. **Email:** nmorel@frd.utn.edu.ar

## Figure-8 fiber laser with dynamically controlled switching characteristic

O. Pottiez, L.A. Rodriguez-Morales, L.M. Gonzalez-Vidal, H.E. Ibarra-Villalon

**Topic(s):** Fiber optics, sensors and optical communications, Laser and laser optics, Nonlinear optics, Ultrafast optics [ID 038]

**Institution(s):** Centro de Investigaciones en Óptica, México; Universidad Autónoma Metropolitana Unidad Azcapotzalco, México

Thanks to their low cost and flexibility, passively mode-locked fiber lasers are attractive sources of short and ultrashort pulses for a broad range of applications. However, many applications, in particular medical and industrial, require intense, high-energy pulses with low ( $\sim$ kHz) repetition rates, which challenges the design of fiber-based sources. Indeed, typical cavity lengths in the order of 10s to 100s of meters yield pulse repetition frequencies in the MHz range; a high repetition rate also reduces the energy per pulse, as the available pump energy is distributed among a larger number of pulses. In principle, pulse energy can be enhanced (and repetition rate decreased) simply by increasing the cavity length. Although such strategy yielded some success in the normal dispersion regime in the  $1\ \mu\text{m}$  spectral region [1], at longer wavelengths (1550 to 2000  $\mu\text{m}$ , anomalous dispersion regime of conventional fiber), which are more attractive in particular for medical applications, the cavity length can hardly be extended beyond the km range [2] as excess nonlinearities and saturable absorber overdriving (which favor multiple pulsing), the buildup of intense interpulse noise and instabilities attributed to uncontrolled birefringence in long cavities all drastically limit pulse energy. Alternatively, the pulse repetition frequency can be reduced by using pulse pickers or acousto-optic modulators, for example, resulting however in increased complexity. Now a regime known as Q-switching mode locking in passive lasers allows increasing the pulse energy, as they are not emitted continuously but only during the “Q-switched-like” modulation windows [3]. In this work, we propose a strategy to tailor the pulse properties, in particular their energy and intensity, through dynamic polarization control. The proposed scheme is a figure-8 fiber laser in which the nonlinear optical loop mirror (NOLM) is polarization imbalanced (PI-NOLM) [4]. Contrary to conventional, power-imbalanced NOLM schemes, the PI-NOLM switching characteristic, in particular its switching power, depends on input polarization [5]. By dynamically adjusting the polarization state at the PI-NOLM input using a polarizer, one can tune the switching characteristic and in this way exert a control in real time on the laser dynamics, and thus on pulse properties, maximizing their energy and intensity. These numerical results are complemented with experimental results.

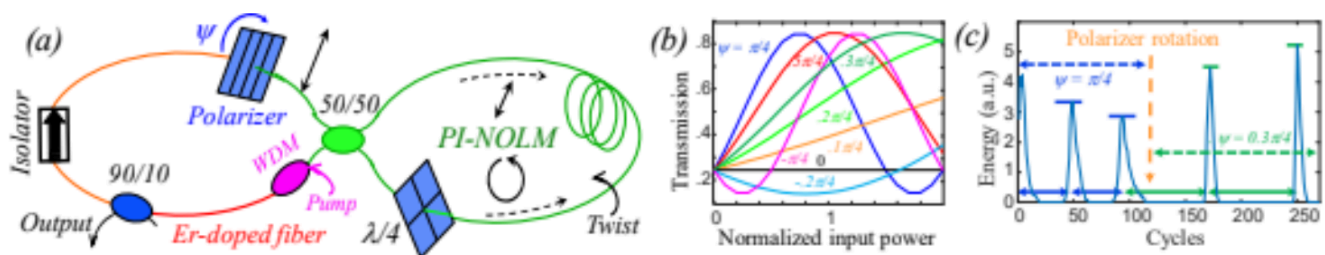


Figure 1: (a) Laser setup, (b) PI-NOLM transmission, (c) Pulse energy oscillations.

This work was supported by CECIHTI “Ciencia Básica y de Frontera” program (grant CBF2023- 2024-612).

### References

- [1] S. M. Kobtsev et al., *Laser Physics* 20, 351 (2010).
- [2] L. A. Rodriguez-Morales et al., *Optics and Laser Technology* 126, 106068 (2020).
- [3] R. Lopez-Estopier et al., *Results in Optics* 5, 100115 (2021).
- [4] O. Pottiez et al., *Applied Optics* 50, E24 (2011).
- [5] O. Pottiez et al., *Optics Communications* 254, 152 (2005).

**Corresponding author:** Olivier Pottiez. **Email:** pottiez@cio.mx

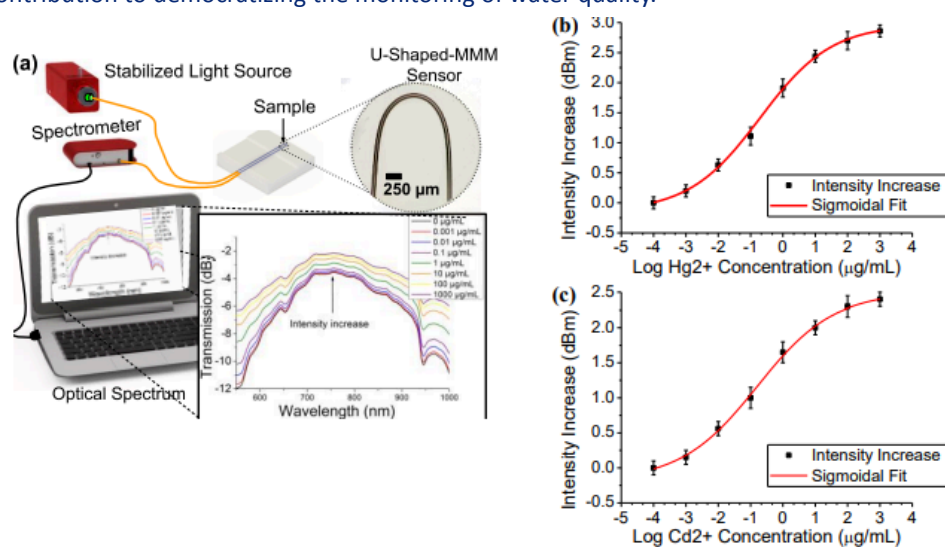
# U-Bent MMM Optical Fiber Sensor for the Detection of Mercury and Cadmium Ions in Aqueous Solutions

Arturo Gaviria-Calderón, Brayan Patiño-Jurado, and Jorge Garcia-Sucerquia

**Topic(s):** Fiber optics, sensors and optical communications [ID 042]

**Institution(s):** Universidad Nacional de Colombia, Colombia

Heavy metal contamination in water, particularly by mercury ( $\text{Hg}^{2+}$ ) and cadmium ( $\text{Cd}^{2+}$ ) ions, means significant environmental and health risks due to their toxicity and tendency to bioaccumulate [1]. Conventional detection methods are often expensive, complex, and time-consuming [2], reducing the opportunities for its democratization. In this work, the development of U-Bent multimode-multimode-multimode (U-MMM) optical fiber sensors for the sensitive and selective detection of  $\text{Hg}^{2+}$  and  $\text{Cd}^{2+}$  ions in aqueous solutions is presented. The simplicity and effectiveness of this proposal constitutes our contribution to democratizing the monitoring of water quality.



**Figure 1: (a) Experimental setup. (b) and (c) Detection results of the U-Bent MMM sensor.**

Multimode interference and enhanced light-medium interaction within a bent multimode fiber segment, are the phenomena that rule the operation of the U-MMM sensor. Figure 1 shows the sensor setup in panel (a) and its performance in panels (b) and (c). For mercury detection, the UMMM sensor surface was functionalized with a chitosan/ $\text{Fe}_2\text{O}_3$  nanocomposite film. Adsorption of  $\text{Hg}^{2+}$  ions into this coating induces changes in the local refractive index, producing measurable increase in the transmitted optical spectrum with detection capabilities down to  $0.001 \mu\text{g/mL}$  (1 ppb) with a sensitivity of  $0.053 \text{ dBm}/\mu\text{g/mL}$ , as shown in panel (b). For cadmium detection, the U-MMM fiber sensor was coated with a green-synthesized gold nanoparticle (AuNP) film stabilized by chitosan and polyvinyl alcohol (PVA). The AuNP-functionalized surface selectively binds  $\text{Cd}^{2+}$  ions, that produce measurable variations in optical transmission to  $\text{Cd}^{2+}$  concentrations up to  $0.001 \mu\text{g/mL}$  (1 ppb) with a sensitivity of  $0.041 \text{ dBm}/\mu\text{g/mL}$ , as presented in panel (c).

## References

- [1] K. G. Pavithra, P. SundarRajan, P. S. Kumar, and G. Rangasamy, "Mercury sources, contaminations, mercury cycle, detection and treatment techniques: A review," *Chemosphere*, vol. 312, p. 137314, Jan. 2023.
- [2] A. Gaviria-Calderón, J. Garcia-Sucerquia, B. Patiño-Jurado, and J. F. Botero-Cadavid, "Competitive fiber optic sensors for the highly selective detection of mercury in water," *Appl. Opt.* Vol. 62, Issue 3, pp. 592-600, vol. 62, no. 3, pp. 592–600, Jan. 2023.

**Corresponding author:** Arturo Gaviria. **Email:** argaviriaca@unal.edu.co

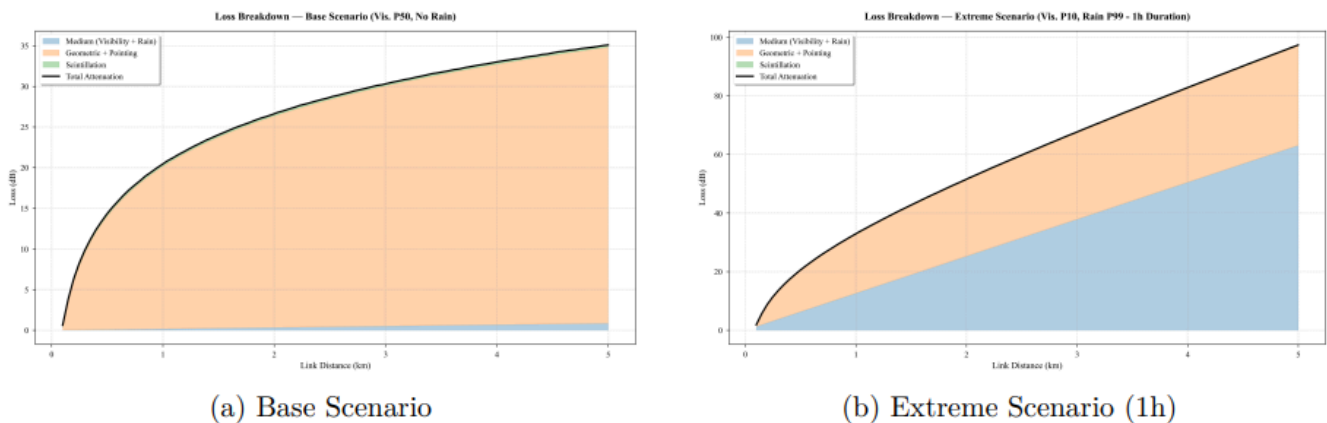
# Analysis of Atmospheric Factors in Free-Space Optical (FSO) Communications for High-Altitude Urban Environments in La Paz, Bolivia

Carlos Gironda, Rene Sosa

**Topic(s):** Fiber optics, sensors and optical communications, Laser and laser optics [ID 072]

**Institution(s):** Universidad Privada Boliviana, Bolivia

Free Space Optical (FSO) communications are a promising technology, whose performance is severely affected by atmospheric conditions. This study provides a comprehensive analysis of FSO link performance in the Bolivian Altiplano, a high-altitude region with distinctive climatic features. Unlike sea-level links where atmospheric turbulence is a critical limiting factor, the conducted analysis reveals that at elevations of approximately 3700 m a.s.l., such as in the municipality of Achocalla (Bolivia), turbulence becomes negligible, contributing only 0.3 dB of attenuation. Through Monte Carlo simulations that incorporate local meteorological data and models for rain and fog attenuation, the dominant factors are identified as geometric and pointing losses (a fixed component of 34 dB at 5 km) and, crucially, attenuation due to precipitation during the wet season. A key finding is the high sensitivity of the link to the duration of rain events, with attenuations ranging between 20.1 dB and 63.1 dB for the same daily rainfall percentile (P99), depending on whether a duration of 6 or 1 hour is assumed, respectively. These results provide essential design criteria for FSO systems in high-mountain regions, indicating that efforts should focus on optimizing the optical design and allocating adequate power margins for rain, while complex turbulence mitigation schemes can be disregarded.



**Figure 1: Breakdown of attenuation components for representative operating conditions.**

## References

- [1] S. A. Al-Gailani, M. F. M. Salleh, A. A. Salem, R. Q. Shaddad, U. U. Sheikh, N. A. Alcelan, and T. A. Almohamad, "A Survey of Free Space Optics (FSO) Communication Systems, Links, and Networks," *IEEE Access*, vol. 9, pp. 7353–7373, 2021.
- [2] S. M. Yasir, N. Abas, S. Raut, N. R. Chaudhry, and M. S. Saleem, "Investigation of optimum FSO communication link using different modulation techniques under fog conditions," *Heliyon*, vol. 8, no. 12, p. e12516, 2022.
- [3] M. A. Khalighi and M. Uysal, "Survey on free space optical communication: A communication theory perspective," *IEEE Communications Surveys & Tutorials*, vol. 16, no. 4, pp. 2231–2258, 2014.

**Corresponding author:** Esteban Gironda. **Email:** estebangironda1@upb.edu

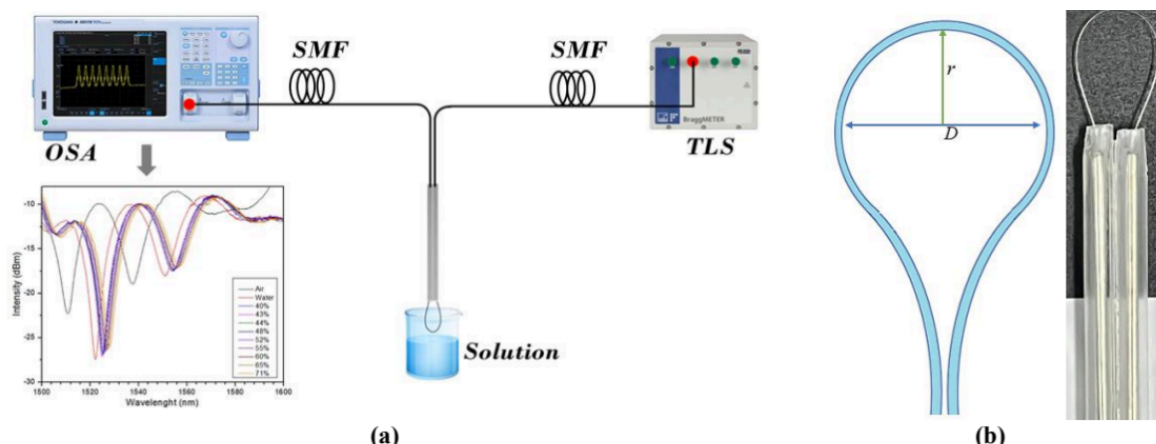
# Optical sensors based on optical fibers in Mach-Zehnder type interferometry configuration for measuring ethanol concentration

L. Espejo-Bayona, Sindi Horta, Duber Avila

**Topic(s):** Fiber optics, sensors and optical communications, Remote sensing and sensors [ID 020]

**Institution(s):** Universidad Popular del Cesar, Colombia

This study presents the development and characterization of an optical device based on a single-mode optical fiber for measuring the concentration of ethanol in an analyte. The proposed configuration consists of a curved, balloon-shaped uncoated optical fiber, whose operating principle is based on Mach-Zehnder type interferometry. This geometric arrangement takes advantage of the high sensitivity of fiber optic interferometers, allowing changes in ethanol concentration to be detected by shifting the peaks of minimum intensity in the interference patterns of the optical signal. The device fabrication involved bending a section of bare single-mode optical fiber into a balloon shape, the ends of which were secured using a standard protective sleeve to ensure mechanical stability. Figure 1a illustrates both the conceptual design and the implemented physical configuration. For the experimental characterization, a setup was used that included a tunable laser source (TLS) in the 1500–1600 nm range and an optical spectrum analyzer (OSA, Yokogawa model AQ6370E), allowing the measurement of the signal transmitted through the device. The results demonstrate that the balloon-shaped configuration improves the interaction between the guided mode and the analyte, thus increasing the sensitivity compared to conventional geometries [1]. This approach offers advantages such as manufacturing simplicity, low cost, and high sensitivity, making it promising for applications in fluid monitoring and quality control in the food and pharmaceutical industries.



**Figure 1: (a) Experimental setup developed in the experiment, (b) Schematic diagram and final device developed.**

In this study, the device's parameters were evaluated, demonstrating its ability to measure ethanol concentrations ranging from 40% to 71%. Analysis of the interference patterns revealed peaks of minimum intensity, associated with destructive interference characteristic of asymmetric Mach-Zehnder interferometers. These peaks exhibited a shift toward longer wavelengths with increasing ethanol concentration, confirming their dependence. The sensor's sensitivity was quantified at 0.109%/nm, highlighting its high reproducibility and repeatability in measurements. Although its sensitivity is comparable to that of traditional devices [1], this configuration offers significant advantages in terms of manufacturing simplicity, low cost, and ease of implementation. These results suggest that the sensor has high potential for applications in the food and pharmaceutical industries.

## References

[1] V. Cardoso, P. Caldas, M. Giraldo, O. Frazão, J. Costa, J.L. Santos, *Sensors* 22, 7652 (2022). "Optical Strain Gauge Prototype Based on a High Sensitivity Balloon-like Interferometer and Additive Manufacturing".

**Corresponding author:** Luis Espejo. **Email:** lespejo@unicesar.edu.co

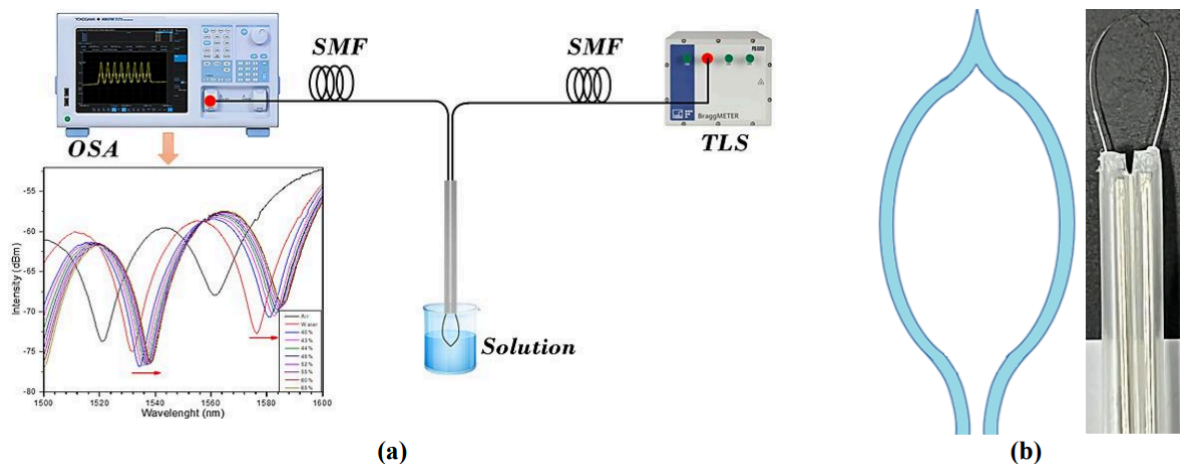
# Optical sensors based on balloon-shaped optical fibers with tip-induced deformation in a Mach-Zehnder interferometer configuration for measuring ethanol concentration

L. Espejo-Bayona, Sindi Horta, Duber Avila

**Topic(s):** Fiber optics, sensors and optical communications, Remote sensing and sensors [ID 045]

**Institution(s):** Universidad Popular del Cesar, Colombia

This study presents the development and characterization of an optical device based on a single-mode optical fiber for measuring ethanol concentration in an analyte. The proposed configuration consists of an uncoated optical fiber curved in the shape of a balloon with a deformation in the sensing zone with a controlled electric arc. This geometric arrangement takes advantage of the high sensitivity of fiber optic interferometers, allowing changes in ethanol concentration to be detected by shifting the minimum intensity peaks in the interference patterns of the optical signal. The device manufacturing involved bending a section of bare single-mode optical fiber into a balloon shape, to which an electric arc was applied over the sensing area of the fiber, to ensure mechanical stability the ends of the fiber were fixed using a standard protective sleeve. Figure 1 illustrates both the experimental design and the physical configuration implemented. For the experimental characterization, a setup was used that included a tunable laser source in the range of 1500–1600 nm and an optical spectrum analyzer, allowing the measurement of the signal transmitted through the device. The results demonstrate that the balloon-shaped configuration with an electric arc improves the interaction between the guided mode and the analyte, thus increasing the sensitivity compared to conventional geometries [1].



**Figure 1: (a) Experimental setup developed in the experiment, (b) Schematic diagram and final device developed..**

In this study, the parameters of the proposed device were evaluated, demonstrating its ability to measure ethanol concentrations ranging from 40% to 65%. Analysis of the interference patterns revealed peaks of minimum intensity, associated with destructive interference characteristic of asymmetric Mach-Zehnder interferometers. These peaks exhibited a shift toward longer wavelengths with increasing alcohol concentration, confirming their dependence. The sensor's sensitivity was measured at 0.183%/nm, highlighting its high reproducibility and repeatability in measurements. Although its sensitivity is comparable to that of traditional devices, this configuration offers significant advantages in terms of manufacturing simplicity, low cost, and ease of implementation.

## References

[1] L. Jing, H. Yu, Z. Tong, W. Zhang, Y. Tao and J. Mu, Applied Physics B 130, 151 (2024). "Temperature-insensitive optical fiber sensor based on SMF-NCF-FMF-NCF-SMF spindle shaped structure for refractive index measurement".

**Corresponding author:** Luis Espejo. **Email:** lespejo@unicesar.edu.co

## Emissions into the atmosphere from the Ing. Héctor R. Lara Sosarefinery, Cadereyta de Jiménez, Nuevo León, México

Claudia I. Rivera Cárdenas, Hugo A. Barrera-Huertas

**Topic(s):** Atmospheric and ocean optics, Instrumentation, measurement and metrology, Remote sensing and sensors, Spectroscopy [ID 036]

**Institution(s):** Universidad Nacional Autónoma de México; Instituto Politécnico Nacional, México

The Ing. Héctor R. Lara Sosa refinery, located in Cadereyta de Jiménez, Nuevo León, México, is one of the eight refineries that form part of the National Refining System of Mexico (in addition to Ciudad Madero, Deer Park, Dos Bocas, Minatitlán, Salina Cruz, Salamanca, and Tula) and was inaugurated in 1979. As part of a research project, several measurement campaigns were carried out during 2025 at the Ing. Héctor R. Lara Sosa refinery with the objective to quantify sulfur dioxide (SO<sub>2</sub>) and nitrogen dioxide (NO<sub>2</sub>) using two compact mobile instruments based on the differential optical absorption spectroscopy methodology (DOAS) [1]. The two mobile DOAS instruments used are composed of a spectrometer with different wavelength ranges, depending on the objective trace gases.

In this case we used a spectrometer covering the wavelength range of 274-432 nm in order to quantify SO<sub>2</sub> and a second spectrometer covering the wavelength range of 357-510 nm to quantify NO<sub>2</sub>). In addition, an optical fiber, a telescope and a GPS were used for each system. The software MobileDOAS [2] was used to acquire spectra in real time along with information about the time and location (latitude and longitude) of each measurement. Further details of the instrument can be found in [3]. Measured spectra were re-evaluated using the QDOAS software version 3.2 [4] using the 307-317 nm wavelength region for SO<sub>2</sub> and the 405-465 wavelength region for NO<sub>2</sub>. This contribution presents preliminary results on the emissions released into the atmosphere from this refinery. These results are part of a series of measurement campaigns that will be carried out in the following years at the Ing. Héctor R. Lara Sosa refinery with the objective of characterizing its emissions to the atmosphere at different times of the year, as well as the horizontal distribution pattern of the quantified emissions.

### References

- [1] U. Platt, U and J. Stutz. (2008). Differential optical absorption spectroscopy: Principles and applications. Springer Verlag.
- [2] Y. Zhang, M. Johansson and D. Norgaard. (2021). Mobile DOAS, Version 6.3.1. Optical Remote Sensing Group, Chalmers University of Technology, Sweden.
- [3] B. Galle, C. Oppenheimer, A. Geyer, A.J.S. McGonigle, M. Edmonds, L. Horrocks. (2002). A miniaturised ultraviolet spectrometer for remote sensing of SO<sub>2</sub> fluxes: a new tool for volcano surveillance. *Journal of Volcanology and Geothermal Research* 119(1-4), 241-254. [https://doi.org/10.1016/S0377-0273\(02\)00356-6](https://doi.org/10.1016/S0377-0273(02)00356-6).
- [4] T. Danckaert, C. Fayt, M. van Roozendaal, I. De Smedt, V. Letocart, A. Merlaud and G. Pinardi. (2017). QDOAS Software user manual Version 3.2. Belgian Institute for Space Aeronomy.

---

**Corresponding author:** Claudia Rivera. **Email:** [claudia.rivera@atmosfera.unam.mx](mailto:claudia.rivera@atmosfera.unam.mx)

---

## The GEMM initiative by OPTICA & AGU and the BEACO2N sensors

Angela M. Guzman H.

**Topic(s):** Atmospheric and ocean optics, Remote sensing and sensors [ID 109]

**Institution(s):** Universidad del Atlántico, Universidad Nacional de Colombia, Colombia

The GEMM Global Environment Measurement & Monitoring initiative [1] is an international initiative of OPTICA and AGU (American Geophysical Union) that seeks to engage universities, research centers, measurement standards agencies, companies, and other scientific societies around the world to form regional GEMM centers. The initiative is led by Professor Ronald Cohen of UC Berkeley (UCB), whose research group has developed the BEACO<sub>2</sub>N sensors [2], which measure CO, CO<sub>2</sub>, NO<sub>x</sub>, and PM<sub>2.5</sub> [3]. Its objective is to create an international network that brings together scientists, technologists, and policy makers to collaborate in the search for regional solutions to critical environmental and climate challenges from a local perspective but geared towards a global framework. The Colombian Caribbean region is in a privileged geographical position to provide climate data to the international community. The Universidad del Atlántico (UA) convened 15 research groups to create a Multidisciplinary Environmental Research Network (RIMA) to develop research in the following areas: (1) Instrumentation and development of environmental sensors, (2) Monitoring of GHG and PM<sub>2.5</sub> through a dense sensor network, (3) Hydrogeological monitoring of coastal areas, and (4) Modeling of environmental phenomena by AI. Recently, UA and UCB signed a collaboration agreement that will allow for the installation of an environmental sensor network in Barranquilla.

### References

- [1]  
[https://www.optica.org/about/newsroom/news\\_releases/2024/september/global\\_environmental\\_measurement\\_and\\_monitoring\\_\(gemm\)\\_initiative\\_expands\\_welcoming\\_the\\_university/](https://www.optica.org/about/newsroom/news_releases/2024/september/global_environmental_measurement_and_monitoring_(gemm)_initiative_expands_welcoming_the_university/)
- [2] J. Kim, A. A. Shusterman, K. J. Lieschke, C. Newman, and R. C. Cohen, *AMT*, 11, 1937–1946 (2018). “The Berkeley Atmospheric CO<sub>2</sub> Observation Network: field calibration and evaluation of low-cost air quality sensors”.
- [3] M. Y. Patel, P. F. Vannucci, J. Kim, W. M. Berelson, and R. C. Cohen. *AMT*, 17, 1051–1060 (2024). “Towards a hygroscopic growth calibration for low-cost PM<sub>2.5</sub> sensors”.

---

**Corresponding author:** Angela Guzmán. **Email:** amguzmanh@unal.edu.co

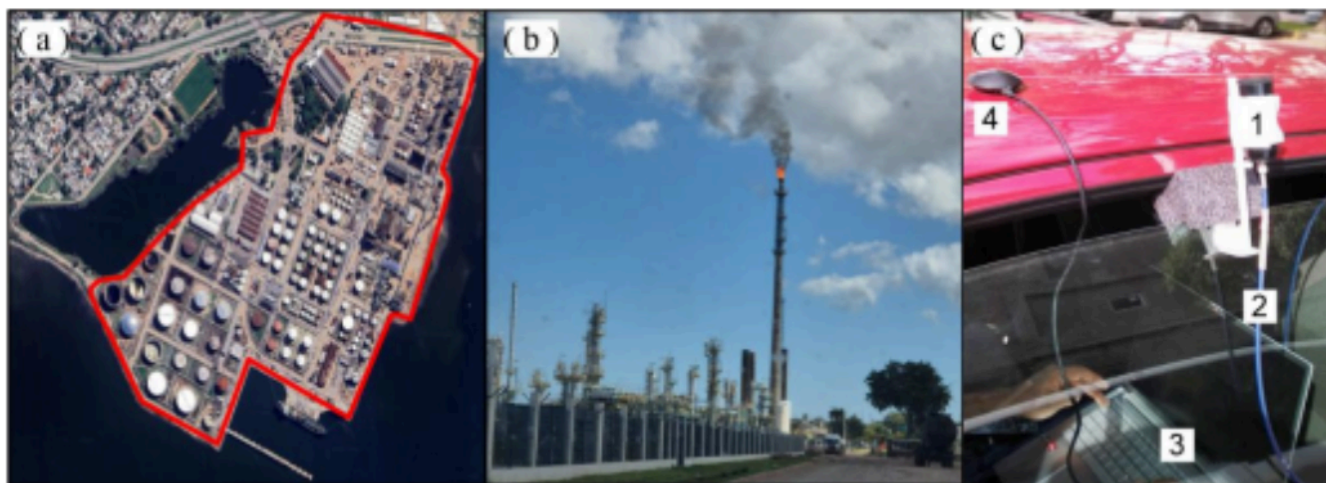
## Analysis of spectral structures influencing the detection of atmospheric trace gases

Adriana Silva, Roberto C. Barragán, Marco Coronato, Matías Osorio, Alejandro Agesta, Nicolás Casaballe, Claudia Rivera, and Erna Frins

**Topic(s):** Atmospheric and ocean optics, Remote sensing and sensors, Spectroscopy [ID 052]

**Institution(s):** Universidad de la República, Uruguay; Universidad Nacional de México, México

Differential Optical Absorption Spectroscopy (DOAS) is widely used to determine atmospheric trace gas abundances from multi-wavelength light measurements and to quantify trace gas emissions from mobile and stationary sources [1]. Mobile DOAS is a technique initially developed to scan and measure fixed emission sources within a specific geographic area, i.e., a volcano, using a zenith-observation DOAS system mounted on a mobile platform [2]. In this work, we present ground-based detection of trace gases and the presence of spectral structures that alter the measurements of atmospheric trace gases. We also discuss various factors that affect these measurements, including wind direction, reflections, and shadows. Mobile DOAS technique was used to register the solar spectral data, and the measurement instruments were mounted on a car while circulating within and around the Refinery "La Teja" in Montevideo, Uruguay. Figure 1(a) shows an aerial view of the refinery (outlined in red). Fig. 1(b) shows an image of a refinery chimney and structures for refining. Fig. 1(c) shows the experimental setup used; a zenith-pointing telescope (1) collects the scattered light, then focuses the light into an optical fiber (2) that directs the light into a spectrometer, which acquires the spectral information and sends the data to a computer (3), where the GPS (4) coordinates are simultaneously received.



**Figure 1: "La Teja" Refinery and Mobile DOAS experimental setup: (a) Aerial view of "La Teja" (b) Photograph of the refinery. (c) Experimental setup used.**

### References

- [1] Platt U., and Stutz J. 2008 *Differential Optical Absorption Spectroscopy: Principles and Applications* (Heidelberg: Springer), <https://doi.org/10.1007/978-3-540-75776-4>
- [2] Galle, B., Oppenheimer, C., Geyer, A., McGonigle, A. J. S., Edmonds, M., and Horrocks, L. (2003). A miniaturised ultraviolet spectrometer for remote sensing of SO<sub>2</sub> fluxes: a new tool for volcano surveillance. *Journal of Volcanology and Geothermal Research*, 119(1-4), 241–254. [https://doi.org/10.1016/s0377-0273\(02\)00356-6](https://doi.org/10.1016/s0377-0273(02)00356-6)

**Corresponding author:** Adriana Silva. **Email:** [adrianas@fing.edu.uy](mailto:adrianas@fing.edu.uy)

# Differentiation of air pollution sources in Montevideo using NO<sub>2</sub>, CO trace gas columns, and atmospheric aerosol properties

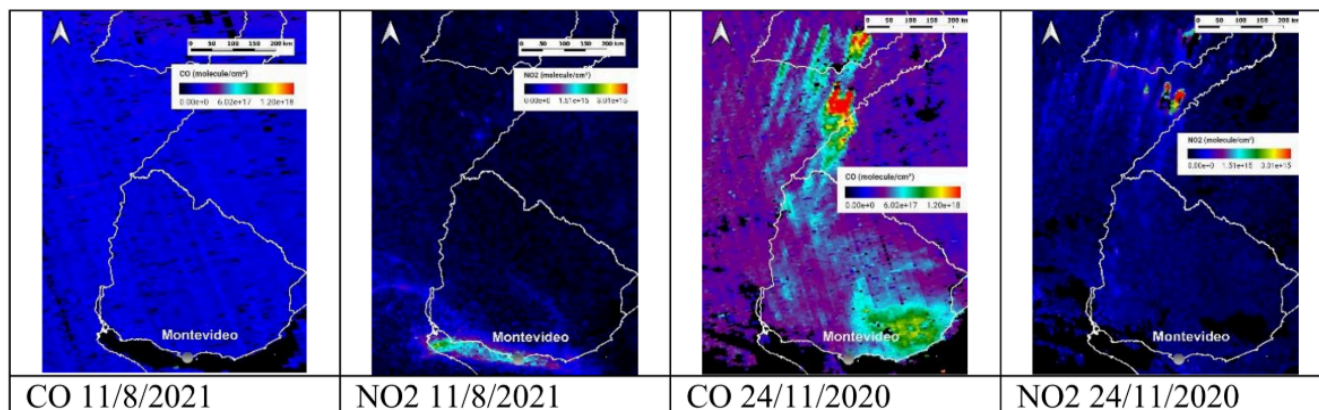
Alejandro Agesta, Erna Frins

**Topic(s):** Atmospheric and ocean optics, Remote sensing and sensors, Spectroscopy [ID 051]

**Institution(s):** Universidad de la República, Uruguay

The differentiation of atmospheric pollution sources is essential for environmental management and air quality studies. In this study we aim to differentiate urban emissions into the atmosphere from emission originating from large-scale biomass burning. This paper analyzes the results of combining satellite data of NO<sub>2</sub> and CO columns (TROPOMI) with aerosol properties from the AERONET station [2, 3] in Montevideo (Montevideo\_FING) to characterize and distinguish between these two types of sources. The analysis is based on the premise that forest fires emit large quantities of NO<sub>2</sub> and CO, with the typical atmospheric half-life of NO<sub>2</sub> being a few hours, while that of CO is several days [1].

Aerosols resulting from biomass burning possess properties that distinguish them from urban aerosols. In comparison, they are smaller in size, exhibit greater absorption of solar radiation, and have higher Angstrom exponent values [4]. On August 11, 2021, satellite images in Montevideo show an episode of high NO<sub>2</sub> column values (likely originating from Buenos Aires) as seen in Fig. 1, an aerosol fine mode fraction (FMF) of 0.79, and an Angstrom exponent of 1.55 according to the AERONET station. However, these increases are not accompanied by high CO column values. In contrast, on November 24, 2020, a CO transport event due to biomass burning (with NO<sub>2</sub> confined near the sources, an event previously studied by Osorio et al. [5]), registered an FMF of 0.94 and an Angstrom exponent of 2.1. These results show the potential of this approach, taking into account various parameters including local instruments and satellites, to identify and separate the contributions of different atmospheric pollution sources in the region.



**Figure 1:** Comparison of NO<sub>2</sub> and CO columns obtained from TROPOMI on 11/8/2021 with those from 24/11/2020. Panels a) and b) show urban pollution, and panels b) and c) show biomass burning.

## References

- [1] Wan, N. et al., (2023). ACP, 23(1), 711–724. <https://doi.org/10.5194/acp-23-711-2023>
- [2] O'Neill, et al., (2001). JGR, 106(D9), 9787–9806. <https://doi.org/10.1029/2000JD900245>
- [3] Dubovik, O. et al., JGR, 105(D16), 20673–20696. <https://doi.org/10.1029/2000JD900282>
- [4] Mattoo, S. et al., [https://doi.org/10.5067/MODIS/MOD04\\_L2.061](https://doi.org/10.5067/MODIS/MOD04_L2.061)
- [5] Osorio, M. et al., <https://doi.org/10.5194/acp-24-7447-2024>

**Corresponding author:** Alejandro Agesta. **Email:** aagesta@fing.edu.uy

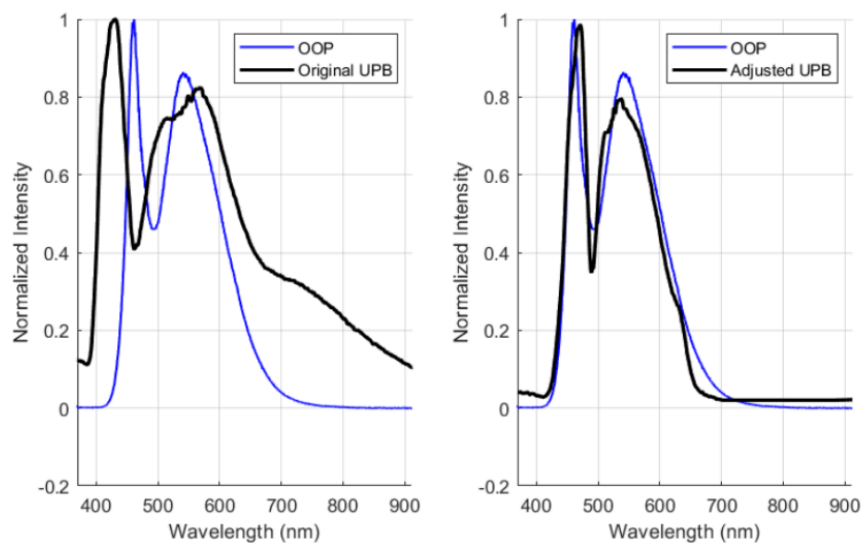
# A Data-based Protocol for a Low-cost Mobile Spectrometer Calibration

Marco De la Fuente Villarroel, Facundo Aliaga, Edgar Salazar

**Topic(s):** Spectroscopy [ID 086]

**Institution(s):** Universidad Privada Boliviana, Bolivia

Spectrometry is a well-established technique that has been extensively used for different purposes, including for example, biomedical, life-sciences and water testing [1]. Nevertheless, dedicated hardware for conducting spectral analysis is expensive, and its price increases with the spectral resolution. Recently, several attempts have been made to design spectrometers with off-the-self components, with similar performance as the one shown by commercial solution, being the one proposed by Ormachea et al. [2] (UPB) highlighted over the others due to its reduced cost and adaptability to mobile phone cameras, as well as its reproducibility. In this study, we propose and develop a comprehensive protocol that allows for the calibration of the UPB spectrometer taking as reference the OCEAN OPTICS USB 4000 (OOP). For that, we simultaneously took spectral signatures with UPB and OOP from a conventional White Light Emitting Diode (LED) under low-light conditions, with previous calibration. Afterwards, we pre-processed the data by point-wise matching the wavelengths with posterior interpolation and intensity normalization. We then implemented a Dynamic Warping (DW) algorithm that finds the minimum distant of the two signatures and, through indexation and interpolation using 14 control points, the UPB curve is adjusted to the OOP. Results of the calibration protocol can be seen in Fig. 1.



**Figure 1: Left: OOP and original UPB White LED spectrum. OOP and adjusted UPB White LED spectrum.**

## References

- [1] A. Das. Portable UV–Visible Spectroscopy–Instrumentation, Technology, and Applications. Portable Spectroscopy and Spectrometry, 179-207, (2021).
- [2] A. Villazon, O. Ormachea, A. Zenteno, & A. Orellan. A low-cost spectrometry remote laboratory. In International Conference on Remote Engineering and Virtual Instrumentation (pp. 198-209). Cham: Springer International Publishing (2022).

**Corresponding author:** Edgar Salazar. **Email:** edgarsalazar@upb.edu

## Enhancement of atomic emission intensity of heavy metals in LIBS using silver nanoparticles to increase the detection sensitivity of Cu and Pb

Elder Espinoza-Sanchez, Jhenry F. Agreda-Delgado, M. A. Valverde-Alva, W. Aldama-Reyna

**Topic(s):** Spectroscopy [ID 078]

**Institution(s):** Universidad Nacional de Trujillo, Perú

The application of the NELIBS technique (nanoparticles-enhanced LIBS) was studied to improve the atomic emission intensity of heavy metals (Cu and Pb) [1]. The samples used were copper (99.9% purity) and lead (99% purity) cubes, both with dimensions of 1 cm × 1 cm × 1 cm. On each sample, 10 μL of a silver nanoparticles (AgNPs) colloid in deionized water, previously synthesized by laser ablation in liquids [2], was deposited using a micropipette. The solvent was evaporated, and to increase the nanoparticles concentration, the process was repeated by adding an additional 10 μL onto the same pretreated surface. The LIBS spectra were obtained by irradiating the samples with a pulsed Nd:YAG laser (1064 nm), operating at  $(10.94 \pm 0.38)$  mJ/pulse for Cu + AgNPs and  $(7.16 \pm 0.42)$  mJ/pulse for Pb + AgNPs. The laser radiation was directed using a high-reflectance mirror and focused onto the sample with a 10 cm focal length lens; the sample was positioned at 7 cm, achieving an irradiation spot size of 1.5 mm. The complete experimental setup is shown in Fig. 1. The analysis of the atomic emission spectra revealed that, in the presence of AgNPs, the intensity of the characteristic Cu emission lines increased threefold compared to the samples without nanoparticles, while the Pb lines showed an approximate 70% enhancement. This signal amplification can be attributed to the coupling of surface plasmon generated by the nanoparticles [3]. These results highlight the potential of the NELIBS technique to improve sensitivity and detection limits in the spectroscopic analysis of heavy metals using LIBS.

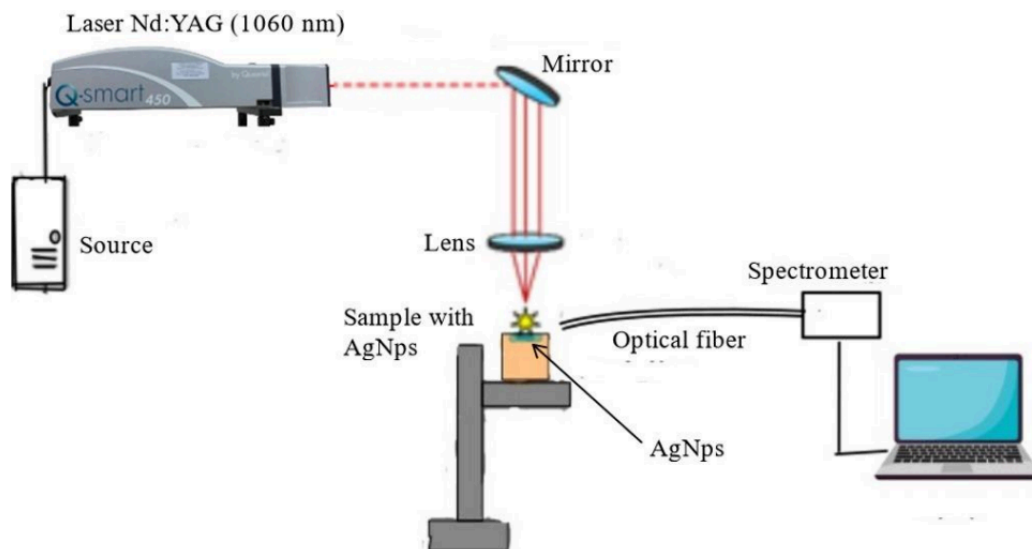


Figure 1: Schematic diagram..

### References

- [1] D. A. Cremers and L. J. Radziemski, Handbook of Laser-Induced Breakdown Spectroscopy, 2nd ed., Wiley, 2013. volume number to make it bold".
- [2] Aldama-Reyna, W., et al. "Photoacoustic study of changes in optical properties of colloids with silver nanoparticles produced by laser ablation." Int. J. Appl. Eng. Res 13 2018: 1408-1414.
- [3] J. Liu et al., "Enhancement mechanisms in nanoparticle-enhanced laser-induced breakdown spectroscopy," Spectrochimica Acta Part B, vol. 87, pp. 43–53, 2013.

**Corresponding author:** Elder Espinoza. **Email:** t1521200121@unitru.edu.pe

---

## Effects of Atmospheric Conditions on Infrared Data Transmission: Experimental Analysis in La Paz, Bolivia

Mariana Vasquez, Rene Sosa

**Topic(s):** Atmospheric and ocean optics, Instrumentation, measurement and metrology, Optics and photonics in the industry [ID 076]

**Institution(s):** Universidad Privada Boliviana, Bolivia

This article aims to verify whether atmospheric conditions in La Paz, such as solar radiation and low atmospheric density significantly degrade the efficiency of voice transmission via infrared (IR) in low-cost systems, in order to evaluate the feasibility of implementing this technology in high-altitude urban environments. Some atmospheric factors at high altitude can increase optical noise in basic receivers, reducing the signal-to-noise ratio (SNR) in unshielded systems. Furthermore, the presence of aerosols and high climatic variability in the Andean region could exacerbate the attenuation of IR signals, particularly in devices with economical components and limited filtering capacity. However, some argue that IR transmitters are less practical than other technologies such as RF or Li-Fi, due to their susceptibility to physical obstacles and limited range in uncontrolled conditions. Nevertheless, IR technology remains relevant in emerging applications, such as IoT security systems and data transmission in electromagnetically restricted environments, where privacy and immunity to interference are critical. In conclusion, this research will not only provide key data to optimize IR systems in Bolivia, considering local atmospheric conditions, but will also assess their competitiveness against other technologies, highlighting scenarios where their implementation would be technically and economically viable.

### References

- [1] Amaya Araujo, C. A., & Celeita Martinez, J. A. (2023). Caracterizacion de un sistema radio sobre comunicaci3n 3ptica inal3mbrica para entornos interiores.
- [2] de Electricidad, V., & Alternativas, E. (2021). Estudio complementario de impacto de la radiaci3n UV en paneles solares (datos UV de un a3o) y otros componentes expuestos en condiciones del altiplano boliviano Gestion 2021.
- [3] Gim3nez de Castro, C. G. (2023). Observando la cromosfera solar en el infrarrojo. Bolet3n de la Asociaci3n Argentina de Astronom3a, 64.

---

**Corresponding author:** Mariana Vasquez. **Email:** marianamontserrathvasquez@gmail.com

---

## Experimental study of polarization in the Normal Zeeman effect

Elian Raul Plata Arguello, Zandra Yoana Lizarazo Mejía

**Topic(s):** Physical optics [ID 056]

**Institution(s):** Optics and Signal Processing Group (GOTS), Universidad Industrial de Santander, Colombia

In the study of the normal Zeeman effect, polarization is traditionally analyzed in two configurations: the transverse mode, where the magnetic field is applied perpendicular to the observation direction of the radiation, in which a triplet ( $\sigma^+$ ,  $\pi$ ,  $\sigma^-$ ) is observed; and the longitudinal mode, where the magnetic field is applied in the same direction as the observation of the radiation, in which a doublet ( $\sigma^+$ ,  $\sigma^-$ ) is observed for  $1P_1$  levels. In both configurations, the observed polarization is well defined [1–2]. These observations are based on the interaction between the orbital magnetic moment and the applied magnetic field [3].

To study the behavior of the polarization of radiation observed at oblique angles to the magnetic field, this work uses the red line from a cadmium lamp. To characterize the polarization states, polarization is analyzed for two different oblique positions, and a triplet is observed in both cases. To determine the polarization state, it is necessary to filter one of the  $\sigma$  or  $\sigma^-$  components, which is achieved by configuring an elliptical polarizer. Based on the + – obtained parameters, the corresponding polarization ellipse is estimated.

From these results, it is inferred that for atoms in the presence of a magnetic field that splits into three Zeeman components, when observed at oblique angles to the applied magnetic field, the polarization is elliptical. This allows for the inference of a correlation between electronic transitions and polarization.

### References

- [1] Pieter Zeeman, On the influence of magnetism on the nature of the light emitted by a substance. The London Edinburgh, and Dublin Philosophical Magazine and Journal of Science, 43(262):226–239, 1897.
- [2] Niels Bohr. Lix. on the effect of electric and magnetic fields on spectral lines. The London, Edinburgh, and Dublin Philosophical Magazine and Journal of Science, 27(159):506–524, 1914
- [3] K. Hentschel et al., Compendium of quantum physics, 862 (2009)

---

**Corresponding author:** Zandra Lizarazo. **Email:** zylizar@uis.edu.co

# A Comparison of Metallic Nanoantenna Configurations for Single-Photon Emitters

Andrea Florez Anteliz, Gabriel Paciaroni, Diego Grosz, María Gabriela Capeluto

Topic(s): Nano photonics and metamaterials [ID 054]

Institution(s): Universidad de Buenos Aires, Argentina

Single-photon sources are essential components in quantum technologies, such as secure communication and optical quantum computing. However, their performance is often limited by spontaneous emission into multiple spatial modes, which reduces photon extraction efficiency. A promising strategy to overcome this limitation relies on coupling the emitter to metallic nanoantennas which can enhance and control emission directionality and intensity [1]. In this work, we present a comparative analysis of two metallic nanoantenna configurations: a dimer of rectangular bars and a dimer of T-shaped structures [2], both designed to couple with a quantum emitter, modeled by a point electric dipole, placed at the center of the gap. Using the finite element method implemented in COMSOL Multiphysics [3], we simulate the electromagnetic response of each system, evaluating the electric field distribution and the Purcell factor (PF). Figure 1 shows a comparison of the PFs obtained for a dimer of rectangular bars (70×20×30 nm) and for a T-shaped antenna, in which the transversal arm length  $b$  is varied while keeping the horizontal section constant. All T-shaped configurations exhibit a double peak: one at approximately 720 nm and another that shifts towards longer wavelengths as  $b$  increases. This behavior demonstrates that the T-shaped geometry enables spectral modulation of the main resonance through adjustments in its structure while providing an augmented Purcell factor.

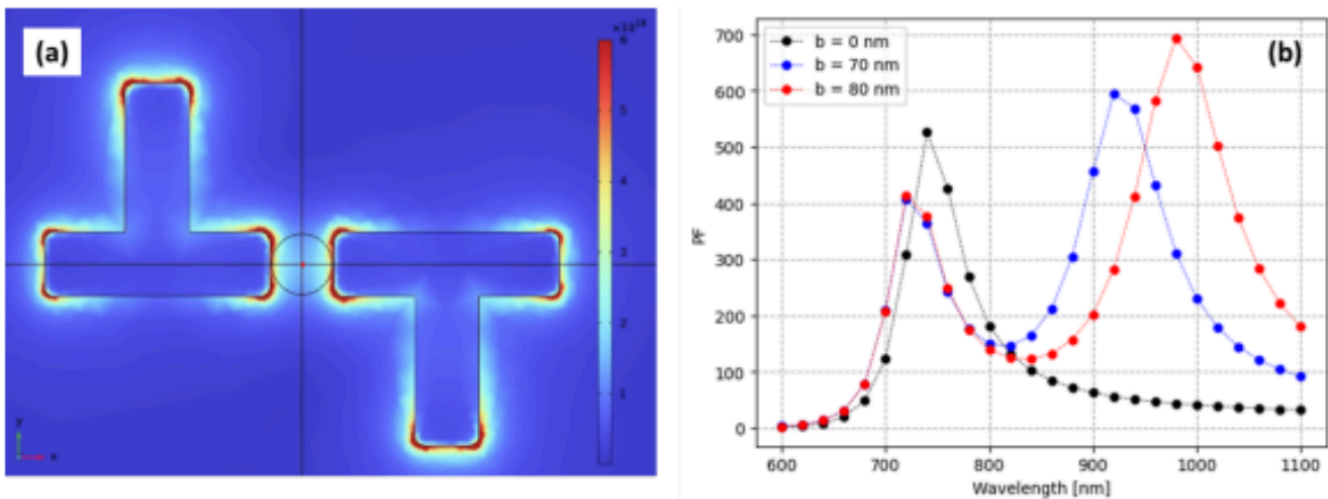


Figure 1: (a) Electric field distribution of a T-shaped antenna. (b) Purcell factors for a rectangular bar dimer ( $b = 0$  nm) and T-shaped antenna dimers with a different arm length.

## References

- [1] A. Mohammadi, V. Sandoghdar, M. Agio, Gold nanorods and nanospheroids for enhancing spontaneous emission, *New Journal of Physics*, 10, 105015, 2008.
- [2] K. Dopf, A. Schraml, J. Becker, M. Hentschel, H. Giessen, Coupled T-Shaped Optical Antennas with Two Resonances Localized in a Common Nanogap, *ACS Photonics*, 2, pp. 1644–1653, 2015.
- [3] COMSOL Multiphysics®, [www.comsol.com](http://www.comsol.com)

Corresponding author: Andrea Florez Anteliz. Email: [aflorez@df.uba.ar](mailto:aflorez@df.uba.ar)

# Optical Bullets with Angular Momentum in Nonlinear Waveguides

Carlos F. Sánchez, Humberto Michinel, and José R. Salgueiro

**Topic(s):** Nonlinear optics [ID 024]

**Institution(s):** Universidad Politécnica Salesiana, Ecuador; Universidade de Vigo, Spain

We investigate the existence, stability, and dynamics of optical pulsed beams that carry a phase singularity and propagate through a nonlinear graded-index waveguide. We explore their stabilization mechanisms through numerical simulations and we demonstrate the existence of stable stationary states due to a balance between nonlinear and linear effects. To our knowledge, this is the first prediction of these types of nonlinear waves.

The physical system is described by a 1+3D Nonlinear Schrödinger Equation with a cubic Kerr focusing response and a cylindrically-symmetric Gaussian modulation of the linear refractive index exclusively along the transverse direction, so no linear trapping is acting on the temporal envelope of the pulse[1]. To calculate the stationary states endowed with angular momentum, we have used a finite differences scheme and the resulting linear problem is iteratively solved using a globally convergent Newton method[2]. Several views of a stable stationary state calculated this way are shown on the left side of Fig.1.

Once the stationary states have been numerically generated, a split-step Fourier method is applied to study their stability during propagation. Some examples of unstable behavior are depicted on the right side of Fig. 1. As it can be seen, both modulational and azimuthal stabilities can destroy the beams, depending on the energy and the propagation constant of the input condition.

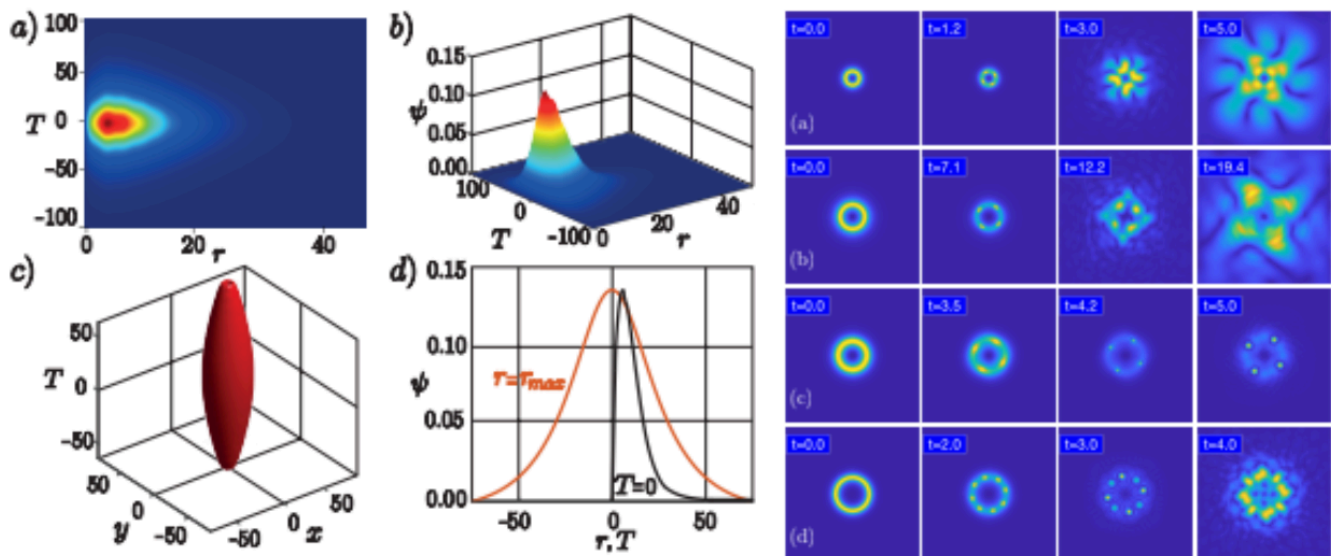


Figure 1: On the left side, we plot several views of a stable solution that is trapped due to the combination of nonlinear effects and a linear waveguide. Variables  $r$  and  $T$  correspond respectively to the radial and temporal cuts in dimensionless units. The right side displays examples of the evolution of several unstable states.

## References

- [1] Mihalache, D et. al Phys. Rev. E 70, 055603(R) (2004).  
 [2] J. R. Salgueiro, D. Olivieri, and H. Michinel, Optical and Quantum Electronics 39, 239 (2007).

**Corresponding author:** Humberto Michinel. **Email:** hmichinel@uvigo.es

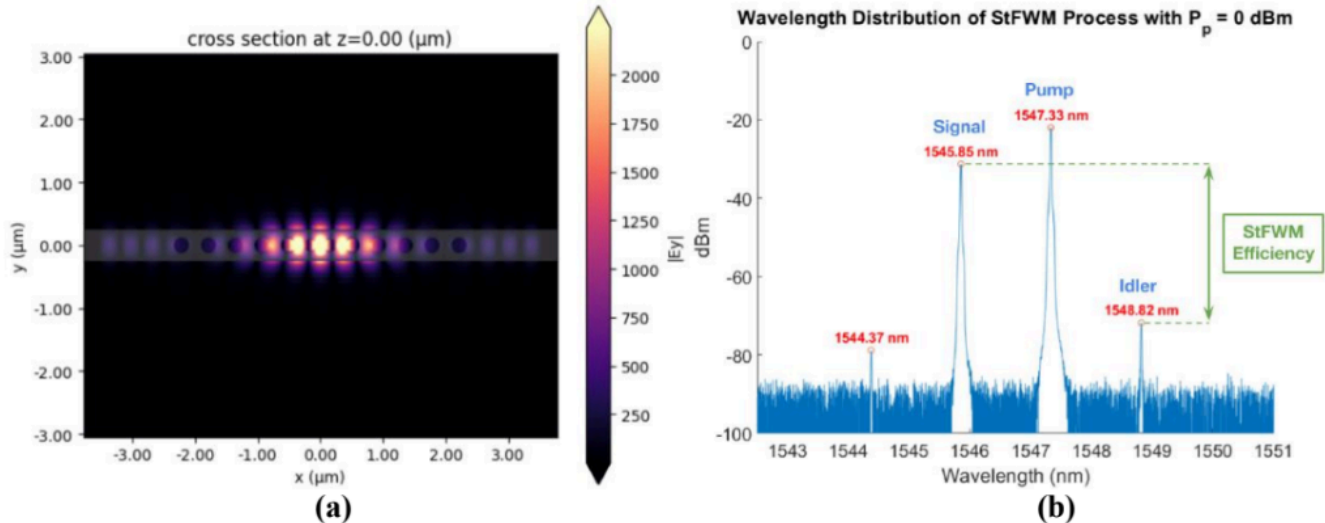
# Design and Simulation of GeSbS-Based Microcavities for Advanced Nonlinear Photonics

Samuel Huertas Rojas, Rafael A. Casalins Hernandez, Camilo Hurtado Ballesteros, Samuel Serna Otálvaro

**Topic(s):** Nonlinear optics [ID 035]

**Institution(s):** Universidad Nacional de Colombia, Colombia; Bridgewater State University, USA

Microcavities are fundamental elements in the development of advanced photonic technologies. For more than a decade, they have been used as key devices for emerging technologies with a high prospect that have the potential to solve key challenges in the design of optical sensors, as well as in the development of nanophotonic and quantum devices [1, 2]. In this context, our work explores the use of the chalcogenide material GeSbS [3] as a medium for the fabrication of microcavities, highlighting its potential for scalability and providing an arsenic (As) free glass to produce high-performance waveguides [4]. Considering the inherent advantages of this material for photonic applications and taking into account that it has a nonlinear refractive index comparable to silicon [4], we performed numerical simulations of various ring-resonators and one-dimensional (1D) micro-cavities, composed of periodic structures of equidistributed holes or also called Bragg reflector distribution [5] (Fig. 1.a). The objective of this paper is to evaluate and compare the optical performance of chalcogenide micro-cavities with respect to their silicon-based counterparts, considering different geometries and to identify those structures with the best figures-of-merit, i.e. low nonlinear losses, high quality factors, resource efficiency in manufacturing, stimulated four-wave mixing (StFWM) (Fig. 1.b), in order to establish optimal design criteria for future experimental implementations on frequency comb generation and entangled pair generation via spontaneous parametric down conversion (SPDC).



**Figure 1:** a) Simulation of a silicon-based Bragg micro-cavity with circular geometry perforations, showing the electric field profile and evidence of a strongly confined optical mode (image on the left). b) Spectral response of the StFWM process within a silicon ring resonator generating an idler signal, this graphic was taken from [6] (image of the right).

## References

- [1] W. B. Veldkamp, Proc. SPIE 1544, 287 (1991).
- [2] H. Kim, B. S. Song, T. Asano, and S. Noda, APL Photonics 8, 12 (2023).
- [3] B. Shen, H. Lin, S. Sharif Azadeh, J. Nojic, M. Kang, F. Merget, et al., ACS Photonics 7, 499 (2020).
- [4] S. Serna, H. Lin, C. Alonso-Ramos, A. Yadav, X. Le Roux, K. Richardson, et al., Photon. Res. 6, B37 (2018).
- [5] P. Velha, J. C. Rodier, P. Lalanne, J. P. Hugonin, D. Peyrade, E. Picard, et al., Appl. Phys. Lett. 89, 171121 (2006).
- [6] P. Brown, New Quantum Information Science Study at BSU: A Theoretical Study and Research Towards PIC Generation of Entangled Photons (2024).

**Corresponding author:** Samuel Huertas. **Email:** shuertas@unal.edu.co

# Optical Characterization of Infrared Key Fiber Materials: Transmission and Kerr Coefficient Measurements

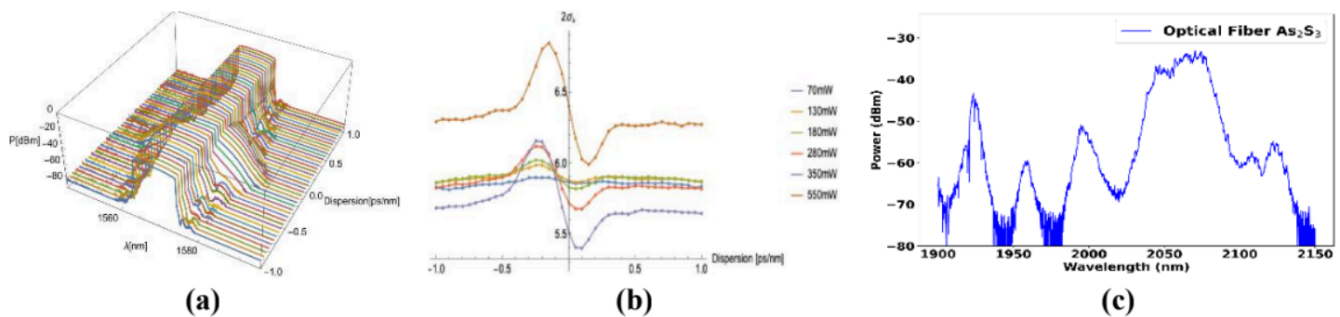
Camilo Hurtado, Samuel Huertas Rojas, Rafael A. Casalins-Hernandez, Pablo Bedoya, Samuel Serna

**Topic(s):** Nonlinear optics, Photonics [ID 050]

**Institution(s):** Universidad Nacional de Colombia, Colombia; Bridgewater State University, USA

The exponential growth of the photonics industry, which seeks to adapt to a wide range of applications in metrology, data transfer, sensing, and telecommunications and thus impacts both the industrial sector and scientific development, makes it necessary to characterize different platforms across multiple wavelength regions. In this work, we explore both the near-infrared (NIR) and mid-infrared (MIR) regimes, in the wavelength range of 1.4  $\mu\text{m}$  to 2  $\mu\text{m}$ . In the NIR region, we evaluate not only the linear response but also the nonlinear response using an ultrafast light source [1].

Furthermore, we present transmission measurements of commercially available optical fibers made of materials  $\text{SiO}_2$ ,  $\text{As}_2\text{S}_3$ , and  $\text{ZrF}_4$ , in the wavelength range of 1.4  $\mu\text{m}$  to 2  $\mu\text{m}$  by using a Chromacity Optical Parametric Oscillator (OPO). We have also performed nonlinear characterization of those fibers by employing the top-hat D-Scan technique [2,3]. This single-beam, non-destructive method, exploits controlled changes in pulse dispersion, enabling the determination of the third-order nonlinear coefficient ( $n_2$ ). We report  $n_2$  values for those fibers at 1.55  $\mu\text{m}$  and provide transmission spectra as a function of wavelength over the 1.4  $\mu\text{m}$ –2  $\mu\text{m}$  range.



**Figure 1: (a) Top-hat output spectrum for a  $\text{SiO}_2$  fiber (b) Spectral r.m.s (c) Transmission spectrum of  $\text{As}_2\text{S}_3$  measured using the optical parametric oscillator (OPO).**

Figure 1a shows the output spectrum measured with an optical spectrum analyzer at a fixed input power while sweeping the dispersion: depending on its sign, the pulse broadens or compresses. Figure 1b displays the root-mean-square (RMS) of the data and in Figure 1c, the transmission spectrum of  $\text{As}_2\text{S}_3$  is shown, illustrating the exploration of these platforms in the mid-infrared. These results highlight the importance of systematically characterizing both linear and nonlinear properties of optical materials across extended wavelength ranges, paving the way for more versatile and efficient photonic systems in next-generation technologies.

## References

- [1] H. Lin et al., "Mid-infrared integrated photonics on silicon: a perspective," *Nanophotonics*, vol. 7, no. 2, pp. 393–420, 2017.
- [2] F. Louradour, E. Lopez-Lago, V. Couderc, V. Messenger, and A. Barthelemy, "Dispersive-scan measurement of the fast component of the third-order nonlinearity of bulk materials and waveguides," *Opt. Lett.*, vol. 24, no. 19, pp. 1361–1363, 1999.
- [3] S. Serna and N. Dubreuil, "Bi-directional top-hat D-Scan: single beam accurate characterization of nonlinear waveguides," *Opt. Lett.*, vol. 42, no. 16, pp. 3072–3075, 2017.

**Corresponding author:** Camilo Hurtado. **Email:** [churtadob@unal.edu.co](mailto:churtadob@unal.edu.co)

---

## From Lab to Factory: Applied Photonics Solutions for Industry

Santiago Cerrotta ,Eneas N. Morel, Jorge R. Torga

**Topic(s):** Optics and photonics in the industry [ID 011]

**Institution(s):** Universidad Tecnológica Nacional, Argentina

The Applied Photonics Group (GFA) has been dedicated to the research and development of photonic technologies for over 20 years, with a strong focus on their transfer to the productive sector [1]. The GFA is located within an engineering faculty and is surrounded by a significant industrial hub in Campana, Buenos Aires, Argentina. The group's main area of expertise is the adaptation of Optical Coherence Tomography (OCT) [2] techniques for industrial applications. In this context, new types of detectors have been developed to extend the maximum measurement range to several centimeters [3,4], targeting applications such as the inspection of glass containers and windshields [5]. Additionally, low-cost equipment has been built to enhance technology transfer to small and medium-sized enterprises (SMEs), and customized processing algorithms have been designed for specific applications. Furthermore, the group has conducted a significant number of feasibility studies, technical services, and reports for various companies, employing a range of optical methods. The aim of this work is to present the motivations behind the development of new techniques, the applications implemented, and the experience gained over the years. We also intend to share practical advice and lessons learned through our interactions with different companies, from the perspective of a university-based research laboratory.

### References

- [1] Cerrotta, Santiago, (2023), "Nuevos detectores de interferometría de baja coherencia para aplicaciones industriales" (Tesis doctoral). <https://ria.utn.edu.ar/items/d6230a11-66b1-45a3-b3d4-b96ee1edfe75>
- [2] Aumann, Silke, et al. "Optical coherence tomography (OCT): principle and technical realization." High resolution imaging in microscopy and ophthalmology: new frontiers in biomedical optics (2019): 59-85.
- [3] Cerrotta, Santiago, et al. "Large axial range frequency-domain optical low coherence interferometry." IEEE Photonics Technology Letters 31.2 (2018): 125-128.
- [4] Cerrotta, Santiago, Eneas Nicolas Morel, and Jorge Román Torga. "Fabry Perot detector for low coherence interferometry." (2023).
- [5] Cerrotta, Santiago, Jorge R. Torga, and Eneas N. Morel. "Long-range frequency domain low-coherence interferometry detector for industrial applications." Journal of the Optical Society of America A 40.4 (2023): C16-C21.

---

**Corresponding author:** Santiago Cerrotta. **Email:** [scerrotta@frd.utn.edu.ar](mailto:scerrotta@frd.utn.edu.ar)

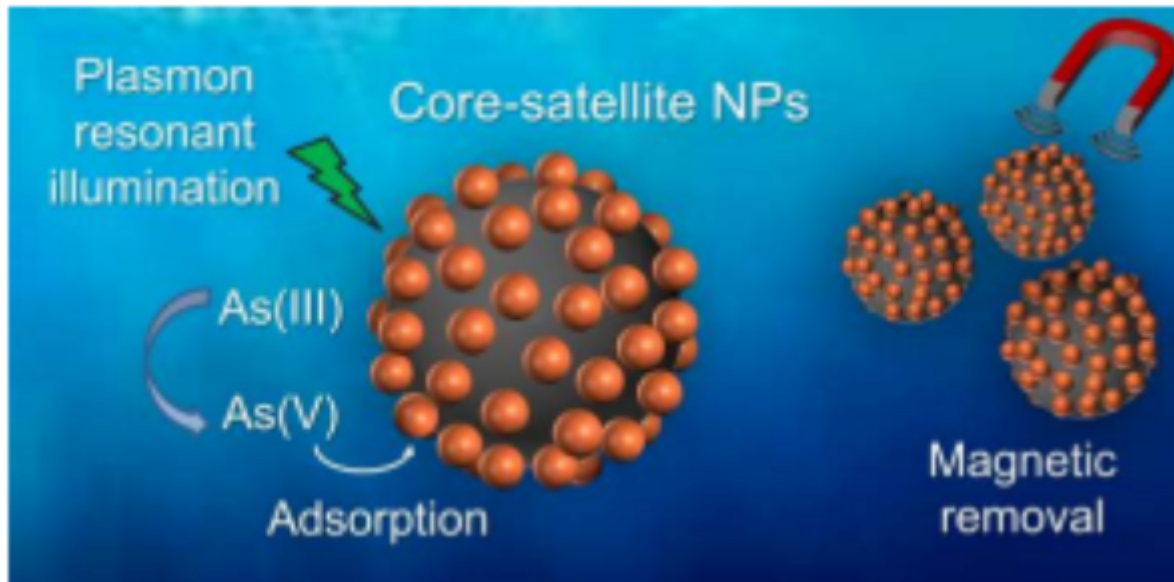
# Plasmonic–Magnetic Hybrid Nanostructures for Efficient Photocatalytic Arsenic Remediation in Water

María Y. Paredes, Bernabé Miralles, Alberto F. Scarpettini

**Topic(s):** Nano photonics and metamaterials [ID 033]

**Institution(s):** Universidad Tecnológica Nacional, Argentina

Arsenic is among the most hazardous elements found in natural waters, with prolonged exposure posing serious health risks. Its efficient removal from groundwater remains a critical environmental challenge. In this work, we present core–satellite hybrid nanostructures composed of plasmonic gold nanoparticles anchored onto magnetic iron oxide cores for the light-assisted remediation of arsenic-contaminated water, as shown in Fig. 1. Our results show that gold nanoparticles catalyze the oxidation of arsenic into less toxic species. Under illumination, both photothermal effects and hot carrier generation contribute to a further enhancement of the reaction rate. The iron oxide cores serve as effective arsenic adsorbents, allowing for the complete removal of both the catalyst and the adsorbed oxidized arsenic species via magnetic separation. We quantitatively assessed the different catalytic contributions and found that the plasmonic effect is comparable in magnitude to the surface catalytic activity [1]. A comparative study between gold and silver nanoparticles shows that while gold exhibits superior catalytic activity, silver achieves an eightfold increase under resonant solar-like illumination, highlighting its potential as a cost-effective photocatalyst [2]. These findings underscore the synergistic interaction between plasmonic catalysts and magnetic iron oxides in enabling efficient, light-assisted arsenic remediation from water sources.



**Figure 1:** The plasmonic-magnetic hybrid catalysts oxidize As(III) to the less toxic As(V), and also enable magnetic removal of the catalyst and the adsorbed contaminant.

## References

- [1] M. Y. Paredes et al., *Environ. Sci.: Nano* 10, 166 (2023).
- [2] B. Miralles et al., *J. Phys. Chem. C* 128, 10017 (2024).

**Corresponding author:** Alberto F. Scarpettini. **Email:** [ascarpettini@frd.utn.edu.ar](mailto:ascarpettini@frd.utn.edu.ar)

# Thin-Film Deposition and Optical Testing of a First-Surface Mirror for Astronomical Applications

Ana Paula Quelopana, Gonzalo Gálvez de la Puente

**Topic(s):** Thin films [ID 091]

**Institution(s):** Pontificia Universidad Católica del Perú, Perú

The fabrication of a first-surface astronomical mirror was completed, encompassing design, manufacturing, and evaluation stages. The design phase utilized optical modeling software to determine the optimal thicknesses and refractive indices for both the aluminum and magnesium fluoride thin-film coatings. These parameters were calculated to maximize reflectivity at the desired wavelengths for astronomical observations. Prior to coating deposition, the glass substrate underwent a thorough cleaning process. This involved initial cleaning with distilled water and isopropyl alcohol, followed by an argon plasma treatment step. The plasma cleaning parameters were controlled in certain values set of voltage, current, pressure and time to eliminate any contaminants that could compromise the quality of the subsequent coatings. The aluminum layer was deposited using physical vapor deposition (PVD) under high vacuum conditions (10<sup>-6</sup> mbar), ensuring a uniform and adherent coating. This was followed by the deposition of the protective magnesium fluoride layer using similar PVD techniques [1][2]. Quality control measures were implemented throughout the manufacturing process. Specifically, the adhesion of the aluminum film to the glass substrate was assessed using the ASTM D3359 standard tape test [3], confirming a robust bond. Post-fabrication, the mirror's performance was thoroughly evaluated.

A spectrophotometer was used to measure the reflectivity across the relevant spectral range. These experimental results were then compared to simulated reflection spectra obtained using the Transfer Matrix Method, validating the accuracy of the design parameters [4][5]. Furthermore, the Ronchi test was employed to characterize the surface figure, assessing the presence and magnitude of optical aberrations [6]. The final mirror, photo 1, demonstrated excellent optical properties, meeting all specifications for its intended astronomical application.



**Photo 1: Aluminum and Magnesium fluoride coated first-surface mirror.**

## References

- [1] G. Gálvez de la Puente et al., Proceedings of SPIE, PP 740–743, 4419 (2001). “Physical effects of evaporated materials in thin films and emission patterns”.
- [2] G. Gálvez de la Puente et al., Proceedings of SPIE, pp. 560–563 107 5622 (2004) “Titanium dioxide thin films: refractive index variation as a function of the deposition rate”.
- [3] <https://store.astm.org/d3359-17.html>
- [4] H. A. Macleod, (1989) McGraw Hill, New York. “Thin Films Optical Filters”.
- [5] H. K. Pulker, (1984) Elsevier, Amsterdam. “Coatings on glass”.
- [6] DOI 10.7149/OPA.51.1.49028.

**Corresponding author:** Gonzalo Gálvez de la Puente. **Email:** ggalvez@pucp.edu.pe

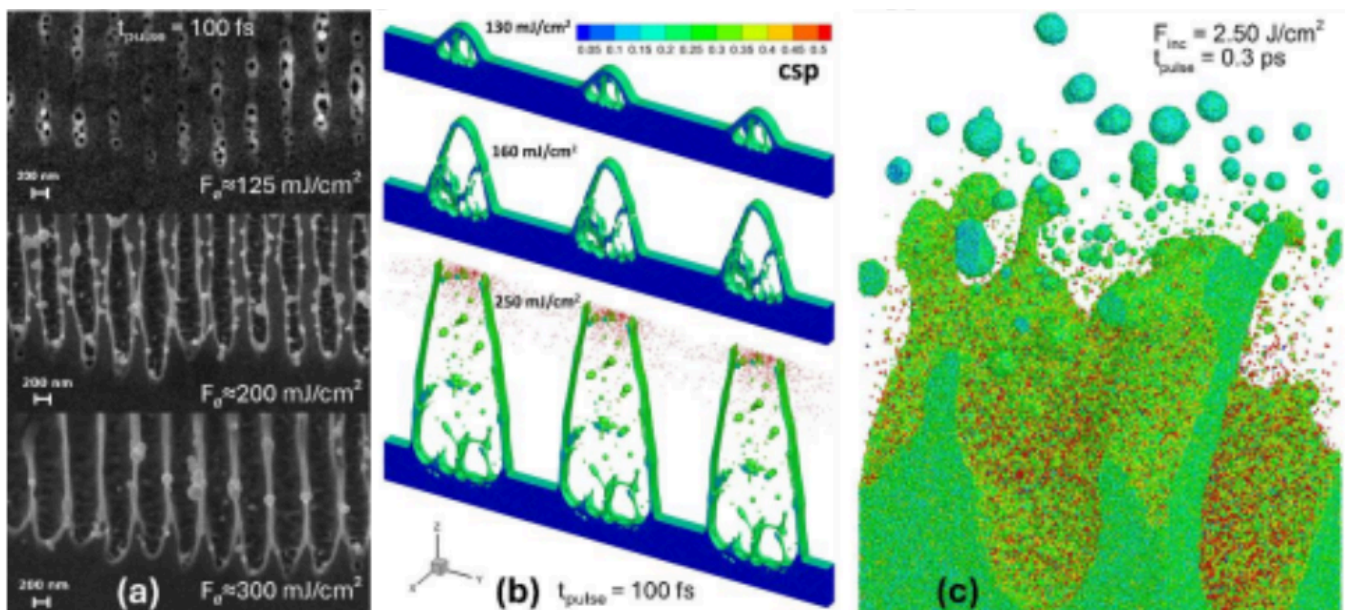
# Modeling of ultrashort laser pulse nanostructuring of materials

Dmitry S. Ivanov

**Topic(s):** Materials processing with lasers [ID 092]

**Institution(s):** University of Kassel, Germany

The possibility of instant and localized energy deposition into material with fs and ps laser pulses make them as perspective methods in precise material modifications at the nanoscale under controlled conditions. The absorbed energy can trigger several laser-induced phase transition processes in solids leading to ablation, formation of voids, nanostructures growth, or nucleation of nanoparticles. The resulting material modifications can change its topological, morphological, magnetic, and optical properties [1]. The functionalized in that way surfaces or resulting colloidal liquids have found a number of applications in micro-optics, waveguiding, Raman spectroscopy, and biomedicine [2]. The controlled material modification, however, requires a detailed understanding of dynamics of fast, non-equilibrium, and interrelated laser-induced processes at the nanoscale. In this work an advanced mesoscopic numerical approach, suitable for the investigation of laser-induced restructuring processes in solids with atomic resolution is proposed [3]. The model is applied to elucidate the mechanisms responsible for laser-induced structuring of solids depending on surrounding media and laser irradiation parameters: wavelength, pulse duration, fluence. Impressive agreement between the modeling and experimental results justifies the proposed approach as a powerful numerical tool revealing the fundamental physics underlying the ablation and nanostructuring processes [4,5]. This will pave the way towards nano-scale pre-designed laser-generated topologies for functionalized surfaces or generation of nanoparticles suitable for biomedical applications.



**Figure 1:** 100 fs laser generation of periodic nanostructures on Au (a), modeling of periodic laser-induced nanostructures due to a single 100 fs pulse (b) atomic snapshot of forming nanoparticles in liquid media due to 300fs laser pulse focused on Au surface. The atoms are colored by Central Symmetry Parameter (SCP) for identification of the local crystal structures as follow: solid  $< 0.08 < \text{liquid} < 0.50 < \text{vapor}$ .

## References

- [1] K. Wieszczycka et al, Coordination Chemistry Reviews 436,213846 (2021).
- [2] S.V. Kaymaz et al, Advances in Colloid and Interface Science 322, 103035 (2023).
- [3] D.S. Ivanov et al, chapter in "Ultrafast Laser Nanostructuring - The Pursuit of Extreme Scales" Springer Nature (2023).
- [4] A. Blumenstein et al, Nanomaterials 10, 1998 (2020).
- [5] D.S. Ivanov et al, Applied Surface Science 643, 158662 (2024).25-7.

**Corresponding author:** Dmitry Ivanov. **Email:** ivanov@uni-kassel.de

## Aniseikonia with Sphero-Cylindrical Lenses

Daniel Malacara-Doblado

**Topic(s):** Optical design and fabrication, Optics at surfaces [ID 013]

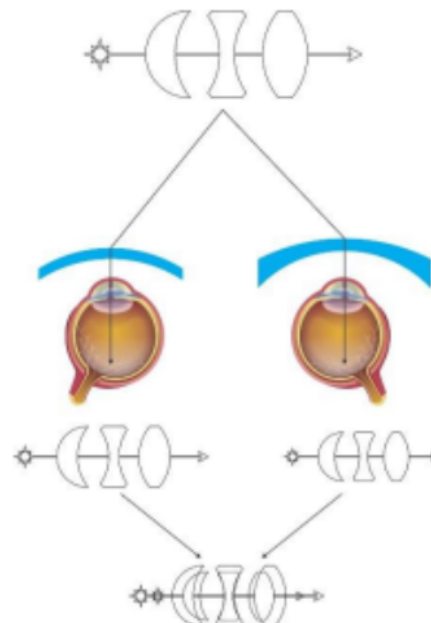
**Institution(s):** Centro de Investigaciones en Óptica, México

Aniseikonia is a binocular vision disorder characterized by a difference in the size and/or shape of the images perceived by each eye, which makes it difficult for the brain to fuse both images into a single, stable visual perception. This discrepancy can cause symptoms such as double vision (diplopia), visual discomfort, spatial distortion, and, in some cases, suppression of the image from one of the eyes by the brain. One of the most frequent causes of aniseikonia is a significant difference in prescription or refractive error between both eyes, known as anisometropia. Sometimes, optical compensation of ametropia with glasses can induce or worsen aniseikonia, especially when there are significant differences in lens power. In the case of astigmatism, cylindrical lenses are used to correct this refractive defect because they modify the focus of light only along one axis.

In summary, aniseikonia due to the use of cylindrical lenses in patients with astigmatism occurs because optical correction alters the size and shape of the retinal image, especially when there are significant differences between both eyes, making binocular vision difficult and causing bothersome visual symptoms.

Arnulf Remole, analyzes the relationship between aniseikonia and anisophoria induced by spectacles, addressing their clinical implications. It explains theoretical aspects, prismatic effects during oblique gaze (such as when reading), and presents a formula to describe these effects. It also describes methods for specifying iseikonic lenses and measuring aniseikonia and anisophoria [1].

In this paper, we will analyze The effects of aniseikonia produced by sphero-cylindrical lenses in eyeglasses as well as in contact lenses. Some solutions to reduce this effect will be proposed. The optimum astigmatism axis orientation will be described.



**Figure 1: Schematic diagram.**

### References

[1] Remole, A., *Optometry and Vision Science*, 66 (10) 659-670 (1989). "Anisophoria and aniseikonia. Part I. The relation between optical anisophoria and aniseikonia".

**Corresponding author:** Daniel Malacara-Doblado. **Email:** dmalacdo@cio.mx

## First Peruvian binoculars: Improvements

Guillermo Baldwin, Franco Gonzales, Alejandro Montoya, Josué Miranda

**Topic(s):** Optical design and fabrication [ID 065]

**Institution(s):** Pontificia Universidad Católica del Perú, Perú

The Physics Section in the Pontificia Universidad Católica del Perú (PUCP) counts on an optical shop managed by the Applied Optics Group (GOA) that allows it to carry out self-sustaining developments through its own optics manufacture [1][2]. Works include developments of different visual instruments such as telescopes [3] and binoculars. A first work on binoculars was presented at the RIOA / OPTILAS 2016 [4], showing a prototype with a non-ergonomic but educative transparent mount. This was an own designed and manufactured Kellner-type eyepiece and an off the shelf objective lens and prisms. A subsequent presentation, at the International Optical Design Conference 2017 [5], showed this binocular with its basic optical characteristics [6]. Binocular improvements will be presented in this congress: ergonomic metal casing, in-house manufacturing of all optical elements [7], superior optical design [8] and better optomechanical design. The manufacturing and interferometric testing of prisms stands out [9]. In relation to the optical design, it should be noted that it includes an optimized Kellner-type eyepiece, and an optimized cemented doublet-type objective [10]. In optomechanical design, the type of prism fastening has been improved, going from using glue to using flexures [11]. Finally, different tests were performed to characterize the binoculars on resolution, field of view, wavefront error of the whole system, and so on.



**Figure 1: Binocular optics and casing**

### References

- [1] Romero, S. M.; Gonzales, F. A. and Baldwin, G. E. (2012). First Works on Multi-Blocking Precision Optics Manufacture in Peru. Case of Elliptical Plane Mirrors. In 8th International Conference on Optics-photonics Design & Fabrication (pp. 265-266). San Petersburg: JSAP.
- [2] Baldwin G., Asmad M, Romero S., Gonzales F., Gálvez G., Sánchez R. and Córdova D., "Advances in optical technologies at Pontificia Universidad Católica del Perú," Proc. SPIE 8001 (2011).
- [3] F. Gonzales, G. Baldwin, S. Romero, W. Tupia, G. Gálvez, "Design and Manufacture of Small Newtonian Telescope for Lunar Observation", Opt. Pura Apl. 51.1.49028:1-12 (2018)
- [4] G. Baldwin, F. Gonzales, "Concepción y Desarrollo de Binoculares", RIOA/OPTILAS 2016
- [5] Guillermo Baldwin, Franco Gonzales, Carlos Pérez S., "First Peruvian binoculars," Proc. SPIE 10590, 2017 IODC, 1059027 (November, 27, 2017); doi: 10.1117/12.2299567
- [6] Johnson B. K., [Optics and optical instruments], Dover Publications, New York, 45 – 77 (1960)
- [7] Karow, Hank, [Fabrication Methods for Precision Optics], Wiley & Sons, N J, 390 - 403 (1993)
- [8] OSLO, "OSLO User Guide," n.d. (18 August 2014)
- [9] Malacara, Daniel, Optical Shop Testing. 3rd Ed., pp 832 John Wiley & Sons Inc. (2007).
- [10] Smith, Warren J., [Modern optical engineering] 4ta ed., McGraw Hill, N Y., 141 – 153 (2008)
- [11] Yoder Jr., P. [Mounting optics in optical instruments] 2da ed., SPIE PRESS, Bellingham, Washington USA, 152 – 156, 673 - 676 (2008)

**Corresponding author:** Guillermo Baldwin. **Email:** gbaldwin@pucp.edu.pe

## Manufacture of aspherical mirrors for the implementation of a classic Cassegrain astronomical telescope

P. Gallardo, A. Romero, A. Escudero, F. Gonzales

**Topic(s):** Optical design and fabrication [ID 044]

**Institution(s):** Pontificia Universidad Católica del Perú, Perú

This work presents the processes of design, manufacturing, and optical testing of aspheric mirrors (paraboloids and hyperboloids) for the implementation of a classical Cassegrain astronomical telescope [1]. The work begins with the simulation of the optical system using Ansys Zemax OpticStudio (student version), where the behavior of the system components (mirrors) is evaluated. This is followed by the manufacturing process of the mirrors according to the design specifications. Subsequently, the final shapes of the reflective optical surfaces (mirrors) are assessed, and a metallic thin film is applied.

Finally, the proposed system is assembled, and its performance is evaluated [2,3]. The material used to fabricating the mirrors is Pyrex glass.

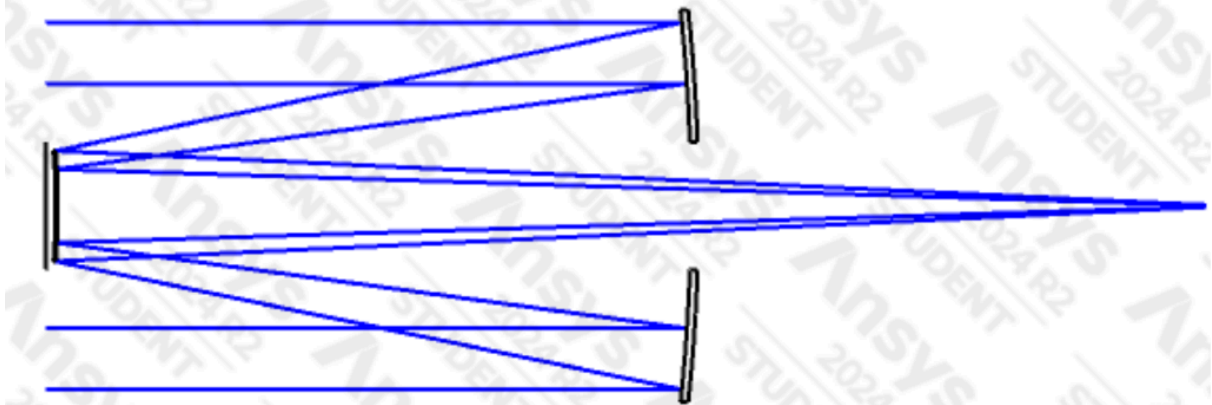


Figure 1: Simulation of the telescope Cassegrain.

### References

- [1] Rutten H., Van Venrooij M. (1988) Telescope Optics. Willmann\_Bell, Inc.
- [2] Baldwin, G., Ochoa, J., & Gonzales, F. Kinematic characterization of a polishing machine for the design of petal tools and its application in the parabolization of reflective optical surfaces. *Óptica Pura y Aplicada* (2022).
- [3] Gonzales, F., Baldwin, G. E., Romero, S., Tupia, W., & Gálvez, G. Design and manufacture of a small Newtonian telescope for lunar observation. *Óptica Pura y Aplicada*, 51. (2018).

---

**Corresponding author:** Pablo Gallardo. **Email:** a20206447@pucp.edu.pe

## Optical design of double lens for the refractor telescope CST-80 KU by G-sum Method

Jenifer Garcia, Franco Gonzales and Ivan Choque

**Topic(s):** Geometrical optics, Optics in computing, Optical design and fabrication [ID 034]

**Institution(s):** Universidad Nacional Jorge Basadre Grohmann; Pontificia Universidad Católica del Perú, Perú

Students of our university are interested in Astronomical Observation, but our telescope, CST-80 KU, was discontinued over 30 years ago, consequently it is impossible to buy a replacement lens, for that reason it is important for us to design an appropriate lens for improving the observation. The present work shows a design of an achromatic doublet lens by the G-sum method. This technique allows us to find parameters for proper correction for spherical, coma and chromatic aberration [1-2]. The design process was first carried out by computer simulation using Ansys Zemax OpticStudio Student. Lens parameters such as: radii curvatures, diameters, thickness, sagittas and refraction indexes are included in the simulation. Glasses N-BK7 and N-SF5 are used in this study, they were chosen by their suitable combination of optical properties, such as dispersion and transmission, which make them compatible and efficient for optical system design [3]. Simulation results allow us to visualize the proposed three-dimensional design, to analyze the mentioned aberrations by spot diagrams, and to optimize the optical system [4]. In the future, the proposed design will facilitate the lens manufacture with a high degree of precision.

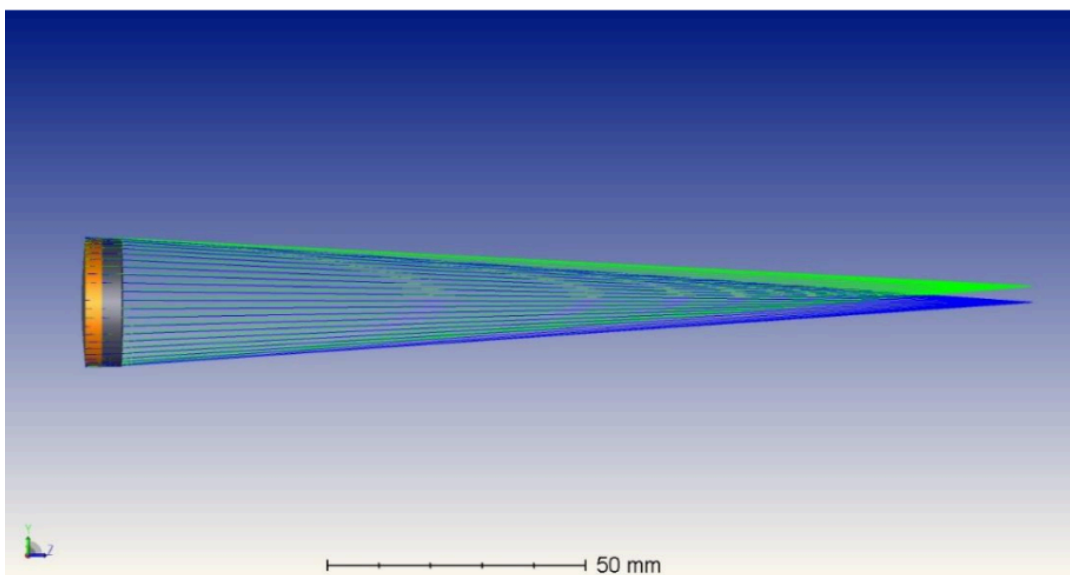


Figure 1: TComputer simulation of a doublet lens by using Zemax OpticStudio.

### References

- [1] Gee AE. The design of telescope objectives by the G-sum method. *Amateur Telescope Making*.1953;III:208.
- [2] Smith JA. Third-order aberration theory and calculation. In: *Modern Optical Engineering*. 4th ed. New York: McGraw-Hill; 2010. p. 105–122.
- [3] Yu SM, Jung MS. Selection of optical glasses using a chromatic-aberration correction method for the whole visible range plus a telecentric lens design applying the method. *Korean J Opt Photonics*. 2015;26(4):217–25.
- [4] Zemax R. Manual del usuario del programa de diseño óptico. Zemax LLC; 2012.

**Corresponding author:** Jenifer Garcia. **Email:** jegarcia@unjbg.edu.pe

## Solar Concentrator

Abraham Lopez Pacheco, María Jose Cervantes Oropeza, Bruno Méndez Sánchez, Omar Cuamani

**Topic(s):** Geometrical optics [ID 073]

**Institution(s):** Benemerita Universidad Autonoma de Puebla, México

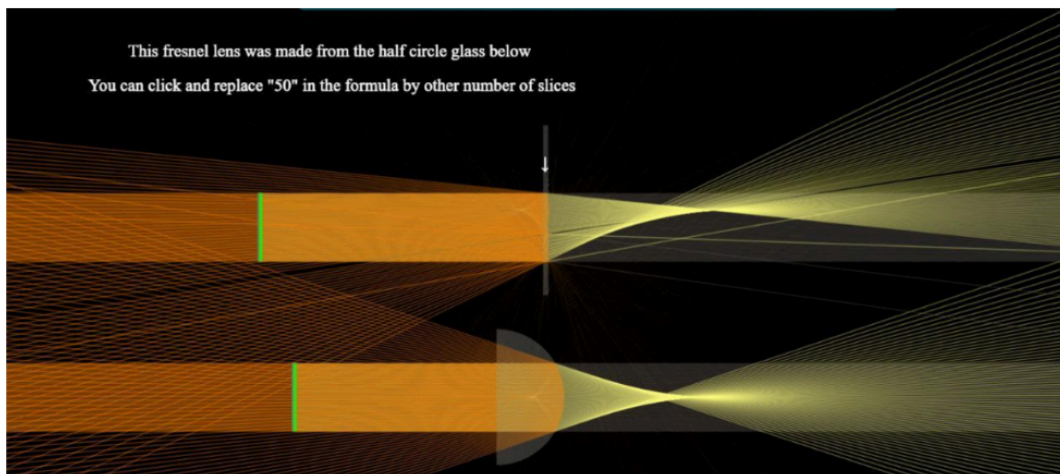
A solar concentrator with a Fresnel lens is a system designed to maximize solar energy capture by concentrating light onto a focal point. This innovative device uses a Fresnel lens, characterized by its thin, flat shape composed of concentric rings that allow solar radiation to be focused with high efficiency. Its main goal is to make the most of solar energy, reducing the costs of electric or thermal generation.

A fundamental aspect of this type of system is the design of an automatic lighting mechanism, which adjusts the concentrator's orientation based on solar intensity. For this, light sensors and solar tracking systems are integrated to ensure precise positioning toward the sun throughout the day. This not only enhances energy performance but also optimizes the use of available resources.

In the optical design, the lens is arranged appropriately to minimize light losses and concentrate the greatest amount of energy on the receiver. Simultaneously, the mechanical design focuses on providing a solid and resistant structure capable of withstanding various environmental conditions and facilitating both maintenance and system operation.

A significant advantage of this type of solar concentrator is its ability to capture diffuse sunlight, making it viable in areas with cloudy or variable climates, where other systems are less effective. This feature broadens its applicability and makes it a versatile option for different regions.

Currently, a functional prototype of the solar concentrator with Fresnel lens has already been developed, with the optical, mechanical, and tracking components completed. The only remaining component to be integrated is the photovoltaic system, which will enable efficient conversion of the concentrated solar energy into electricity.



**Figure 1:** Solar concentrator with a Fresnel lens.

### References

- [1] (s.f.). Fresnel termosolar. <https://laenergiasolar.org/energia-termica-solar/fresnel-termosolar/>
- [2] My Magnifier. (s.f.). Lente Fresnel lineal concentradora solar. <https://www.mymagnifier.com/es/product/Linear-Fresnel-Lens-Solar-+Concentrator.html>
- [3] ScienceDirect. (s.f.). Fresnel concentrator lens. In ScienceDirect Topics. Elsevier. <https://www.sciencedirect.com/topics/engineering/fresnel-concentrator-lens>

**Corresponding author:** Maria Cervantes. **Email:** maria.cervanteso@alumno.buap.mx

---

## Multiple Interferometry Applied to Radio Telescope Techniques

Guillermo Baldwin, Josué Miranda, Juan Jave

**Topic(s):** Diffraction and gratings, Physical optics [ID 074]

**Institution(s):** Pontificia Universidad Católica del Perú, Perú

It is well known that a diffraction grating [1] separates wavelengths to produce light spectra through multiple-beam interferometry, by means of numerous virtual sources located at its slits. This principle can be applied to define key parameters in radio telescopes and radio observatories, aiming to focus the system's response toward specific angular directions—typically in reception for the former, and in transmission-reception for the latter.

This work proposes a methodology inspired by the optical behavior of diffraction gratings to analyze and/or design such systems. The technique of multiple-beam interferometry is applied to model and explain the laser-like behavior of the Jicamarca Radio Observatory [2] in Lima, Peru, considering a half-wavelength ( $\lambda/2$ ) dipole antenna as the elementary radiating unit. Additionally, the design of a radio telescope based on a parabolic antenna from PUCP [3] is presented, configured as the radiating element in a linear array.

### References

[1] Hecht, Eugene, *Optica*, 2023, 5ta Edición Ed, Pearson

[2] <https://www.igp.gob.pe/observatorios/radio-observatorio-jicamarca/>

[3] <https://inras.pucp.edu.pe/proyectos/radioastronomia>

[4] Victor A. Centa, Juan Jave, David Torres, Paulo Mamani, A 3-element portable radio interferometer for 6.7 GHz methanol observations in the Southern Hemisphere, URSI GASS 2023, Sapporo, Japan, 19 – 26 August 2023

---

**Corresponding author:** Guillermo Baldwin. **Email:** [gbaldwin@pucp.edu.pe](mailto:gbaldwin@pucp.edu.pe)

# Remote Automated Laboratory for Real-Time Optimization of Coagulation-Flocculation mediated UV Processes in Arsenic-Contaminated Water Treatment

E.A. Carpio, J.M. Rodriguez

**Topic(s):** Instrumentation, measurement and metrology, Remote sensing and sensors, Solar energy [ID 107]

**Institution(s):** Universidad Nacional de Ingeniería, Perú.

The growing demand for accessible, high-precision experimentation in water treatment necessitates innovative remote solutions [1]. This work presents a fully automated remote laboratory designed to optimize coagulation-flocculation mediated UV processes for arsenic removal [2], enabling researchers and students to conduct complex experiments from any location. The laboratory integrates a hardware platform with a high-precision XY Gantry system for millimeter-accurate positioning of a multisensor probe (pH, conductivity, turbidity, temperature). Peristaltic pumps for controlled dosing of iron (coagulant) and citrate (pH regulator). auxiliary components (UV light, shaker) to enhance reaction kinetics, floc formation and safety mechanisms (emergency stop, power controls).

A multi-platform digital control panel provides Real-time monitoring of four critical parameters (pH, conductivity, turbidity, temperature) through dynamic graphical displays [3]. automated process control for dosing, pH adjustment, mixing, and data logging, manual control for calibration, motor positioning, pump operation, and remote-access management, and advanced configuration of hardware parameters (motor speeds, pin assignments, sampling intervals).

Full operational control and monitoring via web interface, eliminating geographical barriers, Adaptive precision and educational-research synergy. It was validated in educational settings. The system demonstrates more than 90% data fidelity in parameter tracking during coagulation, flexible optimization of reaction conditions (e.g., pH, turbidity) for diverse water matrices, resource efficiency via reduced physical lab dependency and enhanced experimental repeatability.

This remote laboratory establishes a new standard for accessible, data-driven water treatment research, with applications in academic training and environmental engineering. Future work will expand its adaptability to emerging contaminants and AI-driven process optimization.

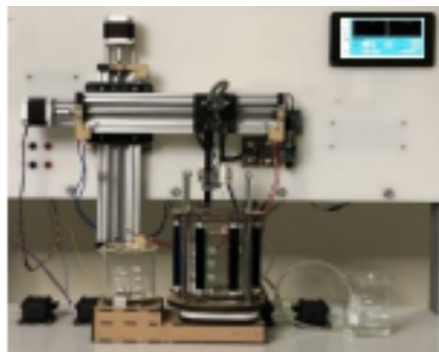


Figure 1: Schematic diagram of the remote lab.

**Acknowledgments:** This work was partially funded by the Erasmus+ project “EU-BEGP” (Project No. 101081473).

## References

- [1] Jacobs, S., Hardebusch, T., Franke, E., Peters, H., Al Amin, R., & Wiese, V. (2024). Design and Development of a Multi- Purpose Collaborative Remote Laboratory Platform. In 2024 IEEE Global Engineering Education Conference (EDUCON).
- [2] C. Jorge, J..Nieto, S..Ponce, J. Rodríguez, J. Solís y W. Estrada, Remoción de Arsénico del agua mediante irradiación solar en Lima, Perú, Cap. 3 en Remoción de arsénico asistida por luz solar en comunidades rurales de América Latina, Ed. Marta Liter y Hector Mansilla, Bs. As. 2003 <https://repositorio.ipen.gob.pe/item/b184b479-f4b9-4063-9d77-fb972a221c04>
- [3] Abeygunawardane, K. W. A. S. R., Dassanayake, D. M. N. D., & Thilakarathna, K. D. W. (2023). Developments of A Remote Online Wind Laboratory Experimental Setup for Repository MOOCs. In 2023 7th International Conference on Information Technology Research (ICITR).

**Corresponding author:** Juan M. Rodriguez. **Email:** [jrodriguez@uni.edu.pe](mailto:jrodriguez@uni.edu.pe)

# A Hybrid Solar Street Lights Remote Laboratory

Boris Pedraza, Alex Villazon, Omar Ormachea, Alfredo Meneses

**Topic(s):** Instrumentation, measurement and metrology, Remote sensing and sensors, Solar energy [ID 112]

**Institution(s):** Universidad Privada Boliviana, Bolivia

Lighting engineering education, in the context of streetlights systems, often lacks tools for students to learn lighting concepts meant to be experienced in a practical way, such as measuring light intensity distribution or validating compliance with standards. Thus, it is more usual to prioritize design over pedagogy by using simulation software tools instead of hands-on experiences [1]. To address this issue, we have developed a hybrid remote lab combining both real-time and ultra-concurrent well-known remote laboratories paradigms [2]. Our remote laboratory enables students to control physical hardware and analyze light distribution in real-world scenarios.

The architecture of our system (Fig. 1) successfully integrates both hardware and software components within three core activities: (1) real-time control of a single street light (adjusting light intensity, capturing light data via a light sensor mesh, and visualizing light distribution), (2) real-time monitoring of five street lights in a real-world campus setup to evaluate compliance with standards, which was improved with the use of pyranometers to measure solar radiation at 2,500 meters above sea level (where the system is installed), and (3) ultra-concurrent analysis of pre-recorded datasets to study light behavior in different scenarios. The platform uses a web interface connected to ESP32 micro-controllers on AC, DC, and inverter-based streetlights. Data is transmitted via MQTT, and a booking system [3] manages access for real-time activities. The remote lab was built to connect theory with practice, allowing students to develop the ability to predict, analyze, and optimize lighting systems. The hybrid approach combines hands-on control, data analysis, and real-world observation, establishing a novel engineering education tool.

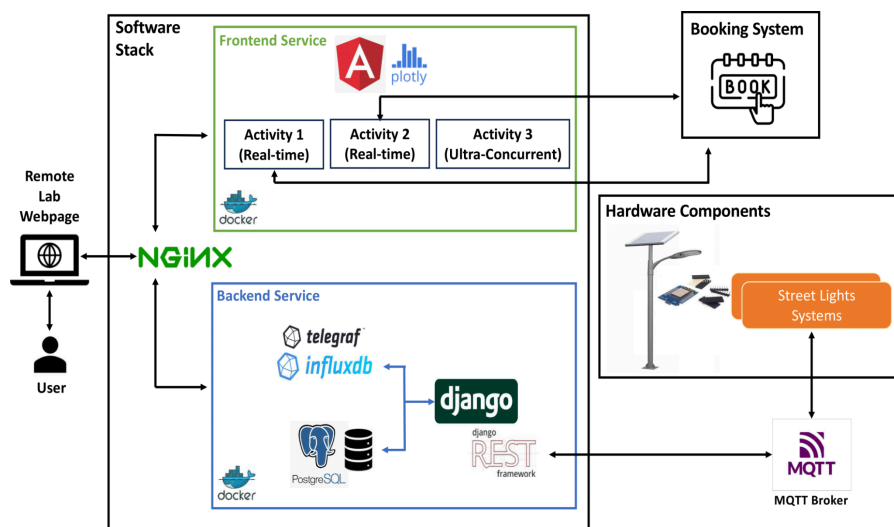


Figure 1: Street Light Remote Lab Architecture.

**Acknowledgments:** This work was partially funded by the Erasmus+ project “EU-BEGP” (Project No. 101081473).

## References

- [1] A. F. C. Vizeu da Silva et al. An Educational Approach to a Lighting Design Simulation using Dialux Evo Software. 2016 51st Int. Universities Power Eng. Conf. (UPEC), 55, 447 (1985).
- [2] J. García-Zubía. Remote Laboratories: Empowering STEM Education with Technology. World Scientific (Europe), 100, 630 (2030).
- [3] A. Villazón et al. A Booking System for Remote Laboratories. In Open Science in Engineering, 341, 348 (2023).

**Corresponding author:** Alex Villazón. **Email:** avillazon@upb.edu

# Bridging Theory and Practice: A Remote Solar Laboratory for Energy Transition Education

Juan Peralta-Jaramilo, Emerita Delgado-Plaza, Doménica León-Moreira, Henry Fuentes

**Topic(s):** Solar energy [ID 111]

**Institution(s):** Escuela Superior Politécnica del Litoral, Ecuador

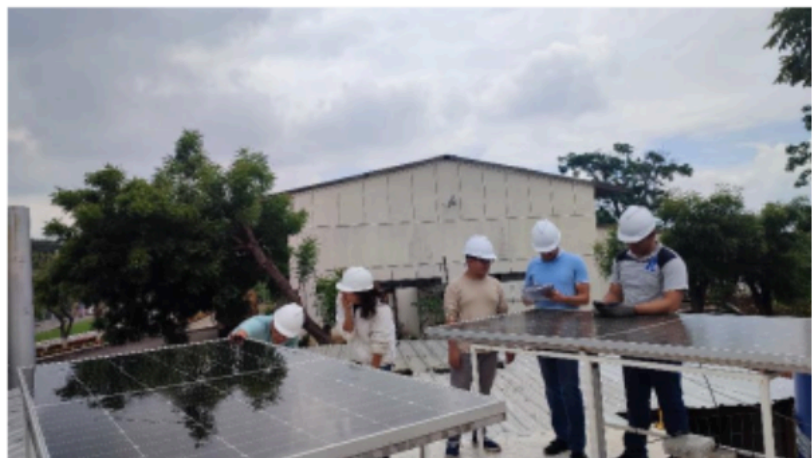
Within the framework of the Erasmus+ project EU-BEGP (Modernising Digital Education in Energy Transition for Circular Economy in Latin America), a remote photovoltaic laboratory has been developed at CDTs–ESPOL to bridge the gap between theoretical learning and real-world practice in renewable energy education. This innovative platform enables undergraduate and postgraduate students to remotely interact with a 1.65 kWp solar PV system (three 550 W panels, 3.3 kW on-grid inverter), instrumented with ESP32 sensors and connected to a SCADA system for real-time acquisition of electrical and environmental variables.

Students can perform hands-on activities such as I–V and P–V curve analysis, evaluation of energy efficiency under different tilt angles, thermographic inspection to detect hotspots, and preventive maintenance procedures. These experiences strengthen analytical, diagnostic, and decision-making skills, allowing learners to understand how environmental conditions and system configurations influence photovoltaic performance and grid integration.

This remote laboratory represents an innovative educational strategy that modernises energy training, expands access to high-quality practical experiences, and enhances the development of professional competences in renewable energy, supporting the goals of energy transition and circular economy promoted by the EU-BEGP project.



Panel de Supervisión y control Solar, Hídrico y Aerotermia



**Figure 1: (a) Panel de supervisión y control del sistema solar, hídrico y aerotérmico conectado al laboratorio remoto del CDTs–ESPOL, (b) Instalación y calibración de los módulos fotovoltaicos de 1.65 kWp desarrollado en el marco del proyecto Erasmus+ EU-BEGP.**

**Acknowledgments:** This work was partially funded by the Erasmus+ project “EU-BEGP” (Project No. 101081473).

## References

- [1] E. Delgado, P. Plaza, D. León-Moreira, J. D. Cabrera Abad, B. M. Briones Morante et al., “Energy efficiency training: Evaluation and optimization of its implementation in secondary education,” Proc. 23rd LACCEI International Multi-Conference for Engineering, Education and Technology (LACCEI): “Engineering, Artificial Intelligence, and Sustainable Technologies in service of society”, January 2025. DOI: 10.18687/LACCEI2025.1.1.2079
- [2] R. S. Herrera, M. A. Márquez, A. Mejías, R. Tirado, and J. M. Andújar, “Exploring the usability of a remote laboratory for photovoltaic systems,” IFAC-PapersOnLine, vol. 48, no. 29, pp. 190–195, Dec. 2015. doi: 10.1016/j.ifacol.2015.11.205

**Corresponding author:** Juan Peralta. **Email:** jperal@espol.edu.ec

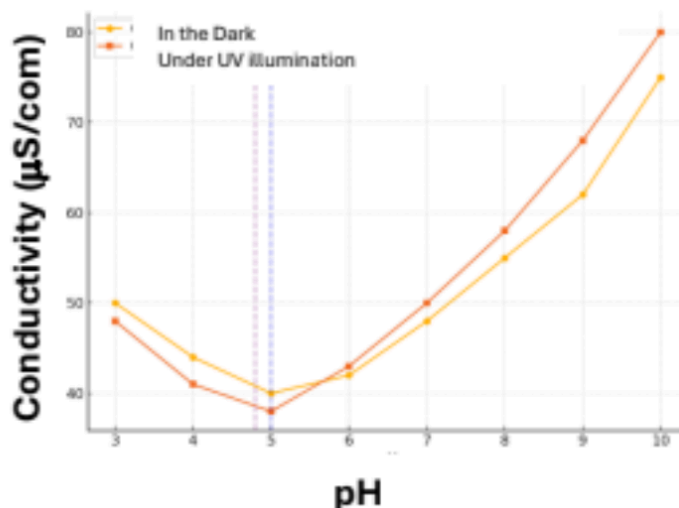
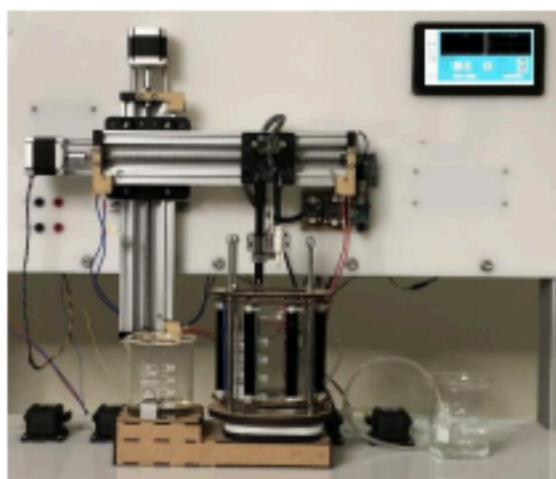
# Remote Multisensor System for Indirect Measurement of Nanoparticle Surface Charge under UV Illumination

E.A. Carpio, J.M. Rodriguez

**Topic(s):** Optics at surfaces, Physical optics, Scattering, Solar energy [ID 108]

**Institution(s):** Universidad Nacional de Ingeniería, Perú

Accurate determination of nanoparticle surface charge is critical for applications in catalysis, nanomedicine, and environmental remediation, yet conventional methods (e.g., zeta potential) remain costly and inaccessible [1]. This study designs and validates a remote automated laboratory for indirect estimation of colloidal nanoparticle surface charge under UV illumination, leveraging correlations between pH-dependent electrical conductivity (EC), turbidity, and the point of zero charge (PZC) [2]. The system integrates a multisensor probe (pH, EC, turbidity, temperature), UV light (365 nm), and automated dosing (HCl/NaOH) within a remotely controlled platform developed in our lab.



**Figure 1: (a) Schematic diagram of the remote laboratory, (b) Electrical conductivity vs pH in the dark and under UV illumination** Obtained results with TiO<sub>2</sub> nanoparticles revealed: Distinct minima in electrical conductivity curves, having a 0.2 difference of the pH in darkness respect to UV, and maxima in turbidity, confirming PZC as the aggregation threshold, indicating photoactivated surface charge and colloidal stability modification. In all obtained results, a consistency higher than 90% in parameter tracking across trials is observed.

The methodology demonstrates high sensitivity to surface chemistry changes, enabling cost-effective characterization of photoactive nanomaterials without specialized instrumentation. Its remote operation eliminates geographical barriers, supporting academic research and industrial quality control. Future work will extend validation to complex matrices and AI-driven optimization.

**Acknowledgments:** This work was partially funded by the Erasmus+ project “EU-BEGP” (Project No. 101081473).

## References

- [1] Kosmulski, M. (2009). Surface Charging and Points of Zero Charge. CRC Press.
- [2] Salley, D. S., Roch, L. M., Rudic, S., et al. (2024). Self-driving laboratories for chemistry and materials science. Chemical Reviews, 124(8), 4567–4602. <https://doi.org/10.1021/acs.chemrev.4c00055>.

**Corresponding author:** Juan M. Rodriguez. **Email:** jrodriguez@uni.edu.pe



# Fringe projection system calibration based on Radon transform

Miguel Mora-Gozalez, Francisco Gerardo Peña-Lecona, Jesús Muñoz-Maciel, Francisco Javier Casillas-Rodríguez, Sergio Álvarez-Rodríguez

**Topic(s):** Imaging systems, Instrumentation, measurement and metrology [ID 085]

**Institution(s):** Universidad de Guadalajara, México

Camera and projector calibration is a key step in three-dimensional measurement and reconstruction technology, such as profilometry and deflectometry, among others [1]. On the other hand, the Radon transform is a mathematical operation that converts a 2D or 3D function into a function defined in the space of lines or planes, respectively, calculating the area under the curve in each of its lines [2]. In this paper, a calibration method for fringe projection systems is presented, which is based on orthogonal Radon transforms. A fringe pattern is projected onto a reference plane, which is captured by the camera, to subsequently obtain the Radon transform of the obtained image. Once the Radon transform results are obtained, micrometric control of the orientations of both the projector and the camera begins, obtaining intermediate Radon transforms to provide feedback to the system and improve its control, as shown in Figure 1. The method was tested with good results both for a system with a projector oblique to the reference plane and a camera perpendicular to the same plane, as well as for a system in which both elements are perpendicular to the reference plane (using a beam splitter). It can be concluded that the Radon transform can be used to calibrate fringe projection systems without the need to modify the system or add extra elements to it.



Figure 1: Flowchart of the calibration system.

## References

- [1] X. Zhang, F. Da, D. Zheng, and L. Rao, Opt. Eng. 58(6), 064104 (2019). "Camera calibration of a near-parallel imaging system based on magnification rate".
- [2] M. Mora-González, J.C. Martínez-Romo, J. Muñoz-Maciel, G. Sánchez-Díaz, J. Salinas-Luna, H.I. Piza-Dávila, F.J. Luna-Rosas, and C.A. de Luna-Ortega, Proceedings of Springer MCP R 2010, in LNCS 6256, 134-143 (2010). "Radon Transform Algorithm for Fingerprint Core Point Detection".

**Corresponding author:** Miguel Mora-Gozalez. **Email:** miguel.mora@academicos.udg.mx

## Fast phase unwrapping by polynomial fitting

Jesús Muñoz-Maciel, Francisco Peña-Lecona, Miguel Mora González

**Topic(s):** Instrumentation, measurement and metrology [ID 053]

**Institution(s):** Universidad de Guadalajara, México

Phase unwrapping is usually the last step to recover the object information from a single or several interferograms. The wrapped phase arises from the use of the arctangent function of the ratio of the sine and cosine functions. Phase unwrapping consists in eliminating the discontinuities that are present in the wrapped phase allowing the correct analysis of the object information encoded in the acquired fringe patterns. In its simplest form phase unwrapping can be achieved by adding or subtracting  $2\pi$  terms to the wrapped phase, however this simple approach may fail with relatively low noise levels. In general terms phase unwrapping methods can be classified in path dependent or independent algorithms. Path dependent are faster but cannot deal with noisy measurements or data with obscurations or irregular pupils. Path independent procedures on the other hand may tolerate higher noise values and avoid missing data or obscurations. In this work we develop a new path independent phase unwrapping algorithm. This new approach is based in a polynomial fitting algorithm between two wrapped maps, the original one and a close version of itself. The sine and the cosine of the wrapped phase are cropped and then resized to the original size to produce a new wrapped data very close to the original. The polynomial fitting is applied to the difference of the two wrapped phases. Then the coefficients of the fitting polynomial procedure are used to reconstruct an unwrapped phase. Depending on the fidelity of the fitting process it may require an additional refinement step. This approach works very fast and can deal with noise measurements. Finally, the proposed method is evaluated in simulated and experimental data with good results.

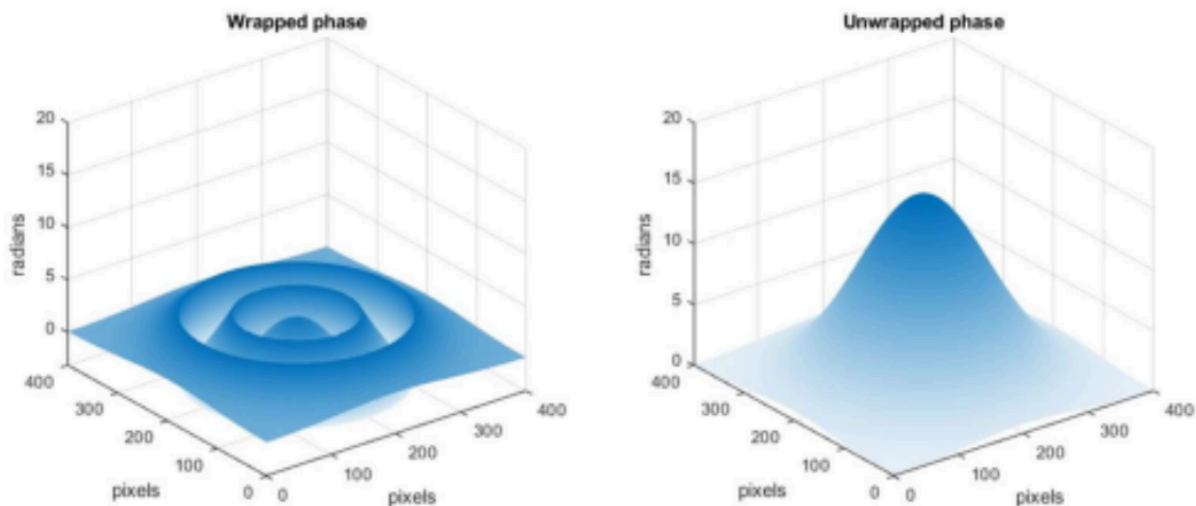


Figure 1: Wrapped and unwrapped phase.

**Corresponding author:** Jesús Muñoz Maciel. **Email:** [jesus.munozm@academicos.udg.mx](mailto:jesus.munozm@academicos.udg.mx)

# Surface Profilometry with a Smartphone-Based Fringe Projection System

Mabel Tesillo, Alejandro Montoya, Heyner Vilchez, Iván Choque, Miguel Asmad

**Topic(s):** Instrumentation, measurement and metrology, Optical devices [ID 100]

**Institution(s):** Universidad Nacional Mayor de San Marcos; Pontificia Universidad Católica del Perú; Universidad Nacional Jorge Basadre G., Perú

This study explores the use of a smartphone as both the illumination and image acquisition system for fringe projection profilometry. A physical grating, illuminated by the phone's built-in light source, projects structured fringes onto the object's surface. The deformed fringe patterns are captured using the smartphone camera and analyzed via Fourier transform techniques to reconstruct the surface topography. We describe the optical setup and demonstrate the resulting digital height map of the tested object, highlighting the potential of low-cost, portable systems for 3D surface measurement.

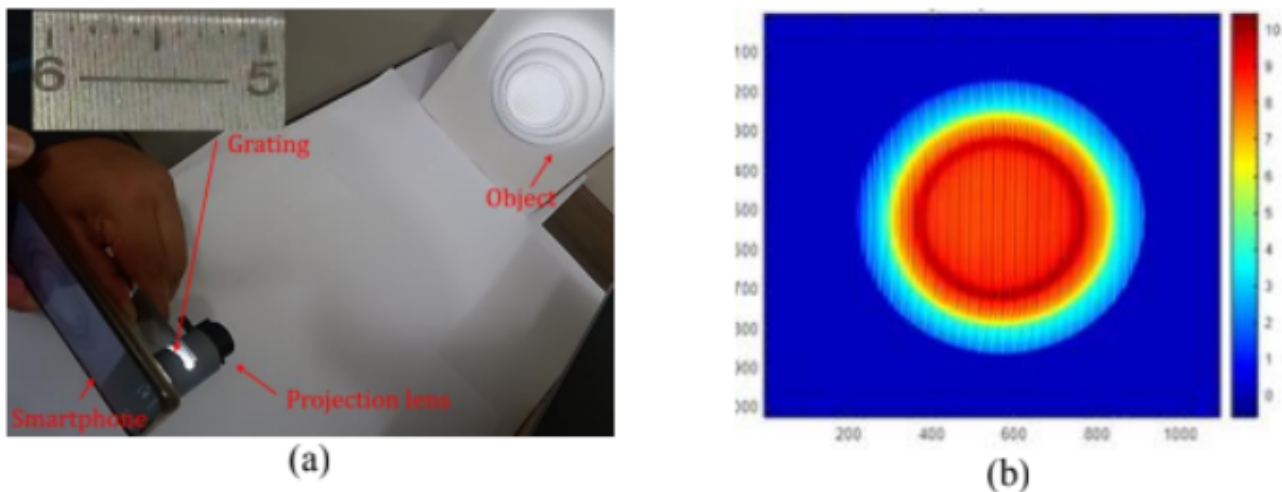


Figure 1: (a) The fringe projection lens using the smartphone's lighting system, b) Height map of the reconstructed object.

## References

- [1] Liu, Yanzhao, et al. "High dynamic range real-time 3D measurement based on Fourier transform profilometry." *Optics & Laser Technology* 138 (2021): 106833
- [2] Liu, Danji, et al. "Fringe projection profilometry with portable consumer devices." 2017 International Conference on Optical Instruments and Technology: Optical Systems and Modern Optoelectronic Instruments. Vol. 10616. SPIE, 2018.

**Corresponding author:** Mabel Tesillo. **Email:** [mabel.tesillo@unmsm.edu.pe](mailto:mabel.tesillo@unmsm.edu.pe)

# Simplified Chromatic Aberration Compensation in Digital Camera Lenses for Fringe Projection Profilometry

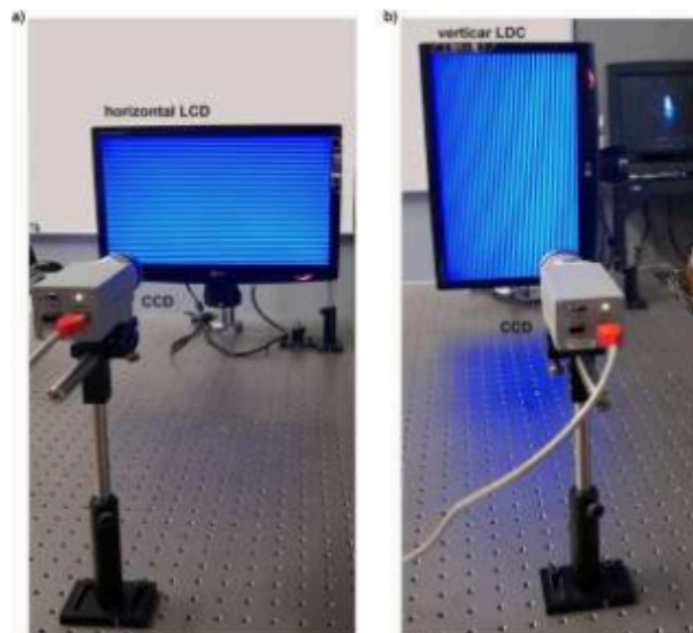
Amalia Martínez- García, Analía Sicardi-Segade, Juan Antonio Rayas-Alvarez

**Topic(s):** Instrumentation, measurement and metrology [ID 084]

**Institution(s):** Centro de Investigaciones en Óptica,, México

Chromatic aberration (CA) is an optical defect arising when different wavelengths of light focus at varying spatial positions, producing colored fringes and degrading image sharpness. In fringe projection profilometry (FPP), such aberrations introduce phase distortions in the projected fringes, leading to inaccuracies in 3D measurements. Although hardware solutions (e.g., achromatic lenses) and advanced coatings can mitigate CA, they are often costly and inflexible. Software-based approaches offer a more cost-effective and adaptable alternative, leveraging image processing techniques to correct color misalignments across RGB channels.

This work presents a simplified software-based method for compensating CA in digital camera lenses used in FPP, building upon the method of Chao Chen et al. [1]. Unlike the original approach, which involves complex geometric modeling and extensive mathematical computation to determine the pixel displacement matrix (PDM), our method reduces the computational burden while maintaining accuracy. Additionally, we address systematic errors introduced by lateral RGB subpixel offsets in the LCD used for fringe projection [2]. The effectiveness of the proposed technique is validated through both numerical simulations and experimental measurements, demonstrating its practical utility in high-precision 3D metrology systems, Fig. 1.



**Figure 1:** Experimental setup. LCD monitor placed in position a) horizontal, and b) vertical.

## References

[1] C. Chao and P. Bing, *Appl. Opt.* 59, 6517 (2020).

[2] A. Sicardi-Segade, J. A. Rayas, A. Martínez-García, *Opt. Contin.* 3, 2006 (2024).

---

**Corresponding author:** Amalia Martínez- García. **Email:** amalia@cio.mx

## Automatic orthogonal recording polarimeter applied to bio-samples

Asticio Vargas, Fabián Torres, Fabiola Zambrano, Vicente Cisternas

**Topic(s):** Imaging systems, Instrumentation, measurement and metrology, Other topic [ID 089]

**Institution(s):** Universidad de La Frontera, Chile

Currently, due to the growing impact of polarized light in the fields of biophysics, medicine, materials science, and chemical processes, polarimetry has advanced using optical and optoelectronic systems optimized for its implementation, data analysis, and error propagation in measurements. In this work, the optical system of a transmission polarimeter is presented, using two cameras for orthogonal polarization state measurements and incorporating the use of variable retarder plates (LCRs) for the Polarization State Generator (PSG) and the Polarization State Detector (PSD) (Figure 1). In this design, the optical system is fully controlled and programmable by a computer. Data is captured using two cameras that capture images with orthogonal states of polarization (SOP) between them. To characterize the polarization response of the sample, the Mueller matrix (MM) is currently widely used and it is composed of 16 elements, obtained with information from 36 images (6 input polarizations combined with 6 output polarizations).

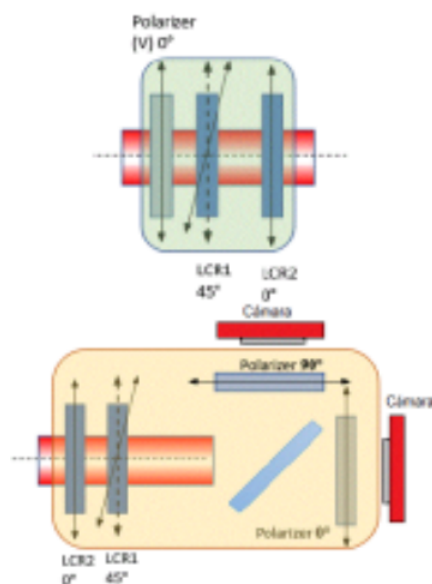


Figure 1. PSG (upper) and PSD (lower) from Polarimeter setup.

This dual-camera design reduces the number of recording iterations by half, still obtaining 36 images but in less time and with less misalignment due to electronically controlled measurement variations, which streamlines and optimizes the process. Additionally, the final calculation of the MM is automated. From there, it is possible to determine the sample's depolarization, polarizance and retardation. From the 36 images obtained, only 16 are needed for the MM calculation [2], which contain all the required polarization data. This significantly reduces recording time and the acquisition process. This polarimeter is applied to biological samples to identify morphological changes in neutrophils during the activation of the mechanism known as NETosis (Figure 2). The results obtained to date demonstrate the possibility of applying whole polarimetric studies to slow-moving objects, with the aim of improving biological models.

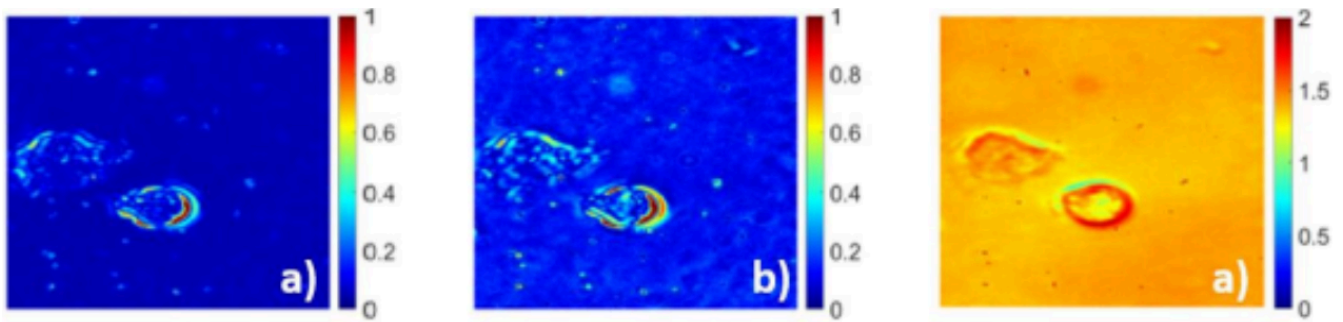


Figure 2: NeTosis formation. (a) polarizance. (b) Diattenuation. (c) Retardance.

#### References

- [1] E. Nabadda, M. M. Sánchez-López, A. Vargas, A. Lizana, J. Campos, and I. Moreno. Journal of the European Optical Society-Rapid Publications, Opt. Comm. 20, 5 (2024).
- [2] Justin S. Baba, Jung-Rae Chung, Aimee H DeLaughter, Brent D Cameron, and Gerard L Cote, Journal of biomedical optics, 7, 341(2002).
- [3] V. Cisternas. Msc Thesis. In progress.

---

**Corresponding author:** Asticio Vargas. **Email:** [asticio.vargas@ufrontera.cl](mailto:asticio.vargas@ufrontera.cl)

## Evaluating gait recognition performance on privacy preserving images

Loana Velasquez-Omonte, Guillermo Sahonero-Alvarez, Edgar Salazar, Laura Galvis

**Topic(s):** Image processing, vision and artificial intelligence, Machine vision, Optics in computing, Other topic [ID 104]

**Institution(s):** Universidad Catolica Boliviana; Universidad Privada Boliviana, Bolivia; Pontificia Universidad Católica de Chile, Chile; Universidad Industrial de Santander, Colombia

The growing concern for privacy in computer vision systems has driven the development of privacy preserving techniques at the optical level, preventing the capture of sensitive visual information during image acquisition. Recent advances in privacy-preserving optics have demonstrated the potential of hardware-level protection by directly degrading sensitive visual information at the point of image acquisition. In this work, we explore the impact of using the privacy-preserving optical encoder proposed by [1], which was originally designed for privacy-preserving human pose estimation, as part of a conventional gait recognition framework. Inspired by the Gait Energy Image (GEI) representation, we computed an average image for the degraded images or Degraded Gait Signature (DGS). Before computing the DGS, all images were binarized by background subtraction, with respect to a reference frame available in the videos, and thresholding. Then, the DGS for each subject and sequence were classified by a deep learning model. For our experiments, we used the OAK-Gait8 dataset that contains 8 subjects, 6 sequences, and 3 variations from 5 camera angles. In total, we used 504 videos for training, 144 for validation and 72 for testing, representing 70%, 20% and 10% of the dataset respectively. The total number of videos used was 720. We only used RGB videos. Our results, based on simulations and comparative analyses show that, although the lens significantly diffuses the image and does not preserve a human-like gait shape, the system is still able to classify individuals with approximately 71% accuracy. This indicates that the optical degradation produces a representation more similar to a spectral or abstract pattern than a recognizable human form, yet it still contains sufficient information for biometric classification. These findings provide insight into the trade-off between privacy protection and biometric recognition when using PSF-based privacy-preserving optics.

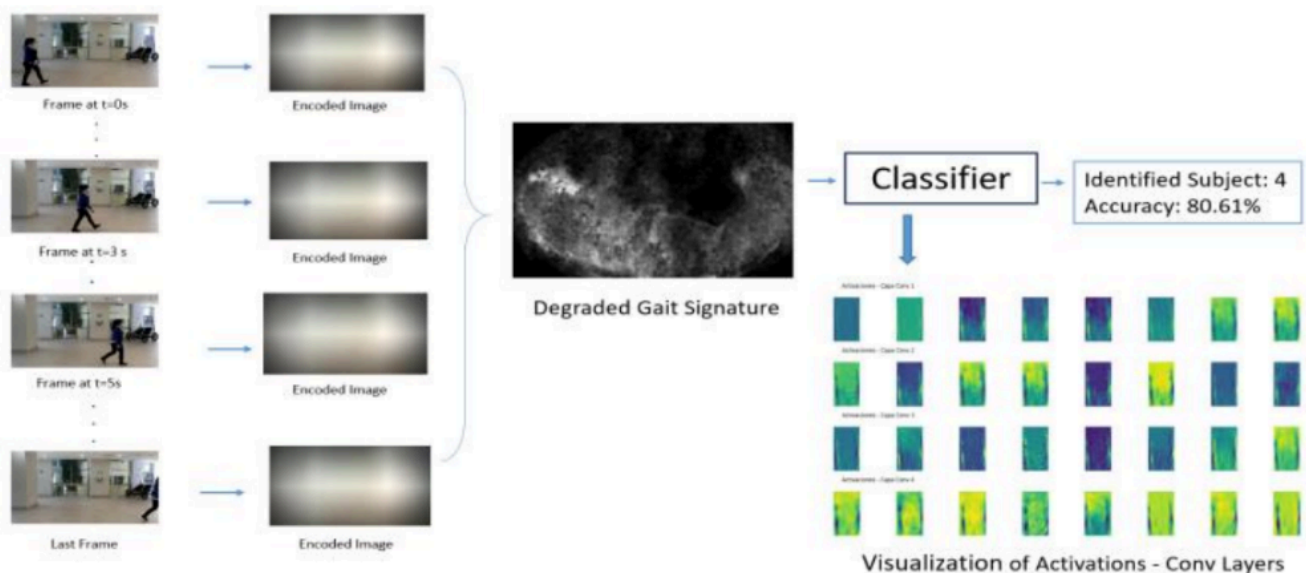


Figure 1: Degraded Gait Signature generation and classification from a video sequence.

### References

[1] C. Hinojosa, J. C. Niebles, and H. Arguello, "Learning Privacy-Preserving Optics for Human Pose Estimation," in Proceedings of the IEEE/CVF International Conference on Computer Vision (ICCV), 2021, pp. 2573–2582. [Online]. Available: <https://carloshinojosa.me/project/privacy-hpe>

**Corresponding author:** Edgar Salazar. **Email:** edgarsalazar@upb.edu

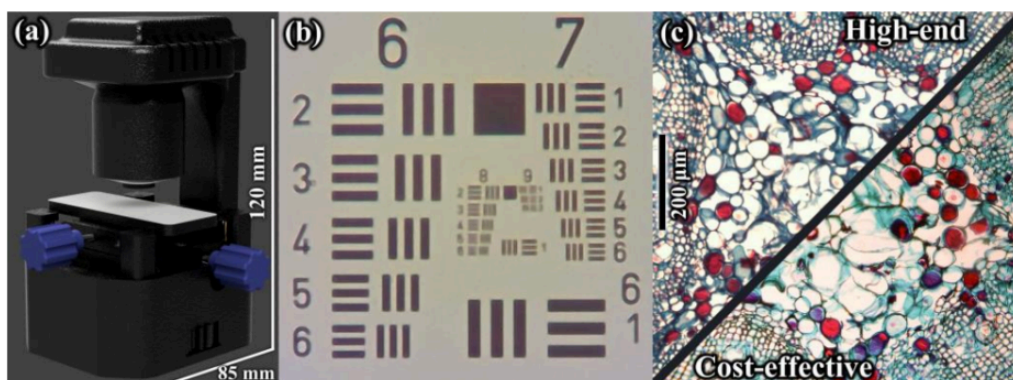
## Cost-effective 3D printed bright-field microscope

Diego A. Londono, Carlos A. Buitrago-Duque, and J. Garcia-Sucerquia

**Topic(s):** Imaging systems, Microscopy [ID 061]

**Institution(s):** Universidad Nacional de Colombia, Colombia

The development of accessible optical tools is essential to support practical science and engineering education. In recent years, various open-source and low-cost microscope initiatives have emerged to address this need [1]. This work contributes to that effort by presenting a digitally integrated, cost-effective bright-field optical microscope. The system is built with off-the-shelf materials: a SonyIMX335 CMOS sensor (available for \$30 USD), frequently used in CCTV systems, and a pair of interchangeable webcam lenses. While previous works have demonstrated the use of similar lens systems for portable microscopy [2], up to the best knowledge of the authors this is the first implementation combining such a lens set with a fully 3D-printed mechanical platform, as illustrated in panel (a) of Fig. 1. The optical setup employs an inverted short focal length (2 or 5 mm) lens operating as the objective; this lens projects the image to infinity when the sample is positioned at its working distance. A second lens with a larger focal length (25 mm), used as the tube lens, then focuses the image onto the sensor. The mechanical platform was fabricated using fused deposition modeling 3D printing and assembled with M3x0.5 screws and 3 mm steel rods, providing up to 20 mm of low-backlash, controlled motion along the X and Y axes and up to 13 mm along the Z axis. The illumination is provided by a diffuse white LED powered via a USB Type-C port, which also serves as the interface for connecting the camera to a computer or mobile device. Panel (b) shows the image of a USAF 1951 resolution target obtained with the proposed microscope prototype; the smallest resolved object is group 8, element 1, corresponding to a feature size of approximately 2 microns, allowing clear observation of typical biological specimens. In panel (c) a direct comparison of the optical performance of the cost-effective microscope and a high-end optical microscope equipped with a Nikon Plan 10x/0.25 objective is presented. While the commercial microscope provided superior image quality with minimal distortions, the cost-effective proposal delivered comparable visible detail, demonstrating its viability as an effective alternative to image complex biological samples as, for instance, a dicotyledonous plant. The total cost of the proposed bright-field microscope is around \$45, inviting its open fabrication and adaptation; its modular design allows users to customize or upgrade the components to meet specific educational or experimental needs, including easily swapping objective lenses for varying magnification.



**Figure 1: Cost-effective 3D printed bright field microscope. (a) Picture of the built microscope. (b) Image of the USAF 1951 test target. (c) Comparison of the imaging performance between a high-end commercial microscope and the cost-effective proposal.**

### References

- [1] J. S. Cybulski, J. Clements, and M. Prakash, PLOS ONE 9, e98781 (2014).
- [2] C. Yu, S. Li, C. Wei, S. Dai, X. Liang, J. Li, Micromachines 13, 869 (2022).

**Corresponding author:** Diego Londono-Zapata. **Email:** dilondonoz@unal.edu.co

# Detection of microstructural patterns in optical coherence tomography images using artificial intelligence tools to differentiate melanoma from melanocytic nevus

Florencia Pinto, Rene Sosa

**Topic(s):** Image processing, vision and artificial intelligence [ID 070]

**Institution(s):** Universidad Privada Boliviana, Bolivia

Optical coherence tomography (OCT) has been established as a non-invasive imaging technique with high spatial resolution, which permits a detailed visualization of tissue microstructure. In melanoma diagnosis, the accurate differentiation between malignant and healthy tissue is crucial for early detection and improved clinical results.

This project proposes the development of a detection model based on convolutional neural networks (CNN's) to identify microstructural patterns in OCT images. To achieve this, publicly available databases will be used, with a focus on cross-validation and robustness against interpatient variability. Additionally, complementary techniques such as transfer learning and data augmentation will be explored to enhance system performance, especially in the context of limited datasets.

The main objective is to achieve high sensitivity and specificity in classification, minimizing false positives and negatives, and ultimately providing a reliable clinical decision-support tool for the early diagnosis of melanoma.

## References

- [1] Ayadh, M., et al. (2025). AI-assisted identification of non-melanoma skin cancer structures based on combined high-resolution morphological imaging and chemical characterisation of skin tissues. *Journal of Biomedical Optics*, 30(7), 076008. <https://doi.org/10.1117/1.JBO.30.7.076008>
- [2] Kulyabin, M., et al. (2024). OCTDL: Optical coherence tomography dataset for image-based deep learning methods. *Scientific Data*, 11, Article 3182. <https://doi.org/10.1038/s41597-024-03182-7>
- [3] Lai, P.-Y., Shih, T.-Y., Chang, Y.-H., Chang, C.-H., & Kuo, W.-C. (2025). Deep learning with optical coherence tomography for melanoma identification and risk prediction. *Journal of Biophotonics*, 18(1), e202400277. <https://doi.org/10.1002/jbio.202400277>
- [4] Naranjo, F. P., et al. (2025). A clinical study of two optical coherence tomography scanners: How resolution and depth affect skin cancer diagnostic accuracy classified by deep neural networks and foundation models. *Optica Open Preprints*. <https://preprints.opticaopen.org/articles/preprint/29492909>
- [5] Rotunno, G., Salvi, M., Deinsberger, J., Krainz, L., Weber, B., Sinz, C., & Liu, M. (2025). DERMA-OCTA: A comprehensive dataset and preprocessing pipeline for dermatological OCTA vessel segmentation. *Scientific Data*, 12, 1473. <https://doi.org/10.1038/s41597-025-05763-6>

---

**Corresponding author:** Florencia Pinto. **Email:** [tabatapinto1@upb.edu](mailto:tabatapinto1@upb.edu)

## Three-dimensional measurement of human face topography using fringe projection profilometry

Riquelme P-Cruz, Ivan Choque, Edith Paredes

**Topic(s):** Instrumentation, measurement and metrology, Optics in computing, Optics at surfaces [ID 032]

**Institution(s):** Universidad Nacional Jorge Basadre Grohmann, Perú

Every year, thousands of people experience deformities in their facial structure as a result of surgical interventions or pathological processes, since the purpose of these procedures is to treat the disease [1]. In this work, the three-dimensional topography of the human face is measured using fringe projection profilometry (FPP). The profilometer comprises a multimedia projector and a monochrome CMOS camera. Human face samples were taken from five volunteers aged between 20 and 40 years. Fringe patterns with sinusoidal profiles were projected onto samples under study, and the phase shift between two consecutive fringe patterns was  $\pi/3$  [2]. Images were recorded and processed in Matlab software. Images were demodulated using a six-step phase-shift algorithm (PSA). Preliminary results display three-dimensional human face topographies with high resolution; this confirms the feasibility of the employed technique. Finally, our results can be useful as recorded morphology for future developments in the design and manufacture of facial prostheses [3].

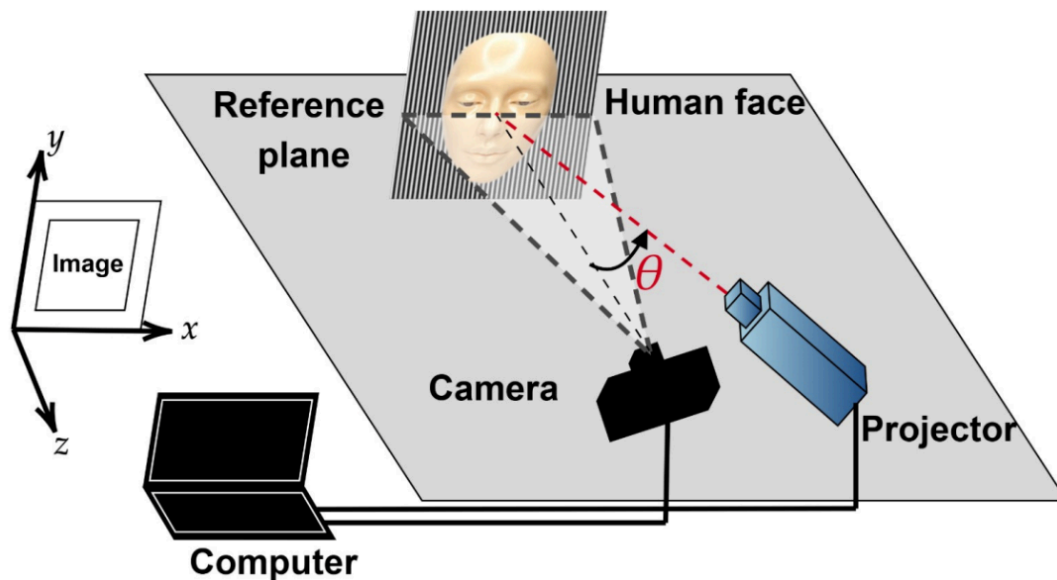


Figure 1: Experimental setup of a Fringe Projection Profilometer (FPP).

### References

- [1] Xue J, Zhang Q, Li C, Lang W, Wang M, Hu Y. 3D face profilometry based on a galvanometer scanner with infrared fringe projection at high speed. Appl Sci. 2019;9(7):1458.
- [2] M. Servin, J. A. Quiroga, J. M. Padilla, et al., Fringe pattern analysis for optical metrology, Wiley Online Library (2023).
- [3] Bockey S, Berssenbrügge P, Dirksen D, Wermker K, Klein M, Runte C. Computer-aided design of facial prostheses by means of 3D-data acquisition

**Corresponding author:** Riquelme P-Cruz. **Email:** riquelmepc@unjbg.edu.pe

# Measurement and characterization of reflective convex surfaces using Ronchi deflectometry

Franco Gonzales, Josep Arasa

**Topic(s):** Instrumentation, measurement and metrology [ID 039]

**Institution(s):** Pontificia Universidad Católica del Perú, Perú; Technical University of Catalunya, Spain

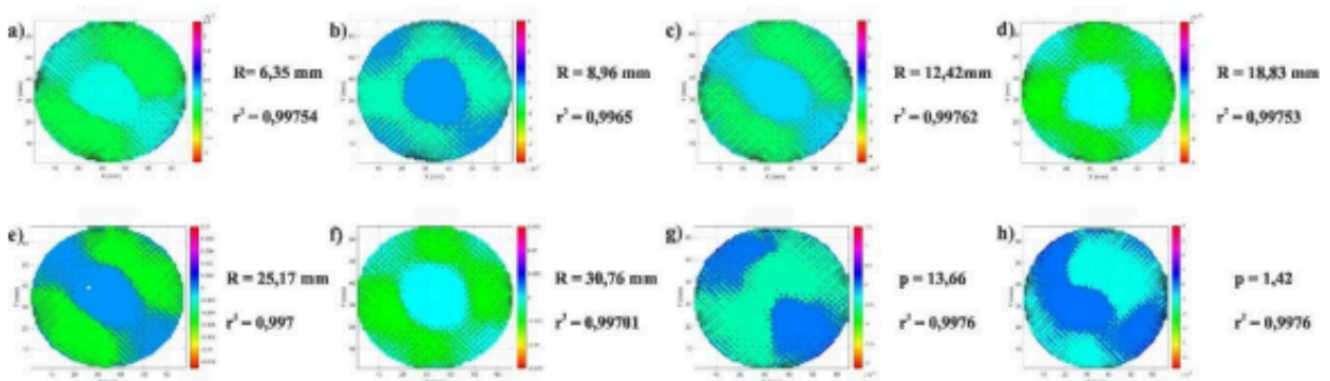
This work presents the measurement and characterization of convex reflective surfaces, both spherical and aspherical, using Ronchi deflectometry. We also describe the implementation of the measurement system using commercial optical components, the evaluation of system-induced errors, and the calibration process [1,2].

Using the technique as mentioned earlier, a set of convex surfaces was measured: six spherical surfaces and two aspherical surfaces. As a result of the measurements, we report the residuals between the sagittal values measured by the system and those obtained from the best-fit surface. Finally, we can conclude that the system measures adequately within its allowed tolerance.

The surface fitting was performed using Equation 1, where  $z$  is the sagitta of the surface,  $R$  is the radius of curvature,  $p$  is the conic constant,  $(x, y)$  are the coordinates of the measured surface points, and  $(a, b)$  are the coordinates of the vertex.

$$z = \frac{\frac{1}{R} [(x - a)^2 + (y - b)^2]}{1 + \sqrt{1 - p \frac{[(x - a)^2 + (y - b)^2]}{R^2}}}$$

For the spherical surfaces, the fitting was carried out using  $p = 1$ , whereas for the aspherical surfaces, the value of  $p$  was determined through the fitting process.



**Figure 1: Results of the measurements of convex spherical (a–f) and aspherical (g and h) surfaces using Ronchi deflectometry.**

## References

- [1] F. Gonzales, J. Arasa, "Optical behavior simulation of the divergence adapter elements in a Ronchi deflectometry configuration for convex surfaces" *Opt. Pura Apl.* V55 - N3, <http://dx.doi.org/10.7149/OPA.55.3.51107> (2022)
- [2] F. Gonzales and J. Arasa, "Determination and Compensation of the Induced Error by Divergence Adapter Systems in the Measurement of Convex Surfaces by Ronchi Deflectometry," in *Optica Latin America Optics and Photonics Conference (LAOP) 2024, Technical Digest Series* (Optica Publishing Group, 2024), paper Tu2B.3.

**Corresponding author:** Franco Gonzales. **Email:** fgonzales@pucp.edu.pe

## Deformation of metallic parts measurement applied shearing interferometry and mechanical sensors

Ernesto Javier Ruiz-Ortega, Francisco Javier Casillas-Rodríguez, Francisco Gerardo Peña-Lecona, Jesús Muñoz-Maciel, Sergio Álvarez-Rodríguez, Miguel Mora-Gozalez

**Topic(s):** Instrumentation, measurement and metrology, Optics and photonics in the industry [ID 088]

**Institution(s):** Universidad de Guadalajara, Mexico

Mechanical deformations are changing that materials experience when they receive impulses or external forces. Usually, to measure these deformations various mechanical sensor techniques are commonly used, such as strain gauges, piezoelectric sensors, load cells, and extensometers, among others, these types of sensors are used as transducers, which transform mechanical energy into an electrical signal [1]. In addition, optical methods such as interferometry can be used; these methods allow the changes measurement of the object under test between its initial state (when it is not being subjected to mechanical stresses) vs. its deformed state when an external force is applied [2].

In this work, different types of metals currently used in the automotive industry for the manufacture of gears, pistons, supports, and structure of automobiles will be evaluated. In which the metal part will be subjected to a tension or compression stress to measure the deformations suffered by the same material. The measurements will be carried out by optical interferometry in conjunction with strain gauges, in shearing and Wheatstone bridge configuration, respectively (as shown in Figure 1).

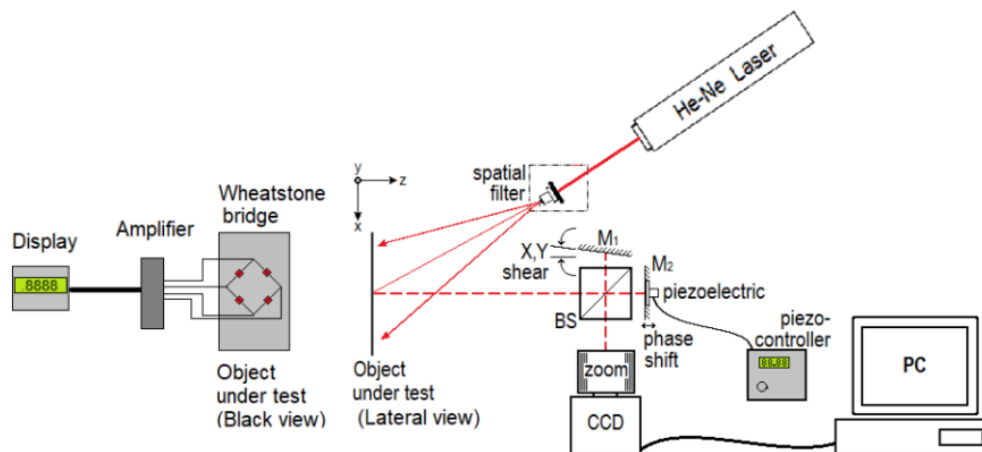


Figure 1: Electrical and optical diagrams.

A mechanical press was used to deform the object under test, a rectangular metal piece (aluminum, steel or stainless steel). The press can deliver deformations of up to 2 tons in compression or in tension configurations, respectively; the experiment has been carried out up to 0.5 tons. The gauge array can measure deformations in the piece from 1 kg up to the limit of the experiment; however, the interferometer begins to detect deformations after 10 kg, but the interferogram phase shows a 3D deformation view and it reaches up to 632nm resolution. Given these results, it can be concluded that both methods work properly for the study of our materials or our objects under test and it is possible to interpret the deformation with any of these methods.

### References

- [1] R. Pallás Areny. *Sensores y acondicionadores de señal*, 4a ed., Marcombo, 2003.
- [2] P. Hariharan. *Optical Interferometry*, 2nd ed. Elsevier Science, 2003.

**Corresponding author:** Miguel Mora. **Email:** miguel.mora@academicos.udg.mx

# Latent Fingerprint Imaging via Modulated-Intensity Maps from Fringe-Pattern Deflectometry

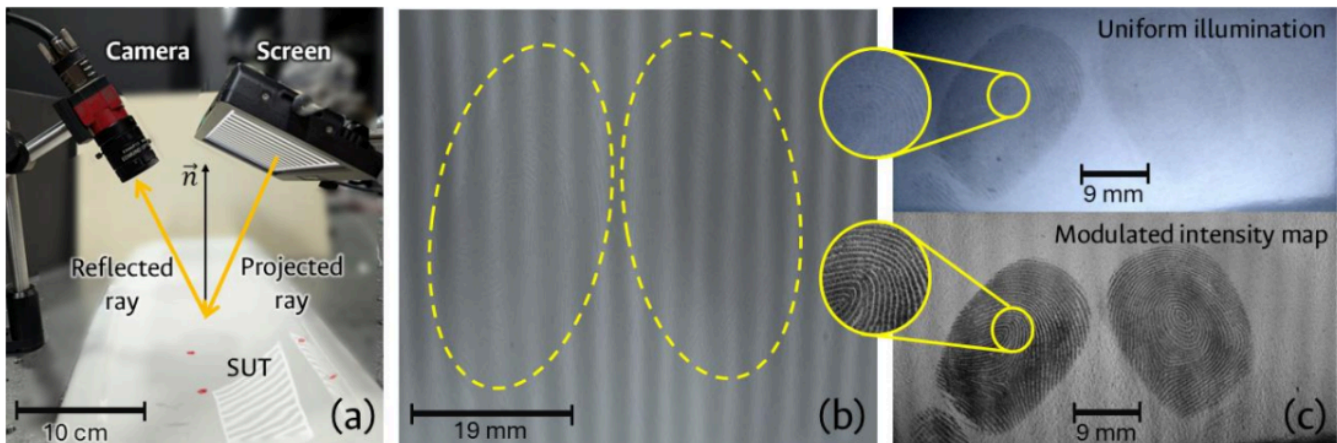
Julian Perez-Carvajal, Carlos A. Buitrago-Duque, and J. Garcia-Sucerquia

**Topic(s):** Image processing, vision and artificial intelligence, Instrumentation, measurement and metrology, Optics and photonics in the industry [ID 066]

**Institution(s):** Universidad Nacional de Colombia, Colombia

Unlike conventional methods for revealing latent fingerprints, which are based on physical or chemical labeling of the surface [1], this work presents a contactless and non-destructive approach for latent fingerprint imaging using fringe pattern deflectometry [2]. The setup of the method is shown in Fig. 1(a). It requires only a regular screen to display a sinusoidal fringe pattern, whose fully- or partially-reflection on a surface under test (SUT) is recorded by a digital camera. The recording codifies height variations of the steady SUT in the form of intensity modulations, as shown in Fig. 1(b). To retrieve the surface information, four controlled phase shifts of  $\pi/2$  steps are introduced into the sinusoidal pattern, such that the recorded intensity can be modeled as  $I_n(x, y) = I_0 + I_m(x, y) * \cos [\varphi(x, y) + n\pi/2]$ .  $n \in [0,3]$  equation (1).

$I_0$ ,  $I_m(x, y)$ , and  $\varphi(x, y)$  correspond to the background intensity, the modulated intensity, and the pattern-phase variations induced by the SUT, respectively [3]. In each recording,  $I_m(x, y)$  codifies the subtle local reflectivity variations of the SUT in the form of changes in the reflected fringe intensity; for case of study in this contribution, those changes can be caused by the presence of oily residues on the surface, such as those left by fingerprint marks [1]. Using a conventional phase-shifting formalism, the modulated intensity can be extracted from the recorded set as  $I_m(x, y) = 1/2\sqrt{(I_3 - I_1)^2 + (I_2 - I_0)^2}$  equation (2). As illustrated in Fig.1(c), the  $I_m$  map, in the lower right corner, provides a significantly enhanced contrast of the fingerprint marks when compared to a direct capture under uniform illumination, as shown in the upper right corner of Fig. 1(c). This method opens new possibilities for contactless forensic analysis and the evaluation of macroscopic alterations in surface reflectivity. Furthermore, the setup simplicity, requiring only a screen for pattern projection and a camera for recording, opens a way for accessible instrumentation innovations and field-ready systems.



**Figure 1:** (a) Experimental deflectometry setup. (b) Fringe pattern recording with distorted intensity by the SUT. (c) Latent fingerprints obtained using uniform illumination (top) and the modulated intensity map (bottom).

## References

- [1] Dhanotia, J., Chatterjee, A., Bhatia, V., & Prakash, S. (2018). A simple low cost latent fingerprint sensor based on deflectometry and WFT analysis. *Optics and Laser Technology*, 99, 214–219
- [2] Burke J, Pak A, Höfer S, Ziebarth M, Roschani M and Beyerer J (2023), Deflectometry for specular surfaces: an overview.
- [3] Huang, L., Idir, M., Zuo, C., & Asundi, A. (2018). Review of phase measuring deflectometry. *Optics and Lasers in Engineering*, 107, 247–257.

**Corresponding author:** Diego Londono-Zapata. **Email:** dilondonoz@unal.edu.co

# Optical Design and prototyping of terrestrial telescope

Miranda Josué, Baldwin Guillermo, Gonzales Franco

**Topic(s):** Optical design and fabrication [ID 018]

**Institution(s):** Pontificia Universidad Católica del Perú, Perú

This work shows progress achieved at the PUCP in the development of telescopes from optical design, manufacturing, prototyping and parameter evaluation [1]. The telescope has a magnification of 28X, a field of view of 1.2°.

**1. Optical Design:** The Telescope designed is 28X magnification and 1,2° of field of view. For this the focal length of the objective and eyepiece are 350 mm and 12.5 mm respectively. The observation of an object for infinity focusses and for close focus is possible if the distance that the light travels from the objective to the eyepiece changes. In binoculars, for example, the eyepieces move, thus increasing the objective-eyepiece distance for close focus and decreasing said distance to focus on more distant objects. In terrestrial telescopes, the focusing system considers the use of a sliding Porro prism (secondary Porro prism) to increase the distance that the light travels from the objective to the eyepiece.

**1.1 Objective Design:** The main requirement of the terrestrial telescope objective is to be corrected for coma, spherical and axial color aberrations. Therefore, the objective to be designed consists of a cemented achromatic doublet. Considering eliminating coma and spherical third-order aberrations for an objective, we have [2]:

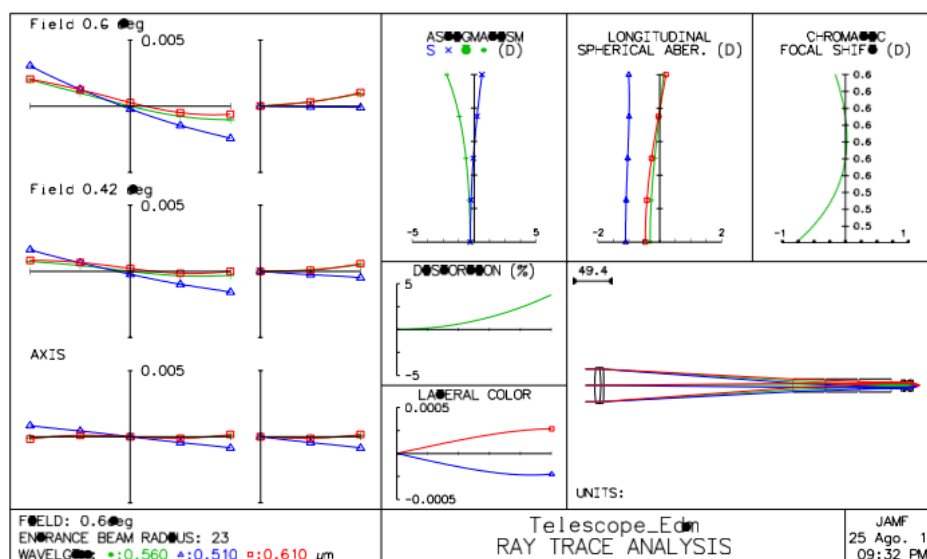
$$c_{a2} = c_{b1} = \frac{n_a V_a \phi - c_{a1} n_a (V_a - V_b) (n_a - 1)}{(V_a - V_b) (n_a - 1)^2 c_{a1} t_a - n_a} \dots (1)$$

$$c_{b2} = \frac{n_b V_b \phi - c_{b1} n_b (V_b - V_a) (n_b - 1)}{(V_b - V_a) (n_b - 1)^2 c_{b1} t_b - n_b} \dots (2)$$

**Figure 1: Temperature fiber sensor experimental setup.**

The glasses available in the PUCP Optical Manufacturing Laboratory are BK7, BAK4, SF10, F2. After simulating and optimizing the design in OSLO.edu, the best results were obtained for the combination of BaK4 and SF10 glasses; for 350 efl and 1,2° field of view, the radii of curvature obtained are  $Ra1= 220.15$  mm;  $Ra2=Rb1=-179.85$  mm y  $Rb2=-625$  mm. The objective is diffraction limited. It has corrected spherical and chromatic aberrations and has very low distortion. [3; 4]

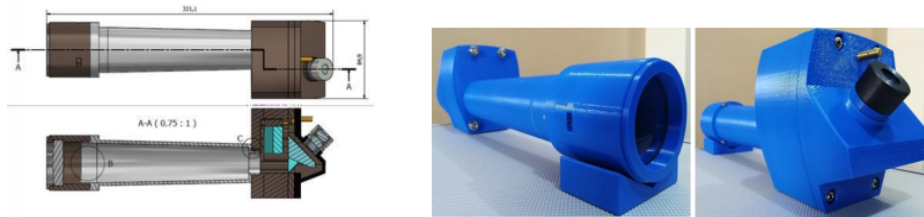
**1.2 The ocular Plössl:** The eyepiece Plössl consists of two identical doublets cemented achromatically. Following the equations (1) and (2), the best results were obtained for the combination of BaK4 and SF10 glasses  $Ra1= 15.63$  mm;  $Ra2 = Rb1 = -12.75$  mm y  $Rb2= -45.21$  mm



**Figure 1: Simulation of terrestrial telescope in OSLO.edu. The spherical aberration has a magnitude of approximately 1 mm at 0.7 of the total field. Astigmatism is 2 diopters.**

**2. Prototyping:** The semi-kinematic design has been considered for the assembly of objective, eyepiece and prisms. Lens assembly is done by generating radial compressions to the lens to secure it to the cell. For this reason, it was considered to use retaining rings and elastic rings as separating elements between lenses. The prisms mounting is using adhesives because it reduces the complexity of the interface, allows compact assembly, and provides adequate mechanical strength to withstand shocks, vibrations and temperature changes [5; 6].

The mechanical parts of the telescope have been printed in 3D. The 3D printer used is a FORTUS 400mc and the thermoplastic material is ABS, which, among other characteristics, is very resistant to impact and has a melting temperature that is between 230 °C to 260 °C. The drawing of the mechanical elements was done in Autodesk Inventor, a software for the design of mechanical parts in 3D. The file corresponding to the part is saved as an STL file and the file is sent to a printer. The FORTUS 400mc printer has a tolerance of 0.15 mm, this is taken into consideration in the design of the mechanical parts of the telescope.



**Figure 2: For the mechanics of the terrestrial telescope, modular prototyping is considered. The objective, eyepiece and prisms are assembled independently and then these are assembled to obtain the terrestrial telescope. The semikinematic design is considered for the assembly of optical elements.**

**3. Evaluations of parameters:** Optical tests are carried out according to following methods proposed by Baldwin G. [1], Jhonson B. [7], Yoder P. & Vukobratovich D. [8]; and Youngworth R. [9]. In the present work, are measured the angular amplification, exit pupil diameter, angular field of view, resolution using USAF cards and to measure the wavefront error of the telescope, a ZYGO 4" GPI XP/D interferometer is used, and two flat reference surfaces of  $\lambda/20$  quality each are used.



**Figure 3: The wavefront error is equivalent to  $0.55\lambda$ . It is within an allowable error close to  $0.5\lambda$  error according to Walker B. [4, p.23]. As can be seen, the total wavefront error indicated by the software is  $1.1\lambda$ ; but, since the wavefront travels through the telescope twice, the wavefront error is half that.**

**4. Conclusions:** The telescope prototype resulted in a visual system with 26.3X magnification; an exit pupil of 1.69 mm in diameter, an angular field of view of  $1.16^\circ$ , a resolution of 102 pl/mm and a wavefront error of  $0.55\lambda$ . This is a great advance in the objective of generating an industry in the field of optical instrumentation for observation in Peru.

#### References

- [1] Baldwin Guillermo, "First Peruvian Binocular", Proceedings of SPIE - vol 10590, U.S.A., 2017.
- [2] Warren Smith, "Modern Optical Engineering", 4th Ed., McGraw-Hill, New York. 2008
- [3] O'Shea Donald, "Elements of Modern Optical Design", A Wiley Interscience Publication John Wiley & Sons, New York, U.S.A., 1985.
- [4] Walker, Bruce, "Optical Design for Visual Systems", SPIE, USA., 2000.
- [5] Yoder Paul, "Optomechanical System Design", 3rd Edition, SPIE, Bellingham, Washington., 2006.
- [6] Vukobratovich Daniel, "Introduction to Optomechanical Design", SPIE Short Course SC014, 2003.
- [7] Jhonson, B. K., "Optics and Optical Instruments", Dover Publications, New York., 1960
- [8] Yoder, Paul Jr. & Daniel Vukobratovich, "Field Guide to Binoculars and Scopes", SPIE, Bellingham, Washington, 2011.
- [9] Youngworth, Richard 2018 SC003 Practical Optical System Design, SPIE. San Diego, California, United States.

**Corresponding author:** Josue Alfonso Miranda Fernández. **Email:** josue.miranda@pucp.edu.pe

# A Remote Solar Photovoltaic Laboratory for Energy Dispatch Analysis

Johnny Villarroel-Schneider

**Topic(s):** Instrumentation, measurement and metrology, Remote sensing and sensors, Solar energy [ID 119]

**Institution(s):** Universidad Mayor de San Simón, Bolivia

The global energy transition needs a highly trained workforce, however, access to essential, hands-on renewable energy education remains limited, particularly in developing countries and remote geographical areas. Traditional laboratories are often cost-prohibitive, leading to significant educational disparities. This work presents the implementation of an innovative Remote Solar Laboratory by the Universidad Mayor de San Simón (UMSS), Bolivia, as a core component of the Erasmus+ EUBEGP project. The goal is to modernize educational strategies and enhance accessibility for graduate students studying the technologies of the energy transition.

The remote laboratory system is designed to replicate and evaluate a rural solar photovoltaic (PV) system configured for Tier 2/3 electricity demand. The hardware setup includes two 50W PV panels, a 280Wh lithium battery, an electricity dispatch controller, and a PLC-based Load Replicator Controller. This replicator simulates diverse, user-defined load demand curves using controlled electrical resistors. Remote interaction is managed via a dedicated web platform, which incorporates a robust reservation and access control system [1]. Users interact with the system by remotely uploading CSV files containing time-based power demand profiles. The platform then executes the simulation and provides real-time data visualization of critical parameters, including generated power, required power, battery voltage, current, and solar radiation. All resulting data is logged and made available for download, allowing students to conduct in-depth analysis and dispatch optimization studies under realistic conditions. By offering open, practical access to system performance data, the laboratory promotes critical thinking, improves research skills, and ensures equitable access to high-quality practical training, supporting the advancement of renewable energy education worldwide [2, 3].



**Figure 1: Equipment and data visualization of the Solar Laboratory.**

**Acknowledgments:** This work was partially funded by the Erasmus+ project “EU-BEGP” (Project No. 101081473).

## References

- [1] A. Villazón et al. A Booking System for Remote Laboratories. In *Open Science in Engineering*, 341, 348 (2023).
- [2] L. Sanchez and M. Gómez. Enhancing STEM Education through Digital Twin Remote Labs. *Journal of Engineering Education*, 45(2), 112–125 (2024).
- [3] J. Smith et al. Real-time Monitoring and Optimization of Microgrids via Cloud-Based Platforms. *Sustainable Energy Technologies and Assessments*, 55, 103987 (2023).

**Corresponding author:** Johnny Villarroel-Schneider. **Email:** [jh.villarroel@umss.edu](mailto:jh.villarroel@umss.edu)

## Nailfold capillaroscopy

Manuel Abraham López Pacheco, María Fernanda Rivera Soto

**Topic(s):** Bio photonics and biomedical applications, Instrumentation, measurement and metrology [ID 079]

**Institution(s):** Benemérita Universidad Autónoma de Puebla, México

Nailfold capillaroscopy is a non-invasive diagnostic technique that enables direct observation of blood capillaries, particularly in the periungual region. Its ability to detect morphological alterations—such as dilations, hemorrhages, architectural disruption, or capillary neoformations— makes it a key tool for the early diagnosis of systemic diseases and for monitoring their progression. Due to its simplicity, low cost, and safety, capillaroscopy has become an important method in both clinical practice and microcirculation research.

However, many commercial capillaroscopes present significant limitations in image quality. Low resolution and poor contrast hinder the accurate extraction of morphological features, which restricts the effective application of Artificial Intelligence (AI) techniques for automated analysis. This project aims to address these issues through a comprehensive upgrade of the device, improving the optical system, user experience, and data communication capabilities. The proposed improvements include:

- **Optical optimization:** Redesign of the light path and selection of high-transmittance aspheric lenses to enhance resolution and detail.
- **Advanced illumination:** Use of adjustable-spectrum LED arrays with PWM control to adapt lighting to different skin phototypes and reduce visual noise.
- **Cross-polarization:** Implementation of linear filters to eliminate specular reflections and improve capillary contrast.
- **Embedded processing:** Integration of FPGA/SoC modules for real-time edge enhancement, noise reduction, and lossless compression.
- **Remote communication:** Wi-Fi connectivity and DICOM protocol support for secure data transmission to medical platforms.
- **Ergonomics and portability:** Structural redesign using 3D printing with lightweight, biocompatible materials to enhance usability in clinical and mobile settings.

These enhancements will enable the capture of high-fidelity images suitable for AI training, accelerating diagnostic workflows and expanding access to more precise and clinically useful capillaroscopy.

### References

- [1] Cantú Pompa, J. J. (2022). Alteraciones capilaroscópicas en lupus eritematoso sistémico [Tesis de especialidad, Universidad Autónoma de San Luis Potosí, Facultad de Medicina]. Hospital Central “Dr. Ignacio Morones Prieto”.
- [2] Juanola, X., Sirvent, E., & Reina, D. (2004). Capillaroscopy in rheumatology units. Uses and applications. *Revista Española de Reumatología*.

---

**Corresponding author:** Manuel López. **Email:** manuel.lopezpa@correo.buap.mx

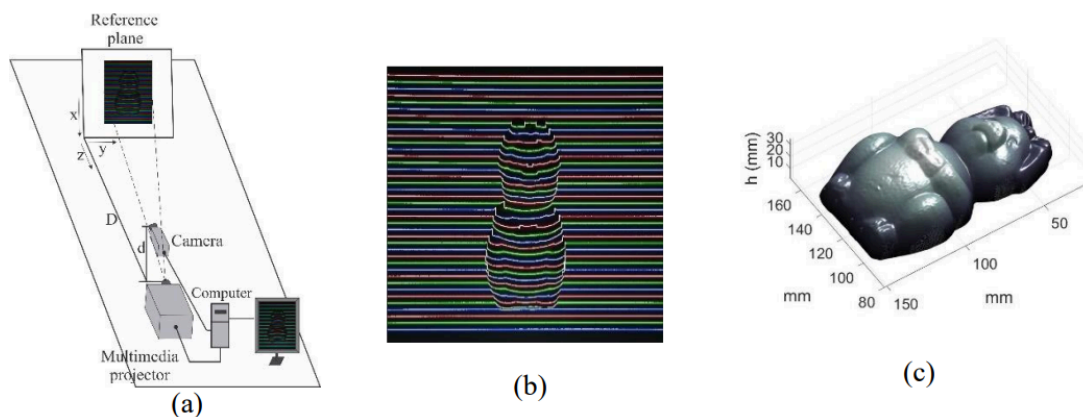
## 3D scanning of objects by color multi-line structured light projection

Heyner Vilchez Rojas, Amalia Martínez García, Juan A. Rayas, Miguel Asmad Vergara, Alejandro Montoya Janampa

**Topic(s):** Image processing, vision and artificial intelligence, Instrumentation, measurement and metrology, Machine vision [ID 043]

**Institution(s):** Pontificia Universidad Católica del Perú, Perú; Centro de Investigaciones en Óptica, México

In this work, we propose an effective method for the 3D reconstruction of objects by color multi-line structured light projection with Gaussian profile. The shape of an object is obtained with high pixel density by calculating the local displacement of the positions of the color lines of a set of gratings projected on an object with respect to a reference plane [1, 2]. In this way, complex phase unwrapping algorithms, which are typically required in phase detection-based profilometry methods, are dispensed with [3]. Additionally, by using a multimedia projector as the light source, the speckle commonly found in laser-based systems is avoided, which otherwise degrades image quality and affects measurement precision [4]. Currently, the main challenge for the calculation of the displacements is the correct recognition of the broken line segments belonging to a single projected light line. To deal with this challenge, our contribution is to propose the independent processing of the lines in their respective color channels (R, G and B), which allows the use of morphological operations to reduce the number of line segments. This is followed by a simple grouping method based on the area of the segments. Once the line segments are grouped, the calculation of the positions of the lines with sub-pixel resolution is carried out by skeletonization using the Bézier curve method. The experimental setup is shown in Figure 1(a). The effectiveness of the proposed methods and algorithms is supported by our experimental results, as shown in Figures 1(b) and 1(c).



**Figure 1: (a) Experimental setup scheme and test object. (b) Skeletonization of the color lines from one of the captured images. (c) 3D shape of the test object with high pixel density.**

### References

- [1] Vilchez-Rojas, H.L., A. Martínez-García and J.A. Rayas, 3D scanning of objects by projection of three incoherent RGB lines with Gaussian profile. *Optik*, 2022. 265: p. 169393.
- [2] Vilchez-Rojas, H.L., J.A. Rayas, and A. Martínez-García, Use of white light profiles for the contouring of objects. *Optics and Lasers in Engineering*, 2020. 134: p. 106295.
- [3] Zhang, S., Absolute phase retrieval methods for digital fringe projection profilometry: A review. *Optics and Lasers in Engineering*, 2018. 107: p. 28-37.
- [4] Li, W., et al., 3D measurement system based on divergent multi-line structured light projection, its accuracy analysis. *Optik*, 2021. 231: p. 166396.

**Corresponding author:** Mariana Vasquez. **Email:** heyner.vilchez@pucp.pe

## Second Harmonic Generation from LIPSS on GaAs

G. V. García-Najar, S. Camacho-López, M. A. García Zarate and A. V. Khomenko

**Topic(s):** Nonlinear optics [ID 105]

**Institution(s):** Centro de Investigación Científica y de Educación Superior de Ensenada, México

Laser-induced periodic surface structures (LIPSS) are a well-documented phenomenon that can be generated on nearly any material via laser irradiation. These structures offer a straightforward and versatile method for tailoring surface optical properties [1]. In this study, we investigate the potential of LIPSS to enhance light confinement at the surfaces of semiconductor crystals with high nonlinear optical coefficients [2]. This localized field enhancement significantly boosts the efficiency of nonlinear optical interactions, paving the way for the development of advanced light sources, including those relevant to quantum optics applications.

In this study, we investigated the formation of LIPSS on GaAs surfaces using a laser scanning method, enabling the fabrication of structures over large areas. The laser system operated at a repetition rate of 5 kHz, with 120 fs pulse duration and a central wavelength of 800 nm. Scanning speeds and beam powers were varied between 2–12 mm/s and 10–120 mW, respectively, to optimize the uniformity of the quasi-periodic surface relief. The laser beam had a diameter of 65  $\mu\text{m}$ . The most uniform and well-ordered structures were achieved at the lowest irradiation powers. A representative scanning electron microscope (SEM) image of the resulting LIPSS is shown in Figure 1a. The structures exhibited an average period of approximately 730 nm, which remained largely consistent across a broad range of beam powers and scanning speeds.

To investigate second harmonic generation (SHG), we employed an ultrashort-pulse laser with a pulse duration of 100 fs, a repetition rate of 60 MHz, and a central wavelength of 830 nm. The resulting second harmonic signal was distributed over a broad angular range, appearing as diffraction orders corresponding to the periodicity of the fabricated LIPSS, as shown in Figure 1b. This measurement was taken at a pump incidence angle of 45°. The observed broadening of the diffraction orders is attributed to the quasi-periodic nature of the LIPSS. We conducted a detailed study of the intensity and polarization of the SHG diffraction orders as a function of the pump beam's polarization. Comparison of the experimental results with theoretical predictions from numerical simulations indicates that the LIPSS exhibit a crystalline orientation aligned with that of the GaAs substrate. Furthermore, our theoretical analysis suggests that SHG efficiency can be enhanced by several orders of magnitude when the structural period and pump wavelength satisfy a specific resonance condition.

We propose that such an optimal condition can be achieved by forming LIPSS on different crystals with zinc-blende symmetry, which inherently possess high second-order optical nonlinearity.

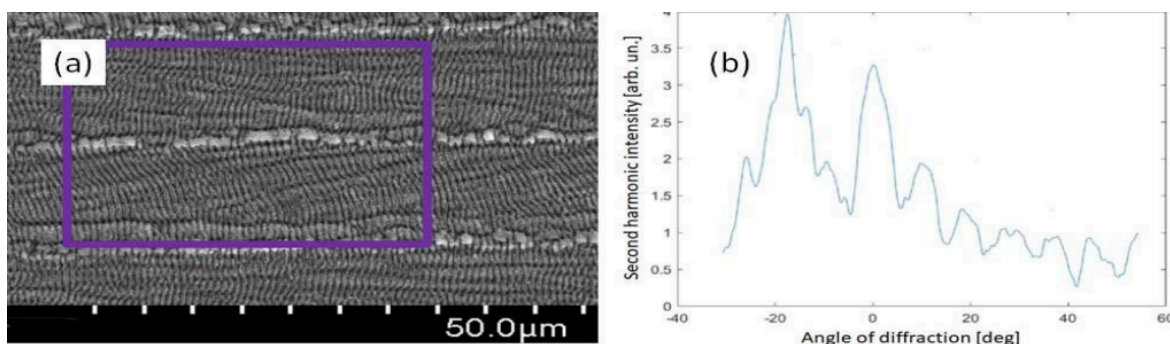


Figure 1: (a) SEM image of LIPSS on GaAs crystal, (b) angular distribution of SH intensity.

### References

- [1] T. Liu et al., *Frontiers in Nanotechnology*, 4, 891892 (2022).  
 [2] C. J. Valencia-Cacedo et al., *Results in Physics*, 37, 105516 (2022).

**Corresponding author:** Anatoly Khomenko. **Email:** akhom@cicese.mx

## Photographs of RIOA-OPTILAS 2025



Official photo RIOA-OPTILAS 2025

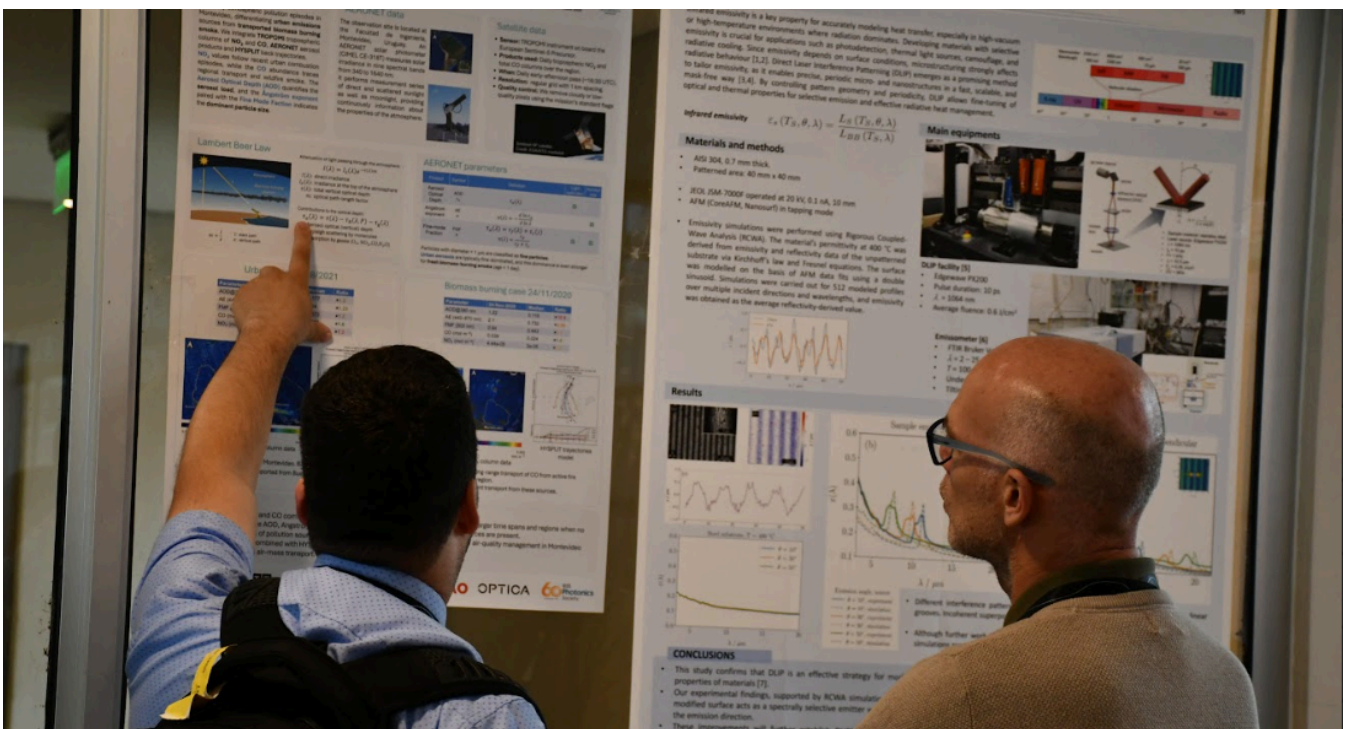


Opening speech at the XII Ibero-American Meeting on Optics / XV Latin American Meeting on Optics, Lasers, and Applications, held in Santa Cruz de la Sierra, Bolivia, in 2025 (Carlos Foronda, PhD, Vice-President of the UPB campus in Santa Cruz).

## Photographs of 1st day of RIOA-OPTILAS 2025



## Photographs of 1st day of RIO-OPTILAS 2025



## Photographs of 1st day of RIOA-OPTILAS 2025



## Photographs of 2nd day of RIOA-OPTILAS 2025



## Photographs of 2nd day of RIO-OPTILAS 2025



## Photographs of 3th day of RIOA-OPTILAS 2025



## Photographs of 3th day of RIOA-OPTILAS 2025



## Photographs of 4th day of RIOA-OPTILAS 2025



## Photographs of 5th day of RIOA-OPTILAS 2025



## Photographs of 5th day of RIOA-OPTILAS 2025



## Photographs of 5th day of RIOAO-OPTILAS 2025



## Photographs from the RIOA-OPTILAS 2025 dinner



## Photographs from the RIOA-OPTILAS 2025 dinner




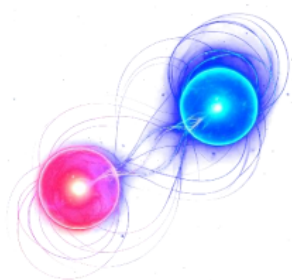
## Detailed Conference Program

### Monday

Monday, November 17th						
Hour						
7:45-08:55	Registration of participants					
9:00-09:30	Opening Ceremony					
<b>Room 01 (Auditorium)</b>						
Monday, November 17th						
Hour	ID	Presentation title	Presenter	Chairman	Topics	
09:30 - 09:50	017	<a href="#">Advanced characterization of oxide nanomaterials using infrared spectroscopy</a>	Iñigo González	Cesar Perez	Bio photonics and biomedical applications	
10:10 -10:30	099	<a href="#">Precision Tissue Classification via LIBS and ML: Toward Intraoperative Pathology Screening</a>	Rene Sosa			
10:30 -10:50	095	<a href="#">Optical Multispectral Characterization of Photonic and Plasmonic Properties of Living Biostructures and Optical Ranging Biodiversity Assessment</a>	Cesar Costa			
10:50 -11:10	025	<a href="#">Spatio-chromatic vision changes following cataract surgery with multifocal diffractive intraocular lens implantation</a>	Maria Millán			
11:30 - 12:30	Plenary 1 Peter de Groot	<b>Physical principles of optical interferometry for surface topography measurement</b>				
12:30 - 13:45	Lunch break					
13:50 - 14:08	098	<a href="#">Ablation volume analysis in laser induced breakdown spectroscopy</a>	Rene Sosa	Cesar Perez		
14:08 - 14:26	094	<a href="#">Application of photonic principles for medical samples transportation: Radiative cooling fabrics in warm tropical weather</a>	Alicia Zelada-Acosta			
14:26 - 14:44	113	<a href="#">Bio-inspired retinal analysis theoretical model based on mantis shrimp vision for monitoring the progression of Sanfilippo syndrome</a>	Mayra Ocampo			
14:44 - 15:02	048	<a href="#">Contouring of residual limb by white light profile for medical prosthetics</a>	Joaquin Sifuentes			
15:02 - 15:20	079	<a href="#">Nailfold capillaroscopy</a>	Manuel López			
15:20 - 15:40	118	Linking Capacity Building & Research in Erasmus+: The EU-BEGP case	A. Villazón / O. Ormachea			
15:40 - 15:55	Coffee break					
16:00 - 17:00	Plenary 2 Carlos Hernández	<b>Structuring ultrafast laser pulses for their application in attosecond science</b>				
17:00 - 18:30	Posters Session / Poster Room / <b>Welcome cocktail (Coffee room)</b>					

## Monday (continuation)

Monday, November 17th			
Room 02 (C1)			
Hour	Activity	Presentation title	Presenter
09:30 - 10:10	First IPS-RIOA Topical Workshop on Quantum Optics - Quantum Optics School	The History of Quantum	Efrain Solarte, Universidad del Valle, Colombia
10:10 - 10:50		From Semi-Classical to Quantum Theory: Understanding Atom-Field Interactions	Imrana Ashraf Zahid, Quaid-i-Azam University, Pakistan 



## Quantum Optics School

November 17 to 20, 2025

Santa Cruz de la Sierra, Bolivia



## Monday (Continuation)

Monday, November 17th			
Posters Session / <b>Hall</b> / 17:00-18:30 / Monday to Wednesday			
#	ID	Presentation title	Authors
1	088	<a href="#">Deformation of metallic parts measurement applied shearing interferometry and mechanical sensors</a>	Ernesto Javier Ruiz-Ortega, Francisco Javier Casillas-Rodríguez, Francisco Gerardo Peña-Lecona, Jesús Muñoz-Maciel, Sergio Álvarez-Rodríguez, Miguel Mora-González
2	042	<a href="#">U-Bent MMM Optical Fiber Sensor for the Detection of Mercury and Cadmium Ions in Aqueous Solutions</a>	Arturo Gaviria-Calderón, Brayan Patiño-Jurado, and Jorge Garcia-Sucerquia
3	061	<a href="#">Cost-effective 3D printed bright-field microscope</a>	Diego A. Londono, Carlos A. Buitrago-Duque, and J. Garcia-Sucerquia
4	066	<a href="#">Latent Fingerprint Imaging via Modulated-Intensity Maps from Fringe-Pattern Deflectometry</a>	Julian Perez-Carvajal, Carlos A. Buitrago-Duque, and J. Garcia-Sucerquia
5	073	<a href="#">Solar Concentrator</a>	Abraham Lopez Pacheco, María Jose Cervantes Oropeza, Bruno Méndez Sánchez, Omar Cuamani
6	091	<a href="#">Thin-Film Deposition and Optical Testing of a First-Surface Mirror for Astronomical Applications</a>	Ana Paula Quelopana, Gonzalo Gálvez de la Puente
7	051	<a href="#">Differentiation of air pollution sources in Montevideo using NO<sub>2</sub>, CO trace gas columns, and atmospheric aerosol properties</a>	Alejandro Agesta, Erna Frins
8	094	<a href="#">Application of photonic principles for medical samples transportation: Radiative cooling fabrics in warm tropical weather</a>	Alicia Zelada-Acosta, Alejandra Oviedo-Cortés, Ariana Y. Miranda-Jimenez, Erwin D. Moreno-Añez
9	044	<a href="#">Manufacture of aspherical mirrors for the implementation of a classic Cassegrain astronomical telescope</a>	P. Gallardo, A. Romero, A. Escudero, F. Gonzales
10	101	<a href="#">Spatial polarization modulation using two LCDs in tandem</a>	Federico Guglielmucci Nazar, Facundo Rouquaud, Sebastián Bordakevich, Silvia Ledesma
11	104	<a href="#">Evaluating gait recognition performance on privacy preserving images</a>	Loana Velasquez-Omonte, Guillermo Sahonero-Alvarez, Edgar Salazar, Laura Galvis
12	087	<a href="#">An Infrared-based Aedes-aegypti Identification Trap</a>	Amina Antonio, Miguel Angel Quiroz, Edgar Salazar
13	086	<a href="#">A Data-based Protocol for a Low-cost Mobile Spectrometer Calibration</a>	Marco De la Fuente Villarroel, Facundo Aliaga, Edgar Salazar
14	072	<a href="#">Analysis of Atmospheric Factors in Free-Space Optical (FSO) Communications for High-Altitude Urban Environments in La Paz, Bolivia</a>	Carlos Girona, Rene Sosa
15	076	<a href="#">Effects of Atmospheric Conditions on Infrared Data Transmission: Experimental Analysis in La Paz, Bolivia</a>	Mariana Vasquez, Rene Sosa
16	070	<a href="#">Detection of microstructural patterns in optical coherence tomography images using artificial intelligence tools to differentiate melanoma from melanocytic nevus</a>	Florencia Pinto, Rene Sosa
17	020	<a href="#">Optical sensors based on optical fibers in Mach-Zehnder type interferometry configuration for measuring ethanol concentration</a>	L. Espejo-Bayona, Sindi Horta, Duber Avila


Monday, November 17th		
Posters Session / Hall / 17:00-18:30 / Monday to Wednesday		
18	045	<a href="#">Optical sensors based on balloon-shaped optical fibers with tip-induced deformation in a Mach-Zehnder interferometer configuration for measuring ethanol concentration</a> L. Espejo-Bayona, Sindi Horta, Duber Avila
19	078	<a href="#">Enhancement of atomic emission intensity of heavy metals in LIBS using silver nanoparticles to increase the detection sensitivity of Cu and Pb</a> Elder Espinoza-Sanchez, Jhenry F. Agreda-Delgado, M. A. Valverde-Alva, W. Aldama-Reyna
20	034	<a href="#">Optical design of double lens for the refractor telescope CST-80 KU by G-sum Method</a> Jenifer Garcia, Franco Gonzales and Ivan Choque
21	032	<a href="#">Three-dimensional measurement of human face topography using fringe projection profilometry</a> Riquelme P-Cruz, Ivan Choque, Edith Paredes
22	048	<a href="#">Contouring of residual limb by white light profile for medical prosthetics</a> Joaquin S. Rivera, Daniel Aquino S., Rodrigo C. Salcedo, Ivan Choque Aquino
23	031	<a href="#">Thickness analysis of South American Camelid Wool Fiber by Fraunhofer Diffraction</a> Jade Aguayo, Ivan Choque and Riquelme P-Cruz
24	111	<a href="#">Bridging Theory and Practice: A Remote Solar Laboratory for Energy Transition Education</a> Juan Peralta-Jaramilo, Emerita Delgado-Plaza, Doménica León-Moreira, Henry Fuentes
25	113	<a href="#">Bio-inspired retinal analysis theoretical model based on mantis shrimp vision for monitoring the progression of Sanfilippo syndrome</a> Adriana M. Suárez Oña, Mayra F. Ocampo Valdivia
26	019	<a href="#">Temperature fiber sensor with variable sensitivity based on the Vernier effect and the bend-induced linear birefringence with tension</a> I. Armas-Rivera, M. Durán-Sánchez, B. Ibarra-Escamilla, M. Delgado-Pinar, A. Díez, J. L. Cruz, and M. V. Andrés
27	028	<a href="#">Stepping stones to engineer pulse propagation through multifrequency nonlinearities</a> M. A. Bosch & M. P. Safont, D. Castelló-Lurbe, E. Silvestre, M. Delgado-Pinar, A. Díez, and M. V. Andrés
28	057	<a href="#">Stochastic Modeling of the Polarization Effect on Light-Induced Mass Transport in Azopolymers</a> Franco Lucio Tambosco, Silvia Adriana Ledesma, María Gabriela Capeluto
29	059	<a href="#">Photoinduced Optical Properties in Layer-by-Layer Azopolymer Films and Polyamines</a> Franco Lucio Tambosco, Candelaria Rico, Gaspar Ariel Casaburi, Florencia Di Salvo, María Gabriela Capeluto
30	016	<a href="#">Laser tuning of IR radiative properties of metals</a> J. Gabirondo López, M. Soldera, J.M. Igartua, A.F. Lasagni, G.A. López
31	075	<a href="#">Optical sensor based on a Mach-Zehnder interferometric curved optical fiber for measuring refractive index</a> Camila Noreña, Sindi Horta, Duber Ávila
32	082	<a href="#">Second-order electrogyration in Bi<sub>12</sub>SiO<sub>20</sub> crystals analyzed by a dualrotation Mueller–Stokes polarimeter</a> María Alejandra Guerrero-V, Luis-A Guerra, Jorge Enrique Rueda-P
33	083	<a href="#">Axial Thermal Gradient Localization and Its Role in LHPG Fiber Integrity</a> Jorge Enrique Rueda-P, João Rodrigues, Antonio Carlos Hernandes
34	106	<a href="#">Optimization of projection selection and measurement time in compressive single-pixel imaging</a> Sebastián Bordakevich, Lorena Rebón, Silvia Ledesma
35	067	<a href="#">Design and production of aplanatic systems for optical imaging using stereolithography 3D printing</a> Angie Sandoval, Alberto Silva, Rafael Torres

## Tuesday

Room 01 (Auditorium)						
Tuesday, November 18th						
Hour	ID	Presentation title	Presenter	Chairman	Topics	
08:30 - 08:47	119	<a href="#">A Remote Solar Photovoltaic Laboratory for Energy Dispatch Analysis</a>	Jhonny Villarroel	Omar Ormachea	Solar Energy, Optics at surfaces, Scattering	
08:47 - 09:05	112	<a href="#">A Hybrid Solar Street Lighting Remotew Laboratory</a>	Alex Villazón			
09:05 - 09:22	111	<a href="#">Bridging Theory and Practice: A Remote Solar Laboratory for Energy Transition Education</a>	Doménica León			
09:22 - 09:40	108	<a href="#">Remote Multisensor System for Indirect Measurement of Nanoparticle Surface Charge under UV Illumination</a>	Edward del Carpio			
09:40 - 09:57	096	<a href="#">A Remote Photovoltaic Laboratory at Latitude 0° for Supporting 24/7 Online Self-learning and Inverted-classroom Teaching</a>	Cesar Costa			
09:57 - 10:15	107	<a href="#">Remote Automated Laboratory for Real-Time Optimization of Coagulation-Flocculation mediated UV Processes in ArsenicContaminated Water Treatment</a>	Juan Rodriguez			
10:15 - 10:34	033	<a href="#">Plasmonic–Magnetic Hybrid Nanostructures for Efficient Photocatalytic Arsenic Remediation in Water</a>	Alberto F. Scarpettini			
10:34 - 10:48	Coffee break					
10:50 - 11:10	053	<a href="#">Fast phase unwrapping by polynomial fitting</a>	Jesús Muñoz	Miguel Mora	Instrumentation, measurement and metrology, Optical device, Imaging systems	
11:10 -11:30	100	<a href="#">Surface Profilometry with a Smartphone-Based Fringe Projection System</a>	Miguel Asmad			
11:30 - 12:30	Plenary 3 Mike McKee	<b>Uncovering Science: Communicating Research to Everyone</b>				
12:30 - 13:45	Lunch break					
14:00 - 14:20	084	<a href="#">Simplified Chromatic Aberration Compensation in Digital Camera Lenses for Fringe Projection Profilometry</a>	Amalia Martínez-García	Miguel Mora / Miguel Asmad		
14:20 - 14:40	022	<a href="#">Upgraded emissometer at the University of the Basque Country based on a new control-design paradigm</a>	Telmo Echániz			
14:40 - 15:00	085	<a href="#">Fringe projection system calibration based on Radon transform</a>	Miguel Mora			
15:00 - 15:20	088	<a href="#">Deformation of metallic parts measurement applied shearing interferometry and mechanical sensors</a>	Ernesto Ruiz-Ortega			
15:20 - 15:40	039	<a href="#">Measurement and characterization of reflective convex surfaces using Ronchi deflectometry</a>	Franco Gonzales			
15:40 - 15:55	Coffee break					
16:00 - 17:00	Plenary 4 John Howell	<b>Triangulation at the Standard Quantum Limit</b>				
17:00 - 17:20	031	<a href="#">Thickness analysis of South American Camelid Wool Fiber by Fraunhofer Diffraction</a>	Jade Aguayo	Telmo Echániz	Laser and laser optics, Optoelectronics, detectors and sources, Nonlinear optics	
17:20 -17:40	029	<a href="#">Photonic Crystal Mode Control in Semiconductor Lasers</a>	Kent Choquette			
17:40 - 18:00	027	<a href="#">Gravity-compensated focus-tunable lenses. Aberration analysis</a>	Maria Millán			
18:00 - 18:20	087	<a href="#">An Infrared-based Aedes-aegypti Identification Trap</a>	Miguel Quiroz			

18:20 - 18:40	056	<a href="#">Experimental study of polarization in the Normal Zeeman effect</a>	Zandra Lizarazo		
18:40 - 19:00	105	<a href="#">Second Harmonic Generation from LIPSS on GaAs</a>	Anatoly Khomenko		

## Tuesday (Continuation)

Tuesday, November 18th			
Room 02 (C1)			
Hour	Activity	Presentation title	Presenter
08:30 - 09:10	First IPS-RIOA Topical Workshop on Quantum Optics - Quantum Optics School	How to use quantum optics for nonlinear optics	Humberto Michinel, University of Vigo, Spain
09:10 - 09:50		Basics of Photoacoustic Spectroscopy and Its Application in Environmental Monitoring Processes	Abdul Rahman, University of Szegeed, Hungary. 

Tuesday, November 18th			
Room 03 (Recreation Room)			
Hour	Activity	Presentation title	Presenter
17:00 - 18:30	Communicating Science to the public	Outreach for Professionals Who Teach in Informal Environments and K-12 Schools	Mike McKee

### **OPTIKS: Outreach for Professionals Who Teach in Informal Environments and K-12 Schools**

It is common for industry professionals, faculty, and graduate students to conduct outreach to K-12 schools and in informal locations such as fairs, science centers, or open houses. But what are the most effective ways to engage participants in activities and how should the information be presented? As part of this workshop, participants will learn how to most effectively present activities in optics and photonics that will maximize engagement while taking into account the audience and the location. They will also learn how to train others using the skills learned in this workshop.

#### **LEARNING OUTCOMES**

This course will enable you to:

- present information taking into account audience and location alter an activity to maximize engagement for their audience
- recognize when a presentation is “over the heads” of a prospective audience adapt their presentation so they “speak simply”
- state the important factors that are required for effective presentations to varying audience
- teach others the approaches learned in the workshop

#### **INTENDED AUDIENCE**

Industry professionals, graduate students or faculty who are interested in conducting outreach and training others how to conduct workshops.

This workshop is for beginners with some experience conducting outreach.

#### **COURSE LEVEL**


Introductory

## Wednesday

Room 01 (Auditorium)					
Wednesday, November 19th					
Hour	ID	Presentation title	Presenter	Chairman	Topics
08:30 - 08:47	091	<a href="#">Thin-Film Deposition and Optical Testing of a First-Surface Mirror for Astronomical Applications</a>	Ana Quelopana, Gonzalo Gálvez	Daniel Malacara / Guillermo Baldwin	Geometrical optics, Optical design and fabrication, Diffraction and gratings, Physical optics
08:47- 09:05	074	<a href="#">Multiple Interferometry Applied to Radio Telescope Techniques</a>	Guillermo Baldwin		
09:05 - 09:22	018	<a href="#">Optical Design and prototyping of terrestrial telescope</a>	Franco Gonzales		
09:22 - 09:40	065	<a href="#">First Peruvian binoculars: Improvements</a>	Guillermo Baldwin		
09:40 - 09:57	044	<a href="#">Manufacture of aspherical mirrors for the implementation of a classic Cassegrain astronomical telescope</a>	Pablo Gallardo		
09:57 - 10:15	034	<a href="#">Optical design of double lens for the refractor telescope CST-80 KU by G-sum Method</a>	Jenifer Garcia		
10:15 - 10:34	073	<a href="#">Solar Concentrator</a>	Maria Cervantes		
10:34 - 10:48	Coffee break				
10:50 - 11:10	013	<a href="#">Aniseikonia with Sphero-Cylindrical Lenses</a>	Daniel Malacara	Guillermo Baldwin	
11:10 - 11:30	068	<a href="#">Coexistence of Aplanatism and Achromatism in Optical System Design</a>	Rafael Torres		
11:30 - 12:30	Plenary 5 Emiliano Descrovi	<b>Light Manipulation in Multilayered Photonic Structures</b>			
12:30 - 13:45	Lunch break				
14:00 - 14:20	009	<a href="#">Fiber-based acoustic and optic fused couplers</a>	Miguel Andrés	Rene Sosa	Fiber optics, sensors and optical communications, Remote sensing and sensors
14:20 - 14:40	014	<a href="#">Point sensors and fiber characterization techniques based on forward stimulated Brillouin scattering</a>	Miguel Andrés		
14:40 - 15:00	041	<a href="#">Optical Fiber Sensor Based on CS-TA Functionalized E-SMS Structure for the Selective Detection of Microplastics in Water</a>	Brayan Patiño-Jurado		
15:00 - 15:20	007	<a href="#">Sensing Fiber Twist through State of Polarization-Induced Phase Shifts</a>	Susana Silva		
15:20 - 15:40	010	<a href="#">Low-Coherence Interferometry for Analog Optical Communication</a>	Eneas Nicolas Morel		
15:40 - 15:55	Coffee break				
16:00 - 17:00	Plenary 6 Martin E. Garcia	<b>Ultrafast structural dynamics in solids driven by femtosecond laser pulses: from nonthermal bond breaking to surface nanostructuring</b>			
17:00 -17:20	038	<a href="#">Figure-8 fiber laser with dynamically controlled switching characteristic</a>	Olivier Pottiez	Rene Sosa	
17:20 - 17:40	042	<a href="#">U-Bent MMM Optical Fiber Sensor for the Detection of Mercury and Cadmium Ions in Aqueous Solutions</a>	Arturo Gaviria		
17:40 - 18:00	072	<a href="#">Analysis of Atmospheric Factors in Free-Space Optical (FSO) Communications for High-Altitude Urban Environments in La Paz, Bolivia</a>	Esteban Girona		

18:00 - 18:20	020	<a href="#">Optical sensors based on optical fibers in Mach-Zehnder type interferometry configuration for measuring ethanol Concentration</a>	Luis Espejo		
18:20 - 18:40	045	<a href="#">Optical sensors based on balloon-shaped optical fibers with tip-induced deformation in a Mach-Zehnder interferometer configuration for measuring ethanol concentration</a>	Luis Espejo		

### Wednesday (Continuation)

Wednesday, November 19th			
Room 02 (C1)			
Hour	Activity	Presentation title	Presenter
08:30 - 09:10	First IPS-RIOA Topical Workshop on Quantum Optics - Quantum Optics School	Precision measurement in optics and quantum optics	John Howell, Chapman University, USA
09:10 - 09:50		Optical quantum communications	Yaseera Ismail, Stellenbosch University, South Africa. 

Wednesday, November 19th			
Room 02 (C1)			
Hour	Activity	Presentation title	Presenter
17:00 - 18:30	RIOA OPTILAS General Assembly	RIOA OPTILAS General Assembly	Eric Rosas

Wednesday, November 19th			
Yotau All Suites Hotel			
Hour	Activity	Place	Presenter
19:00 - 23:00	<b>Official Event Dinner</b>		All together

## Thursday

Room 01 (Auditorium)						
Thursday, November 20th						
Hour	ID	Presentation title	Presenter	Chairman	Topics	
10:00 - 10:15	Coffee break					
10:20 - 10:40	035	<a href="#">Design and Simulation of GeSbS-Based Microcavities for Advanced Nonlinear Photonics</a>	Samuel Huertas	Eric Rosas	Nonlinear optics, photonics, Optics and photonics in the industry, Nano Photonics	
10:40 - 11:00	050	<a href="#">Optical Characterization of Infrared Key Fiber Materials: Transmission and Kerr Coefficient Measurements</a>	Camilo Hurtado			
11:00 - 11:20	011	<a href="#">From Lab to Factory: Applied Photonics Solutions for Industry</a>	Santiago Cerrotta			
11:20 - 11:40	092	<a href="#">Modeling of ultrashort laser pulse nanostructuring of materials</a>	Dmitry Ivanov			
11:40 - 12:40	Plenary 7 Erna Frins	<b>Some contributions to improving atmospheric observations through solar spectral analysis</b>				
12:40 - 13:55	Lunch break					
14:00 - 14:20	024	<a href="#">Optical Bullets with Angular Momentum in Nonlinear Waveguides</a>	José Ramón Salgueiro	Eric Rosas		
14:20 - 14:40	054	<a href="#">A Comparison of Metallic Nanoantenna Configurations for Single-Photon Emitters</a>	María Gabriela Capeluto			
14:40 - 15:00	036	<a href="#">Emissions into the atmosphere from the Ing. Héctor R. Lara Sosarefinery, Cadereyta de Jiménez, Nuevo León, México</a>	Claudia Rivera	Iñigo González de Arrieta		
15:00 - 15:20	109	<a href="#">The GEMM initiative by OPTICA &amp; AGU and the BEACO2N sensors</a>	Angela Guzmán			
15:20 - 15:40	052	<a href="#">Analysis of spectral structures influencing the detection of atmospheric trace gases</a>	Adriana Silva			
15:40 - 15:55	Coffee break					
16:00 - 17:00	Plenary 8 Orlando Frazão	<b>Future Perspectives of Optical Fiber Sensors</b>			Atmospheric and ocean optics, Instrumentation, measurement and metrology, Spectroscopy	
17:00 - 17:20	051	<a href="#">Differentiation of air pollution sources in Montevideo using NO<sub>2</sub>, CO trace gas columns, and atmospheric aerosol properties</a>	Alejandro Agesta	Iñigo González de Arrieta		
17:20 - 17:40	086	<a href="#">A Data-based Protocol for a Low-cost Mobile Spectrometer Calibration</a>	Edgar Salazar			
17:40 - 18:00	078	<a href="#">Enhancement of atomic emission intensity of heavy metals in LIBS using silver nanoparticles to increase the detection sensitivity of Cu and Pb</a>	Elder Espinoza			
18:00 - 18:20	076	<a href="#">Effects of Atmospheric Conditions on Infrared Data Transmission: Experimental Analysis in La Paz, Bolivia</a>	Mariana Vasquez			

## Thursday (Continuation)

Thursday, November 20th			
Room 02 (C1)			
Hour	Activity	Presentation title	Presenter
10:15 - 11:30	First IPS-RIAO Topical Workshop on Quantum Optics - Quantum Optics School	An Introduction to High Harmonic Generation and Attosecond Laser Pulses	Carlos Hernández García

Thursday, November 20th			
Room 02 (Recreation Room)			
Hour	Activity	Presentation title	Presenter
17:00 - 19:00	Hands-on Activity	IPS-Peer review ethics / IPS-Entrepreneurship	Carmiña Londoño / Natalia Cañas

### IEEE Ethics Guidelines and the Peer Review Process

Did you know that Albert Einstein did not like the peer review process? Have you been asked to be an IEEE peer reviewer? Have you published your research in an IEEE journal? Even if your answer is no, come to this interactive workshop to discuss the IEEE ethics requirements for authors and the IEEE peer review process. We will review basic principles and engage in fun exercises to really understand what it really takes to be a thorough peer reviewer that helps the scientific and engineering community document its contributions to society. And find out what alternative review process Einstein suggested!

### IPS-Entrepreneurship

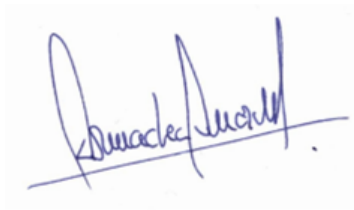
In this talk, Natalia Cañas Estrada will present the recent work of the IEEE Photonics Society across Latin America, highlighting key efforts carried out in countries like México and Brazil, share insights from the entrepreneurship workshops organized in the region, and discuss how these initiatives aim to strengthen and encourage the growth of the optics and photonics community in Latin America. This session will also offer a space for open discussion, collaboration, and networking among participants.

## Friday

Room 01 (Auditorium)						
Friday, November 21st						
Hour	ID	Presentation title	Presenter	Chairman	Topics	
08:30 - 08:50	066	<a href="#">Latent Fingerprint Imaging via Modulated-Intensity Maps from Fringe-Pattern Deflectometry</a>	Julian Perez-Carvajal	Edgar Salazar	Image processing, Imaging system, vision and artificial intelligence, Fourier optics and signal processing	
08:50 - 09:10	070	<a href="#">Detection of microstructural patterns in optical coherence tomography images using artificial intelligence tools to differentiate melanoma from melanocytic nevus</a>	Florencia Pinto			
09:10 - 09:30	061	<a href="#">Cost-effective 3D printed bright-field microscope</a>	Diego Londono			
09:30 - 09:50	104	<a href="#">Evaluating gait recognition performance on privacy preserving images</a>	Loana Velasquez-Omonte			
09:50 - 10:10	089	<a href="#">Automatic orthogonal recording polarimeter applied to bio-samples</a>	Asticio Vargas			
10:10 - 10:30	106	<a href="#">Optimization of projection selection and measurement time in compressive single-pixel imaging</a>	Sebastián Bordakevich			
10:30 - 10:40	Coffee break					
10:40 - 11:00	101	<a href="#">Spatial polarization modulation using two LCDs in tandem</a>	Sebastián Bordakevich	Edgar Salazar		
11:00 - 11:20	032	<a href="#">Three-dimensional measurement of human face topography using fringe projection profilometry</a>	Riquelme P-Cruz			
11:20 - 11:50	043 / 040	<a href="#">3D scanning of objects by color multi-line structured light projection</a> <a href="#">Application of structured light projection for the digital reconstruction with color texture of archaeological objects</a>	Miguel Asmad			
11:50 - 12:50	Plenary 9 Marina Sparvoli	<b>Applications of Gallium Oxide-Based Photomemristors in Neuromorphic Engineering</b>				
12:50 - 13:50	<b>CLOSING CEREMONY COCKTAIL (Recreation Room)</b>					

## Final Comments

The RIOAO OPTILAS 2025 Meeting, represented an opportunity to organize a prestigious Ibero-American Meeting, to learn about current research in the field of optics, photonics, and lasers, to promote students vocations in these areas, and to provide a space for the exchange of information and collaboration for students and researchers in the region and our country.

A handwritten signature in blue ink, which appears to read "Ormachea Ormachea", is written over a horizontal line.

Omar Ormachea, Ph.D., Chairman  
Dean of the Faculty of Engineering and Architecture  
Director of the Optical and Energy Research Center  
UPB, Cochabamba, Bolivia